Electronic Thesis and Dissertation Repository

8-15-2016 12:00 AM

Microwave and Ultrasound Assisted Zeolitization of Coal Fly Ash

Syed Salman Raza Bukhari, *The University of Western Ontario*

Supervisor: Prof. Sohrab Rohani, *The University of Western Ontario*
A thesis submitted in partial fulfillment of the requirements for the Doctor of Philosophy degree
in Chemical and Biochemical Engineering
© Syed Salman Raza Bukhari 2016

Abstract

Coal fly ash (CFA) is a major bi-product of coal fired power plants and is a liability for coal power industry. Coal fly ash has been accumulating rapidly around the globe and has been known to be accident prone, resulting in $1.65 billion in clean-up costs and fines. Given the environmental damage CFA is capable of causing, it is a great interest for scientists to recycle this material. Utilization of novel energy such as microwave and ultrasound has been of research interest for the zeolitization of coal fly ash.

This research produced zeolites from CFA utilizing microwave and ultrasound power. Single mode microwave which significantly decreases was utilized to produce zeolite with 300 W power in 30 min. The amount of irradiation was also related to zeolite the growth of crystals and phase purity. Ultrasound assisted zeolitization resulted in single phase zeolite-A crystals with high crystallinity and smaller crystal sizes at 85°C compared to 95°C with conventional synthesis. Ultrasound probe was shown to produce the results with only $1/10^{th}$ of energy as previously reported works. The Recycling of waste stream for zeolitization process was also investigated this can contribute to lower the financial costs of zeolite production. A novel design of a microwave reactor is introduced in this work that utilizes the microwave energy efficiently this design can result in cost savings in the production of zeolites through microwave energy. It is a first step in industrializing the zeolitization of CFA utilizing microwave energy which can result in a cleaner coal energy in world where it is a significant source of power generation and can offer the option of using CFA waste accumulated decreasing the likelihood of future accidents causing environmental damages and legal liabilities.

This work has shown that microwave and ultrasound irradiation can significantly decrease the time of zeolitization process. Single mode microwave has been shown to be much more effective in producing the same results at a third of the power rating for a multimode microwave. Similarly, utilization of ultrasound probe produced a single phase zeolite at a tenth of power reported using ultrasound bath. Ultrasound assisted zeolitization was observed at 85°C, about 10°C lower than conventional synthesis. Waste stream recycling was shown to be effective for a couple of runs indicating that waste from zeolitization can be reduced. A

pilot scale microwave reactor with a novel design was commissioned can be utilized in future from microwave synthesis.

Keywords

Dedicated

To:

The memory of my grandfather

Syed Anwar Ali Shah

and

My dear parents

Mrs. Syeda Narjis Imtiaz and Mr. Syed Imtiaz Hussain Bukhari

Co-Authorship Statement

Chapter 2

Article Title: Conversion of coal fly ash zeolite utilizing microwave and ultrasound energies: A review
Authors Syed Salman Bukhari, Jamshid Behin, Hossein Kazemian, Sohrab Rohani
Article Status Published, Fuel
The paper was written and compiled by S. S. Bukhari. J. Behin assisted in collecting the references and complete Tables. 2 and Table 3. This work was supervised by S. Rohani. Various drafts of the paper were reviewed by H. Kazemian and S. Rohani.
Bukhari, S.S., Behin, J., Kazemian, H., and Rohani, S (2015). Conversion of coal fly ash zeolite utilizing microwave and ultrasound energies: A review. Fuel, 140, 250-266.

Chapter 3

Article Title: Synthesis of zeolite Na-A using single mode microwave irradiation at atmospheric pressure: The effect of microwave power
Authors Syed Salman Bukhari, Jamshid Behin, Hossein Kazemian, Sohrab Rohani
Article Status Published, The Canadian Journal of Chemical Engineering
S.S. Bukhari wrote the manuscript, conducted experiments and analyzed the product synthesized. J. Behin assisted in conducting experiments, collecting and compiling the data. The work was supervised by S. Rohani. Various drafts of the paper were reviewed by H. Kazemian and S. Rohani.
Bukhari, S.S., Behin, J., Kazemian, H., and Rohani, S (2015). Synthesis of zeolite Na-A using single mode microwave irradiation at atmospheric pressure: The effect of microwave power. The Canadian Journal of Chemical Engineering, 93(6), 1081-1090.

Chapter 4

Article Title: A comparative study using direct hydrothermal and indirect fusion methods to produce zeolites from coal fly ash utilizing single-mode microwave energy
Authors Syed Salman Bukhari, Jamshid Behin, Hossein Kazemian, Sohrab Rohani
Article Status Published, Journal of Materials Science
S.S. Bukhari wrote the manuscript, conducted experiments and analyzed the product synthesized. J. Behin assisted in collecting and compiling the data. The work was supervised by S. Rohani. Various drafts of the paper were reviewed by H. Kazemian and S. Rohani.
Bukhari, S.S., Behin, J., Kazemian, H., and Rohani, S (2015). A comparative study using direct hydrothermal and indirect fusion methods to produce zeolites from coal fly ash utilizing single-mode microwave energy: Journal of Materials Science, 49(24), 8261-8271.

Chapter 5

Article Title: Effect of ultrasound energy on the zeolitization of chemical extracts from fused coal fly ash
Authors Syed Salman Bukhari, Hossein Kazemian, Sohrab Rohani
Article Status Published, Ultrasonics Sonochemistry
This work was supervised by S. Rohani. Various drafts of the paper were reviewed by H. Kazemian and S. Rohani. All the experiments and data analysis were conducted by S.S. Bukhari.
Bukhari, S.S., J., Kazemian, H., and Rohani, S (2016). A comparative study using direct hydrothermal and indirect fusion methods to produce zeolites from coal fly ash utilizing single-mode microwave energy: Journal of Materials Science, 49(24), 8261-8271.

Chapter 6

Article Title:
Microwave assisted zeolitization of coal fly ash using landfill leachate as the solvent
Authors
Syed Salman Bukhari, Hecham Omar, Sohrab Rohani
Article Status
Submitted to Journal of Hazardous Materials for publication
All experiments were conducted by S.S. Bukhari with the assistance of H. Omar. The manuscript was prepared by S.S. Bukhari and H. Omar. The work was supervised by S. Rohani and various drafts of the paper were reviewed by S. Rohani.
Bukhari, S. S., Omar, H., Rohani, S. Microwave assisted zeolitization of coal fly ash using landfill leachate as the solvent. Journal of Hazardous Materials (Submitted 2016).

Chapter 7

Article Title:
Continuous large flow synthesis of zeolite-A utilizing microwave irradiation with recycled liquid stream
Authors
Syed Salman Bukhari and Sohrab Rohani
Article Status
Intended for submission
This work was supervised by S. Rohani. Various drafts of the paper were reviewed by S. Rohani. All the experiments and data analysis were conducted by S.S. Bukhari.

Appendix A

Article Title:
Using coal fly ash and wastewater for microwave synthesis of LTA zeolite
Authors
Jamshid Behin, Syed Salman Bukhari, Vahid Dehnavi, Hossein Kazemian, Sohrab Rohani
Article Status

Published, Chemical Engineering & Technology
Experimental protocol was established by S. S. Bukhari. Waste water was provided by V. Dehnavi. All experiments were conducted by Jamshid Behin with the assistance of S. S. Bukhari. Analysis were conducted by and Jamshid Behin and S. S. Bukhari. The manuscript was prepared by Jamshid Behin with the assistance of S. S. Bukhari and V. Dehnavi. The work was supervised by S. Rohani and various drafts of the paper were reviewed by H. Kazemian and S. Rohani.
Behin, J., Bukhari, S.S., Dehnavi, V., Kazemian, H., and Rohani, S (2014). Using Coal Fly Ash and Wastewater for Microwave Synthesis of LTA zeolite. Chemical Engineering & Technology, 37(9), 1532-1540.

Appendix B

Article Title: Developing a zero liquid discharge process for zeolitization of coal fly ash to synthetic NaP zeolite
Authors Jamshid Behin, Syed Salman Bukhari, Hossein Kazemian, Sohrab Rohani
Article Status Published, Fuel
All experiments were conducted by Jamshid Behin with the assistance of S. S. Bukhari. Analysis were conducted by J. Behin and S. S. Bukhari. The manuscript was prepared by Jamshid Behin with the assistance of S. S. Bukhari. The work was supervised by S. Rohani and various drafts of the paper were reviewed by H. Kazemian and S. Rohani.
Behin, J., Bukhari, S.S., Kazemian, H., and Rohani, S (2015). Developing a zero liquid discharge process for zeolitization of coal fly ash to synthetic NaP zeolite. Fuel, 171, 195-202.

Appendix C

Article Title: Comparison of cation exchange capacity of zeolites using Kjeldahl method and UV-Vis spectroscopy
Authors Syed Salman Bukhari, Hecham Omar, Sohrab Rohani
Article Status Intended for submission
All experiments were conducted by S.S. Bukhari with the assistance of H. Omar. The manuscript was prepared by S.S. Bukhari and H. Omar. The work was supervised by S. Rohani and various drafts of the paper were reviewed by S. Rohani.

Acknowledgments

Table of Contents

List of Tables

List of Figures

Chapter 1

1 INTRODUCTION

Coal fired power is an important corner store of Canadian energy production. In 2006 production of energy from coal accounted for 13% of Canadian energy [1]. Canada has 8.7 billon tons of proved and an additional 190 billion tons of estimated coal resource. Coal fly ash is a by-product of the combustion of pulverized coal in coal-fired power plants and is considered a pollutant. Canada produced 37.7 million tons of thermal coal in 2010 of which 33.2 million tons were utilized locally for electricity generation. National Energy Board (NEB) of Canada estimates that about 14% of Canadian electric generation comes from coal and will be 6% of electricity generation of Canada in year 2035 [2]. According to CIRCA (Association of Canadian Industries Recycling Coal Ash) Canada produced upwards of 6 million tons of coal fly ash in 2010 and only 25% was recycled. Furthermore, 38 million tons of CFA have accumulated in landfills from 1997-2007 in Canada. In order to move towards clean coal energy, we need to recycle CFA being produced in coal power plants and the CFA that has accumulated in Ontario and Canada. One of the attractive solutions is to convert coal fly ash into zeolites which are multipurpose crystals utilized for various applications in industries such as petrochemical, agriculture, and health [3]. They are used for hydrothermal cracking, Fischer-Tropsh reaction, slow release fertilizers, antibacterial agents, and for removing of heavy metal elements from water [4] among many other uses.

1.1 Motivation and Objective

Conversion of CFA into zeolite serves two purposes simultaneously, it advances green technologies and also makes coal power a cleaner source of energy. Reducing the environmental hazards from coal power production would enable countries and regions rich in coal deposits utilize their natural resources to produce cheaper and greener energy.

The conversion of CFA into zeolite is a hydrothermal reaction. It is a prevalent opinion that a ton of CFA used in a cement mixture saves the use of an equivalent of nearly one barrel of oil [5]. Since the pioneering work of zeolitization [6–8] of CFA utilizing

conventional heating methods, there have been many reported CFA zeolitization with microwave (MW) and ultra sound (UTS) energies. This project focused on CFA zeolitization research from lab scale to pilot scale. CFA has been previously zeolitized utilizing MW and UTS energies, however, this work has been largely limited to small lab scale experiments using altered house hold microwave [9–13] and ultrasound baths [14–18].

The focus of this thesis was to consider more efficient methods of microwave and ultrasound irradiation for the zeolitization of coal fly ash. In the case of microwave experiments, a laboratory scale single mode microwave unit manufactured by CEM cooperation was used. In a single mode microwave, electromagnetic irradiation is directed through a precisely designed wave guide that produces a standing wave, this is unlike an altered home microwave system which produces waves with different phase shifts resulting in multimode microwave irradiation. This results in an energy field density to be higher and more uniform in a single mode microwave compared to a multimode microwave system. This thesis also introduces utilizing of ultrasound probe to directly irradiate the zeolitization reaction with ultrasound energy unlike the previously conducted works that have used ultrasound water bath. A pilot scale reactor system has also been fabricated and manufactured for the purpose of conducting this research at a larger scale.

1.2 Approach and Methodology

The following work was conducted in order to meet the above mentioned objectives.

1.2.1 Pure Chemical Synthesis

Three primary methodologies were used to prepare zeolite-A from pure chemical precursors in lab scale reactor of about 20 mL. Na-A zeolite was synthesized using a single mode microwave heating method (single mode, 2.45 GHz, CEM cooperation, Discover, USA). The synthesis solution with the composition of 3.165 Na_2O:1 Al_2O_3:1.926 SiO_2:128 H_2O was aged for two hours. It was demonstrated that the microwave energy released to a synthesis mixture at atmospheric pressure can produce pure zeolite A. The presence of zeolite Na-A and Na-X crystals was verified by both

XRD, and SEM. The BET surface area and the Cation Exchange Capacity (CEC) of the zeolite produced utilizing microwave were compared to the zeolite produced by conventional synthesis. Producing zeolite through microwave synthesis significantly shortens (50%) the production time of the zeolite compared to the conventional heating and both methods result in comparable BET surface area The microwave irradiation power plays a significant role in producing a single phase zeolite, furthermore, the total amount of microwave irradiated energy also strongly influenced the purity of the zeolite produced. Higher power and total energy irradiation produce pure Na-A compared to a mixture of Na-X and Na-A at lower power and energy irradiation [19].

1.2.2 CFA Zeolitization

Pure chemical synthesis of zeolite was followed by CFA zeolitization utilizing both MW and UTS energies.

1.2.2.1   Lab Scale Microwave Reaction

CFA was converted into Na-A zeolite using a single mode microwave heating. Two methods of converting CFA were investigated (direct hydrothermal and indirect fusion). The effects of three factors (power, time, aluminate concentration) were studied. The synthesis solution with composition of 4.714 Na2O:1 Al2O3:1.780 SiO2:192 H2O for high level aluminum mole composition and 4.714 Na2O: 0.582 Al2O3:1.780 SiO2:192 H2O for low level aluminum mole composition in factorial design of experiment were used. It was demonstrated that the microwave energy released to a synthesis mixture at atmospheric pressure can produce pure zeolite A at atmospheric pressure. Zeolite-A produced from CFA (CFAZA) was characterized using FTIR, XRD, BET, TGA, and (CEC). The hydrothermal and fusion products were comparable to each other in their characteristics, however, hydrothermal CFAZA performed better at immobilizing heavy metal ions and showed better crystalline structure whereas, fusion CFAZA had a higher BET surface area and a slightly higher CEC. It is suggested that the differences between the properties of the two different CFAZA are due to the difference in the dissolution of aluminum and silicon content of CFA in the reaction mixture. It was also observed that

the XRD peaks for hydrothermal conversion are sharper with bigger area under the peaks indicating a better crystallinity.

1.2.2.2   Ultrasound Reaction

The precursor reaction solution was prepared by extracting the constituents of CFA. The zeolitization process was conducted with conventional heating and with the assistance of UTS energy. UTS assisted synthesis at 95°C reduced the induction time of the zeolitization process by 20 min and also increased the crystal growth rate compared to conventional heating. However, as the reaction progressed, the synthesized zeolite-A converted to a more stable zeolite phase, namely hydroxysodalite. This conversion is discernable sooner and is much more rapid in the case of the UTS assisted synthesis compared to conventional synthesis. Hydroxysodalite XRD peaks are detectable at and after 60 min of reaction time for UTS synthesis at 95°C and these peaks gradually increase in height linearly as the peaks for zeolite-A decrease exponentially. Whereas, hydroxysodalite peaks are not observable until after 100 min into the reaction for conventional synthesis at 95°C. Reaction conducted at 85°C showed that UTS energy in addition to reducing the induction time and an increasing the crystal growth rate, produces a single phase zeolite-A, while the conventional heating showed production of small amounts of both zeolite-A and hydroxysodalite. SEM images showed that UTS energy at 85°C produced the purest single phase zeolite-A with smooth crystalline surface and smaller crystal sizes. However, conventional synthesis at 85°C resulted in zeolitic crystals with amorphous debris on the surface, generally with larger crystal sizes and presence of hydroxysodalite crystals. TGA analysis showed that the products have high water content. The zeolites produced by UTS had 3 % higher water carrying capacity by weight compared to zeolite synthesized by conventional heating. The UTS energy plays a positive role in the production of zeolite. It can expedite the production of zeolitic crystals and at a lower temperature while producing a pure single phase crystals of smaller size.

1.2.2.3   Bench Scale Microwave Reaction

The Milestone FlowSynth MW reactor was used to conduct direct conversion of CFA to zeolite at a larger scale (1 L of reaction slurry compared to 20 mL). A typical zeolite-synthesis procedure from coal fly ash (CFA) was carried out by adding 109 g of sodium hydroxide granules with 91 g of fly ash (NaOH/CFA ratio of 1.2) to 850 mL deionized water, and mixed at 60 ℃ for 16 h. Afterwards, 150 mL aqueous sodium aluminate solution (concentration: 0.155 g/mL) was also added. These experiments explored the effect of microwave power on the zeolitization process and further investigated the reuse of liquid waste stream produced during this process. The observations indicated that the microwave power can significantly increase the crystal growth, however, there was an optimal conversion beyond which higher crystallinity could not be achieved regardless of the microwave power. Furthermore, it was found that the waste stream from the zeolitization process could not be indefinitely used for the production of zeolite-A.

1.2.2.4   Pilot Scale Microwave Reactor System

The technical data gathered during the course of lab scale and bench scale tests were used to design a customized MW reactor. This pilot scale reactor was fabricated and commissioned to meet CSA (Canada Standards Association) requirements.

1.3   Thesis Outline and Organization

This thesis is organized in an integrated article format as specified by The School of Postgraduate Studies at the University of Western Ontario.

Chapter 2 of this thesis gives a thorough literature review of zeolitization of CFA with specific focus on the work done utilizing novel energies such as Microwave and Ultrasound. It briefly introduces CFA and its current uses and the future prospect of its use as a precursor material for crystallization of zeolite. It also highlights the differences of zeolite formed by different zeolitization processes and their relevant applications

Chapter 3 describes the production of zeolite-A (LTA framework) utilizing pure chemical precursors with a single mode microwave irradiation at atmospheric pressure. It quantitatively relates the total microwave irradiation energy with the crystallinity of the

zeolite produced. It can be concluded from this study that production of a single phase zeolite-A is directly related to the total microwave irradiation power.

Two major methods of zeolitization of CFA are compared in Chapter 4. Direct hydrothermal conversion and dry fusion followed by hydrothermal conversion are the two most widely used methods to produce zeolites from CFA. Characterization of the zeolites produced by two of these methods indicated that the zeolites are comparable in their properties. Therefore, either method of zeolitization can be used depending on economic feasibility. For our future bench and pilot plant it was decided that direct synthesis would be more practical and economically feasible.

Chapter 5 contains the experiments done on zeolitization of CFA utilizing ultrasound energy. It was concluded that ultrasound can produce a single phase zeolite-A at a lower temperature (85℃) compared to the hydrothermal synthesis.

Chapter 6 explores the effects of heavy metals in reactant solution on the crystallization of zeolites. Leachate solution which had multiple light and heavy metals was utilized as the reactant solution.

Bench scale experiments and pilot scale reactor system are discussed in Chapter 7. This chapter investigates the effects of microwave irradiation power on the zeolitization process at a bench scale in a continuous flow regime. It also explores the possibility and the limitations of utilizing the waste stream from the process in successive zeolitization. It also describes the pilot scale reactor system. It familiarizes the reader with the unique design and operation of the system. The specifications and capabilities of the system are discussed and a section devoted to the operations.

Chapter 8 presents the general conclusions of this thesis based on the experimental results, and the carried out analyses. Major findings are summarized and further endorses recommendations for future work.

Three appendices are included two of which consist the publications on the work conducted by this researcher who appears as the second author. Appendix A presents the work conducted to produce zeolite-A by utilizing two waste streams, a solid stream from

coal fired plants and a liquid stream from a plasma electrolytic oxidation (PEO) process. This work shows that these two waste streams can be successfully utilized to produce zeolitized CFA through the application of microwave irradiation.

Appendix B shows the work conducted to produce zeolite-P from CFA with recycled liquid waste stream resulting in a zero liquid discharge process. The zero liquid discharge technique introduced in this work minimizes the consumption of freshwater and sodium hydroxide remarkably.

A new methodology for calculating Cation Exchange Capacity (CEC) is introduced in Appendix C. This new suggested methodology would dramatically decrease the time and effort needed to calculate CEC in comparison to the Kjeldahl method.

1.4   References

[1]   Government of Canada NEB. Energy Reports - Coal-Fired Power Generation - An Overview - Energy Brief 2008.

[2]   Vision 2050: The Future of Canada's Electricity System. Canadian Electricity Association; 2014.

[3]   Bukhari SS, Behin J, Kazemian H, Rohani S. Conversion of coal fly ash to zeolite utilizing microwave and ultrasound energies: A review. Fuel 2015;140:250–66.

[4]   Attari M, Bukhari SS, Kazemian H, Rohani S. Mercury Removal from Aqueous Solution by Zeolitized Coal Fly Ash: Equilibrium and Kinetic Study. Chemosphere n.d.

[5]   Hollman GG, Steenbruggen G, Janssen-Jurkovičová M. A two-step process for the synthesis of zeolites from coal fly ash. Fuel 1999;78:1225–30.

[6]   Holler H, Wirsching U. Zeolite formation from fly ash. Fortschr Mineral 1985;63:21–43.

[7]   Shigemoto N, Hayashi H, Miyaura K. Selective formation of Na-X zeolite from coal fly ash by fusion with sodium hydroxide prior to hydrothermal reaction. J Mater Sci 1993;28:4781–6.

[8]   Behin J, Bukhari SS, Dehnavi V, Kazemian H, Rohani S. Using Coal Fly Ash and Wastewater for Microwave Synthesis of LTA Zeolite. Chem Eng Technol 2014;37:1532–40. doi:10.1002/ceat.201400225.

[9]   Bukhari SS, Behin J, Kazemian H, Rohani S. A comparative study using direct hydrothermal and indirect fusion methods to produce zeolites from coal fly ash utilizing single-mode microwave energy. J Mater Sci 2014;49:8261–71.

[10]   Bukhari SS, Rohani S, Kazemian H. Effect of ultrasound energy on the zeolitization of chemical extracts from fused coal fly ash. Ultrason Sonochem 2016;28:47–53. doi:10.1016/j.ultsonch.2015.06.031.

[11]   Belviso C, Cavalcante F, Lettino A, Fiore S. Effects of ultrasonic treatment on zeolite synthesized from coal fly ash. Ultrason Sonochem 2011;18:661–8.

[12]   Inada M, Tsujimoto H, Eguchi Y, Enomoto N, Hojo J. Microwave-assisted zeolite synthesis from coal fly ash in hydrothermal process. Fuel 2005;84:1482–6.

[13]   Querol X, Alastuey A, López-Soler A, Plana F, Andrés JM, Juan R, et al. A fast method for recycling fly ash: microwave-assisted zeolite synthesis. Environ Sci Technol 1997;31:2527–33.

[14]   Querol X, Moreno N, Umana J t, Alastuey A, Hernández E, López-Soler A, et al. Synthesis of zeolites from coal fly ash: an overview. Int J Coal Geol 2002;50:413–23.

[15]   Bukhari SS, Behin J, Kazemian H, Rohani S. Synthesis of zeolite NA-A using single mode microwave irradiation at atmospheric pressure: The effect of microwave power. Can J Chem Eng 2015;93:1081–90.

Chapter 2

2 CONVERSION OF COAL FLY ASH TO ZEOLITE UTILIZING MICROWAVE AND ULTRASOUND ENERGIES: A REVIEW[1]

Abstract

The ever increasing consumption of coal around the world has given rise to the by-product coal fly ash that requires an urgent attention and is gaining much needed research attention. This paper introduces pioneering work on zeolitization of coal fly ash utilizing conventional heating methods and reviews the progress made in the conversion of coal fly ash to zeolite and its applications while strongly focusing on the utilization of microwave and ultrasound energies in achieving this goal. An introduction to coal fly ash and zeolitic materials is given and the conversion of the formal to the latter is discussed. Zeolites are multi-utility crystals that have attracted much attention in the research community. Zeolites synthesized from pure chemical precursors are inherently different from zeolites produced from coal fly ash therefore; published works which have investigated the application of zeolites produced from coal fly ash are also discussed. Microwave and ultrasound energies have been reported to dramatically decrease reaction times due to the influences on the induction periods and nucleation. In the last few years these novel energies have blossomed in a useful technique for many applications. As novel energies they hold great promise in rapid and efficient conversion of coal fly ash to value added materials such as zeolites.

2.1 Introduction

Coal is the world's most abundant and widely distributed fossil fuel, with global proven reserves totaling nearly 1,000 billion tones. Coal fuels most of the electricity production in many countries, such as South Africa (93%), Poland (92%), China (79%), India (69%)

---

[1] This Chapter is published in the Journal Fuel. S.S. Bukhari, J. Behin, H. Kazemian, S. Rohani, Fuel 140 (2015) 250–266.

and the United States (49%). Moreover, the growing energy needs of the developing world are likely to ensure that coal remains a key component of the power generation mix in the foreseeable future, regardless of climate change policy [1]. Coal-fired power plants accounted for 41% of global electricity production in 2006 and are expected to account for 44% in 2030 [2]. The coal consumption has increased globally for the decade of 2002-2012 [3]. The increase in the global consumption of coal is led by the Asian and Oceania followed by countries in Central and South America, Middle East, Eurasia, and Africa, while there was a slight decrease in this trend in Europe and North America. Figure 2-1 outlines the coal consumption around the world.
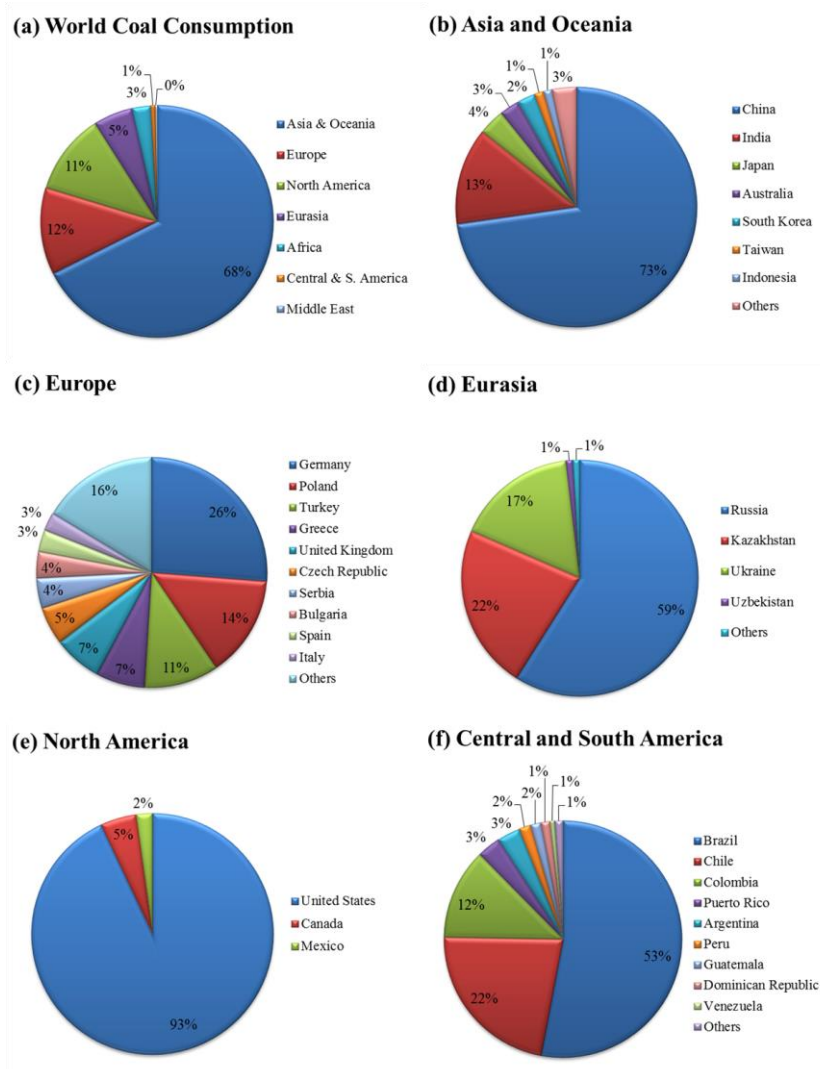
Figure 2-1. Global and Continental Coal Consumption for 2012

Burning of pulverized coal in coal-fired power plants produces residue of fine particles that rise with the flue gas, this residual gas is called fly ash. It is removed by dust collectors from the exhaust gases in the power plants. When fly ash is mixed with the residual coal ash (bottom ash) that does not rise, coal ash is obtained. Coal fly ash (CFA) is a mixture of about 80% fly ash and 20% bottom ash [4]. It a fine grained powder and it is mainly composed of spherical glassy particle (about 80%). CFA is the largest by-product of combusted coal in a power plant. It accounts for 75-85% of the total ash produced after the burning process [5]. The constituents of CFA can vary depending on many factors, such as the mineralogical composition of the coal, degree of coal pulverization, type of furnace and oxidation conditions [5].

CFA has adverse effects as a particulate pollutant and also leachate pollutant. CFA is classified as a human carcinogen and is composed of small particles with diameter less than 75 μm [6,7]. These small particles of CFA can easily be carried away by air, while particles smaller than 2.5 μm are considered to be the most harmful, as when inhaled can penetrate deep into the lungs [8]. Coal-fired power plants without effective fly ash capture systems are one of the largest sources of human-caused background radiation exposure. In vitro studies of CFA independent of type of coal combustion, origin or precipitation-exerts cytotoxicity in tests using animal lung cells, human red blood cells and hamster ovary cells [6]. Coal-fired power plants cause nearly 24,000 premature deaths annually in the United States, including 2,800 from lung cancer. Annual health cost in Europe from use of coal to generate electricity is $55 billion [4]. The amorphous CFA particles are insoluble in water, however, the enriched surface maybe soluble in water and can leach out of the solid waste. The leachates of CFA can demonstrate a great variability, toxicity studies suggest the leachates may adversely affect aquatic ecosystems, while the solid material may be hazardous to terrestrial ecosystems by direct external reactions or reactions in the respiratory or alimentary canal. Some of the constituents in the CFA such as heavy metals, polycyclic aromatic hydrocarbons and silica are considered toxic. Generation of hundreds of millions of tons of waste products that contain mercury, uranium, thorium, arsenic, and other heavy metals is major concern as it has the potential to adversely affect human health and the environment. It is imperative to decrease the environmental impact of burning coal in power plants for an

environmentally friendly and greener utilization of coal. China, USA, India and European Union produced 395, 118, 105, and 52.6 million metric tons of coal combustion by products in 2010, respectively and 67.1, 42.1 13.8 and 90.9% of the produced CFA are recycled in the respective countries. The world produced 780 million metric tons of coal combustion by product and recycled 52.6% [9].

It is important to dispose of CFA in a manner that is not harmful to the environment which could be a financial liability, therefore it is wise to utilize this waste product and convert it to a value added product. The abundance of coal and the advantages [10] of using coal in the production of energy dictate that more investment should be made in clean coal energy. It is necessary to find a novel method that is energy efficient and economically feasible to utilize it in manufacturing of value added materials. The use of CFA can have important economic and environmental implications. Employment of CFA to produce value added compounds could be one way of reducing the negative impact of coal power plants on the environment.

One major use for CFA is in the manufacturing of cement due to its pozzolanic properties. Since the 1950, CFA has been used in concrete and cement manufacturing. It is a prevalent opinion that a ton of CFA used to replace cement saves the use of an equivalent of nearly one barrel of oil [4]. USA and EU utilize about 6 and 9 million tons of CFA, respectively each year. It is a prevalent opinion that a ton of CFA used to replace cement saves the use of an equivalent of nearly one barrel of oil [4]. United States produced about 180 million cubic meters of ready mix concrete with about 50% utilizing CFA as a supplemental cementitious material. Leaching of toxic elements from concrete produced with CFA has shown to be much lower than contamination levels [11,12] while the strength [13] and modulus of elasticity increased [14]. Production of zeolite from CFA would result in a higher value added good compared to cement.

Zeolites are multi-utility crystals largely composed of Al and silicate framework. Zeolites are precipitated from aluminosilicate solutions in basic media at elevated temperatures. Generally, aluminate and silicate compounds such as but not limited to aluminum isopropoxide, aluminum hydroxide, alumina trihydrate, sodium aluminate, sodium

silicate, silica sol, are used as the Al and Si source for the synthesis of zeolites [15–20]. However, it has been shown that CFA which is largely composed of Al and Si can also be used as aluminosilicate source in the synthesis zeolites. Since the first reported conversion of CFA into zeolite by Holler and Wirsching [21] there have been hundreds of publications and tens of patents. The conversion of CFA into zeolite is a hydrothermal reaction conducted in high pH solution. The conventional methods of zeolite preparation using CFA involve dissolution of Al and Si sources, in addition to nucleation, and crystal growth. Creation of zeolite from CFA is energy intensive, this conversion occurs under high temperature provided through conventional heating methods. The most novel solution is to use microwave radiation and ultrasound energy instead of conventional heating to produce the desired product. It has been suggested that using microwave (MW) and ultrasound (UTS) energy sources could decrease the reaction time remarkably [22,23] thus making zeolitization of CFA an economically viable process. This will not only solve the problem of waste, but also produce a value added compound, zeolite, a multipurpose crystalline aluminosilicates that can be used for purifying air and water, and many other industrial uses. Since their discovery there has been a keen interest in the research of these materials.

2.2 Novel Energies

There is a lot of interest in using MW and UTS energies in recent years; this can be deduced from the number of publications reported synthesis utilizing MW and UTS.

2.2.1 Microwave Energy

MW lie in between infrared waves and radio waves on electromagnetic spectrum. Typical operation frequency of MW is 915 ± 15 and 2450 ± 15MHz. The use of 2450 MHz is more prevalent due to the fact that energy absorption is maximum for water at this frequency and also magnetrons at this frequency are more widely available in commercial microwave and chemistry equipment [24]. The mechanism of energy transfer due to MW is starkly different from conventional heating, thus giving it a unique advantage over conventional synthesis. The energy transfer is due to the interaction of dielectric molecules with MW. Dielectric heating occurs when dipoles of polar molecules follow

the inversion of alternating electric field. The dipole molecules in the irradiated field tend to orient them with the magnetic field, as the magnetic field oscillates the molecules also follow the oscillations. Their motion is resisted by inter-particle interactions and electric resistance. The induced energy dissipates in the form of heat through molecular friction resulting in uniform distribution of heat compared to conventional heating. Furthermore, beyond thermal effects non-thermal effects have also been reported. It has been shown that MW irradiation elevates the boiling point of the solvent. This is called "super heating" effect caused due to retardation of nucleation of gas vapors in MW radiation. However, the nucleation retardation can be overcome by stirring the reaction mixture [25]. The activation energy is also observed to decrease during MW irradiation compared to conventional heating that might be due to higher atomic mobility in the crystal lattice [26]. MW irradiation can also be used for non-polar molecules by addition of susceptors. These materials efficiently absorb MW and then transfer the absorbed energy as thermal energy to the molecules in the vicinity that are weak at absorbing MW [27,28]. The unique properties of MW energy they have been utilized in the production of zeolites from pure chemical precursors [18,20,29] and CFA as discussed later in the paper.

2.2.2 Ultrasound Energy

UTS irradiation can initiate reactions that may not be initiated under conventional methods; furthermore, UTS can also accelerate chemical reactions. UTS causes cavitation events that refer to the growth and violent collapse of micro-bubbles in a liquid medium. These cavitations cause chemical (sonochemical-SC) and physical (light emission sonoluminescence-SL) phenomena due to ultrasonically driven growth and collapse of gas nuclei in a liquid [30]. Broadly there are two types of sonochemical reactions, homogenous sonochemistry that results from the formation of radicals or radical intermediates while heterogeneous sonochemistry is influenced primarily through the mechanical effects of cavitation, such as surface cleaning, particle size reduction, and improved mass transfer [31]. The sonochemical effects do not come from a direct interaction between sound field and molecular species, but due to acoustic cavitation [32]. These cavitations are produced when gas nuclei that are present in the liquid go through oscillations expanding and compressing, during the expansion in ultrasonic field,

a vacuum is created into which gas in the liquid diffuses. During the compression half of the cycle the gas within the bubble diffuses back into the host liquid, however, due to the smaller surface area not all the gas that diffused into the bubble diffuses out. After multiple expansion and compression, micro-bubbles reach a critical size resulting in bubble collapse during one compression cycle. Collapse of these bubbles results in adiabatic heating of gas and vapour inside the bubble. These cavitations produce radicals inducing sonochemical reactions. A simplified model of adiabatic bubble collapse can be used to calculate the maximum local temperature [30]. These hot spots can reach a temperature of 5000 °C, the local pressure can go as high as 20 MPa with high cooling rates of 107 °C/s these cavitations result in particle collisions at high velocities [23,33,34]. UTS energy can also be used for the synthesis of metal and semiconductor particles, polymers, organic compounds, cleaning of industrial equipment, leather processing, drug delivery, inter-particle collisions and coupled with electrochemical reactions [30]. There have been many reported works where zeolites have been synthesized utilizing US energy [19,35–38].

2.3 Coal Fly Ash characteristics

The major chemical constituents and properties of CFA are greatly influenced by the properties of coal being burned (anthracite, bituminuous, sub-bituminuous and lignite) [7,39] combustion method, heating and cooling regimes in the coal boiler [5] as well as emission control devices, storage and handling [40]. CFA may contain different phases of alumina and silica, such as mullite, quartz, hematite, and calcite, while also containing other inorganic compounds such as lime and sulphates [41]. Besides the mineral compounds, CFA is largely composed of amorphous solid and hollow spheres [39]. There are two major classes of CFA, class F and class C. Class F contains less than 20% of CaO and is mostly produced by higher ranked coal such as anthracite and bituminous coal, while class C contains more than 20% CaO and is mostly a result of burning of lower grade coal such as sub-bituminous and lignite [41,42]. Quartz and mullite are the major crystalline compounds found in low calcium CFA where as high calcium CFA consists of quartz, tricalcium aluminate, calcium silicate, and tetracalcium aluminosilicate [7]. Despite the variability of CFA around the globe, they have been successfully used to

synthesize zeolite in different countries including but not limited to Australia [43], Bulgaria [44], Canada [45,46], Italy [37,38], India [47], Japan [48–52], Poland [42,53,54], South Africa [55,56], South Korea [57–59], Spain [60,61], and United States [62].

2.4 Zeolitized Coal Fly Ash

2.4.1 Structure and Characteristics of Zeolite

Zeolites are crystalline aluminosilicates consisting of alkaline and alkaline-earth elements. In addition to be found in nature, zeolites are also synthesized using different chemical precursors and raw materials. Natural zeolites are abundant and low cost resources, which are crystalline hydrated aluminosilicates with a framework structure containing pores occupied by water and metallic cation.

Zeolite structure is based on silicate chemistry with tetrahedron structure similar to aliphatic carbon chemistry. Tetrahedron is a polyhedron composed of four triangular faces. Three of these triangular faces meet at the vertex while the forth triangle composes the base of the structure. Silicate (SiO_4) unit within a structure is linked to other silicate through shared oxygen atoms. Zeolite frameworks exclusively contain Al^{+3} and Si^{+4}, therefore producing a negative charge in the frameworks. These frameworks contain cations to electrochemically balance the negative charge introduced by Al atoms present in aluminosilicates. It can be inferred that higher ratio of Al^{+3} would result in higher cation exchange capacity. Cations neutralize the excess anionic charge; these cations should be able to undergo reversible ion exchange in order to be considered zeolite. Sometimes the frameworks of aluminosilicates are so compact that these cations are trapped at the normal temperature. However, in zeolite molecules the frameworks are wider. These wide frameworks are open to cations in addition to salts and water molecules. Zeolite frameworks are also rigid which enables them to remains unaltered when water is sorbed or desorbed. The unit cell formula is generally written as follows.

$$M_{2/n}O \cdot Al_2O_3 \cdot XSiO_2 \cdot YH_2O \hspace{4cm} (\text{Eq. 2-1})$$

Where M represents the exchangeable cations, generally from group I or II ions, although other metallic, non-metallic, or organic cations may be used to balance the charge on the framework; n represents the cation valence. These cations are present either during synthesis or through post synthesis. The value of X is equal to or greater than 2, as alumina tetrahedron does not occupy adjacent tetrahedral sites. Y represents the degree of hydration [63].

The amount and location of Al present in the zeolite affect heavily the properties of the compound produced. The amount of Al can vary greatly. The Si to Al ratio can range from 1 to ∞, where later is complete siliceous compound, SiO_2. The lower limit of Si to Al ratio of 1 is observed, it is suggested by Lowenstein that $[AlO4]^{-1}$ tetrahedra are not placed adjacent to each other because the negative charge on them repel each other [64]. Al introduces negative charge into the compound that gives it the ability to exchange cations and catalyze reactions. The hydrophobicity and hydrophilicity also strongly depend on the Al content. Adsorption of polar and non-polar molecules by zeolites is also affected by Al content. Controlling the above properties can have a significant impact on the utilization of zeolite. The hydrophobic and cation exchange properties would be advantageous properties in water purification. Adsorption of polar and non-polar molecules could be useful in cases of purification of mixtures dissolved in polar or non-polar solvents. Some zeolites also show adsorption of anions and organics from aqueous solution. Modification of zeolites can be achieved by several methods such as acid treatment, ion exchange, and surfactant functionalization, endowing the modified zeolites higher adsorption capacity for organics and anions [65].

Silicate and aluminate tetrahedra are the primary building units of zeolites. Whereas, secondary building units are the characteristic arrangements of tetrahedra giving rise to frameworks in the zeolite's structure. The framework structures are listed in the publications of Atlas of Zeolite Framework Types which in its sixth edition lists 176 unique zeolite framework structures each assigned a 3-letter code by the commission of International Zeolite Association [66] (however these framework structures have currently reached 218 [67]). One way to view zeolite structure that involves stacking units along a particular axis. A six-ring unit can be vertically stacked over it to generate

hexagonal prism or offset to generate a different structure. There is an infinite number of ways of stacking that leads to four-connected three-dimensional framework structure, however out of 1000 theoretical structures built; only 10% of the frameworks have been experimentally observed [68]. Some of the common zeolite framework structures are illustrated in Figure 2-2 and Table 2-1 that give a brief property description and provide examples of the zeolites with those frameworks.
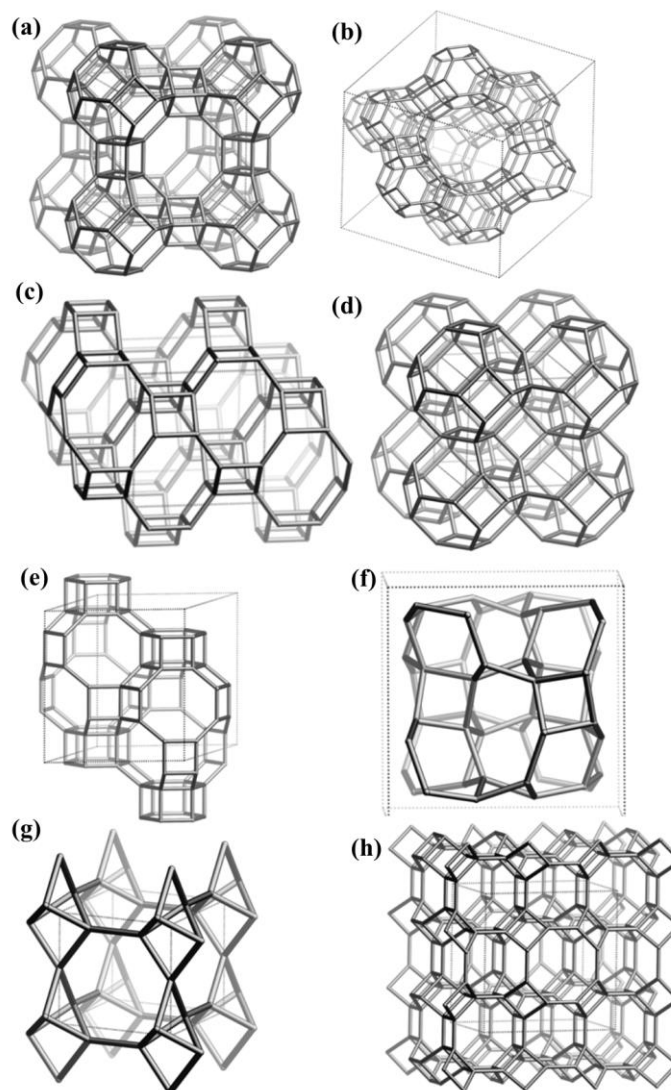
Figure 2-2. Structure of some common zeolite frameworks (a) LTA (b) FAU (c) GIS (d) SOD (e) CHA (f) ANA g(EDI) (h) MER [66]

Table 2-1. Common frameworks with their idealized cell parameters, composite building blocks and examples of zeolites

Frame work	Idealized Cell			CBU	Zeolites
	Shape	Space Group	Parameters		
LTA	Cubic	Pm-3m	a=11.9 Å	d4r, sod, lta	Zeolite-A, SAOP-42
FAU	Cubic	Fd-3m	a=24.3 Å	d6r, sod	Faujasite, Na-X, Na-Y, SAPO-37, ZSM-20
GIS	Tetragonal	I4$_1$/amd	a=9.8 Å, c=10.2 Å	gis	Gismondine, Na-P, Na-P1, Na-P2, SAPO-43
SOD	Cubic	Im-3m	a=9.0 Å	sod	Sodalite, hydroxysodalite, AlPO-20
CHA	Trigonal	R-3m	a=13.7 Å, c =14.8 Å	d6r, cha	Chabazite, AlPO-34, SAPO-34. SAPO-47
ANA	Cubic	Ia-3d	a=13.6 Å		Analcime, AlPO-24,
EDI	Tetragonal	P-4m2	a=6.9 Å, c=6.4 Å	nat	Edingtonite, K-F, Linde F, Zeolite N
MER	Tetragonal	I4/mmm	a=14.0 Å, c=10.0 Å	dcc, d8r, pau	Merlinoite, K-M, Linde W, Zeolite W

2.4.2 Structure and Characteristics of CFA-Zeolite (CFAZ)

The zeolites that are produced from CFA are mostly characterized by using multiple techniques such as X-ray diffraction (XRD), Fourier Transform Infra-red spectroscopy (FTIR), Inductively Coupled Plasma spectroscopy (ICP) and Scanning Electronic Microscopy (SEM). The structure of zeolites synthesized from CFA depends on the synthesis steps taken during the procedure. CFA can be converted to zeolite without filtering out solids from the reaction mixture or filtering out of the undissolved CFA in the reaction mixture after ageing. Without filtering out the solids results in the production of CFA particles with a surface covered in zeolitic crystals, such as Na-A, Na-X, K-CHA,

SOD etc. for different reaction conditions. Examples of these types of CFAZ structure is given in the Figure 2-3.
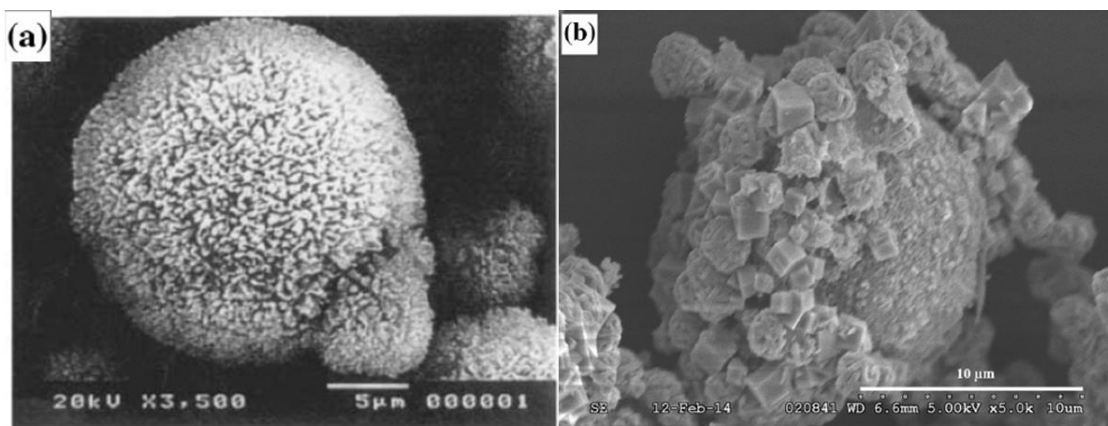
Figure 2-3. SEM of CFAZ crystallized on the surface of CFA particle (a) Na-P1 [69] (b) Na-A [46]

CFAZ synthesized with filtration of undissolved soluble produces zeolites with crystalline shapes such as cubes (for Na-A and Na-X), needle like structures (Na-P1) and flower shapes (SOD). Some examples of this type of CFAZ structure are given in the Figure 2-4.
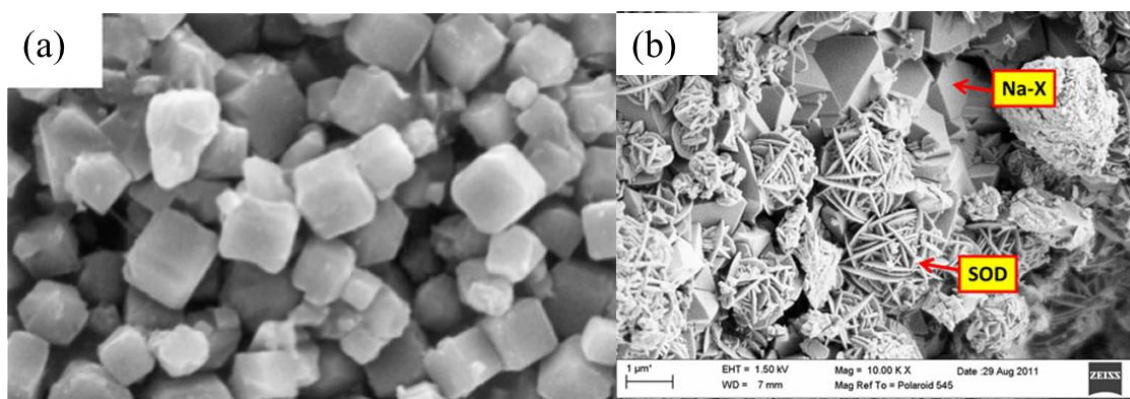
Figure 2-4. SEM of zeolites synthesized from leached CFA (a) LTA (Na-A) [70] (b) FAU (Na-X) and SOD [71]

2.4.3 Applications of CFA-Zeolites (CFAZ)

Natural and synthetic zeolites are well known for their ability to act as catalysts, ion exchangers, adsorbents and membrane. Due to these abilities they find many potential applications in the fields of pollution control [72], radioactive waste management [73,74], petrochemical reactions [75,76], water purification [77–80], purification of gasses [81–83], and agriculture [84]. Na-A zeolite possesses unique structural properties and is extensively used in the industrial field for drying gasses and liquids, washing builder, and the separation of normal from branched paraffins. However, because the Na-A zeolite obtained from CFA processes is a mixture of CFA, the aforementioned properties are inferior to those of pure Na-A [70]. Zeolites produced utilizing CFA might not be used for all the applications that pure zeolites can be used. Zeolitized CFA also contains heavy metal ions, due to this restriction there has been a lot of interest in researching the use of CFA-zeolites (CFAZ) for different applications. This section tries to summarize the applications where CFAZ have been utilized.

Srinivasan and Michael [81] produced Zeolite-X, Y and Na-P1 from class F fly ash and utilized it for SO_2 adsorption from a stack gas containing 2000 ppm SO_2 (~0.2% by volume). The adsorption capacity of the best sample which was prepared by treating CFA for 7 days at 150 °C was around 6-7 mg of SO_2 per g of product. Majchrzak-Kucęba and Nowak [85] used a flue gas with a volumetric composition of 10% CO_2, 10% O_2 and 80% N_2 to investigate the CO_2 adsorption by zeolite produced using CFA. It was reported that zeolite Na-A produced from CFA had the adsorption capacity of 52 mg CO_2 per g of product. Wdowin et al. [83] produced zeolite Na-A and Na-P1 utilizing CFA and impregnated with silver. Modified CFAZ can be promising for Hg removal. Querol et al. [86] produced zeolite from CFA and measured the CEC of the product utilizing procedure outlined by International Soil Reference and Information Centre [87]. The CEC for zeolite-4A, Na-P1, Na-CHA, KM, Linde F, Na-ANA, SOD and original CFA were reported as 4.7, 2.7, 2.1, 1.9, 1.9, 0.6, 0.3, and less than 0.05 meq/g, respectively. The best CFAZ produced had a gas sorption capacity for CO_2, SO_2, NH_3 of 74, 297, 111 mg/g, respectively.

Some of the prevalent applications of CFAZ arise from its cation exchange capacity (CEC). This property can be utilized for the sorption of metallic cations from wastewater. It is of great interest to produce CFAZ with high CEC capacity. Berkgaut and Singer [88] produced zeolite from CFA and used procedure outlined by Polemio and Rhoades [89] with minor modifications replacing Na^+ with NH_4^+ reporting CEC ranging from 5.78-6.12 meq/g. Woolard and Horst [55] modified 100 g CFA in 1 dm3 of NaOH with a molarity ranging from 1-8 M for 21 h at 90°C. CEC was measured from the procedure outlined by Hesse [90] and were reported as high as 3.00 meq/g and lead absorption capacity as high as 1.00 meq/g at a pH of 5. CFAZ produced have been shown that they can be used to reduce pollution in wastewater by removal of heavy metal cations such as Ar [61,72], Cd [52,61,72,91,92], Co [61,72,91,93,94], Cr [61,72,94], Cu [52,91–94], Pb [61,72,91,92,92,93], Sb [61,72], Mo [61,72], Ni [52,61,72,92–94], Tl [61,72], U [61,72], V [61,72] and Zn [91,93,94] from aqueous solution. CFAZ has also shown the potential to act as an immobilizing agent of metallurgical wastes [95]. Fotovat et al. [96] showed CFAZ loaded with cobalt nanoparticles can be utilized for catalysis of Fischer-Tropsh synthesis. The CFAZ loaded with cobalt particle and pure zeolite loaded with cobalt nanoparticles produced comparable results. Klamrassamee et al. [97] used CFAZ to adsorb water from ethanol solution. The CFAZ produced with the best result was able to increase the ethanol percentage of the solution from 95% to 99% which was the same as commercial-grade molecular-sieve. CFAZ modified by potassium has also shown promise as a catalyst in biodiesel production [76]. Zeolites have also been functionalized for utilizing in oil spill remediation. Sakthivel et al. [62] utilized CFAZ for oil sorption to investigate their application in oil spill clean-up. CFAZ produced were functionalized with alkyltrimethoxysilanes with propyl, octyl, and octadecyl alkyl groups to have a high contact surface with water so they float on the surface water and sorp spilled oil. The contact angles achieved were up to 147° while the sorption capacity in was found to be 1.2 g of product per g of sorbent, making it a great environmentally friendly sorbent for oil spill clean-up. Ahmaruzzaman [7] in his review of CFA utilization also discusses the applications and utilization of zeolites produced from CFA. There are many venues for the utilization of zeolites produced from CFA. There is increasing work on their applications; these applications include but are not limited to water purification, gas and

sorption, catalysis, and environmental remediation. Given all the benefits achieved from zeolites produced from CFA and their comparable performance with pure zeolites and other alternatives, the conversion of the increasing CFA by-product is a huge motivation to utilize this waste to produce value added zeolites.

2.5   Conversion of CFA to zeolite

CFA and zeolite are mainly composed of Al and Si [4]. However, the major difference between the two is the crystalline structure. Zeolite has a well-defined crystalline structure, whereas, CFA is composed mostly of amorphous structure. Due to these similarities in the composition between CFA and zeolite, CFA has been viewed as a potential candidate for conversion to zeolite [98]. The main component of fly ash, aluminosilicates, is converted to zeolitic crystals by alkali hydrothermal reaction. The aluminosilicates dissolve into the reaction mixture and then cluster, nucleate and grow as crystals on the CFA surface. This is illustrated in the Figure 2-5.
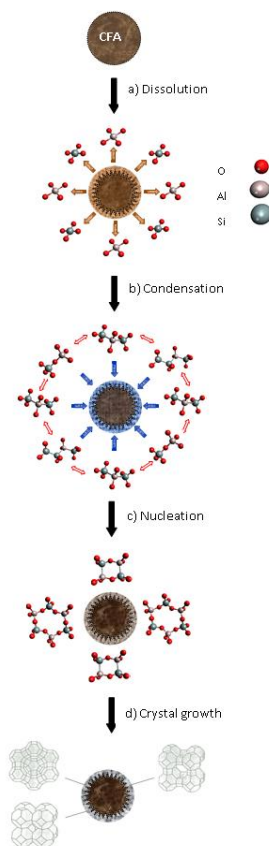
Figure 2-5. Schematic illustration of heterogeneous zeolitization process of CFA particle a) Dissolution of Al and Si content of CFA into the solution b) Condensation of Al and Si polymers (dimers, trimmers etc.) on the surface of CFA particle c) Nucleation of zeolites d) Crystal growth of zeolites

Amorphous aluminosilicates in CFA are dissolved into the reaction mixture. Dissolution of aluminosilicates not only determines the percent conversion but also the conversion rate [98]. The concentration of Si and Al may vary locally in a given sample, however particular zeolite maybe produced by adjusting the average ratio by addition of deficient constituents. The crystallization of zeolitic material from CFA is different from normal zeolite synthesis because the source of Si and Al are relatively less reactive and the presence of other cations in CFA may hinder or aid the crystallization process [98]. The presence of CaO in the CFA can reduce mullite giving higher conversion, trace elements such as TiO_2, MnO, MgO, Na_2O and K_2O along with anions such as carbonate, sulphate, appear to promote nucleation and crystallization [99]. Iron oxides may decrease the

desirability of the product by incorporating themselves into the zeolite matrix giving the product a brownish tinge [99]. Furthermore, these cations may favor one type of zeolite over another; therefore, it would be important to choose the specific zeolite that can be produced from a particular CFA. The lower reactivity of the Al and Si source present in the CFA may be due to the issue of dissolution of the aluminosilicates into the solution for reaction. Products from CFA conversion even after a conversion time of 1 to 3 days still contain significant amount of residual CFA [47,100]. This is further indicated by the lower cation ion exchange capacity of zeolite produced through CFA conversion and pure zeolite [100]. The presence of crystalline structure in the CFA can also be a hurdle in the conversion. Whereas aluminosilicate glass and crystalline quartz can be converted to zeolite, mullite stays resilient during the hydrothermal reaction [98]. There have been an increasing number of publications regarding CFA and zeolite, this trend is indicated in Figure 2-6 as well as the publications regarding CFA, zeolites and novel energies.
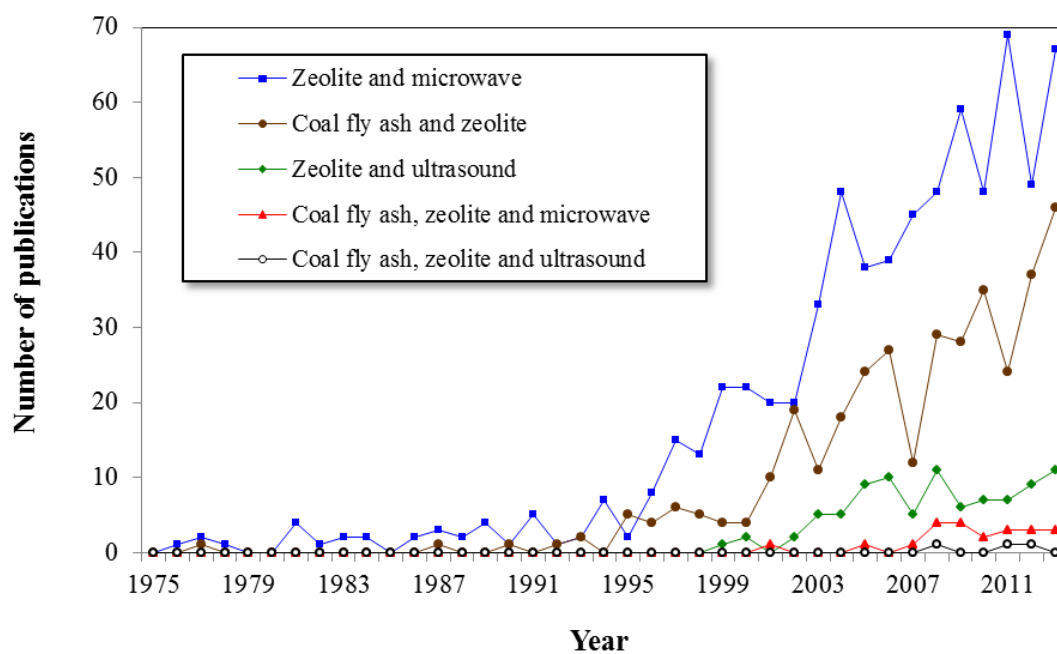
Figure 2-6. Keyword search regarding coal fly ash, zeolites, and novel energies on scopus.com

2.5.1 Hydrothermal Treatment (Direct Conversion)

2.5.1.1   Conventional Hydrothermal Conversion

Direct hydrothermal method for converting CFA into zeolite consists of dissolving CFA in alkaline solution such as NaOH or KOH to extract aluminate and silicate constituents followed by heat treatment to produce zeolite crystals from the reaction mixture. Aluminate or silicate compounds can be added to adjust the ratio of Si/Al to produce the desired type of zeolite. The resulting material may vary between zeolite X [62,81,100–102], A [47,94,100–102], P [59,69,102–106], analcime [81,86,107], chabazite [86,106,108], or hydrosodalite [53,81,86,106,109] depending on the reaction conditions such as temperature, pressure, reaction time, Si/Al ratio, alkaline solution, pH, seeding etc.

Wirsching [110] utilized volcanic glass to produce zeolite by hydrothermal treatment in an alkaline solution at varying temperatures of 180, 200 and 250 °C to produce chabazite, phillipsite and analcime establishing that zeolites can be produced utilizing raw materials with high concentration of alumina and silica. Hollar and Wirsching [21] treated CFA in a similar manner to produce zeolite ushering in an era of scientific inquiry in the conversion of CFA to zeolite that continues to this day. Hollman et al. [100] conducted direct hydrothermal synthesis of zeolite Na-P1 by mixing 500 g of fly ash in 1.25 dm^3 of 2 M NaOH followed by 96 h of heat treatment at 90°C. Samples of 10-15 samples were drawn from the reaction mixture at equal intervals for analysis. During the conversion Si concentration reached a maximum of 10,000 mg/dm^3 before stabilizing at 6800 mg/dm^3. The XRD results showed that the maximum of Si concentration corresponded with the start of crystallization. Al concentration reached a maximum at the start of the reaction and within one hour of the beginning of crystallization process and decreased to almost zero. It is suggested that it is due to an induction period, during which fly ash particles dissolve releasing their Al and Si contents. Zeolite nuclei form on the surface of the particles. Crystallization starts at the moment the size of these nuclei reach a certain minimum. Direct hydrothermal conversion was extended to a two-step process where the 500 g of fly ash (500 g) was mixed with in a volume of 1.25 dm^3, 2 M sodium hydroxide solution and incubated at 90 °C for 6 h. Incubation was followed by filtration, the solid

residue was dried and filtrate was adjusted to a molar ratio of Si/Al to 0.8-2. The adjusted filtrate was incubated at 90 °C for 48 h after which the resulting reaction mixture was filtered and the recovered residues dried. The new filtrate was added to the fly ash residue from the earlier incubation of 6 h. This fly ash mixture was incubated at 90 °C for 24 h, subsequently filtered and the residue dried. Whereas one step direct hydrothermal synthesis was conducted by producing same reaction mixture, however this reaction mixture was treated for 96 h at 90 °C. There have been many studies conducted in converting CFA into zeolite utilizing conventional heating methods. These studies are indicated in Table 2-2.

Table 2-2. Zeolite synthesized by conventional oven assisted hydrothermal method

| Reference | NaOH/CFA | Hydrothermal conditions | | | Zeolite | Remarks |
		NaOH (M)	T (ºC)	t (h)		
Zhao et al. [98]	0.86	2.5	50	48	Na-Y	with seeding
Querol et al. [103]	0.07-0.7	0.1-1.0	150-200	8-100	Na-P1	
Ma et al. [104]	0.28-0.5	2.8-5.0	25	48	Na-P1	Crystallization: 100 ºC, 144 h
Steenbruggen and Hollman [105]	-	2	90-150	12	Na-P1	
Hollman et al. [100]	0.20	2.0		54-96	Blend	Na-A, Na-X, Na-P1

Srinivason and Grutzeck [81]	0.3	3	90	24-72	Na-X	
				168	Blend	Na-P1, Na-Y
			150	24	ANA	
				72-168	Blend	ANA, SOD
Park et al. [59]	0.5	3.0	103	12	Na-P1	
Woolard et al. [55]	0.4-1.2	1-3	90	21	Na-P1	
	2-3.2	5-8	90	21	SOD	
Moreno et al. [102]	0.24	2.0	80-90	39	Blend	Na-A, Na-X, using wastewater
Querol et al. [108]	-	0.5-5	150-200	3-48	Na-P1	Herschelite, KM, Linde F, K-CHA
Moreno et al. [102]	-	3	125	8	Na-P1	
	-	2	150	24	Na-P1	
Murayama et al. [69]	0.08-0.64	0.5-4.0	120	3-24	Na-P1	
Murayama et al. [106]	0.08-0.64	0.5-4.0	120	3-24	Na-P1,SOD	K-CHA
Miyake et al. [127]	0.5-3.5	0.5-3.5	60	10-48	Na-A	Pretreatment with HCl at 800°C
			100-120		Na-P1	
Querol et al. [86]	1.6	5	150	8	Na-CHA	
	0.96	3	125	9	Na-P1	
	0.72	1	200	24	Na-ANA	
	2.16	3	150	24	SOD	

	0.99	1	200	48	KM	KOH
	1.18	3	150	24	Linde-F	KOH
Molina and Poole [101]	1.0-2.0	2.9-5.9	25	24	Blend	Crystallization: 40-90 ºC, 2-96 h, Na-A, Na-X, Na-P1
Inada et al. [109]	0.64, 1.12	2.0, 3.5	100	5, 24	Blend	Na-P1, SOD
Moriyama et al. [107]	0.09-0.16	2.5-3.5	25-150	5	Blend	GIS, Analcime
Hui and Chao [128]	0.8	2.0	100	2	Na-A	Crystallization: 90 ºC, 1.5 h
			25	0.5	Na-A	Crystallization: 95 ºC, 2.5 h
Derkowski et al. [91]	0.8	1	105	24	Na-P1	Adding 3M NaCl solution
	2.4	3	75	24	Na-X	
	8	5	105	24	SOD	Adding 3M NaCl solution
Juan et al. [129]	0.06	0.5	150	48	Na-P1	HS, CHA
Tanaka and Fujii [130]	0.23.	2.2	85	12	Na-A	Crystallization: 85 ºC, 24 h, Si/Al:2-4
					Na-X	Si/Al:4.5
Musyoka et al. [131]	1	-	47	48	SOD	Crystallization: 140 ºC, 48 h, using industrial waste brine solution
Chauhan and Talib [132]	0.8	2	100	2	Na-A	Crystallization: 90 ºC, 1.5 h
			25	0.5	Na-A	Crystallization: 95 ºC, 2.5 h
Nascimento et al. [133]	0.5-1.6	2-5	100-150	0.5-6	Na-A	

Shoumkova and Stoyanova [44]	0.84	3.1-6.2-	100	7	SOD	
					EDI	Using KOH (M:6.2-12.5)
Sakthivel et al. [62]	-	10	120	-	Na-X	
	-	3.1	80	-	Blend	Na-A, Na-P1
Algoufi and Hameed [134]	1.12	-	160	8	-	K-zeolite (calcined at 900 °C for 3 h), using KOH (M:5)
Wdowin et al. [54]	0.6	3.3	80	36	Na-P1	
Franus et al. [53]	0.33	3	75	24	Na-X	
	0.33	3	95	24	Na-P1	
	0..21	5	95	24	SOD	0.4 dm^3 of 3M NaCl added
Musyoka [135]	1	-	100	12-48	Na-P1	

2.5.1.2   Microwave Assisted Hydrothermal Conversion

Querol et al. [60] produced zeolite-A utilizing CFA with a Si/Al ratio of 1.85 with 62 % amorphous phase while the crystal phases included mullite (13 %), magnetite (13 %), quartz (7 %), anhydrite (0.7 %) and anorthite (0.3 %). Two different alkaline agents, NaOH and KOH, were used to convert the CFA in to zeolite crystals. The molarities were varied from 1.0 to 5.0 M and temperature range was 150 to 225 °C using both conventional and microwave energy. Microwave used was Milestone MLS-1200 MEGA at the highest available power of 1000 W. The crystallization time range was reduced from 8 to 98 h in conventional synthesis to 10 to 30 min for microwave assisted synthesis. By varying the mentioned parameters multiple different zeolites were produced namely, Na-P1, hydroxysodalite, hydroxycancrinite, analcime, Linde type F, tobermorite, kalsilite. CEC of the samples produced ranged from 2.0-3.1 meq/g using conventional heating method and microwave heating methods were compared and the values were in

close agreement. It was reported that the activation time of the production of zeolite from CFA using microwave was reduced from 24-48 h to 30 min.

Experiments conducted by Inada et al. [48] have shown that microwave induced heating played a positive role in the production of zeolite Na-P1 from CFA. CFA of Si/Al ratio of 1.10 was added in 2M of NaOH, this mixture was treated for 2 h at 100 °C for both microwave and conventional heating. The microwave oven used was a house hold microwave with 2.45 GHz and 500 W. CEC was measured for the synthesized products at different intervals during the 2 h reaction time. It is observed that the CEC for products treated with microwave increased much faster than conventional heating. CEC of the products after 1 h (60 min) of treatment was 0.25 meq/g and 0.60 meq/g for conventional and microwave heating, respectively. However, after 60 min of reaction the CEC for conventional treatment increases rapidly to 1.25 meq/g while the CEC for microwave lags off to 0.65 meq/g. In another run both conventional and microwave heating were combined. The microwave was applied for 15 min in the course of conventional heating in which the vessel was moved from oil bath to the microwave. It was observed that microwave application in the first 15 min of the two hour synthesis produced the best result with the highest CEC (~2.00 meq/g) and high XRD peak intensity, as 15 min microwave treatment was moved from 0-15 min, 15-30 min 30-45 min and so on. Microwave irradiation at 45-60 min during the two hour reaction time produced the worst results with lowest XRD peak intensity and CEC (1.00 meq/g), after this interval the CEC increased however, it still was much lower about 1.25 meq/g compared to CEC observed when microwave was irradiated for the first 15 min. It was suggested irradiation schedule should be controlled over the course of the reaction to achieve the best results. It was further hypothesized that microwave assists in the dissolution of alumina and silica in the reaction mixture thus assisting the reaction.

Fukui et al. [50] used fly ash with Si/Al ratio of 2.39 procured from a Japanese coal power plant and treated it with NaOH solution at 100 °C using microwave heating and conventional heating to produce phillipsite. The reaction mixture was produced by mixing 2.0 g of fly ash in 50 mL of NaOH solution with a molarity of 2.0 M. The temperature for both microwave and conventional heating was controlled utilizing a PID

controller, while 2.45 GHz microwaves were produced using a magnetron. In case of the microwave the temperature reached the set temperature of 100 °C with 3 min while conventional heating took 15 min. SEM images of both methods showed that the particle size for phillipsite were smaller in case for microwave treatment. The concentration of Si and Al in the reaction mixture was measured using ICP. It was observed that both Si and Al concentration rapidly increase. Al reaches the peak concentration of about 35 mmol/dm^3 within an hour and a half after which it sharply decreases until it reaches an equilibrium concentration of 5 mmol/dm^3. While Si concentration logarithmically increases reaching a plateau of 750 mmol/dm^3. The concentration observations were similar for both microwave and conventional heating. It was observed that while microwave increases the nucleation rate, however, it decreases the crystal growth rate. Therefore, another experiment was conducted in which microwave was irradiated for the first two hours followed by conventional heating producing both faster nucleation and crystal growth. Fukui et al. [49] produced phillipsite using fly ash with Si/Al ratio of 1.38 a lower Si constituent compared to fly ash used in the previous study [50], however this Si was substituted by rick husk that contained 86.5% Si. 40 g of fly ash was dissolved into 1.01 dm3 of 2 M NaOH solution at 100°C for 1 h in an electric oven before separating filtrate from insoluble solids. Rice husk into 50 cm^3 of the filtrate and then treated with microwave and conventional heating for 9 h. It was shown that with addition of rice husk increased the adsorption of ammonium in the product to a maximum of 80 mg/g of ammonium adsorption per gram of product. Samples produced with microwave heating required the addition of more rice husk compared to conventional heating 0.4 g and 0.55 g of rice husk added, respectively. SEM images showed that the crystals produced with microwave treatment were smaller. It was also observed the product powder synthesized with microwave had a relatively higher sodalite phase. Both conventional and microwave heating showed an increase of phillipsite in the product until reaching a peak at about at about once hour after which it decreased and stabilized while the composition of hydroxysodalite increased after 1 h indicating that phillipsite converts into hydroxysodalite as the reaction continues. It was hypothesized that the carbon present in the rice husk may have been heated by to a high temperature locally by microwave and these hot spots may have enhanced the generation of hydroxysodalite,

however this was refuted by the experiments conducted with using pure chemical silica source instead of rice husk, therefore it is concluded that microwave promotes the growth of hydroxysodalite crystals.

Tanaka et al. [70] introduced a two-step process utilizing house hold microwave with frequency of 2.45 GHz and power rating of 600 W to assist in zeolite Na-A production. The fly ash used for this process had a Si/Al ratio of 2.76 with amorphous constituents of 49.4%. 6.0 g of fly ash was added in 109 cm^3 of NaOH solution of 2.2 M. This mixture was pretreated by refluxing at the boiling point temperature of the solution under microwave irradiation for 60 min. This resultant solution was treated under microwave irradiation for an additional 60 min. After the second microwave treatment the solid product was separated for further analysis. During the pretreatment it was observed that amorphous phase in the raw material decreased while no other phase change was observed. This suggests that Si and Al constituents of the fly ash dissolved into the reaction solution. At the end of the pretreatment the concentration of Si and Al was detected at 80.6 and 4.7 $mmol/dm^3$, respectively. This concentration increases about two-folds if the fly ash is milled before pretreatment to 142.7 and 10.7 mmol/dm3. After the pretreatment the solution was filtered and NaAlO2 solution was added into the filtrate to control SiO_2/Al_2O_3 mass ratio to 0.5-4.0. This ratio played a critical role in the yield of the product, for the ratio of 0.5 and 1.0 the yield remained about 0.4 g of Na-A to 1.0 g of fly ash used. However, this yield decreased to about 0.2 and 0.1 for the Si/Al ratios of 2 and 4 respectively. It was further observed that the Na-A produced had the CEC of 4.70 meq/g compared to 5.50 meq/g of commercially available Na-A zeolite. Kim and Lee [57] also combined microwave heating and conventional heating to produce zeolite Na-4A with a CEC capacity of 5.5 meq/g. An industrial microwave (Korea High Frequency Inc., KMIC-2KW) with working frequency of 2.45 GHz and variable power range of 0-2 kW was used. The CFA used had Si/Al ratio of 2.07, 500 g of solids were dissolved in 1000 cm3 of 5 M NaOH solution and heated utilizing microwave and conventional oven for 1-8 h. 130 g of sodium aluminate, 132 g of NaOH and 790 mL of distilled water were added to the filtrated form this treatment to adjust the molar ratio of the reaction mixture to 1·Si:1·Al: 2.5·Na: 100·H2O. It was seen that the microwave was able to dissolve the Si and Al content in the CFA more efficiently than conventional microwave. It was

observed that microwave irradiation and conventional irradiation both dissolved the same amount of Si and Al content from CFA after two hours of treatment, however where the concentrations stayed constant for conventional heating, while they dramatically increased for microwave heating reaching a peak at 5 h of treatment after which the concentration started decreasing and this can be associated with the formation of zeolite-P and hydroxysodalite. Zeolite synthesis after the pretreatment step was conducted under both conventional heating (2 h), microwave heating (2 h) and conventional heating (1 h) followed by microwave heating (1 h). It was found that the CEC were 1.1, 2.5, and 5.5 meq/g and BET surface area 209, 250, and 980 m3/g, respectively. Zeolite-A produced through the combination of both conventional heating and microwave heating also performed much better in removing heavy metals such as Cd, Pb, Zn. The samples prepared from the combination of the two methods was 100 % efficient compared to microwave alone and conventional alone efficiencies ranging from 15-40 %.

Behin et al. [45] produced Na-A using CFA from Canadian power plant with Si/Al ratio of 2.13 and wastewater from Plasma Electrolytic Oxidation (PEO) process. 1.82 g of CFA and NaOH each was mixed with 17 cm^3 of PEO wastewater and then stirred at 60°C for 12 h followed by addition of 3 cm^3 of sodium aluminate solution (0.155 g/dm^3 in PEO wastewater) and mixture aged for 2 h at 20 °C. This solution was subjected to single mode 2.45 GHz MW (CEM Corp. Discover, USA) for varying time. It was found that high MW power and time of irradiation directly related to the higher crystallinity of the product. CFAZ produced had a CEC of 1.82 meq/g compared to 0.3 meq/g of the starting CFA, while the surface area of CFAZ also improved to 47.14 m^2/g from the surface area of CFA of 15.47 m^2/g. It was reported that a single mode MW that produces only single standing wave compared to more prevalent multimode MW could save energy in the zeolitization process of CFA.

2.5.1.3   Ultrasound Assisted Hydrothermal Conversion

Wang and Zhu [43] used CFA provided from a coal power plant in Western Australia with a Si/Al ratio of 1.9. The experiments were conducted in alkaline solution of varying NaOH concentration from 1 M to 5 M and a solid to liquid ratio of 0.5 g/cm^3. The slurry mixture was sonicated at room temperature at varying times between 30 min and 2 h in

an ultrasonic bath of 300 W. The XRD analysis of the sonicated and the unsonicated alkaline CFA slurry showed no phase change however, it was reported that both sonicated alkaline treated CFA had a much higher surface area compared to raw CFA (35.4 m^2/g compared to 5.6 m^2/g). The ultrasonic treated CFA also performed much better in the adsorption of methylene blue compared to raw CFA (1.5×10-5 mol/g compared to 8.0 ×10-6 mol/g) [43]. In preceding study conducted by Woolard et al. [111] CFA obtained from South African power plant with Si/Al ratio of 1.37 were treated for a longer period of time 21 h compared to 6 h in a higher alkaline solution of 7 M compared to 5M without the use of ultrasound energy and showed a phase change of CFA to hydroxysodalite, the surface area of raw CFA increased from 0.9 to 7.4 m^2/g after ultrasound treatment. Both results produced comparable adsorption capacities while considerably decreasing the treatment time by the introduction of ultrasonic energy.

2.5.2 Fusion followed by Hydrothermal Treatment (Indirect Conversion)

2.5.2.1 Fusion followed by Conversion Hydrothermal Treatment

Shigemoto et al. [51] introduced a fusion step prior to hydrothermal treatment to produce zeolites from CFA. The starting material was fused with NaOH in solid phase at high temperatures. This solid fused mixture is further mixed into an aqueous solution and aged. All of the mineral phases such as mullite and quartz present in the CFA were dissolved after fusion and ageing steps in the alkali solution, due to the destruction of the minerals' structures [112]. The dissolution of these insoluble mineral phases introduced more aluminosilicates into the solution thus ultimately increasing the conversion rate of the CFA; furthermore, the increase of BET surface area of the crystallized product through the fusion step was reported to be ten times more than the crystallization without fusion [62]. In addition, zeolite produced by fusion method also have been reported to have a higher cation exchange capacity and better crystallinity [101]. It has been further reported that fusion method favoured the production of zeolite X, or zeolite A (for an Al rich CFA), compared to non-fusion method yielding a mixture of Na-P1, Na-X and hydroxysodalite [51]. Many of the experiments reported converting CFA to zeolites

utilizing fusion followed by hydrothermal treatment with conventional oven are summarized in Table 2-3.

Table 2-3. Zeolite synthesized by fusion followed by hydrothermal synthesis utilizing conventional heating (Fusion at 550 -600 ºC for 1-2 h)

Reference	NaOH	Hydrothermal dissolution		crystallization		Zeolite	Remarks
	C (M)	T (ºC)	t (h)	T (ºC)	t (h)		
Shigemoto et al. [51]	3	25	12	100	6	Na-X	
Berkgaut and Singer [88]		25	12	100	6	Na-P1	
Chang and Shih [136]	3-72	-	-	-	-	SOD	
Park et al. [59]						SOD	0.7 g fly ash, 0.3 g NaOH, and 1 g salt (NaNO$_3$ or KNO$_3$)
Rayalu et al. [99]	N.A	N.A.	8	100	2.5-3	Na-A	
Molina and Poole [101]	2.9-5.9	25	24	40-90	6-24	Na-X	
Kumar et al.[137]		25	8	90	2	Na-A	
Somerset et al. [138]		100	24				
Yaping et al. [139]	1.5	B.P.		100	0.5		Fused using Na$_2$CO$_3$
Fotovat et al. [140]	2.7	25	8	100	12	Blend	Na-A, Na-X, Na-Y
Ruen-ngam et al. [141]	3	30	12	90	4	Na-X	
Belviso et al. [142]	N.A.	25	24	35-60	48	Na-X	ZK-5 , using sea water
Kazemian et al. [143]	0.8	70	0.5	120	4	Na-P1	
Klamrassamee et al. [97]	5.6	25	12	90	4	SOD	

Zhang et al. [144]	2.5						
Chareonpanich et al. [145]	-	120	4			Na-A	HCl pretreatment and using Na$_2$CO$_3$ instead of NaOH
Musyoka et al. [146]	6	25	2	80	9	Na-X	using mine water
Izidoro et al. [147]	3	25	16	100	24	Na-A	
	1.5	25	16	100	7	Na-X	
Sakthivel et al. [62]	-	25	18	90	60	Na-X	Pretreatment of CFA with HCl
Musyoka [135]	-	47-48	48	100	12-48	Na-P1	

2.5.2.2 Fusion followed by Microwave Assisted Hydrothermal Conversion

There is only one paper published to the best of our knowledge that utilize microwave heating in hydrothermal synthesis after fusion step. Bukhari et al. [46] have conducted experiments that utilize microwave in hydrothermal treatment following the fusion step. Fusion synthesis experiments for production of zeolite Na-A from CFA were carried out by fusing. 2.18 g of sodium hydroxide (granules) and 1.82 g of CFA at 550 °C for 2 h followed by the addition of 17 cm^3 deionized water. The slurry was then mixed using a mechanical stirrer for 2 h at 20 °C. Afterwards 3 cm^3 sodium aluminate solution with a molality of 0.155 g/dm^3 was added to the reaction mixture and this mixture was irradiated with single mode microwave irradiation (CEM Corp., Discover, USA) for varying time and power under reflux. The CFAZ produced was Na-A and had a CEC value of 2.42 meq/g. It was also found that CFAZ produced was able to immobilize heavy metal cations such as Ba, Cu, Cr, Mn, Ni, Pb, and V in the original CFA. The study found the power and the time of microwave irradiation increased the crystallinity of the CFAZ produced. The BET surface area of the product was dramatically higher at 42 m^2/g compared to CFA surface area of 15 m^2/g. The CFAZ produced also immobilized the heavy metal ions in the original CFA [46].

2.5.2.3 Fusion followed by Ultrasound Assisted Hydrothermal Conversion

Park et al. [113] have reported using kaolin, which is an aluminosilicate source, to produce Na-A of higher crystallinity utilizing UTS energy compared to conventional heating. Koalin used had a Si/Al ratio of 1.15 and the molar batch composition of the reaction mixture was $Al_2O_3:1.94 \cdot SiO_2:4 \cdot Na_2O:100 \cdot H_2O$. Ultrasonic treatment in an ultrasound bath at a frequency of 47 kHz and 130 W was found to produce a relative crystallinity of 68% compared to 0% for the same condition of 60°C and 4 h as in conventional treatment. One hundred percent crystallinity was achieved at 70°C and 4 h of treatment in ultrasonic treatment compared to 82% in conventional treatment, therefore leading to the conclusion that ultrasonic treatment fared much better results in terms of crystallinity compared to conventional heating.

Musyoka et al. [114] have converted CFA in zeolite A with UTS assistance. The CFA procured from South African power plant with a Si/Al ratio of 1.65 was fused with NaOH in a ratio of 1 to 1.2 at 550°C for 1.5 h. Hydrothermal treatment was conducted for varying times from 1-2 h at 100°C. The ultrasound energy during the ageing phase for 40 min prior to the hydrothermal synthesis reduced the synthesis time of single phase zeolite A from 2 h to 1 h by enhancing crystallization. Belviso et al. [37] also conducted similar work to convert CFA obtained from Italian power plants with different Si/Al ratios of 1.65, 1.86, and 1.95. The CFA was fused with NaOH with a ratio of 1 to 1.2 at 550°C for 1 h, followed by 1 h of sonication treatment in an ultrasonic bath of 240 W. This ultrasonic treated fused CFA slurry was incubated for 4 days at varying temperatures from 25-60°C. The US treated samples produced zeolite-X at 25°C and higher compared to untreated ones which did not show crystallization of zeolite until temperatures higher than 40°C. The work reported a phase change after UTS treatment, the phase observed after treatment was hydroxysodalite. However, hydroxysodalite was not observed after incubation for 4 days for all samples. The different CFA used from different power plants produced different crystallinity at the same reaction conditions indicating that the Si/Al ratio of CFA is an important factor in the zeolite production. Belviso et al. [38] utilized

sea water to conduct the preceding and reached the same conclusion that UTS treatment reduces the required temperature for crystallization.

There has been some work conducted utilizing UTS to observe zeolitization process instead of using UTS energy to convert CFA in to zeolite. The work conducted on using UTS to study the zeolitization process and modeling it is briefly discussed below:

Musyoka et al. [115] produced zeolite-A utilizing clear solution extracted from class F CFA with a molar composition of Al_2O_3:31 Na_2O:4 SiO_2:415 H_2O. The CFA was fused under identical condition as work done in [114]. The fused CFA was dissolved in demineralized water in weight ratio 1:5. This slurry was stirred for 2 h at room temperature and then filtered and centrifuged to produce a clear solution. In-situ UTS attenuation monitoring was conducted using ultrasonic transducer during the reaction progress to better understand the mechanism of CFA to zeolite conversion. This in-situ monitoring was complemented with ex-situ analysis such as XRD, FTIR, ICP, and SEM conducting on 4 cm3 of aliquots drawn at varying times (0, 30, 60, 90, 120, 150, 200, 210, 220, 240 and 360 min) during the progress of the reaction. The filtrate obtained from filtering fused CFA did not show immediate cloudiness of the precursor solution unlike precursor solution prepared by pure chemical. However, this precursor solution started becoming cloudy and viscous after 60 min like precursor solution obtained from pure chemicals. This event was also accompanied by the peak attenuation observed in UTS signifying a physical and chemical change in the reaction mixture. The concentration of Al and Si start from a maximum of 1800 mg/dm^3 and 1000 mg/dm^3 and decrease over the period of 360 min of reaction to 900 mg/dm3 and 150 mg/dm3, respectively. There was a decrease in the concentration of both elements in the solution in the first 30 min; however, the decrease in Si concentration of 20% was more dramatic than for Al which was about 11%. There was a slight fluctuation in the concentrations of Si and Al followed by a dramatic decrease after 220 min when both concentration decrease to a minimum. This eventual dramatic decrease in the concentration is accompanied with the observation of intense peaks observed in the XRD analysis of the samples collected after 220 min. This work divides the reaction process in to the a) dissolution of gel, b) formation of secondary amorphous gel which is pseudo-steady-state intermediate, c) nucleation and

formation of "islands of order," d) crystal growth, e) breakdown of gel structure complemented by further crystal growth. During step a) dramatic decrease in the concentrations of Al and Si ions are observed followed by b) and c) where fluctuation in the concentration was observed, however no significant change was observed. It is suggested that the interface between solid and solvent during the nucleation process stage move too fast to observe any significant changes in the concentration during the nucleation stage. A further dramatic decrease in the Al and Si concentration is observed after 220 min of reaction corresponding to the breakdown of gel structure which releases nuclei that have nucleated in the gel leading to more crystal growth and formation while the solution provides the required Al and Si ions thus decreasing their concentration in the reaction solution. The different reaction stages are also corroborated with ex-situ analysis such as XRD, FTIR, and SEM and with in-situ observation of UTS attenuation. There were two distinct inflection points that were observed during the crystallization process, one before the destruction of the gel structure and one after.

Musyoka et al. [116] used a clear solution obtained with the same procedure as before to produce zeolite-X, however the difference was the weight ratio of fused CFA to demineralized water in the dispersion step. In the previous work they had used a weight ratio of fused CFA to water as 1:5 while to produce zeolite-X they used a ratio of 1:2.5. A clear solution extracted from fused CFA with a molar regime of Al_2O_3:56.80 Na_2O:16.62 SiO_2:954.05 H2O. The work only observes in-situ UTS attenuation during the 1050 min of reaction at three different temperatures of 80, 90 and 94 °C. There were four regions outlined depending on the observation of UTS attenuation. The first region was where the UTS attenuation decreases until reaching a minimum and isothermal temperature was reached; this region was ascribed to induction period. Attenuation signal hump observed in the production of zeolite-A was not observed for zeolite-X therefore indicating secondary amorphous gel formation was not significant event as it is for the formation of zeolite-A. This is followed by nucleation where the UTS fluctuation was observed. This fluctuation was ascribed to the rapid interfacial changes taking place between nucleation sites in condensation of precursor species. The nucleation was followed by crystal growth where the UTS attenuation gradually increases and eventual constant attenuation reading. The period of 360 min required for complete crystallization was shorter than similar

experiments conducted to produce zeolite-A (1050 min). This difference was attributed to structural difference between the two zeolites. Zeolite-X has a more complex structure (D6R) and less dense structure compared to zeolite-A (D4R). Furthermore, it was also suggested that the nucleation process of the two zeolites is different, zeolite-A is dependent on the formation of secondary amorphous gel also referred to as pseudo-steady-state intermediate, while the nucleation for zeolite-X is only a solution phase-mediated mechanism according to reported in-situ UTS data. The investigation on the effect of temperature indicated significant change in the UTS attenuation thus the induction, nucleation and crystal growth regions. Increase in the temperature led to decrease in the induction, nucleation and crystal growth time. The induction and nucleation region indicated by UTS attenuation decreased to 40 % and 54 % as the temperature of the reaction mixture was increases by 10°C and 14°C, respectively. Crystal growth region also decreases by 40% and 75% for the same temperature change. Furthermore, XRD results indicated that there were zeolite-P and hydroxysodalite peaks in the product synthesized at 80 °C while for higher temperature of 90 and 94°C there was only pure zeolite-X observed. BET analysis indicated that the mesopore volume for the crystals for the produced at temperature of 80 °C was higher than the ones produced 90 and 94°C. Hums et al. [71] have used the data produced from [115] and [116] to calculate reaction rate, reaction order and activation energy for both Na-A and Na-X produced from clear solution extracted from CFA.

2.5.3 Effects of Zeolitization Parameters

The formation of a particular zeolite is determined by many factors such as the composition of the raw CFA, the concentration of cations and anions, alkalinity of the aqueous phase, and the heating method such as MW and UTS.

2.5.3.1   Role of Cations and Anions

The presence of different alkali metal cations in otherwise identical gels results in crystallization of different zeolites with particular frameworks. The interactions between the negatively charged aluminosilicates and cations in the solution phase are extremely important in determining the final zeolite structure. The ability of the cationic species to

favor one zeolite structure over another is called "structure-direction." Many organic molecules are also used as structure-directing agents [112].

Murayama et al. [69] investigated the role of cations Na^+ and K^+ on the production of zeolite from CFA. One hundred g of CFA with a Si/Al ratio of 2.48 was mixed in 400 cm3 different solutions of NaOH, Na_2CO_3 and KOH and their combinations followed by hydrothermal treatment in conventional heating oven at 100 °C. It was observed that Na^+ can play a significant part in the crystallization of zeolite Na-P1. Na^+ speeds up the reaction process for both either zeolite P or chabazite production. Lower amount of Na^+ slows the crystallization speed; however, with higher Na+ ions the reaction is faster. K^+ concentration produces chabazite crystals, with the addition of Na^+ ions with K^+ ions produces chabazite within three hours compared to 24 h for only K^+ present in the reaction solution. The lowering of crystallization time maybe associated with the role Na^+ plays in the dissolution of CFA as mentioned earlier. Knowing the ratios of Na^+ and K^+ cations exchange sites is important in order to understand the role of these cations in the reaction mechanism. When the ratio of Na^+ ions to K^+ ions is 1, the concentration of K^+ ions captured into the cation ion exchange sites of zeolite produced is about twice as much. However, we would like to point out that in the study mentioned, a mixture of zeolite P and chabazite is produced. Therefore, it cannot be predicted with certainty if either zeolite produced is balanced by a single cation or a combination of the two. It has been reported further that Cs^+ ions give rise to edingtonite just as Na^+ and K^+ produces zeolite P (or zeolite A [117]) and chabazite respectively. In the authors' opinion it would be an interesting experiment to conduct with reaction mixture containing both Na^+ and Cs^+. If a reaction mixture of Na^+ and Cs^+ produces edingtonite and the reaction time is shorter compared to a reaction mixture with only Cs^+ ions present in the solution mixture, then such a result would indicate that Na^+ may only play a role in the dissolution of CFA and not necessarily a structural directing ion. Studying the effects of a single ion in the reaction would be a difficult task because the introduction of cations into the solution is coupled with the inclusion of anions. In case of NaOH the anions are OH^- while Na_2CO_3 introduces CO_3^{-2}. Deconvolution of the effects of anions and cations in a reaction mixture is a difficult task. The cations introduced in to the reaction mixture also play a vital role in the crystallization process. Hydrothermal reaction in NaOH have produced CFAZ such

as Na-phillipsite, hydroxysodalite, hydroxycancrinite, tobermorite, analcime and herschelite while KOH produced CFAZ such as hydroxysodalite, zeolite Barrer-KF, K-chabazite and zeolite Linde Type F under the same conditions [118]. Different cations produce different types of zeolitic materials. These zeolitic materials are metastable and under different conditions different zeolitic materials can be crystallized. The cations can significantly alter the reaction path to one crystal type to another. The addition of Na$^+$ can promote the crystallization of zeolite P, while the addition of K$^+$ in the form of KOH produces chabazite [69]. It is intriguing to observe that the zeolite P and chabazite not only have different resident cations in their frameworks but completely different frameworks as well. Furthermore, it should be noted that in addition to the frameworks the SBU's and CBU's are also different. Zeolite P crystals are composed of 4, 6, 8 atom rings giving rise to d6R and CHA CBU's. On the other hand, chabazite crystals are composed of 4 and 8 ring SBU's and GIS CBU's. Given the difference between the two structures on such a fundamental level suggests that the cations in the reaction play a very significant role in determining the type of zeolite produced.

During the conversion of CFA into zeolite it has been reported that the concentration of Al ions and Si ions vary as the reaction progresses. While the Al quickly dissolves into the solution and its concentration rapidly increases in the beginning of the heating stage then slowly decreases in the solution (while the concentration of Si ions concentration linearly increases until it reaches lag phase) until both Si and Al components reach an equilibrium concentration. The lag phase concentration corresponds to the decline of Al concentration to a minimum [69,100,119]. There is a possibility that the Al concentration plays a role in the dissolution of Si ions into the solution.

Wu et al. [120] conducted an experiment adding NaF and NaCl into the reaction mixture during the conversion of CFA into zeolite. 15 g of CFA with a ratio of SiO2/Al2O3 of 3.25 in 150 mL of aqueous solution with varying NaOH molarity of 0.5,1 and 2M followed by hydrothermal synthesis at 95°C for 24 h under atmospheric pressure and another set conducted at 120°C for 24 h in autogenous pressure. Addition of NaF and NaCl increased the CEC by 43.0% and 16.4%, respectively. Furthermore, it was observed that autogenous pressure produced CFAZ with a higher CEC compared to the one

produced at atmospheric pressure i.e. 0.55 mol/g and 1.63 mol/g, respectively. This study indicates the addition of anions such as F$^-$ and Cl$^-$ produce CFAZ with higher crystallinity and CEC [120]. Addition of Cl$^-$ in form of NaCl into the reaction solution during the conversion of CFA to zeolite produces zeolites with better crystallinity and higher CEC [120,121].

2.5.3.2   Role of Alkalinity

Amorphous aluminosilicates in CFA are dissolved into the reaction mixture. Dissolution of aluminosilicates not only determines the conversion percent but also the conversion rate [98]. Si component in CFA is dissolved with a linear relation as a function of time. Alkalinity of the solution plays a significant role by contributing to the dissolution of Si^{+4} and Al^{+3} in CFA [69]. The major crystal present in CFA is quartz that dissolves in higher pH, while mullite crystal structure stays resilient in increasing pH. Lower mullite phase in CFA encourages the production of zeolite; lower mullite phase can be attributed to higher concentration of CaO in the CFA. Therefore, CFA containing higher concentration of CaO might be a better candidate for the production of zeolite [99]. Dissolution of quartz in the higher pH in the reaction solution pushes the reaction towards the products. However, further increase of pH leads to production of hydroxysodalite via co-crystallization between zeolite and hydroxysodalite [69]. Changes in the crystal structure from zeolite to hydroxysodalite do not occur through hydrothermal reaction, instead they deposit at the beginning of crystallization reaction as first crystals [69]. Implication of this statement is that the first crystals of both zeolite and hydroxysodalite are born in the solution; however different pH values aid the growth of respective zeolitic or hydroxysodalite crystals. The pH of a solution is increased by the addition of OH$^-$ ions; however, the addition of this anion mostly is coupled with the addition with a cation such as Na$^+$ or K$^+$. It has been suggested that the behavior of Na$^+$ and OH$^-$ is independent of each other during the hydrothermal reaction [69].

2.5.3.3   Role of Seeding

Seeding is an important technique in zeolite synthesis in order to obtain pure crystalline phase [98]. Zeolites are metastable crystals; therefore, a single crystal form of zeolite is

not formed in a reaction, but actually multiple forms of zeolite maybe formed in a reaction. It is the optimization of the reaction conditions that can lead to favorable condition for the production of a desired zeolite. Seeding is a method that has proven to push the reaction towards a particular zeolite. In addition to using natural and commercial zeolites as seeds [99], aluminosilicate-gel slurry has also shown to be used as seeds to produce zeolite Y without the presence of other significant zeolite-like impurities [98]. Furthermore, seeds play an important role in selectively producing one zeolite over another [98,119]. Slangen et al. [119] synthesized zeolite-A with molar ratio of $SiO_2:Al_2O_3:1.5 \cdot Na_2O:96.5 \cdot H_2O$ utilizing kitchen microwave where the mixture was aged for varying time (5, 60, 120, 180, 240, 1200 min) which produced zeolite-A with different crystallinity (0, 0, 0, 80, 90, 100%) after conventional and microwave heat treatment. The conventional heating was conducted for 2 h whereas, microwave heating for 1 min was sufficient to produce zeolite-A. It was further noted that when aged sample was mixed with unaged sample the unaged sample produced zeolite-A with better crystallinity, therefore indicated that ageing the samples before heat treatment is essential to the production of zeolite-A crystals [119]. This result could be due to seeds formed in the aged solution.

2.5.3.4   Role of Microwave Energy

Arafat et al. [18] produced zeolite-Y and ZSM-5 using pure chemicals and stablished oxide molar ratios of precursor solution. Molar ratio used for the synthesis of zeolite-Y was $8\text{-}10 \cdot SiO_2:Al_2O_3:3\text{-}4 \cdot Na_2O:100\text{-}135 \cdot H_2O$ whereas the molar ratio used to synthesize ZSM-5 was $12.2 \cdot SiO_2:Al_2O_3:20 \cdot Na_2O:20 \cdot (TPA)_2O$, where TPA is tetraproplyammonium produced from Tetraproplyammonium bromide. It was reported that reaction time of zeolite Y production from pure chemicals was reduced from 10-50 hours to 10 minutes using microwaves instead of conventional heating, whereas, ZSM-5 conversion occurred in 30 minutes compared to several days. Fast dissolution of gel in the MW is associated with relatively fast crystallization of zeolite from precursor gel. Microwave heating produce purer zeolite crystals due to nucleation occurring at 120 ℃ while crystallization occurred at 100 ℃, therefore nucleation and crystal growth of other types of zeolite did not happen. The rapid synthesis of zeolite may indicate the absence of induction period;

however, this cannot be concluded from the given data [18]. Bukhari et al. [29] used single mode microwave to produce Na-A with the molar ratio of the precursor solution of 3.165 Na_2O:1 Al_2O_3:1.926 SiO_2:128 H_2O.It was reported that the amount MW energy irradiated to the reaction mixture is strongly correlated to the crystallinity of the product. Furthermore, MW irradiation was also directly proportional to the phase selection of Na-A over Na-X. Many studies have combined both microwave energy and conventional heating. It is observed that microwave energy produces a faster nucleation rate however the crystal growth rate is decreased under microwave irradiation therefore the best results have been seen when both microwave and conventional heating are combined. In addition to the increase in nucleation rate it is further noted that microwave irradiation increases the dissolution of the Al and Si content of amorphous CFA [48,49,57,70]. However, this Si and Al concentrations in the liquid reach equilibrium as the reaction progresses. From observation of SEM images of the zeolites produced it can be hypothesized that Si and Al ratio reach an equilibrium because the zeolite crystals are deposited over the amorphous surface of the CFA and further grow on the surface. The zeolite crystals form a thick layer over the amorphous CFA, the remaining aluminosilicates are trapped inside this zeolite layer unavailable for further reaction. Furthermore, it can be concluded that smaller amorphous CFA particles would yield higher zeolite as the smaller particles higher available for aluminosilicates to dissolve out into the solution.

2.5.3.5   Role of Ultrasound Energy

Ultrasound energy accelerates Al/Si dissolution and strengthens the bonds at the solid particle/gel phase interface [37]. This increases the condensation process thus speeding up the zeolite crystallization process. Ageing of source of Al or Si, either from pure chemical precursors or CFA using UTS energy has been shown to reduce the crystallization time [36,122]. Solution aged with UTS has the shortest crystallization time in the second step, followed by mechanically stirred solution and static solution. From this result it can be assumed that the mixing ability of UTS bath reduces the time for crystallization. The mixing abilities of UTS bath is assumed to provide soluble silica required to produce the zeolite. Reduction in induction time can also be associated with

UTS ageing. Induction time is the time that elapses between the achievement of super saturation and the appearance of crystals and can be influenced by initial conditions, super saturation, state of agitation, presence of impurities, and seeding [123]. It is known that the amount of agitation produced due the cavitation caused by UTS is higher than the agitation produced through mechanical stirring. Reduction of induction time due to agitation caused by UTS can be a reason for the observation by [122]. Furthermore, the cavitation bubbles caused by the UTS can provide nucleation sites for the species resulting in secondary crystallization, high speed collisions caused by UTS field in the mixture could be another source of secondary nucleation reducing induction time thus decreasing the crystallization time.

UTS irradiation throughout ageing and conventional hydrothermal synthesis crystallization was studied and it was found that longer ageing time corresponded to shortening of the nucleation period and the eradication of secondary amorphous phase [115,124]. Experiments conducted in UTS bath have also been reported to decrease the time of crystallization between conventional water bath and UTS bath [19]. The time for UTS crystallization that is reported is longer than expected suggesting that UTS would dramatically decrease the reaction time [22,23]. This difference could be because UTS is not introduced into the solution in the same manner. The UTS introduced by [116] and [19] is indirect, the UTS energies are outside the reaction solution, and ultrasound field has to travel through water or the reaction vessel to interact with the reactant solution. However, if UTS energy is introduced directly into the crystallizing solution through an UTS probe, zeolite crystals could be produced much faster. We suggest for the crystallization of zeolite a direct probe should be immersed into the reaction mixture for shorter reaction time.

2.6 Summary and Conclusion

CFA is not only a waste but also an environmental hazard, disposal of which is a financial liability. As the demand for electricity increases around the globe and given the advantages of production of electricity, the production of CFA is only expected to increase. This increasing financial liability can be converted into a financial advantage through its use as a reactant for value added goods, namely zeolites. Zeolites have many

uses including sorption, catalysis, ion-exchange, and many uses as substitute for creating environmentally friendly products. Conversion of CFA into zeolite serves two purposes simultaneously, is produces green technologies such as products that are better for the environment and also make coal power a cleaner source of energy. Reducing the environmental hazards from coal power production would enable countries and regions rich in coal deposits to utilize their natural resources to produce cheaper and greener energy.

There has been much work done investigating the utilization of zeolite produced from coal fly for different applications. CFA is only composed of about 40-60% aluminosilicate components resulting in the production of zeolites that have significant residual impurities thus limiting their applications. However, CFAZ have been shown to be an effective gas adsorbent for SO_2 and after Ag impregnation for CO_2. CFAZ have also been functionalized to be utilized for oil spill remediation. Production of CFAZ with high CEC is also of great interest due to the ability of CFAZ to remove heavy metallic ions from wastewater. Utilization of microwave energy in conjunction of conventional heating has shown great promise in the production of CFAZ with high CEC values. Further investigation of these novel energies in the production of CFAZ are needed to produce better products that could have a wide range of applications.

The mechanism of the conversion of CFA into zeolite through a hydrothermal reaction is complicated and not well understood, however there have been many experiments conducted to study the effects of different reaction conditions on the crystallization of zeolite from CFA. Some of the most important reaction conditions studied include ageing of the mixture, temperature of ageing, alkalinity of the reaction mixture, effects of different cations in the reaction mixture, temperature of reaction and the time of reaction. It has been shown that many different zeolitic materials can be produced by changing reaction parameters. The discussion of the experiments conducted with different reaction condition would help understand the importance of the parameters in the zeolitization of CFA. Despite all the published work on the investigation of these parameters, the mechanism of zeolitization is still not well understood. UTS energy has been utilized in some research to better understand the mechanism of zeolitization. It has been found that

the mechanism of zeolitization can be different for different types of zeolites. Therefore, the mechanism of each type of zeolite and its framework need to be investigated. Authors suggest that these parameters be further explored and mechanism of different zeolite further researched.

Considering the research conducted previously to successfully enhance a reaction using microwave and ultrasonic energies and the current work being conducted on utilizing these novel techniques for zeolite production, we purpose to conduct further experiments and research to perfect this technique. Novel energy sources such as MW and UTS have been utilized to speed up chemical reactions and produce more desirable products efficiently. There have been reports of using these novel energies to produce zeolites from both pure chemicals and CFA. MW energy in conjunction with conventional heating produced zeolites with better CEC and BET surface area. MW was shown to significantly reduce the reaction time and produced smaller sized crystals. Microwave irradiation has also reported to increase the dissolution of the Al and Si content of amorphous CFA thus resulting in a better conversion. UTS also reduced reaction time and produced better performing CFAZ when compared to conventional heating methods. Both sonochemical and sonophysical effects of UTS can produce a desirable CFAZ. It has been reported that UTS treatment even in the absence of phase change can increase the performance of the CFA in the adsorption of organic dyes. It is suggested that more studies can be conduct to perfect a technique of using these novel methods to produce zeolitic materials from CFA. We also purpose a combination of the two methods for zeolitization of CFA. Furthermore, all the experiments discussed are conducted on a lab scale. In order to produce zeolites from abundant CFA around the world utilizing novel energies, more research has to be conducted on pilot scale and industrial scale. There are many challenges associated with larger scale MW [125] and UTS [126] which need to be surmounted for a future where zeolitization of CFA utilizing novel energies is conducted on a larger scale.

If such novel methods are perfected and made feasible for larger industrial use they can be very beneficial to the environment and have a very significant impact towards achieving a greener technology for the future.

2.7 References

[1]   Burnard K, Bhattacharya, Sanker. Power Generation From Coal 2011.

[2]   Mehmood S, Reddy BV, Rosen MA. Energy analysis of a biomass co-firing based pulverized coal power generation system. Sustainability 2012;4:462–90.

[3]   International Energy Statistics n.d. http://www.eia.gov/cfapps/ipdbproject/IEDIndex3.cfm?tid=1&pid=1&aid=2 (accessed August 27, 2014).

[4]   Querol X, Moreno N, Umana J t, Alastuey A, Hernández E, López-Soler A, et al. Synthesis of zeolites from coal fly ash: an overview. Int J Coal Geol 2002;50:413–23.

[5]   Siddique R. Performance characteristics of high-volume Class F fly ash concrete. Cem Concr Res 2004;34:487–93.

[6]   Borm PJA. Toxicity and occupational health hazards of coal fly ash (CFA) A review of data and comparison to coal mine dust. Ann Occup Hyg 1997;41:659–76.

[7]   Ahmaruzzaman M. A review on the utilization of fly ash. Prog Energy Combust Sci 2010;36:327–63.

[8]   Juda-Rezler K, Kowalczyk D. Size distribution and trace elements contents of coal fly ash from pulverized boilers. Pol J Env Stud 2013;22:25–40.

[9]   Heidrich C, Feuerborn, H, Weir, A. Coal Combustion Products: a Global Perspective. World Coal Ash WOCA, Lexington, KY: 2013.

[10]   Government of Canada NEB. Energy Reports - Coal-Fired Power Generation - An Overview - Energy Brief 2008.

[11]   Garrabrants AC, Kosson DS, DeLapp R, van der Sloot HA. Effect of coal combustion fly ash use in concrete on the mass transport release of constituents of potential concern. Chemosphere 2014;103:131–9.

[12]   Liu R, Durham SA, Rens KL. Effects of post-mercury-control fly ash on fresh and hardened concrete properties. Constr Build Mater 2011;25:3283–90.

[13]   Poon CS, Lam L, Wong YL. A study on high strength concrete prepared with large volumes of low calcium fly ash. Cem Concr Res 2000;30:447–55.

[14]   Duran-Herrera A, Juarez CA, Valdez P, Bentz DP. Evaluation of sustainable high-volume fly ash concretes. Cem Concr Compos 2011;33:39–45.

[15]   Robson HE, Lillerud KP. Verified syntheses of zeolitic materials. 2nd ed. Amsterdam, The Netherlands: Elsevier; 2001.

[16]   Ginter, D. M., Bell, A. T., Radke, C. J. The Chemistry of NaY Crystallization from Sodium Silicate Solutions. Synth. Microporous Mater. Mol. Sieves, vol. 1, Van Nostrand Reinhold; 1992, p. 6–30.

[17]   Goto, Y., Saegusa, H., Koizumi, M. Synthesis of Zeolite Y in Geelatin Solution. Synth. Microporous Mater. Mol. Sieves, vol. 1, Van Nostrand Reinhold; 1992, p. 31–41.

[18]   Arafat A, Jansen JC, Ebaid AR, Van Bekkum H. Microwave preparation of zeolite Y and ZSM-5. Zeolites 1993;13:162–5.

[19]   Andaç Ö, Tatlıer M, Sirkecioğlu A, Ece I, Erdem-Şenatalar A. Effects of ultrasound on zeolite A synthesis. Microporous Mesoporous Mater 2005;79:225–33.

[20]   Stojkovic SR, Adnadjevic B. Investigation of the NaA zeolite crystallization mechanism by i.r. spectroscopy. Zeolites 1988;8:523–5.

[21]   Holler H, Wirsching U. Zeolite formation from fly ash. Fortschr Mineral 1985;63:21–43.

[22]   Gordon J, Kazemian H, Rohani S. Rapid and efficient crystallization of MIL-53 (Fe) by ultrasound and microwave irradiation. Microporous Mesoporous Mater 2012;162:36–43.

[23]   Sabouni R, Kazemian H, Rohani S. A novel combined manufacturing technique for rapid production of IRMOF-1 using ultrasound and microwave energies. Chem Eng J 2010;165:966–73.

[24]   Li Y, Yang W. Microwave synthesis of zeolite membranes: A review. J Membr Sci 2008;316:3–17.

[25]   Perreux L, Loupy A. A tentative rationalization of microwave effects in organic synthesis according to the reaction medium, and mechanistic considerations. Tetrahedron 2001;57:9199–223.

[26]   Binner JGP, Hassine NA, Cross TE. The possible role of the pre-exponential factor in explaining the increased reaction rates observed during the microwave synthesis of titanium carbide. J Mater Sci 1995;30:5389–93.

[27]   Glasnov TN, Kappe CO. Microwave-Assisted Synthesis under Continuous-Flow Conditions. Macromol Rapid Commun 2007;28:395–410.

[28]   Leadbeater NE, Torenius HM. A study of the ionic liquid mediated microwave heating of organic solvents. J Org Chem 2002;67:3145–8.

[29]   Bukhari SS, Behin J, Kazemian H, Rohani S. Synthesis of zeolite Na-A using single mode microwave irradiation at atmospheric pressure: The effect of microwave power. Can J Chem Eng 2014. Accepted for publication.

[30]   Ashokkumar M, Grieser F. Ultrasound assisted chemical processes. Rev Chem Eng 1999;15:41–83.

[31]   Baig RN, Varma RS. Alternative energy input: mechanochemical, microwave and ultrasound-assisted organic synthesis. Chem Soc Rev 2012;41:1559–84.

[32]   Suslick KS, Hyeon T, Fang M. Nanostructured materials generated by high-intensity ultrasound: sonochemical synthesis and catalytic studies. Chem Mater 1996;8:2172–9.

[33]   Suslick KS. Sonochemistry. Science 1990;247:1439–45.

[34]   Flint EB, Suslick KS. The temperature of cavitation. Science 1991;253:1397–9.

[35]   Abrishamkar M, Azizi SN, Kazemian H. Ultrasonic-Assistance and Aging Time Effects on the Zeolitation Process of BZSM-5 Zeolite. Z Für Anorg Allg Chem 2010;636:2686–90.

[36]   Azizi SN, Yousefpour M. Static and Ultrasonic-assisted Aging Effects on the Synthesis of Analcime Zeolite. Z Für Anorg Allg Chem 2010;636:886–90.

[37]   Belviso C, Cavalcante F, Lettino A, Fiore S. Effects of ultrasonic treatment on zeolite synthesized from coal fly ash. Ultrason Sonochem 2011;18:661−8.

[38]   Belviso C, Cavalcante F, Fiore S. Ultrasonic waves induce rapid zeolite synthesis in a seawater solution. Ultrason Sonochem 2013;20:32–6.

[39]   Zacco A. Review of fly ash inertisation treatments and recycling. Environ Chem Lett 2014;12:153–75.

[40]   Jankowski J, Ward CR, French D, Groves S. Mobility of trace elements from selected Australian fly ashes and its potential impact on aquatic ecosystems. Fuel 2006;85:243–56.

[41]   Hower JC. Petrographic examination of coal-combustion fly ash. Int J Coal Geol 2012;92:90–7.

[42]   Franus W. Characterization of X-type zeolite prepared from coal fly ash. Pol J Env Stud 2012;21:337–43.

[43]   Wang S, Zhu ZH. Sonochemical treatment of fly ash for dye removal from wastewater. J Hazard Mater 2005;126:91−5.

[44]   Shoumkova A, Stoyanova V. Zeolites formation by hydrothermal alkali activation of coal fly ash from thermal power station "Maritsa 3", Bulgaria. Fuel 2013;103:533–41.

[45]   Behin J, Bukhari SS, Dehnavi V, Kazemian H, Rohani S. Using Coal Fly Ash and Wastewater for Microwave Synthesis of LTA Zeolite. Chem Eng Technol 2014;37:1532–40.

[46]   Bukhari SS, Behin J, Kazemian H, Rohani S. A comparative study using direct hydrothermal and indirect fusion methods to produce zeolites from coal fly ash utilizing single-mode microwave energy. J Mater Sci 2014;49:8261–71.

[47]   Chauhan YP, Talib M. A Novel and green approach of synthesis and characterization of nano-absorbant (zeolites) from coal fly ash: A review. Sci Rev Chem Commun 2012;2:12–9.

[48]   Inada M, Tsujimoto H, Eguchi Y, Enomoto N, Hojo J. Microwave-assisted zeolite synthesis from coal fly ash in hydrothermal process. Fuel 2005;84:1482–6.

[49]   Fukui K, Kanayama K, Yamamoto T, Yoshida H. Effects of microwave irradiation on the crystalline phase of zeolite synthesized from fly ash by hydrothermal treatment. Adv Powder Technol 2007;18:381–93.

[50]   Fukui K, Arai K, Kanayama K, Yoshida H. Phillipsite synthesis from fly ash prepared by hydrothermal treatment with microwave heating. Adv Powder Technol 2006;17:369–82.

[51]   Shigemoto N, Hayashi H, Miyaura K. Selective formation of Na-X zeolite from coal fly ash by fusion with sodium hydroxide prior to hydrothermal reaction. J Mater Sci 1993;28:4781–6.

[52]   Jha VK, Nagae M, Matsuda M, Miyake M. Zeolite formation from coal fly ash and heavy metal ion removal characteristics of thus-obtained Zeolite X in multi-metal systems. J Environ Manage 2009;90:2507–14.

[53]   Franus W, Wdowin M, Franus M. Synthesis and characterization of zeolites prepared from industrial fly ash. Environ Monit Assess 2014:1–9.

[54]   Wdowin M, Franus M, Panek R, Badura L, Franus W. The conversion technology of fly ash into zeolites. Clean Technol Environ Policy 2014;16:1217–23.

[55]   Woolard CD, Petrus K, Van der Horst M. The use of a modified fly ash as an adsorbent for lead. WATER SA-PRETORIA- 2000;26:531–6.

[56]   Musyoka NM, Petrik L, Hums E. Synthesis of Zeolite A, X and P from a South African Coal Fly Ash. Adv Mater Res 2012;512:1757–62.

[57]   Kim JK, Lee HD. Effects of step change of heating source on synthesis of zeolite 4A from coal fly ash. J Ind Eng Chem 2009;15:736–42.

[58]   Park M, Choi CL, Lim WT, Kim MC, Choi J, Heo NH. Molten-salt method for the synthesis of zeolitic materials: I. Zeolite formation in alkaline molten-salt system. Microporous Mesoporous Mater 2000;37:81–9.

[59]   Park M, Choi CL, Lim WT, Kim MC, Choi J, Heo NH. Molten-salt method for the synthesis of zeolitic materials: II. Characterization of zeolitic materials. Microporous Mesoporous Mater 2000;37:91–8.

[60]   Querol X, Alastuey A, López-Soler A, Plana F, Andrés JM, Juan R, et al. A fast method for recycling fly ash: microwave-assisted zeolite synthesis. Environ Sci Technol 1997;31:2527–33.

[61]   Moreno N, Querol X, Ayora C, Pereira CF, Janssen-Jurkovicová M. Utilization of Zeolites Synthesized from Coal Fly Ash for the Purification of Acid Mine Waters. Environ Sci Technol 2001;35:3526–34.

[62]   Sakthivel T, Reid D, Goldstein I, Hench L, Seal S. Hydrophobic High Surface Area Zeolites Derived from Fly Ash for Oil Spill Remediation. Environ Sci Technol 2013.

[63]   Ali Zaidi SS, Rohani S. Progress towards a dry process for the synthesis of zeolite - A review. Rev Chem Eng 2005;21.

[64]   Breck DW. Zeolite Molecular Sieves: Structure, Chemistry and Use. Anal Chim Acta 1975;75:493.

[65]   Wang S, Peng Y. Natural zeolites as effective adsorbents in water and wastewater treatment. Chem Eng J 2010;156:11–24.

[66]   Baerlocher, Ch., McCusker, L.B., Olson, D.H. Atlas of Zeolite Framework types. 6th ed. New York, NY, USA: Elsevier Science; 2007.

[67]   Zeolite Framework Type http://izasc.ethz.ch/fmi/xsl/IZA-SC/ft.xsl (accessed August 25, 2014).

[68]   Auerbach SM, Carrado KA, Dutta PK. Handbook of zeolite science and technology. CRC Press; 2003.

[69]   Murayama N, Yamamoto H, Shibata J. Mechanism of zeolite synthesis from coal fly ash by alkali hydrothermal reaction. Int J Miner Process 2002;64:1–17.

[70]   Tanaka H, Fujii A, Fujimoto S, Tanaka Y. Microwave-Assisted Two-Step Process for the Synthesis of a Single-Phase Na-A Zeolite from Coal Fly Ash. Adv Powder Technol 2008;19:83–94.

[71]   Hums E, Musyoka NM, Baser H, Inayat A, Schwieger W. In-situ ultrasound study of the kinetics of formation of zeolites Na–A and Na–X from coal fly ash. Res Chem Intermed n.d.:1–16.

[72]   Moreno N, Querol X, Ayora C, Alastuey A, Fernández-Pereira C, Janssen-Jurkovicová M. Potential Environmental Applications of Pure Zeolitic Material Synthesized from Fly Ash. J Environ Eng 2001;127:994–1002.

[73]   Malekpour A, Millani MR, Kheirkhah M. Synthesis and characterization of a NaA zeolite membrane and its applications for desalination of radioactive solutions. Desalination 2008;225:199–208. doi:10.1016/j.desal.2007.02.096.

[74]   Sinha PK, Panicker PK, Amalraj RV, Krishnasamy V. Treatment of radioactive liquid waste containing caesium by indigenously available synthetic zeolites: A comparative study. Waste Manag 1995;15:149–57.

[75]   Landau MV, Vradman L, Valtchev V, Lezervant J, Liubich E, Talianker M. Hydrocracking of heavy vacuum gas oil with a Pt/H-beta-Al2O3 catalyst: Effect of zeolite crystal size in the nanoscale range. Ind Eng Chem Res 2003;42:2773–82.

[76]   Babajide O, Musyoka N, Petrik L, Ameer F. Novel zeolite Na-X synthesized from fly ash as a heterogeneous catalyst in biodiesel production. Catal Today 2012;190:54–60.

[77]   Savage N, Diallo MS. Nanomaterials and water purification: opportunities and challenges. J Nanoparticle Res 2005;7:331–42.

[78]   Theron J, Walker JA, Cloete TE. Nanotechnology and Water Treatment: Applications and Emerging. Nanotechnol Water Treat Appl 2010:43–69.

[79]   Shoumkova A. Zeolites for water and wastewater treatment: An overview. Res Bull Aust Inst High Energ Mater Spec Issue Glob Fresh Water Short 2011;2:10–70.

[80]   Fan Y, Zhang F-S, Zhu J, Liu Z. Effective utilization of waste ash from MSW and coal co-combustion power plant—Zeolite synthesis. J Hazard Mater 2008;153:382–8.

[81]   Srinivasan A, Grutzeck MW. The Adsorption of SO2 by Zeolites Synthesized from Fly Ash. Environ Sci Technol 1999;33:1464–9.

[82]   Cheung O, Hedin N. Zeolites and related sorbents with narrow pores for CO2 separation from flue gas. RSC Adv 2014;4:14480–94. doi:10.1039/C3RA48052F.

[83]   Wdowin M, Wiatros-Motyka MM, Panek R, Stevens LA, Franus W, Snape CE. Experimental study of mercury removal from exhaust gases. Fuel 2014;128:451–7.

[84]   Khan AZ, Nigar S, Khalil SK, Wahab S, Rab A, Khattak MK, et al. Influence of synthetic zeolite application on seed development profile of soybean grown on allophanic soil. Pak J Bot 2013;45:1063–8.

[85]   Majchrzak-Kucęba I, Nowak W. A thermogravimetric study of the adsorption of CO2 on zeolites synthesized from fly ash. Thermochim Acta 2005;437:67–74.

[86]   Querol X, Moreno N, Umaña J, Juan R, Hernández S, Fernandez-Pereira C, et al. Application of zeolitic material synthesised from fly ash to the decontamination of waste water and flue gas. J Chem Technol Biotechnol 2002;77:292–8.

[87]   Reeuwijk L van. Procedures for soil analysis. Tech Pap 1992;9.

[88]   Berkgaut V, Singer A. High capacity cation exchanger by hydrothermal zeolitization of coal fly ash. Appl Clay Sci 1996;10:369–78.

[89]   Polemio M, Rhoades JD. Determining cation exchange capacity: A new procedure for calcareous and gypsiferous soils. Soil Sci Soc Am J 1977;41:524–8.

[90]   Hesse PR. A textbook of soil chemical analysis 1971.

[91]   Derkowski A, Franus W, Beran E, Czímerová A. Properties and potential applications of zeolitic materials produced from fly ash using simple method of synthesis. Powder Technol 2006;166:47–54.

[92]   Jha VK, Matsuda M, Miyake M. Sorption properties of the activated carbon-zeolite composite prepared from coal fly ash for Ni2+, Cu2+ , Cd2+ and Pb2+ . J Hazard Mater 2008;160:148–53.

[93]   Qiu W, Zheng Y. Removal of lead, copper, nickel, cobalt, and zinc from water by a cancrinite-type zeolite synthesized from fly ash. Chem Eng J 2009;145:483–8.

[94]   Hui KS, Chao CYH, Kot SC. Removal of mixed heavy metal ions in wastewater by zeolite 4A and residual products from recycled coal fly ash. J Hazard Mater 2005;127:89–101.

[95]   Fernández-Pereira C, Galiano YL, Rodríguez-Piñero MA, Vale J, Querol X. Utilisation of zeolitised coal fly ash as immobilising agent of a metallurgical waste. J Chem Technol Biotechnol 2002;77:305–10. doi:10.1002/jctb.584.

[96]   Fotovat F, Kazemeini M, Kazemian H. Novel utilization of zeolited fly ash hosting cobalt nanoparticles as a catalyst applied to the Fischer–Tropsch synthesis. Catal Lett 2009;127:204–12.

[97]   Klamrassamee T, Pavasant P, Laosiripojana N. Synthesis of Zeolite from Coal Fly Ash: Its Application as Water Sorbent. Eng J 2010;14:37–44.

[98]   Zhao XS, Lu GQ, Zhu HY. Effects of ageing and seeding on the formation of zeolite Y from coal fly ash. J Porous Mater 1997;4:245–51.

[99]   Rayalu SS, Udhoji JS, Munshi KN, Hasan MZ. Highly crystalline zeolite—a from flyash of bituminous and lignite coal combustion. J Hazard Mater 2001;88:107–21.

[100]   Hollman GG, Steenbruggen G, Janssen-Jurkovičová M. A two-step process for the synthesis of zeolites from coal fly ash. Fuel 1999;78:1225–30.

[101]   Molina A, Poole C. A comparative study using two methods to produce zeolites from fly ash. Miner Eng 2004;17:167–73.

[102]   Moreno N, Querol X, Plana F, Andres JM, Janssen M, Nugteren H. Pure zeolite synthesis from silica extracted from coal fly ashes. J Chem Technol Biotechnol 2002;77:274–9.

[103]   Querol X, Plana F, Alastuey A, López-Soler A. Synthesis of Na-zeolites from fly ash. Fuel 1997;76:793–9.

[104]   Ma W, Brown PW, Komarneni S. Characterization and cation exchange properties of zeolite synthesized from fly ashes. J Mater Res 1998;13:3–7.

[105]   Steenbruggen G, Hollman GG. The synthesis of zeolites from fly ash and the properties of the zeolite products. J Geochem Explor 1998;62:305–9.

[106]   Murayama N, Takahashi T, Shuku K, Lee H, Shibata J. Effect of reaction temperature on hydrothermal syntheses of potassium type zeolites from coal fly ash. Int J Miner Process 2008;87:129–33.

[107]   Moriyama R, Takeda S, Onozaki M, Katayama Y, Shiota K, Fukuda T, et al. Large-scale synthesis of artificial zeolite from coal fly ash with a small charge of alkaline solution. Fuel 2005;84:1455–61.

[108]   Querol X, Umaña JC, Plana F, Alastuey A, Lopez-Soler A, Medinaceli A, et al. Synthesis of zeolites from fly ash at pilot plant scale. Examples of potential applications. Fuel 2001;80:857–65.

[109]   Inada M, Eguchi Y, Enomoto N, Hojo J. Synthesis of zeolite from coal fly ashes with different silica–alumina composition. Fuel 2005;84:299–304.

[110]   Wirsching U. Experimente zum Einfluß des Gesteinsglas-Chemismus auf die Zeolithbildung durch hydrothermale Umwandlung. Contrib Mineral Petrol 1975;49:117–24.

[111]   Woolard CD, Strong J, Erasmus CR. Evaluation of the use of modified coal ash as a potential sorbent for organic waste streams. Appl Geochem 2002;17:1159–64.

[112]   Wajima T, Sugawara K. Material conversion from various incinerated ashes using alkali fusion method. Int J Soc Mater Eng Resour 2010;17:47–52.

[113]   Park J, Kim BC, Park SS, Park HC. Conventional versus ultrasonic synthesis of zeolite 4A from kaolin. J Mater Sci Lett 2001;20:531–3.

[114]   Musyoka NM, Petrik LF, Hums E. Ultrasonic assisted synthesis of zeolite A from coal fly ash using mine waters (acid mine drainage and circumneutral mine water) as a substitute for ultra pure water. Int. Mine Water Assoc., Aachen, Germany: 2011, p. 423–8.

[115]   Musyoka NM, Petrik LF, Hums E, Baser H, Schwieger W. In situ ultrasonic monitoring of zeolite A crystallization from coal fly ash. Catal Today 2012;190:38–46.

[116]   Musyoka NM, Petrik LF, Hums E, Baser H, Schwieger W. In situ ultrasonic diagnostic of zeolite X crystallization with novel (hierarchical) morphology from coal fly ash. Ultrasonics 2014;54:537–43.

[117]   Khodabandeh S. Synthesis of Alkaline-Earth Zeolites. California Institute of Technology, 1997.

[118]   Ríos R. CA, Williams CD, Roberts CL. A comparative study of two methods for the synthesis of fly ash-based sodium and potassium type zeolites. Fuel 2009;88:1403–16.

[119]   Slangen PM, Jansen JC, Van Bekkum H. The effect of ageing on the microwave synthesis of zeolite NaA. Microporous Mater 1997;9:259–65.

[120]   Wu D, Zhang B, Yan L, Kong H, Wang X. Effect of some additives on synthesis of zeolite from coal fly ash. Int J Miner Process 2006;80:266–72.

[121]   Fukui K, Katoh M, Yamamoto T, Yoshida H. Utilization of NaCl for phillipsite synthesis from fly ash by hydrothermal treatment with microwave heating. Adv Powder Technol 2009;20:35–40.

[122]   Wang B, Wu J, Yuan Z-Y, Li N, Xiang S. Synthesis of MCM-22 zeolite by an ultrasonic-assisted aging procedure. Ultrason Sonochem 2008;15:334–8.

[123]   Tavare NS. Industrial crystallization. Plenum Press; 1995.

[124]   Wu J, Wang B, Li N, Xiang S. Effect of Aging with Ultrasound on the Synthesis of MCM-49 Zeolite. Chin J Catal 2006;27:375–7.

[125]   Morschhäuser R, Krull M, Kayser C, Boberski C, Bierbaum R, P. A. Püschner, T. Glasnov, K.C. Oliver. Microwave-assisted continuous flow synthesis on industrial scale. Green Process Synth 2012;1:281–90.

[126]   Gogate PR, Sutkar VS, Pandit AB. Sonochemical reactors: important design and scale up considerations with a special emphasis on heterogeneous systems. Chem Eng J 2011;166:1066–82.

[127]   Miyake M, Tamura C, Matsuda M. Resource Recovery of Waste Incineration Fly Ash: Synthesis of Zeolites A and P. J Am Ceram Soc 2002;85:1873–5.

[128]   Hui KS, Chao CYH. Effects of step-change of synthesis temperature on synthesis of zeolite 4A from coal fly ash. Microporous Mesoporous Mater 2006;88:145–51.

[129]   Juan R, Hernández S, Andrés JM, Ruiz C. Synthesis of granular zeolitic materials with high cation exchange capacity from agglomerated coal fly ash. Fuel 2007;86:1811–21.

[130]   Tanaka H, Fujii A. Effect of stirring on the dissolution of coal fly ash and synthesis of pure-form Na-A and -X zeolites by two-step process. Adv Powder Technol 2009;20:473–9.

[131]   Musyoka NM, Petrik LF, Balfour G, Gitari WM, Hums E. Synthesis of hydroxy sodalite from coal fly ash using waste industrial brine solution. J Environ Sci Health Part A 2011;46:1699–707.

[132]   Chauhan YP, Talib M. A novel and green approach of synthesis and characterization of nano-adsorbents (zeolites) from coal fly ash: a review. Sci Rev Commun 2012;2:12–9.

[133]   Nascimento M, Soares PSM, Souza VP de. Adsorption of heavy metal cations using coal fly ash modified by hydrothermal method. Fuel 2009;88:1714–9.

[134]   Algoufi YT, Hameed BH. Synthesis of glycerol carbonate by transesterification of glycerol with dimethyl carbonate over K-zeolite derived from coal fly ash. Fuel Process Technol 2014;126:5–11.

[135]   Musyoka NM. Hydrothermal synthesis and optimisation of zeolite Na-P1 from South African coal fly ash. University of Western Cape, 2009.

[136]   Chang H-L, Shih W-H. A general method for the conversion of fly ash into zeolites as ion exchangers for cesium. Ind Eng Chem Res 1998;37:71–8.

[137]   Kumar P, Rayalu S, Dhopte SM. Flyash based zeolite-A: a suitable sorbent for lead removal. Indian J Chem Technol 2004;11:227–33.

[138]   Somerset VS, Petrik LF, White RA, Klink MJ, Key D, Iwuoha EI. Alkaline hydrothermal zeolites synthesized from high SiO2 and Al2O3 co-disposal fly ash filtrates. Fuel 2005;84:2324–9.

[139]   Yaping Y, Xiaoqiang Z, Weilan Q, Mingwen W. Synthesis of pure zeolites from supersaturated silicon and aluminum alkali extracts from fused coal fly ash. Fuel 2008;87:1880–6.

[140]   Fotovat F, Kazemian H, Kazemeini M. Synthesis of Na-A and faujasitic zeolites from high silicon fly ash. Mater Res Bull 2009;44:913–7.

[141]   Ruen-ngam D, Rungsuk D, Apiratikul R, Pavasant P. Zeolite formation from coal fly ash and its adsorption potential. J Air Waste Manag Assoc 2009;59:1140–7.

[142]   Belviso C, Cavalcante F, Fiore S. Synthesis of zeolite from Italian coal fly ash: differences in crystallization temperature using seawater instead of distilled water. Waste Manag 2010;30:839–47.

[143]   Kazemian H, Naghdali Z, Ghaffari Kashani T, Farhadi F. Conversion of high silicon fly ash to Na-P1 zeolite: Alkaline fusion followed by hydrothermal crystallization. Adv Powder Technol 2010;21:279–83.

[144]   Zhang X, Tang D, Jiang G. Synthesis of zeolite NaA at room temperature: The effect of synthesis parameters on crystal size and its size distribution. Adv Powder Technol 2013;24:689–96.

[145]   Chareonpanich M, Jullaphan O, Tang C. Bench-scale synthesis of zeolite A from subbituminous coal ashes with high crystalline silica content. J Clean Prod 2011;19:58–63.

[146]   Musyoka NM, Petrik LF, Fatoba OO, Hums E. Synthesis of zeolites from coal fly ash using mine waters. Miner Eng 2013;53:9–15.

[147]   Izidoro J de C, Fungaro DA, Abbott JE, Wang S. Synthesis of zeolites X and A from fly ashes for cadmium and zinc removal from aqueous solutions in single and binary ion systems. Fuel 2013;103:827–34.

Chapter 3

3   SYNTHESIS OF ZEOLITE NA-A USING SINGLE MODE MICROWAVE IRRADIATION AT ATMOSPHERIC PRESSURE: THE EFFECT OF MICROWAVE POWER[1]

Abstract

This paper investigates the effects of single mode microwave irradiation on the synthesis of zeolite Na-A from sodium aluminate and sodium silicate gel at atmospheric pressure. Microwave irradiation has shown to accelerate zeolitization process from several hours to several minutes. The microwave irradiation employed was produced in a single mode lab scale microwave, which enabled control of irradiated power and temperature of the reaction mixture, while the pressure was controlled by affixing a condenser on a Teflon reactor vessel with a working volume 20 mL. Two sets of experiments were conducted, first with three levels of temperature and reaction time, and second with three levels of power and reaction time. The characteristics and physical properties of the synthesized samples were analyzed by means of different instrumental techniques including XRD including Rietveld refinement, SEM, BET, TGA, and by determination of cation exchange capacity (CEC). It was observed that the crystallinity of the product was influenced by both power and time of microwave irradiation; moreover, power and time of microwave irradiation influenced the phase selection between Na-A and Na-X. Single phase zeolite Na-A was achieved with a crystallinity of 80 % at 300 W using single mode microwave irradiation at atmospheric pressure after 30 min of exposure to radiation.

3.1   Introduction

Microwave radiations (MW) lie in between infrared waves and radio waves on the electromagnetic spectrum. The energy transfer occurs due to the interaction of dielectric

molecules with MW. Dielectric heating occurs when dipoles of polar molecules follow the inversion of alternating electric field. The dipole molecules in the irradiated field orient themselves with the magnetic field and oscillate with the magnetic field oscillations. Their motion is resisted by inter-particle interactions and electric resistance. The induced energy dissipates in the form of thermal energy through molecular friction resulting in a uniform distribution of thermal energy compared to the conventional heating [1]. Microwave produces volumetric heating in the reaction vessel; furthermore, beyond thermal effects, there are also non-thermal effects. The activation energy is also observed to decrease during MW irradiation; this decrease in the activation energy compared to the conventional heating might be due to higher atomic mobility in the crystal lattice [2].

Microwave-assisted synthesis of zeolites and nanozeolites have been reported in many previous works [3–8] and has been found to assist shortening the crystallization time, accelerating nucleation, producing narrower size distributions, reducing undesirable phases and obtaining different morphologies [9–11]. Furthermore, the employment of the microwave technique in the synthesis of nanoporous materials has been shown to produce multiple effects, for instance, short heating times, inductive heating, specific energy dissipation via microwave energization of the hydroxylated surface or associated water molecules in the boundary layer, and formation of the high potential active water molecules [12–16]. According to various authors, the reduction of time using the microwave energy source is a consequence of two main effects: a relatively fast rate of reaction and a rapid homogeneous heating of the synthesis mixture that lead to a more abundant nucleation at tiny hot spots [17,18].

In a conventional autoclave reactor, the heat is transferred from the heating source (oven) to the water medium through its surface, and the rate of heat flow is limited by temperature difference and thermal diffusivity. The conventional heating requires a long synthesis time above 48 h to produce the zeolite [15,19]. However, it was found that aging (pre-crystallization) is a prerequisite step and extra care is needed for the successful rapid synthesis of Na-A. This is in contrast to the conventional synthesis. During the aging, mixing on a molecular scale allows the formation of nuclei necessary for the

subsequent growth of Na-A, whereas an extra aging step is not required in conventional synthesis because the mixing and nucleation takes place during the heat-up of the reaction mixture [17]. It can be deduced that nucleation occurs during the aging step, the aged gel supplies the seeds to produce zeolite in fresh un-aged gel mixture [17,20]. The presence of zeolite nuclei in the reaction gel has been confirmed in previous publications [21,22]. Infrared spectroscopy (IR) investigation shows the presence of a band at 560 cm-1 that corresponds to double membered ring such as D4R, D5R and D6R, the composite structure of Na-A and Na-X [23]. before the formation of zeolitic crystals [21]. In the first reported attempt of microwave synthesis of zeolite Na-A, crystallization of zeolite was achieved in 12 min but the product was contaminated with hydroxysodalite (HS) phase, even when the mixture was aged for 2 h at room temperature before microwave heating [12]. Slangen et al. (1997) were able to obtain pure zeolite A in 5 min crystallization at 100 ℃ and autogenous pressure in a household type microwave oven, but only after the gel was aged for 20 h at room temperature. The output power of microwave equipment varied from 180 to 1800 W. In the microwave synthesis the mixture was rapidly heated to 120 ℃ (90 s) and it was kept at 100 ℃ for 5 min, subsequently. They obtained more than 80 % Na-A after 3 h of aging. After 4 h of aging 90 % Na-A was produced with hydrosodalite (HS) as the major impurity [17]. Bonaccorsi and Proverbio (2003) modified the microwave oven by the introduction of a water condenser to conduct synthesis experiments under atmospheric pressure. They used two steps microwave exposure to achieve high purity Na-A product. Irradiation at the power of 360 W for 50 min followed by 900 W in 10 min resulted in 89 % Na-A. However, irradiation at the power of 900 W for 10 min followed by 360 W in 50 min resulted in 99 % Na-A [18]. Yuan et al. (2011) reported the synthesis of Na-A zeolite from sodium silicate and sodium aluminum oxide, while using tetramethylammonium hydroxide as an organic template and structural directing agent (SDA). Pre-crystallization aging was performed at 60 ℃ for 1.5 to 3 h, followed by crystallization at 70-90 ℃ in a modified kitchen microwave oven for 15-35 min under autogenous pressure. The optimal microwave heating time was 25 min [24]. Sapawe et al. (2013) reported 15 min to be the optimum microwave irradiation time for the synthesis of Na-A at autogenous pressure,

which is about sixteen times shorter than using conventional heating technique in an oven at 105 ºC for 4 h [25].

In a single mode microwave, electromagnetic irradiation is directed through a precisely-designed wave guide that produces a standing wave, whereas in multimode microwave there is no single standing wave but a mixture of many waves with different phase shifts. The microwave field density in a single mode microwave is much higher compared to multimode microwave, therefore similar results can be achieved in single-mode microwave using lower power than in high power multimode microwave [26]. Atmospheric pressure has been chosen because atmospheric hydrothermal synthesis is the common method for manufacturing zeolite A on a commercial scale and allows an easy change of reaction parameters, like stirring or vessel geometry for continuous application. Furthermore, it is much more cost effective to work at atmospheric pressure compared to elevated pressures. The choice of single mode microwave was made because it further increases the advantage of using microwave irradiation as a heating source.

In the present work, zeolite Na-A has been prepared under single mode microwave and ambient pressure to achieve the reduction in synthesis time. The microwave irradiation power that has been used ranges from 100 W to 300 W much lower than the other reported experiments [17,18]. Microwave irradiation energy has also been related to crystallinity of the product and phase selection of Na-A over Na-X. Na-A is chosen as a synthesis candidate due to its well-known structure, good ion exchange, and catalytic properties. Thereby, a better understanding may be obtained on the influence of microwave heating on the synthesis of zeolite Na-A.

3.2 Materials and Methods

3.2.1 Materials

Sodium aluminate $Na_2O:Al_2O3:3H_2O$ (Anachemia, Canada), sodium metasilicate, $Na_2SiO_3:5H2O$ (Sigma-Aldrich, USA), sodium hydroxide (Alphachem, Canada) were all of analytical grade and used as received. Other chemicals used for characterization tests were of analytical grade. Deionized water was used for the preparation of the solution.

3.2.2 Hydrogel Preparation

The experiments were performed with an aluminosilicate gel consisting of a mole composition of 3.165 Na_2O:1 Al_2O_3:1.926 SiO_2:128 H_2O. The preparation procedure of the gel [27] was as follows: (a) Sodium aluminate (8.258 g) and sodium metasilicate (15.48 g) were dissolved in an 0.22 M solution of sodium hydroxide (40 mL), separately. After 30 min of stirring at room temperature, clear solutions were obtained. (b) The solutions were mixed and then the gel was aged at ambient temperature (23±2 °C) for 2 h. (c) The obtained gel (20 mL) was subjected to microwave irradiation. Synthesis mixture was mixed thoroughly to ensure formation of silica-alumina oligomers. This mixing on a molecular scale is essential for the nucleation of Na-A. The constant aging time of 2 h was chosen as the optimum-short aging time mentioned in the literature [24].

3.2.3 Crystallization Method

A cylindrical PTFE vessel (28 mm ID × 108 mm) attached to a reflux condenser was placed in the microwave chamber for varied periods of time and temperatures. The time was varied between 10 and 30 min while the temperature was varied between 100 and 120 ºC. Two sets of experiments were conducted, the first set were the temperature was kept constant with the adjustment of microwave irradiation power while the other set was performed at a constant power. The experiments were performed in a self-adjusting, microwave oven (single-mode, 2.45 GHz, CEM cooperation, Discover, USA), where the reaction temperature and power were monitored automatically. The temperature was measured using infrared pyrometer installed in the microwave chamber. The infrared pyrometer detects the temperature at the bottom of the reactor vessel. This temperature can be higher than the temperature of the solution inside the vessel. Figure 3-1 shows the overview of the crystallization system. The system consists of a microwave generator, a condenser and a laptop computer to record power and temperature profiles. After a given period of MW irradiation, the solid products were filtered off, washed with deionized

water until the pH reached around 8, and dried overnight at 100 ºC in an electric oven. The zeolite produced utilizing conventional oven by following verified method published by International Zeolite Association (IZA) [27].

Figure 3-1. Photograph of the single mode microwave set-up used of Na-A zeolite under atmospheric condition

3.2.4 Characterization

A MiniFlex powder diffractometer (Rigaku, Woodlands, USA) was used to collect XRD data of the synthesized samples using CuKα (λ for Kα = 1.54059 Å) over the range of 5°<2θ<40° with step width of 0.05°. The peaks appeared at the 2θ of 6.12° for Na-X and 7.20° for Na-A were chosen for further calculations of the crystallinity and phase purity of the products [28]. The ratios of the two peaks were calculated using MDI-Jade v 7.5 software. The crystallinity of the products was determined by "peak fitting" algorithm in the software. The crystallinity was defined as the amount of crystals synthesized from the amorphous gel. The algorithm used utilized the areas corresponding to characteristic zeolite peaks and amorphous hump to calculate crystallinity. The XRD peak areas were used for these calculations because the intensity of the peaks is related to size of the crystals which was not investigated in this study. The Furrier transform infrared (FTIR) spectra of the samples were recorded on solid state by a Vector 22 spectrometer (Canada). The sample scan time was 32 s over the 400–4000 cm^{-1} spectral region with resolution of 4 cm^{-1}. Crystal size distribution and morphology of zeolite were studied by scanning electron microscope (SEM) JSM 600F (Japan) operating at 10 keV of acceleration voltage. Specific surface area and pore size of the prepared samples were measured by means of a BET analyzer (Micrometrics ASAP 2010). Known amounts of samples (e.g., 50-80 mg) were loaded into the BET sample tube and degassed under vacuum (10-5 Torr) at 125 °C for 6 h. The thermal analyses were performed using a Mettler Toledo TGA/SDTA 851e model (Mississauga, ON, Canada) with version 6.1 Stare software. The samples were heated from 30 °C to 600 °C at heating rate of 10 °C/min under nitrogen purge. Cation exchange capacity (CEC) was measured using ammonium acetate saturation method (5 days) based on method introduced by Bain and Smith [29].

3.2.5 Experimental Design

The zeolite Na-A synthesis was statistical analysed by using a three-level, double-factorial design. Design-Expert 7.1.5 software (StatEase, Minneapolis, USA) was used to investigate the effect of each reaction parameter on the crystallinity and the ratio of Na-X and Na-A. The effects of time and power for continuous MW irradiation at atmospheric

pressure were investigated. The effect of power irradiation on the crystallinity of the product was investigated. Detailed indications of the factor levels employed for the experimental technique are summarized in Table 3-1.

Table 3-1. Experimental design for the synthesis of zeolite A

Run no.	Power (W)	Reaction time (min)
1	100	10
2	300	10
3	100	30
4	300	30
5	100	20
6	300	20
7	200	10
8	200	30
9	200	20

3.3 Results and Discussion

During the course of the gel preparation, it is observed that when the sodium aluminate and sodium metasilicate solutions are combined in the reaction vessel, the two liquids form a thick gel. After vigorous shaking the gel is homogenized. It is observed that the turbid gel phase diminishes in height and clear supernatant is formed with the crystalline phase below it, which is in agreement with the literature [27]. The crystallinity of the Na-

A zeolite synthesized with less than 2 h of aging is relatively low. Furthermore, formation of zeolite Na-X occurs for aging time longer than 3 h [24]. Therefore, in this work, gel was aged for 2 h in order to improve the nucleation and growth of Na-A zeolite particles, exclusively. A series of experiments with microwave irradiation time varying from 10 to 30 min were carried out. The results revealed that microwave irradiation time plays a significant role on the crystallinity and the purity of the synthesized Na-A zeolite without the presence of any other phases such as Na-X or hydroxysodalite. All experiments, with different power levels, temperature level, and times of exposure to MW, are listed in Table 2.

Table 3-2. Two sets of MW exposure experiments with 3.165 Na2O:1 Al2O3:1.926 SiO2:128 H2O

Constant Temperature		Constant Power	
Temperature (^{o}C)	*MW irradiation time (min)*	*Power (W)*	*MW irradiation time (min)*
100	10-30	100	10-30
110	10-30	200	10-30
120	10-30	300	10-30

For the first set of experiments the microwave power level was reduced after desired temperature was reached to get constant temperature for crystallization period. In order to minimize the temperature overshoot during the initial phase of the reaction, the microwave power was set to a predefined maximum irradiation output. The irradiation output was kept at a maximum of 100 W, 200 W, and 300 W to control the desired temperature to 100 °C, 110 °C, and 120 °C, respectively. Due to this setup the temperature reached the set point smoothly and without any significant overshoot. Therefore, the high initial irradiation associated with the high initial temperature over-shoot, may lead to the synthesis of Na-A zeolite and investigating the individual effect of

these two factors would become convoluted. Synthesis mixtures were first heated using a relatively low power of the magnetron, 100 W, to reach 100 °C in 2 min. Subsequently, the power decreased; the temperature was kept at 100 ± 3 °C with a power adjustment to 7 ± 2 W for 28 min. It is assumed that the initial crystal growth takes place in the high-temperature/high power regions; the subsequent crystal growth at low temperature. As the clear supernatant phase starts to separate from the crystal precipitate, a slight increase in the temperature is observed under constant power setting, however when a constant temperature is set, a power decrease is observed. It can be concluded that crystal phase and the supernatant start to separate inside the vessel early in the reaction during microwave irradiation. Figure 3-2 shows a typical power and temperature profiles during irradiation of the reaction mixture with microwave radiation. The area under the power curve represents the energy irradiated to the sample.
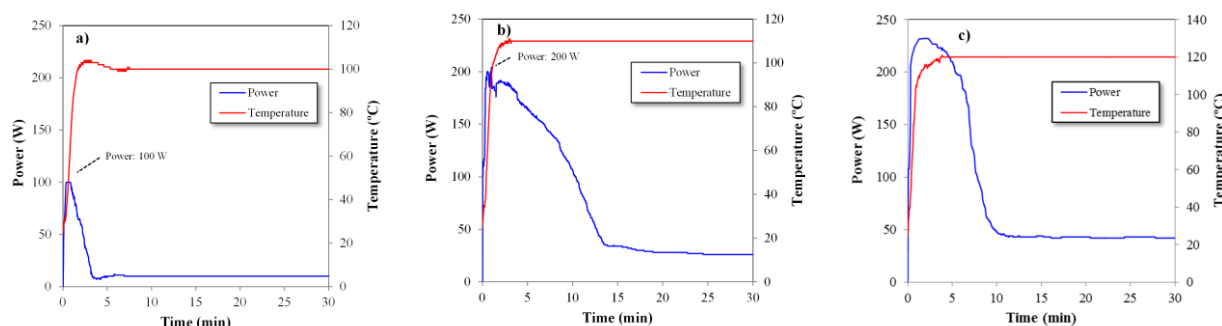
Figure 3-2. Power irradiation and temperature profiles versus time inside the reaction vessel during crystallization

The other set of experiments was conducted with constant MW power applied to the reaction mixture. Figure 3-3 shows the temperature-time profiles of the experiments during constant microwave irradiation of 100 W, 200 W, and 300 W, using single-mode microwave applicator. After several minutes of irradiation at each constant power level, the quasi-steady state temperature (with a tolerance of 6 ºC) was achieved.
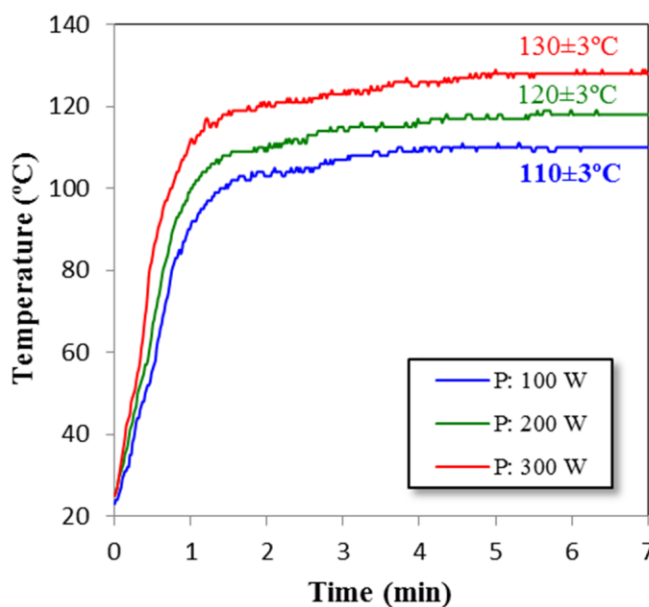
Figure 3-3. Temperature profile during crystallization at constant microwave irradiation power

3.3.1 XRD Results

Preliminary experiments conducted with constant temperature and variable MW power showed that at least 30 min of irradiation was required for significant crystal growth to occur that is detectable by XRD. In addition to irradiation time, irradiation power is also an important factor in the production of zeolite crystals. Higher MW irradiation produced sharper XRD peaks confirming the production of zeolite crystals. There was no zeolite observed with a maximum MW power of 100W and a constant temperature of 100 °C. However, as the temperature and the maximum MW power was increased the observed crystallinity increased significantly from 0.46 % to 74.81 %. The energy irradiated to the reaction mixture is a function of both irradiation time and MW power. The difference of the MW energy irradiated can be estimated graphically by observing the area under the power curve in Figures 2a-c. The amount of energy irradiated in this set of experiment was 4.06 kJ/g, 19.77 kJ/g and 20.50 kJ/g resulting in a crystallinity of 0.46 %, 56.75 % and 74.81 %, respectively. Prepared gel needs to be homogenized to allow nucleation of the desired phase. Only after nucleation can a sharp rise of temperature lead to the growth of pure zeolite crystals. This action is, strongly accelerated by microwave interaction.

Rotation of water dipoles and dissipation of energy as heat are the main results of exposing an aqueous solution to microwaves. Under the action of the electromagnetic field, water molecules are dissociated from each other and dipoles acquire a higher potential for dissolution of the gel phase than in hydrogen bonded water [30]. Dissolution and depolymerisation of the silica and alumina polymeric groups linked together to form the gel, have been recognized by several authors [31,32] to be the main mechanism for the crystallization of zeolites. It appears that in the liquid phase, dissolved oligomers form stable nuclei capable of inducing crystal growth [18]. However, if inadequate amount of energy is transferred to the reaction mixture, then the crystal growth would not be observed. Figure 3-4 indicates the observed crystallinity difference for different temperatures and the corresponding MW irradiation power.
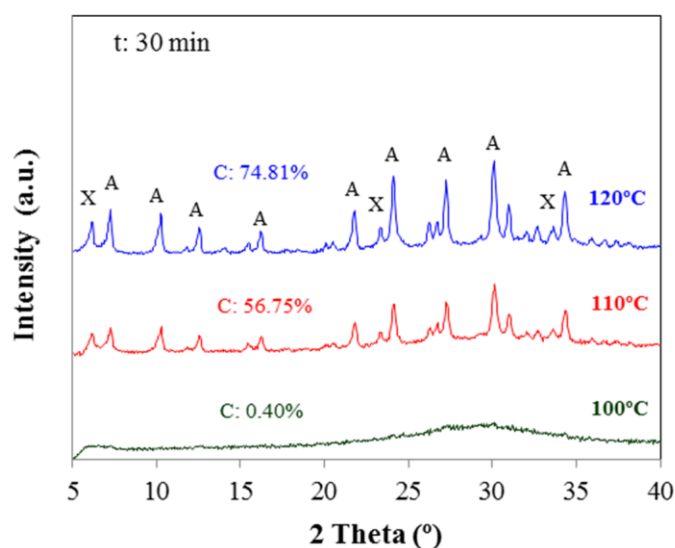
Figure 3-4. XRD patterns of synthesized Na-A zeolite at different crystallization temperatures for constant temperature experiments (A: Na-A peaks, X: Na-X peaks)

A series of characteristic peaks were observed at the 2θ of 7.25º, 10.25º, 12.55º, 16.20º, 21.80º, 24.10º, 27.25º, 30.10º, and 34.35º, which were in agreement with reference peaks that belong to Na-A zeolite. Other peaks at the 2θ values of 6.20°, 23.35°, 33.65° belong to Na-X zeolite [28], indicating only two zeolite phases. With increasing temperature, the

intensity of the characteristic peaks of both Na-A and Na-X zeolite increased, as well as the crystallinity.

The XRD patterns of the prepared Na-A at three different microwave irradiation powers of 100, 200 and 300 W and different times ranging from 10 to 30 min, and the results are shown in Figure 5. The amount of energy irradiated in this set of experiment with constant power ranged from 8.67 kJ/g to 32.30 kJ/g, resulting in a crystallinity ranging from 3.62 % to 83.35 %. The peak intensity of Na-A increased as microwave irradiation time was increased. With increasing power, the oscillating electromagnetic field in the microwave oven is active for longer time, leading to a stronger dissolution effect [33]. The crystallinity increased when microwave power increased. Moreover, Na-X began to disappear at a relatively higher microwave power. The irradiation power influenced both the crystallinity of the product and also the ratio of Na-X to Na-A. As the power irradiation was increased the ratio of Na-X to Na-A also decreased. This could be attributed to difference in their structure, Na-X has a larger structural unit (D6R) compared to Na-A (D4R) which are more condensed. Another reason that can attributed to the selection of Na-A over Na-X at higher irradiation power could be attributed to the difference in their formation mechanism. Na-X has been shown to have only a solution phase-mediated mechanism unlike Na-A which has an extra "secondary amorphous phase" before conversion to Na-A [34,35]. Higher MW irradiation might favour the mechanism of formation of Na-A crystallization over Na-X. The ratio was found to be the highest at irradiation power of 100 W and while the characteristic Na-X peak was not observed at 300 W. Hence a moderate level of 100-300 W microwave power would be more suitable for the synthesis of Na-A zeolite in industrial case [24].
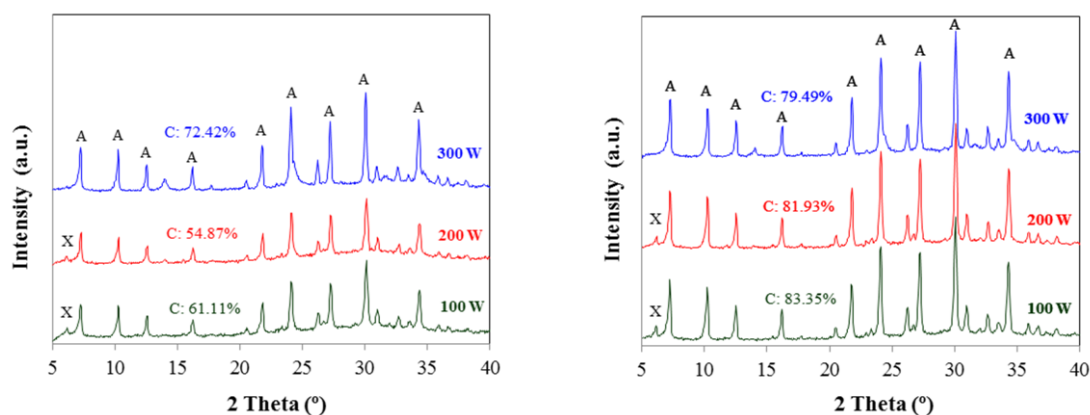
Figure 3-5. XRD patterns of synthesized Na-A zeolite with different crystallization times for constant power experiments (A: Na-A peaks X: Na-X peaks) (a) 20 min (b) 30 min

The product produced at 300 W 30 min in Figure 3-5(b) has a high crystallinity and phase purity. The crystallinity is measured using the peak fitting in MDI jade v7.5 software, this algorithm calculates the crystallinity by adding all the peak areas that are observed in the XRD. At high crystallinity the multi-phase product have higher crystallinity compared to single phase product due to the addition of peak areas of both Na-A and Na-X, therefore a higher crystallinity is observed for the mixed phase produced at 100 W and 200 W compared to the single phase product produced at 300 W in Figure 3-5(b).

Rietveld refinement was used to determine the crystalline group and the crystalline parameters of the zeolite produced. The crystalline groups of the two phases present in some of the samples were determined as Fm-3c and Fd-3m which correspond to Na-A and Na-X respectively [28]. Whereas, samples produced at higher microwave irradiation consisted of only one crystalline group, Fm-3c, corresponding to Na-A. Both crystalline groups Fm-3c and Fd-3m have cubic structure that is confirmed through the SEM images where the crystal products show distinctively cubic structure.

3.3.2 FTIR Results

The FTIR spectra of the zeolite synthesize at constant MW power of 300 W are illustrated in Figure 3-6. The FTIR data validate the observations made through XRD.

The FTIR spectrum of the zeolite during and after termination of crystallization contains a number of characteristic vibration bands in the regions 1100-900 cm-1, 700-650 cm^{-1}, and 560 cm-1. Band at about 1000 cm-1 corresponding either to the stretching vibrations of Si-O bonds in SiO4 or to the skeleton of bonded SiO4 tetrahedra, shows the greatest change during crystallization [21,36].

The spectrum band at 560 cm^{-1} corresponds to D4R vibration. In the FTIR conducted, the band corresponding to D4R is seen increasing as the crystallinity time increases. The band corresponding to SiO4 (about 1000 cm^{-1}) is also seen increase with the increase in the crystallinity time.
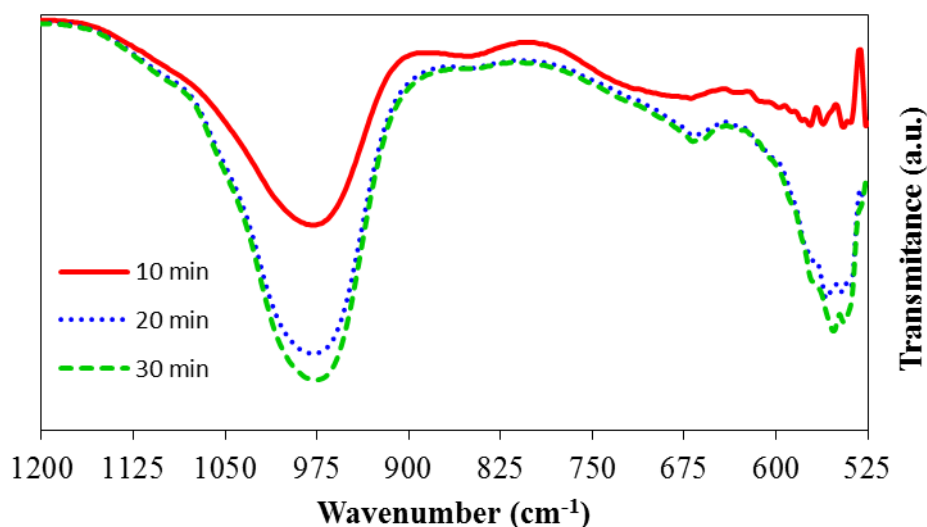
Figure 3-6. FTIR spectra of samples synthesized at 300 W constant irradiation

3.3.3 Scanning Electron Microscope Results

The scanning electron microscope (SEM) images (Figure 3-7) were taken for Na-A crystals using conventional oven and for microwave synthesis at different irradiation times to compare the growth of zeolite crystals. The samples produced through conventional method and microwave irradiation showed crystal structure of the same morphology, i.e., cubic structure as expected from literature and simulated data [28]. Figure 3-7(a) shows the cubic structure of zeolite A formed under conventional synthesis with hydroxysodalite phase. Figure 3-7(b)-(d) shows the progression of crystallization as

the microwave irradiation time increases from 10 to 30 min. While Figure 3-7(b) has a high ratio of amorphous phase with cubic crystals embedded in, however, for the succeeding SEM images it can be observed that only cubic crystals are present. The SEM images validate the XRD data, showing the amorphous structure decreases as the irradiation time is increased and more cubic crystals appear. After 10 min of MW irradiation at 300 W a few cubic structures appear, however, the cubic structures are not abundant and are embedded into the amorphous structure. One of the explanations that can be offered for the embedment of zeolite crystals in the amorphous structure is that these crystals are nucleated and grow on the surface of the amorphous gel, concurring with the literature that zeolite crystals form through heterogonous crystallization. As the MW irradiation time increases the abundance of cubic zeolite crystals increases significantly, indicating that the crystal growth is strongly dependent on the MW irradiation time.
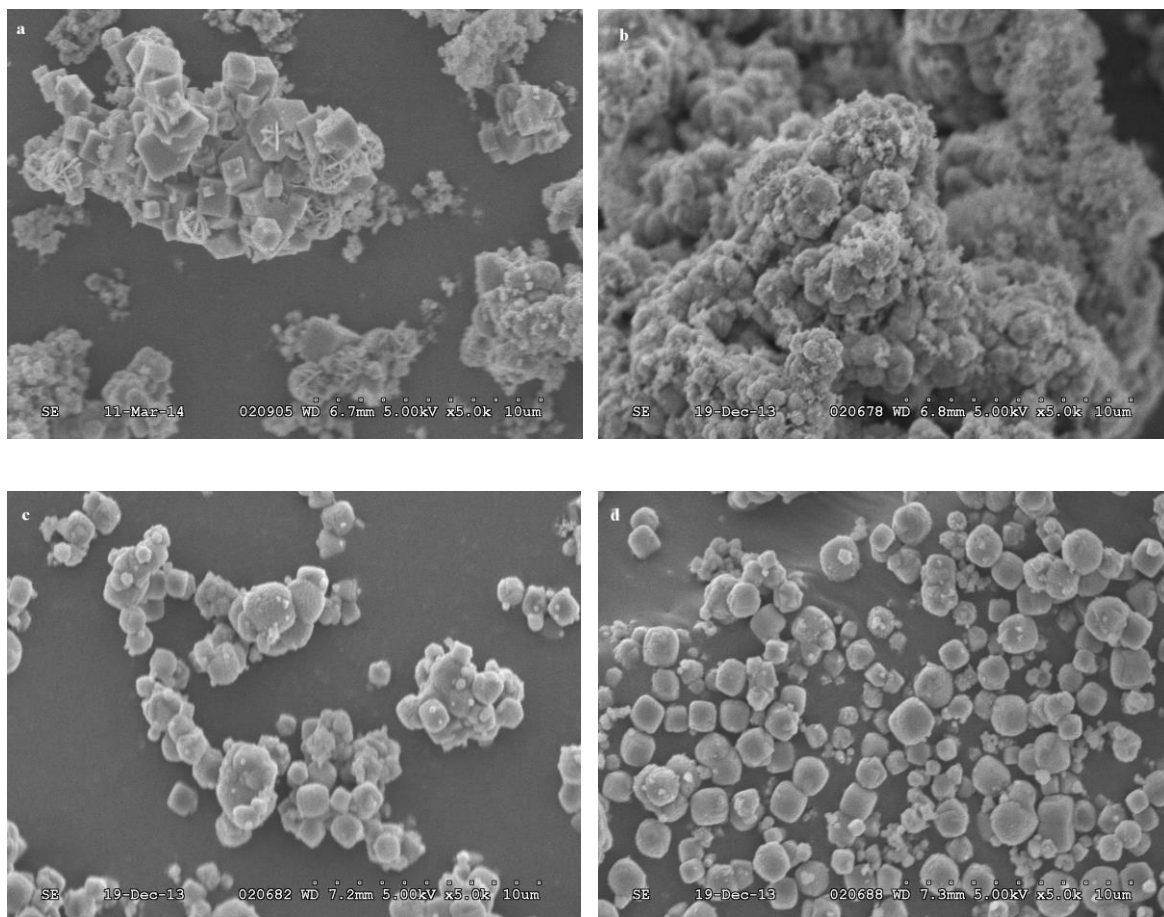
Figure 3-7. SEM images of the samples synthesized (a) with conventional heating (b) at MW irradiation of 300 W at different crystallization times t = 10 min (c) t = 20 min (d) t = 30 min

3.3.4 BET Results

BET surface area of the best sample synthesized at 300 W and 30 min was determined to be 50 m^2/g. At the optimum conditions of experimentations that yielded a single phase Na-A zeolite with the highest crystallinity (300 W and 30 min), the micropore area and external surface area were 42 m^2/g and 7 m^2/g, respectively therefore indicating that more than 86 % of the surface area consists of micropore. The BET surface area was compared to Na-A prepared using the conventional oven under autogenous pressure which was found to be about two and a half times higher at 130 m^2/g. Whereas the micropore area and external surface area were found 110 m^2/g and 13 m^2/g, respectively, therefore

indicating similar percentage of micropore (89 %) as the Na-A produced with microwave assisted synthesis at atmospheric condition. The isotherms of both Na-A prepared through microwave synthesis and conventional oven synthesis are shown in Figure 3-8(a)-(b).

The shape of the isotherm and its hysteresis pattern can be used to qualitatively predict the types of pores present in the zeolite (Figure 3-8). Based on International Union of Pure and Applied Chemistry (IUPAC) isotherm classification [37,38], the adsorption branch of the isotherm curve of sample has a general shape like Type I isotherms. A purely microporous adsorbent will exhibit a concave-shaped isotherm with very high monolayer adsorption at low relative pressure (less than 0.01) before it reaches a plateau. The narrow micropores result in overlapping adsorption potential fields of opposite walls. This overlapping potential energy creates an enhanced absorbent-adsorbate interaction resulting in high adsorption uptake at low relative pressures (micropore filling phenomenon). The limiting uptake (plateau) depends on the cumulative accessible micropore volume present in the sample.

The hysteresis loop type is mostly found in materials with platy particles having slit-shaped pores, but is associated with micropores in general. Another important feature is the forced closure of desorption branch to adsorption one where relative pressures is low. Disappearance of the hysteresis is due to the instability of the hemispherical meniscus during capillary evaporation in micropores of zeolite. In these micropores, the surface tension forces are stronger than the tensile strength of the liquid causing the meniscus collapse which leads to a spontaneous evaporation of the bulk liquid phase.
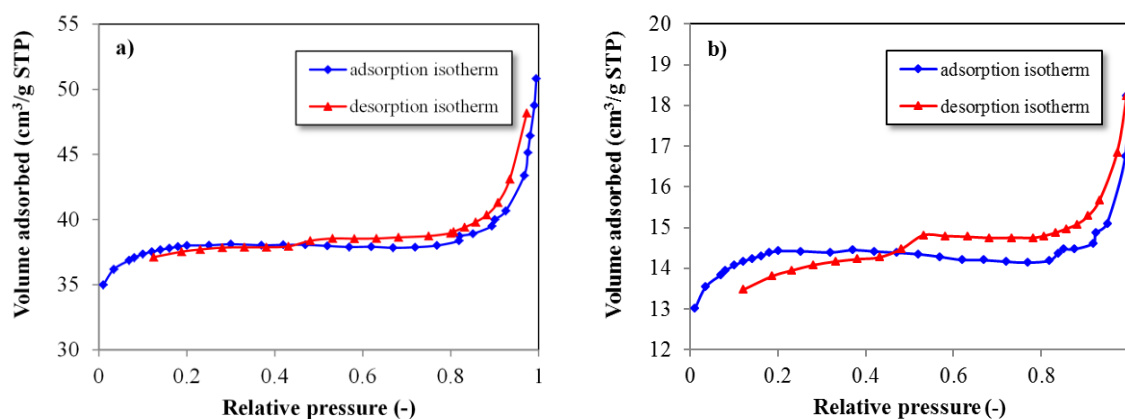
Figure 3-8. (a) N2 adsorption-desorption isotherms at 77 K for Na-A synthesized with conventional oven for 3.5 hours (b) N2 adsorption-desorption isotherms at 77 K for Na-A synthesized with single-mode microwave oven at 300 W 30 min

3.3.5 Thermogravimetric Analysis (TGA) Results

An important property of zeolite is its ability to sorb water into its framework. Thermogravimetric analysis (TGA) of the best sample of this work (300 W and 30 min) showed a weight loss of 19.6 % compared to conventionally synthesised sample of 22.04 % (Figure 3-9), with most of the weight loss occurring at 193.3 ℃ for both samples. This weight loss indicates that the water content in the sample is relatively high confirming the obtained BET surface area. The high potential of water adsorption is one of the characteristic of zeolite. The point of inflection at temperature much higher than 100 ℃ is not related to the reversible adsorption of atmospheric moisture on external surface and macropore of sample. It could be attributed to evaporation of adsorbed water molecules in capillary micropores of synthesised zeolite.
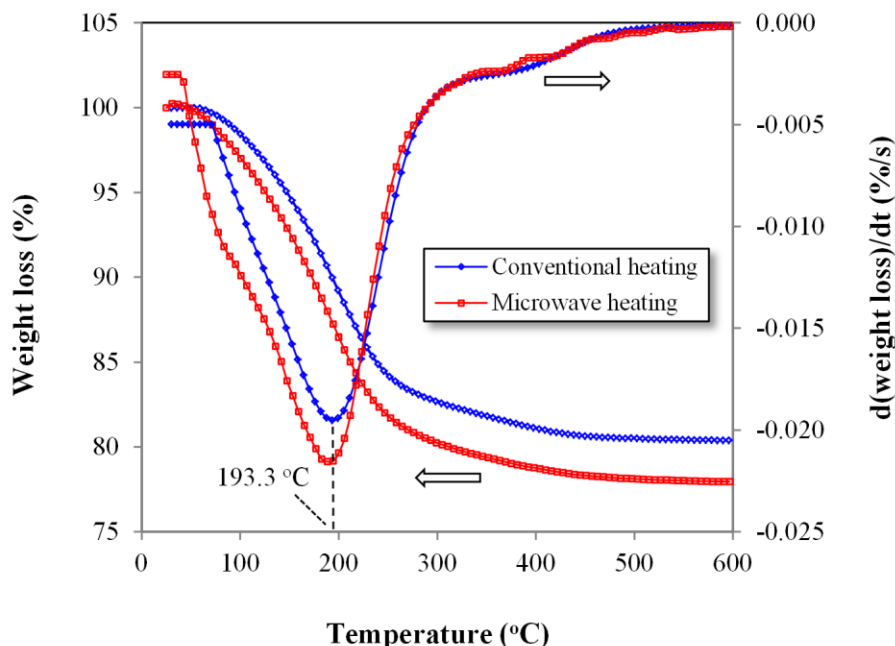
Figure 3-9. TGA pattern of Na-A zeolite

3.3.6 The Cation Exchange Capacity (CEC)

The cation exchange capacity (CEC) CEC is an important physical property of zeolite that determines its quality and utility. CEC of best sample was found to be 2.63 meq/g which is comparable with CEC values obtained in preceding works [39–44] and to the CEC of the zeolite produced using conventional method. The CEC of the conventional synthesis was found to be 3.13 meq/g. Therefore, the CEC of the best sample produced through microwave synthesis is within 84 % of the CEC of the zeolite produced through conventional synthesis.

3.3.7 Analysis of Variance (ANOVA)

Analysis of variance (ANOVA) was used to study which synthesis variables significantly influenced crystallinity and Na-X to Na-A ratio. Empirical models were constructed and assigned alphabetically coded input factors (i.e., P for MW Power, θ for MW time) (Table 3-3 and Table 3-4).

Table 3-3. Summary of the ANOVA of the model equation for the product crystallinity as a function of MW irradiation and time

Source	Sum of Squares	Degrees of Freedom	Mean Square	F value	p value
Model	8324.70	5	1664.94	74.88	0.0024
P	162.14	1	162.14	7.29	0.0738
θ	7333.21	1	7333.21	329.81	0.0004
P.θ	190.44	1	190.44	8.56	0.0612
P^2	115.98	1	115.98	5.22	0.1066
θ^2	522.94	1	23.52	23.52	0.0167

Table 3-4. Summary of the ANOVA of the model equation for Na-X/Na-A peak area ratio as a function of MW irradiation and time

Source	Sum of Squares	Degrees of Freedom	Mean Square	F value	p value
Model	0.046	3	0.015	6.16	0.0392
P	0.021	1	0.021	8.60	0.0325
θ	0.017	1	0.017	6.97	0.0460
P.θ	7.283×10^{-3}	1	7.283×10^{-3}	2.92	0.1484

3.3.8 Response Surface Analysis

The first response curve (RC1) indicating the empirical model of crystallinity. The Model F-value of 74.88 implies the model is significant and there is only a 0.24 % chance that a

Model F-Value this large could occur due to noise. The model equation with significance of 99.9 % is as follows:

$$RC_1 = -84.41 - 0.115P + 11.34\theta - 6.9 \times 10^{-3}P.\theta + 7.61$$

$$\times 10^{-4}P^2 - 0.161\theta^2$$

(Eq. 3-1)

The second response curve (RC2) indicating the empirical model of the Na-X to Na-A ratio. The Model F-value of 5.91 implies the model is significant and there is only a 3.81 % chance that a Model F-Value this large could occur due to noise. The model equation with significance of 99.95 % is as follows:

(Eq. 3-2)

$$RC_2 = -0.0829 - 5.98 \times 10^{-4}P + 5.38 \times 10^{-3}\theta$$

The energy irradiated to the reaction vessel directly influenced the crystallinity of the final product. These results are summarized in Table 3-5. Higher MW power irradiation increases the crystallinity of the products. The advantage of working at a higher power level is that the oscillating electromagnetic field is active for a longer time, leading to a stronger dissolution effect. The experimental results can be more easily compared if energy per gram (kJ/g) transferred in each run to the reaction mixture is considered. These values have been calculated by time-integrating the released output energy by the total weight of material.

The total energy irradiated per gram of product, E, is related to the crystallinity of the product according to the following equation:

$$\text{Crystallinity} = 100\,(1 - 1.504\,e^{-0.071E})\text{where E} > 5.75 \text{ kJ/g}$$

(Eq. 3-3)

The above equation was obtained by fitting the data from Table 3-5. The R^2 value of over 0.92 shows that the exponential model fits well with the experimental data.

Table 3-5. Crystallinity and transfer of energy

Controlled variable		Transferred Energy	Response
Time (min)	Power (W)	kJ/g product	Crystallinity
30	variable	4.06	0.46
30	variable	19.77	56.75
30	variable	20.50	74.81
10	100	8.67	3.62
20	100	18.27	61.11
30	100	28.34	83.35
10	200	8.99	4.03
20	200	19.11	54.87
30	200	29.73	81.93
10	300	9.80	27.36
20	300	21.99	72.42
30	300	32.30	79.49
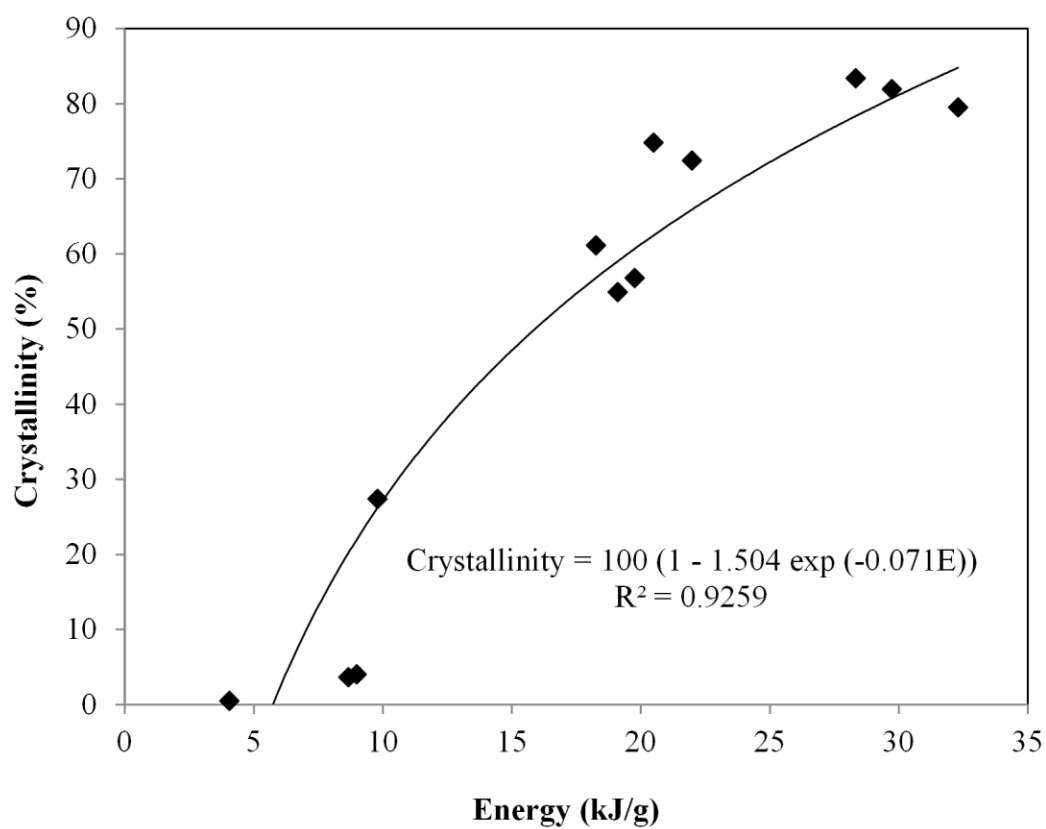
Figure 3-10. Effect of irradiation energy on crystallinity of the Na-A zeolite product

The total energy irradiated per gram of product also has a strong trend with the purity of the zeolite produced. While the ratio of Na-X to Na-A is at its maximum at lowest amount of energy irradiated this ratio quickly drops to zero as the amount of microwave irradiation is increased. This strong linear trend is calculated from the data in Table 3-6 and shown in Figure 3-11.

Table 3-6. Experiments using the formula (3.165 Na$_2$O:1 Al$_2$O$_3$:1.926 SiO$_2$:128 H$_2$O)

after 30 minutes irradiation

Microwave expositions		Transferred Energy	Response	
Controlled variable		kJ/g product	Na-X/Na-A Peak Area	Crystallinity
Temperature (°C)	Power (W)			
100	variable	4.06	N/A	0.46
110	variable	19.77	0.943	56.75
120	variable	20.50	0.659	74.81
variable	100	28.34	0.171	83.35
variable	200	29.73	0.152	81.93
variable	300	32.30	0.000	79.49
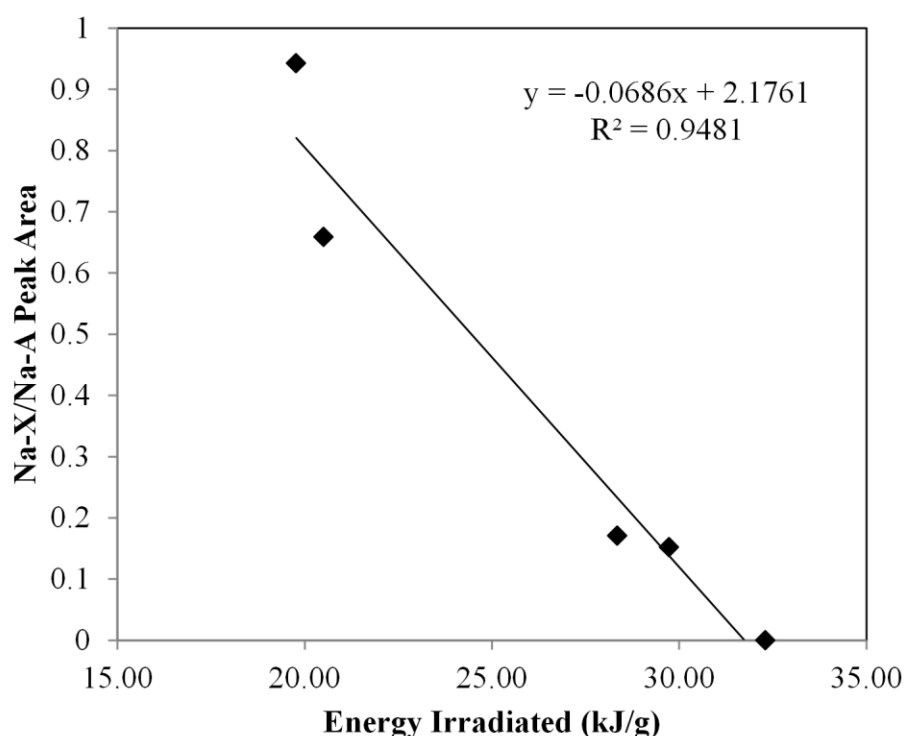
Figure 3-11. Effect of energy irradiation on the phase purity of the MW synthesized zeolite

A linear trend line can be drawn through the data collected in Table 3-6. The R^2 of 0.94 shows that the purity of zeolite crystal phases produced is strongly related to both MW irradiation energy (function of both MW power and MW irradiation time). It can be concluded that the MW irradiation energy strongly influences both the crystallinity and the purity of the final product.

3.4 Conclusions

Na-A zeolite was synthesized using a single mode microwave heating method. The synthesis solution with the composition of 3.165 Na_2O:1 Al_2O_3:1.926 SiO_2:128 H_2O and aged for two hours. Two sets of experiments were performed, the first set with constant temperatures of 100, 110, and 120 °C and variable microwave power, while the other set with constant powers of 100, 200, and 300 W microwave heating for 30 min at atmospheric pressure. It was demonstrated that the microwave energy released to a

synthesis mixture at atmospheric pressure can produce pure zeolite A. The presence of zeolite Na-A and Na-X crystals was verified by both XRD and SEM. The BET surface area and the CEC of the zeolite produced utilizing microwave were compared to the zeolite produced by conventional synthesis. Producing zeolite through microwave synthesis significantly shortens (50%) the production time of the zeolite compared to conventional heating and both methods result in comparable BET surface area. The CEC of Zeolite produced by microwave is within 85% compared to conventional synthesis. The microwave irradiation power plays a significant role in producing a single phase zeolite, furthermore, the total amount of microwave irradiated energy also strongly influences the purity of the zeolite produced. The constant temperature product had lower crystallinity due to the fact that the overall microwave energy irradiated to the samples were lower comparted with the set of experiments conducted with constant power. Higher power and total energy irradiation produce pure Na-A compared to a mixture of Na-X and Na-A at lower power and energy irradiation. Single mode microwave is also more effective in the production of zeolite as relatively low power is required to achieve the same results. In this study power of 100 W and 300 W were used from a single mode microwave source compared to many previous studies where the power source was as high as 1000 W. A condenser attached to the reaction vessel maintained the reaction mixture at atmospheric pressure. The setup naturally requires more energy because the condenser refluxes the evaporated water from the reaction mixture back into the Teflon vessel.

3.5   REFERENCES

[1]   Li Y, Yang W. Microwave synthesis of zeolite membranes: A review. J Membr Sci 2008;316:3–17.

[2]   Perreux L, Loupy A. A tentative rationalization of microwave effects in organic synthesis according to the reaction medium, and mechanistic considerations. Tetrahedron 2001;57:9199–223.

[3]   Abrishamkar M, Azizi SN, Kazemian H. The Effects of Various Sources and Templates on the Microwave-assisted Synthesis of BZSM-5 Zeolite. Z Für Anorg Allg Chem 2011;637:312–6.

[4]   Gordon J, Kazemian H, Rohani S. Rapid and efficient crystallization of MIL-53 (Fe) by ultrasound and microwave irradiation. Microporous Mesoporous Mater 2012;162:36–43.

[5]   Mehdipourghazi M, Moheb A, Kazemian H. Incorporation of boron into nano-size MFI zeolite structure using a novel microwave-assisted two-stage varying temperatures hydrothermal synthesis. Microporous Mesoporous Mater 2010;136:18–24.

[6]   Sabouni R, Kazemian H, Rohani S. A novel combined manufacturing technique for rapid production of IRMOF-1 using ultrasound and microwave energies. Chem Eng J 2010;165:966–73.

[7]   Sistani S, Ehsani MR, Kazemian H, Didari M. Microwave Assisted Synthesis of Nano Zeolite Seed for Synthesis Membrane and Investigation of its Permeation Properties for H2 Separation. Iran J Chem Chem Eng Res Note Vol 2010;29.

[8]   Song H, Wan X, Sun X. Preparation of Agy zeolites using microwave irradiation and study on their adsorptive desulphurisation performance. Can J Chem Eng 2013;91:915–23.

[9]   Cundy C, Zhao J. Remarkable synergy between microwave heating and the addition of seed crystals in zeolite synthesis—a suggestion verified. Chem Commun 1998;14:1465–6.

[10]   Katsuki H, Furuta S, Komarneni S. Microwave-versus Conventional-Hydrothermal Synthesis of Hydroxyapatite Crystals from Gypsum. J Am Ceram Soc 1999;82:2257–9.

[11]   Madhusoodana CD, Das RN, Kameshima Y, Okada K. Microwave-assisted hydrothermal synthesis of zeolite films on ceramic supports. J Mater Sci 2006;41:1481–7.

[12]   Chu P, Dwyer FG, Vartuli JC. Crystallization method employing microwave radiation. 4,778,666, 1988.

[13]   Kim DS, Chang J-S, Hwang J-S, Park S-E, Kim JM. Synthesis of zeolite beta in fluoride media under microwave irradiation. Microporous Mesoporous Mater 2004;68:77–82.

[14]   Gharibeh M, Tompsett GA, Yngvesson KS, Conner WC. Microwave synthesis of zeolites: effect of power delivery. J Phys Chem B 2009;113:8930–40.

[15]   Muraza O, Bakare IA, Tago T, Konno H, Adedigba A, A. M. Al-Amer, Z.H. Yamani, T. Masuda. Controlled and rapid growth of MTT zeolite crystals with low-aspect-ratio in a microwave reactor. Chem Eng J 2013;226:367–76.

[16]   Park S-E, Kim DS, Chang J-S, Kim WY. Synthesis of MCM-41 using microwave heating with ethylene glycol. Catal Today 1998;44:301–8.

[17]   Slangen PM, Jansen JC, Van Bekkum H. The effect of ageing on the microwave synthesis of zeolite NaA. Microporous Mater 1997;9:259–65.

[18]   Bonaccorsi L, Proverbio E. Microwave assisted crystallization of zeolite A from dense gels. J Cryst Growth 2003;247:555–62.

[19]   Zhang X, Tang D, Jiang G. Synthesis of zeolite NaA at room temperature: The effect of synthesis parameters on crystal size and its size distribution. Adv Powder Technol 2013;24:689–96.

[20]   Zhao XS, Lu GQ, Zhu HY. Effects of ageing and seeding on the formation of zeolite Y from coal fly ash. J Porous Mater 1997;4:245–51.

[21]   Stojkovic SR, Adnadjevic B. Investigation of the NaA zeolite crystallization mechanism by i.r. spectroscopy. Zeolites 1988;8:523–5.

[22]   Valtchev VP, Bozhilov KN. Evidences for Zeolite Nucleation at the Solid−Liquid Interface of Gel Cavities. J Am Chem Soc 2005;127:16171–7.

[23]   Auerbach SM, Carrado KA, Dutta PK. Handbook of zeolite science and technology. New York, NY, USA: CRC Press; 2003.

[24]   Yuan W, Chen H, Chang R, Li L. Synthesis and characterization of NaA zeolite particle as intumescent flame retardant in chloroprene rubber system. Particuology 2011;9:248–52.

[25]   Sapawe N, Jalil AA, Triwahyono S, Shah MIA, Jusoh R, Salleh NFM, et al. Cost–effective microwave rapid synthesis of zeolite NaA for removal of methylene blue. Chem Eng J 2013;229:388–98.

[26]   Morschhäuser R, Krull M, Kayser C, Boberski C, Bierbaum R, P. A. Püschner, T. Glasnov, K.C. Oliver. Microwave-assisted continuous flow synthesis on industrial scale. Green Process Synth 2012;1:281–90.

[27]   Robson HE, Lillerud KP. Verified syntheses of zeolitic materials. 2nd ed. Amsterdam, The Netherlands: Elsevier; 2001.

[28]   Treacy MMJ, Higgins JB. Collection of simulated XRD powder patterns for zeolites. Amsterdam, The Netherlands: Elsevier; 2007.

[29]   Bain DC, Smith BFL. Chemical Analysis. Handb. Determinative Methods Clay Mater., Glasgow : New York: Blackie ; Chapman and Hall; 1987, p. 248–74.

[30]   Jansen JC, Arafat A, Ebaid AR, Van Bekkum H. Microwave Techniques in Zeolite Synthesis. Synth. Microporous Mater. Mol. Sieves, vol. 1, Van Nostrand Reinhold; 1992, p. 507–21.

[31]   Barrer RM. Hydrothermal chemistry of zeolites. Toronto, Canada: Academic; 1982.

[32]   Breck DW. Zeolite Molecular Sieves: Structure, Chemistry and Use. Anal Chim Acta 1975;75:493.

[33]   Block E, Gillies JZ, Gillies CW, Bazzi AA, Putman D, L.K. Revelle, D. Wang, X. Zhang. Allium chemistry: microwave spectroscopic identification, mechanism of formation, synthesis, and reactions of (E, Z)-propanethial S-oxide, the lachrymatory factor of the onion (Allium cepa). J Am Chem Soc 1996;118:7492–501.

[34]   Musyoka NM, Petrik LF, Hums E, Baser H, Schwieger W. In situ ultrasonic diagnostic of zeolite X crystallization with novel (hierarchical) morphology from coal fly ash. Ultrasonics 2014;54:537–43.

[35]   Musyoka NM, Petrik LF, Hums E, Baser H, Schwieger W. In situ ultrasonic monitoring of zeolite A crystallization from coal fly ash. Catal Today 2012;190:38–46.

[36]   De Man AJM, Van Santen RA. The relation between zeolite framework structure and vibrational spectra. Zeolites 1992;12:269–79.

[37]   Sing K, Everett D, Haul R, Moscou L, Peirotti R, Rouquerol J. IUPAC commission on colloid and surface chemistry including catalysis. Pure Appl Chem 1985;57:603–19.

[38]   Rouquerol F, Rouquerol J, Sing KSW. Adsorption by powders and porous solids. Waltham, MA, USA: Academic Press; 1999.

[39]   Qiu W, Zheng Y. Removal of lead, copper, nickel, cobalt, and zinc from water by a cancrinite-type zeolite synthesized from fly ash. Chem Eng J 2009;145:483–8.

[40]   Shoumkova A, Stoyanova V. Zeolites formation by hydrothermal alkali activation of coal fly ash from thermal power station "Maritsa 3", Bulgaria. Fuel 2013;103:533–41.

[41]   Chareonpanich M, Jullaphan O, Tang C. Bench-scale synthesis of zeolite A from subbituminous coal ashes with high crystalline silica content. J Clean Prod 2011;19:58–63.

[42]   Juan R, Hernández S, Andrés JM, Ruiz C. Synthesis of granular zeolitic materials with high cation exchange capacity from agglomerated coal fly ash. Fuel 2007;86:1811–21.

[43]   Liu H, Peng S, Shu L, Chen T, Bao T, Frost RL. Magnetic zeolite NaA: Synthesis, characterization based on metakaolin and its application for the removal of Cu^{2+}, Pb^{2+}. Chemosphere 2013;91:1539–46.

[44]   Tanaka H, Fujii A, Fujimoto S, Tanaka Y. Microwave-Assisted Two-Step Process for the Synthesis of a Single-Phase Na-A Zeolite from Coal Fly Ash. Adv Powder Technol 2008;19:83–94.

Chapter 4

4 A COMPARATIVE STUDY USING DIRECT HYDROTHERMAL AND INDIRECT FUSION METHODS TO PRODUCE ZEOLITES FROM COAL FLY ASH UTILIZING SINGLE MODE MICROWAVE ENERGY[1]

Abstract

This paper investigates the effects of microwave irradiation on the synthesis of zeolite Na-A from coal fly ash at atmospheric pressure. Microwave irradiation has shown to accelerate zeolitization from several hours to several minutes. A single mode laboratory scale microwave was employed, which enabled control of irradiated power and temperature of the reaction mixture, while the pressure was controlled by affixing a condenser on the 40 mL Teflon reactor vessel with a working volume 20 mL. Design of Experiment was used to compare two methods of converting CFA to zeolite-A, direct hydrothermal method and indirect fusion method. Experiments conducted were two level four factorial design. The first factor considered was the categorical factor of conversion method (hydrothermal vs fusion), while the other three factors investigated were power (P), time (θ), aluminate concentration (δ). Zeolite produced from CFA (CFAZA) was characterized using XRD, FTIR, SEM, TGA, BET, and Cation Exchange Capacity (CEC). It was observed that the crystallinity of the product was influenced by factors such as, conversion method, power, time and aluminate concentration. The hydrothermal and fusion products were comparable to each other in their characteristics, however, hydrothermal CFAZA performed better at immobilizing heavy metal ions and showed better crystalline structure whereas, fusion CFAZA had a higher BET surface area and a slightly higher CEC. Regardless of the performance of the categorical factors the other

---

factors, i.e. power, time and aluminate concentration followed the same trend for both types of CFAZA.

4.1   Introduction

Coal-fired power is an important corner store of world energy production. About half of the world's electric energy is generated using coal. It is imperative to decrease the environmental impact of burning coal in power plants for an environmentally friendly and greener utilization of coal. Employment of coal fly ash (CFA) to produce value added compounds could be one way of reducing the negative impact of coal power plants on the environment. Burning of pulverized coal in coal-fired power plants produces residue of fine particles that rise with the flue gas, this residual is called fly ash. According to Association of Canadian Industries Recycling Coal Ash (CIRCA), Canada produces upwards of 4,679,000 tons of coal fly ash (CFA) and only 31% is recycled compared to 88% recycling in Europe. The world produced 780 million metric tons of coal combustion by product and recycled 52.6 % [1]. One major use for coal fly ash is in the manufacturing of cement due to its pozzolanic properties. Since the 1950, CFA has been used in concrete and cement manufacturing; USA and EU utilize about 6 and 9 million tons of CFA, respectively each year. It is a prevalent opinion that a ton of CFA used to replace cement saves the use of an equivalent of nearly one barrel of oil [2]. United States produced about 180 million cubic meters of ready mix concrete with about 50 % utilizing CFA as a supplemental cementitious material. Leaching of toxic elements from concrete produced with CFA has shown to be much lower than contamination levels [3,4] while the strength [5] and modulus of elasticity increased [6]. CFA is classified as a human carcinogen [7]; therefore, it is necessary to find a novel method that is energy efficient and economically feasible to utilize it in manufacturing of value added materials. The use of CFA can have important economic and environmental implications. It is opined that a ton of CFA recycled saves the use of an equivalent of nearly one barrel of oil [2].

CFA is largely composed of Al and Si that can be used as starting materials to synthesis zeolites. Zeolites are multipurpose crystalline aluminosilicates that can be used to purify air and water, catalyze reactions and for countless more industrial uses. The conversion

of CFA into zeolite is a hydrothermal reaction. The conventional methods of zeolite preparation using CFA involve digestion and dissolution, nucleation, and crystal growth. This conversion occurs under high temperature provided through conventional heating methods. It has been suggested that microwave (MW) and ultrasound (US) can be used as alternate sources of energy for synthesizing porous materials. MW and US energy sources could decrease the reaction time remarkably. [8–11] The significant decrease in the reaction time would mean that zeolitization of CFA would be a more attractive option for industrialization of the process. This will not only solve the problem of waste, but also produce value added compound (i.e. zeolite) that can be used for purifying of air, water and soil and for many other industrial uses.

There have been different methods introduced for conversion of CFA into zeolite, such as direct hydrothermal method [12], indirect fusion followed by hydrothermal conversion [13,14], two step hydrothermal method [15] and molten salt liquid free method [16]. Many pioneering work done in the conversion of CFA in zeolite with direct hydrothermal method [12–14,16–20,20] and indirect fusion method [14,21,22], has utilized conventional heating methods. There are also work utilizing novel energy methods such as microwave and ultrasound energies to convert CFA to zeolite, however, little work is done in comparing the two methods. There has been some work done previously to compare direct hydrothermal conversion method and indirect fusion method of converting CFA to zeolite using conventional heating source [23,24]. Molina and Poole [23] evaluated direct hydrothermal and indirect fusion methods at different reaction conditions of temperature, time, and proportion of NaOH to CFA. The crystallinity and CEC was consistently higher for the zeolite produced through fusion compared to hydrothermal conversion. Sakthivel et al. [24] converted CFA to zeolite for cleaning up of oil spills. It was reported that zeolites produced through fusion performed better with higher oil absorption capacity. However, there is no work done to our knowledge that compares the two methods while using microwave irradiation at atmospheric pressure. This paper utilizes novel energy method, i.e. single mode microwave to accelerate crystallization at atmospheric pressure instead of conventional heating method at autogenous pressure. The two methods are compared utilizing microwave irradiation during crystal growth and exploring the effects of microwave irradiation power,

irradiation time and aluminate concentration in the precursor solution and their interactions on the quality of zeolite produced. Multiple characterization techniques are used to compare the two conversion methods.

4.2 Materials and Methods

4.2.1 Materials

Coal fly ash was obtained from coal fired power plant (OPG, Nanticoke) located in the Ontario province of Canada and was stored in seal container before use. Sodium hydroxide (Alphachem, Canada), sodium aluminate anhydrous (Sigma-Aldrich, USA) and sodium metasilicate, (Sigma-Aldrich, USA) were of analytical grade and used as received. Deionized (DI) water was used for the preparation of the solutions. Other chemicals used for characterization tests were of analytical grade. The experiments were performed with a precursor composition of: 4.714 Na_2O:1 Al_2O_3:1.780 SiO_2:192 H_2O for high level aluminum mole composition and 4.714 Na_2O: 0.582 Al_2O_3:1.780 SiO_2:192 H_2O for low level aluminum mole composition in factorial design of experiment.

4.2.2 Direct Hydrothermal Conversion

Coal fly ash (CFA) was converted into LTA zeolite by a single step hydrothermal alkaline treatment [12]. A typical zeolite-synthesis procedure from coal fly ash (CFA) was carried out as follows: 2.18 g of sodium hydroxide granules with 1.82 g of fly ash (NaOH/CFA ratio of 1.2) were dissolved in 17 ml deionized water, and mixed at 60 ºC for 12 h using a mechanical stirrer. Afterwards, 1 mL aqueous sodium aluminate solution (concentration: 0.155 g/mL) was added to the above mixture to bring the mole composition of the reactant mixture to 4.714 Na_2O: 0.582 Al2O3:1.780 SiO_2:192 H_2O for low-level aluminum mole composition in factorial design of experiment. For high-level aluminum mole composition, however, 3 mL of the aqueous sodium aluminate solution was added to bring the molar composition of the crystallization gel to 4.714 Na_2O:1 Al_2O_3:1.780 SiO_2:192 H_2O. Subsequently the mixture was subjected to microwave radiation for crystallization. The crystallization experiments were carried out using single mode microwave heating under atmospheric pressure. A cylindrical PTFE vessel (28 mm ID$\times$ 108 mm) attached with a reflux condenser was placed in the microwave chamber for

varied periods of time and temperature. The experiments were performed in a self-adjusting, microwave oven (single-mode, 2.45 GHz, CEM cooperation, Discover, USA), where the reaction temperature and power were monitored automatically. In a single mode microwave, electromagnetic irradiation is directed through a precisely-designed wave guide that produces a standing wave, whereas in multimode microwave there are is no single standing wave but a mixture of many waves with different phase shifts. The microwave field density in a single mode microwave are much higher compared to multimode microwave therefore similar results can be achieved in single-mode microwave using lower power than in high power multimode microwave [25]. The temperature was measured using infrared pyrometer installed in the microwave chamber and was constantly monitored and controlled through a PID built-in controller in the MW. The system consists of a microwave generator, a condenser and a laptop computer to record power and temperature profiles. After a given period of MW irradiation, the solid products were filtered off, washed with deionized water until the pH reached around 8, and dried overnight at 100 ºC in an electric oven.

4.2.3 Indirect Fusion Conversion

Indirect fusion method for the conversion of coal fly ash (CFA) converted to Na-A zeolite (CFAZA) introduces fusion of dry NaOH with CFA at high temperature prior to hydrothermal treatment [14]. Fusion synthesis experiment for production of zeolite Na-A from coal fly ash was carried out as following.1.82 g of sodium hydroxide (granules) and 1.82 g of fly ash were fused at 550 °C for two hours then added in 17 ml deionized water. The mixture was then stirred for 2 h at 20°C. Afterwards sodium aluminate solution was added to the reaction mixture [26] to a final reaction mixture composition of 4.714 Na_2O: 0.582 Al_2O_3:1.780 SiO_2:192 H_2O for low level aluminum mole composition in factorial design of experiment and 4.714 Na_2O:1 Al_2O_3:1.780 SiO_2:192 H_2O for high level. Hereon, the procedure was identical to direct hydrothermal synthesis.

The zeolite produced from pure chemical precursors utilizing conventional oven by following verified method published by International Zeolite Association (IZA) [27].

4.2.4 Characterization

Chemical composition of the CFA sample was determined by means X-ray fluorescence spectroscopy (XRF) utilizing PANalytical PW2400 Wavelength Dispersive. Rigaku–Miniflex powder diffractometer (Japan) was used to collect XRD data of the raw CFA sample and the synthesized zeolites using CuKα (λ for Kα = 1.54059 Å) over the range of 5°<2θ<40° with step width of 0.02°. The obtained crystalline phase was indicated based on standard peaks in literature [28]. The peak areas of the products were determined by "peak fitting" algorithm in the MDI-Jade v 7.5 software (Livermore, California). A series of characteristic peaks were observed at the 2θ of 7.25º, 10.25º, 12.55º, 16.20º, 21.80º, 24.10º, 27.25º, 30.10º, and 34.35º, which were in agreement with reference peaks that belong to Na-A zeolite. The Fourier transform infrared (FTIR) spectra of the samples were recorded on solid state by a Vector 22 spectrometer (MA, USA). Spectra were performed on the 550-2000 cm^{-1} spectral region, with resolution of 4 cm^{-1} and 32 scan. Crystal size distribution and morphology of zeolite were studied by scanning electron microscope (SEM) JSM 600F (Joel, Japan) operating at 10 keV of acceleration voltage. The thermo-gravimetrical analyses (TGA) of the samples were performed using a Mettler Toledo TGA/SDTA 851e model (Switzerland) with version 6.1 Stare software. The samples were heated from 30 °C to 600 °C at heating rate of 10 °C/min under nitrogen purge. Specific surface area and pore size of the prepared samples were measured by means of BET technique (Micrometrics ASAP 2010). Known amounts of samples (e.g. 50-80 mg) were loaded into the BET sample tube and degassed under vacuum (10-5 Torr) at 125 °C for 6 h. Cation exchange capacity (CEC) was measured using ammonium acetate saturation method (5 days) based on Bain and Smith [29]. Inductively coupled plasma-atomic emission spectroscopy (ICP-AES) is used to measure the elemental concentration of different ions inside the solution. To measure the leaching resistance of the FCA and produced zeolite, supernatant liquid obtained by soaking the sample in de-ionized water (after 7 days) was measured by Vista Pro CCD Simultaneous ICP-AES (Varian, Australia) using ICP expert software (version: v 4.0). The percent yield of zeolite demonstrating the efficiency of the zeolite synthesis procedure was calculated by dividing the dried solid product by dry solid CFA and NaOH added in the solution.

4.2.5 Experimental Design

The conversion process of CFA to Na-A zeolite was designed by means of a statistical approach using a four-level, double-factorial design. Design-Expert 7.1.5 software (StatEase, Minneapolis, USA) was used to investigate the effect of each reaction parameter on the crystallinity of Na-A produced. The effects of conversion method (fusion vs direct hydrothermal), power, time and aluminum concentration for continuous MW irradiation at atmospheric pressure were investigated. Detailed indications of the four factors and two levels employed for the experimental technique and the response examined are summarized in Table 4-1.

Table 4-1. Detailed experimental design for the conversion of CFA into zeolite Na-A

Experiment	Run	Method	Power (W)	Time (min)	Al (M)	Peak Area
1	8	Fusion	100	10	0.0945	0
2	1	Hydrothermal	100	10	0.0945	1200
3	12	Fusion	300	10	0.0945	0
4	4	Hydrothermal	300	10	0.0945	1572
5	6	Fusion	100	30	0.0945	861
6	2	Hydrothermal	100	30	0.0945	709
7	11	Fusion	300	30	0.0945	1327
8	13	Hydrothermal	300	30	0.0945	1417
9	15	Fusion	100	10	0.284	209
10	5	Hydrothermal	100	10	0.284	1866
11	14	Fusion	300	10	0.284	1314

12	16	Hydrothermal	300	10	0.284	1747
13	9	Fusion	100	30	0.284	1105
14	7	Hydrothermal	100	30	0.284	2025
15	10	Fusion	300	30	0.284	2049
16	3	Hydrothermal	300	30	0.284	2206

4.3 Results and Discussion

4.3.1 X-ray analysis (XRF and XRD)

The chemical composition of the CFA that was used as starting materials and the main source of Si and Al for fusion and hydrothermal zeolitization process are summarized in Table 4-2. The loss on ignition can be related to the presence of unburnt carbon in the CFA samples. The SiO2/Al2O3 ratio was found to be 2.13, which was a good predictor of the potential to synthesize low silica zeolite crystallites such as LTA type zeolite. According to the XRD data, the main components of CFA are amorphous aluminosilicate as well as quartz and mullite that exist as crystalline as indicated in Table 4-2.

Table 4-2. XRF analysis of chemical composition of CFA

Parameter	Weight percent (%)
Major oxide	
SiO_2	41.78
Al_2O_3	19.61
CaO	13.64
Fe_2O_3	5.79
MgO	3.23
TiO_2	1.39
K_2O	1.1
Na_2O	0.94
P_2O_5	0.71

BaO	0.36
SrO	0.25
Cr_2O_3	0.01
MnO	0.02
Loss On Ignition	10.89
Total	99.72
Phases analysis	
Amorphous aluminosilicate	88
Quartz (SiO_2)	8
Mullite ($3Al_2O_3.2SiO_2$)	3
Others	1

*SiO_2/Al_2O_3: 2.13

The XRD patterns of the CFA used and the fused CFA (FCFA) with NaOH are depicted in Figure 4-1. It can be clearly seen that the characteristic peaks of crystalline structure of quartz, mullite, calcite and hematite significantly decrease after fusion of CFA with NaOH. The reason for the breakdown of these crystalline structures is associated with high temperature and diffusion of liquid NaOH into the CFA structure [14]. The XRD pattern of the fused CFA shows that new peaks can be observed and these peaks are associated with soluble aluminates and silicates originally present in the CFA [30]. The soluble aluminates and silicates are formed due to the incorporation of NaOH into the framework of the amorphous and crystalline phases present in the CFA which makes it easier to dissolve into the liquid than amorphous aluminosilicates present in unfused CFA [14,23].
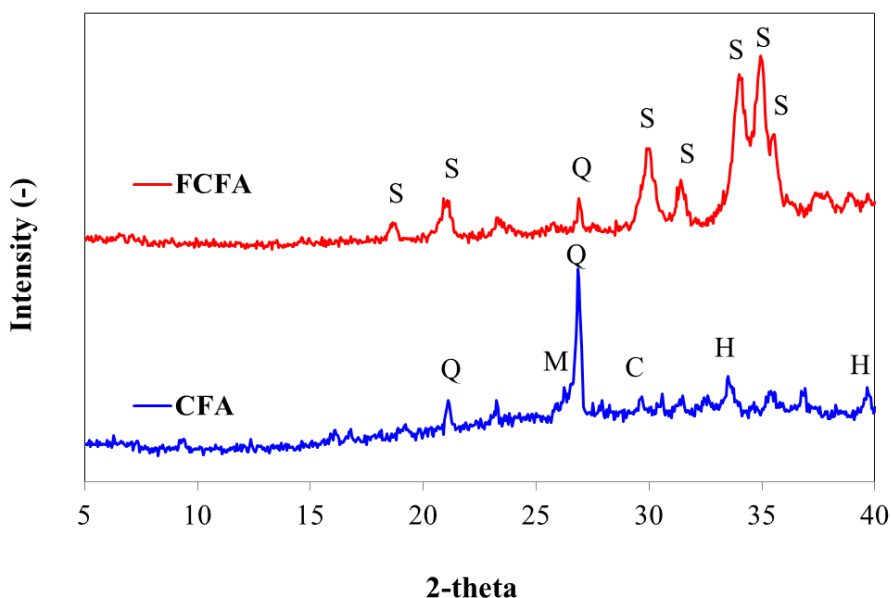
Figure 4-1. XRD patterns of CFA and Fused CFA (Characteristic Peaks C: Calcite, H: Hematite, M: Mullite, S: Soluble Fused CFA, Q: Quartz)

This incorporation of solid NaOH into the CFA not only affects the dissolution of CFA into the reaction solution but also plays a significant role in the yield. It can be observed that the yield of fused CFA is much higher than hydrothermal CFA. It can be concluded by performing t-test analysis that the yield of the two methods is statically significant with 99 % confidence interval. Table 3 outlines the experiments and the yield of the dried product.

Table 4-3. Yield Percentage of CFAZA produced through Hydrothermal and Fusion methods with respect to dissolved solids and with respect to CFA dissolved. CFA: 1.82 g, NaOH: 2.18 g

Experiment	Power (W)	Time (min)	Al (M)	Method	$\frac{CFAZA}{CFA+NaOH}(\%)$
2	100	10	0.0945	Hydrothermal	33.75

4	300	10	0.0945	Hydrothermal	34.75
6	100	30	0.0945	Hydrothermal	32.00
8	300	30	0.0945	Hydrothermal	35.75
10	100	10	0.284	Hydrothermal	35.50
12	300	10	0.284	Hydrothermal	37.00
14	100	30	0.284	Hydrothermal	35.50
16	300	30	0.284	Hydrothermal	36.00
1	100	10	0.0945	Fusion	48.50
3	300	10	0.0945	Fusion	48.75
5	100	30	0.0945	Fusion	52.75
7	300	30	0.0945	Fusion	53.75
9	100	10	0.284	Fusion	48.85
11	300	10	0.284	Fusion	47.60
13	100	30	0.284	Fusion	50.85
15	300	30	0.284	Fusion	47.60

The XRD patterns of CFAZA synthesized by microwave crystallization through hydrothermal and fusion methods are presented in Figure 4-2 (a,b), respectively for precursor solution of 4.714 Na2O:1 Al2O3:1.780 SiO2:192 H2O. The XRD patterns for the lower aluminate mole ratio followed the same trend however, had a smaller peak height and peak area as indicated in Table 1. The characteristic peaks of most zeolites appear at low 2θ value of less than 10° [28]. The peaks appear at 2θ ranging from 5 to 24 degree and match with those for zeolite Na-A, which confirm successful formation of

LTA zeolite as the major crystalline phase of the zeolitized CFA [27,28]. It is observed that XRD peaks for CFAZA produced through hydrothermal conversion are smooth, while for fusion methods the XRD peaks are rough and noisy. This could be explained through the difference in the dissolution mechanism of the two methods.

In the case of hydrothermal conversion, the coal fly ash slowly dissolves into the alkaline solution over a longer period of time, after the dissolution of CFA, zeolite nuclei form on the surface of the residual CFA particles [15]. As the amorphous CFA is mostly covered with crystalline CFAZA therefore the XRD pattern is smooth. However, in the case of fusion method the fused soluble aluminosilicate quickly dissolve into the reaction mixture [21] and the aluminosilicate crystallize while residue CFA still persist in the solution, therefore showing noisy XRD peaks.
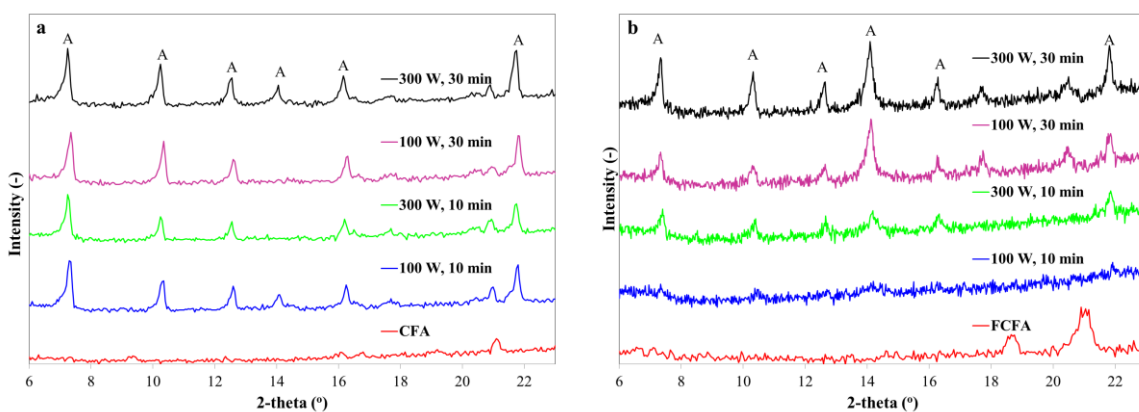
Figure 4-2. XRD of a) CFA and hydrothermal CFAZA b) fused CFA and fusion CFAZA (Characteristic Peaks A= Zeolite A)

4.3.2 Fourier transform infrared (FTIR)

Figure 4-3 depicts the FTIR results of the CFAZA produced through direct hydrothermal synthesis method and indirect fusion synthesis method at higher alumina ratio, along with the FTIR of raw CFA and the fused CFA, respectively. It can be noted that in Figure 4-3, there is no peak present at 560 cm^{-1} or 960 cm^{-1} for the CFA; however, sharp peaks can be observed in the case of CFAZA, clearly demonstrating the production of zeolite. The FTIR spectrum of the zeolite during and after termination of crystallization contains a number of characteristic vibration bands in the regions 1100-900 cm^{-1}, 700-650 cm^{-1}, and

560 cm^{-1}. Band at about 960 cm-1 corresponding either to the stretching vibrations of Si-O bonds in SiO4 or to the skeleton of bonded SiO4 tetrahedra, shows the greatest change during crystallization [31,32]. Band at 670 cm^{-1} indicates that the

Si is liberation in the zeolite framework and substitution by additional Al and Na [32]. The spectrum band at 560 cm^{-1} corresponds to D4R vibration. The presence of water in the zeolite sample corresponds to bending and stretching of water molecules at 1625 cm^{-1} [33,34]. The band at 1625 cm-1 like the bands at 560 cm^{-1}, 670 cm^{-1} and 960 cm^{-1} increases sharply as the power and time of the microwave irradiation increases, indicating better water sorption capacity and higher crystallinity. Similar trend is observed for CFAZA produced with lower level of alumina however, the peaks' intensities observed are smaller.
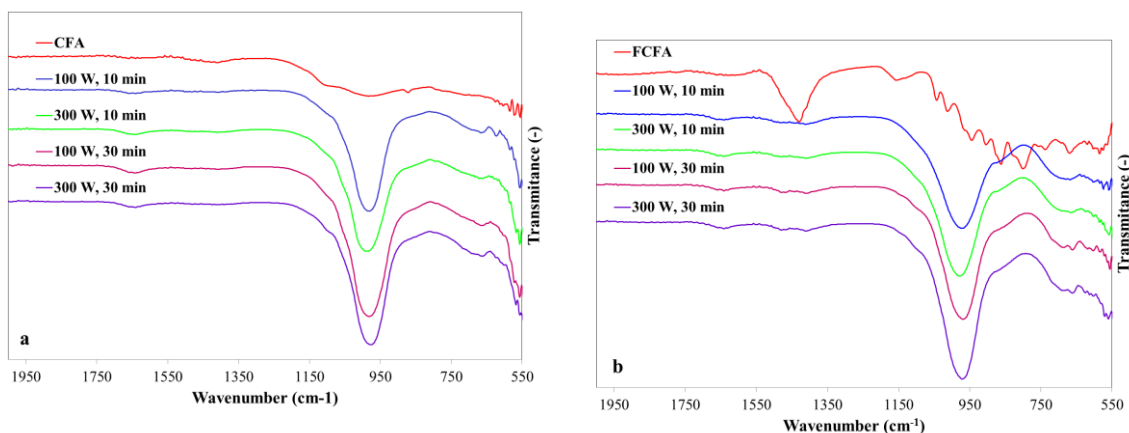
Figure 4-3. FTIR results a) CFA and hydrothermal CFAZA b) fused CFA and Fusion CFAZA

4.3.3 Scanning Electron Microscope (SEM)

Scanning electron microscope (SEM) images of the raw CFA and the synthesized zeolites are illustrated in Figure 4-4 (a-d). Evidence of characteristic cubic crystallites of Na-A zeolite validates the XRD data. The Na-A zeolite morphology is characterized by regulated cubic shaped crystals with approximate dimensions of 2-5 μm. The SEM data corroborates the explanation provided above about two different rates of dissolution resulting in CFAZA formed either on the surface of CFA or as agglomerated chunks in

the liquid. It can be seen in the SEM Figure 4-4 (b) that the CFAZA produced through a direct hydrothermal treatment is deposited on the surface of the amorphous spherical phase of the CFA, while the CFAZA produced through fusion step is agglomerated together and have nucleated and grown regardless of the lack of amorphous CFA presence. It can be seen in Figure 4-4 (d) that CFAZA produced with fusion step have amorphous debris deposited around them. The presence of this debris can be associated with the roughness of XRD peaks observed. The morphology of the CFAZA produced with indirect fusion conversion is similar to the morphology of zeolite produced through pure chemicals using verified synthesis techniques (Figure 4-4 (c)), in both samples the cubes have sharp edges, however in the case of hydrothermal conversion the crystal cubes are deposited on amorphous CFA structure. The SEM images of indirect fusion conversion show chamfered-edged cube. This difference might be associated with the same phenomenon that produces the difference between the two methods in XRD results.
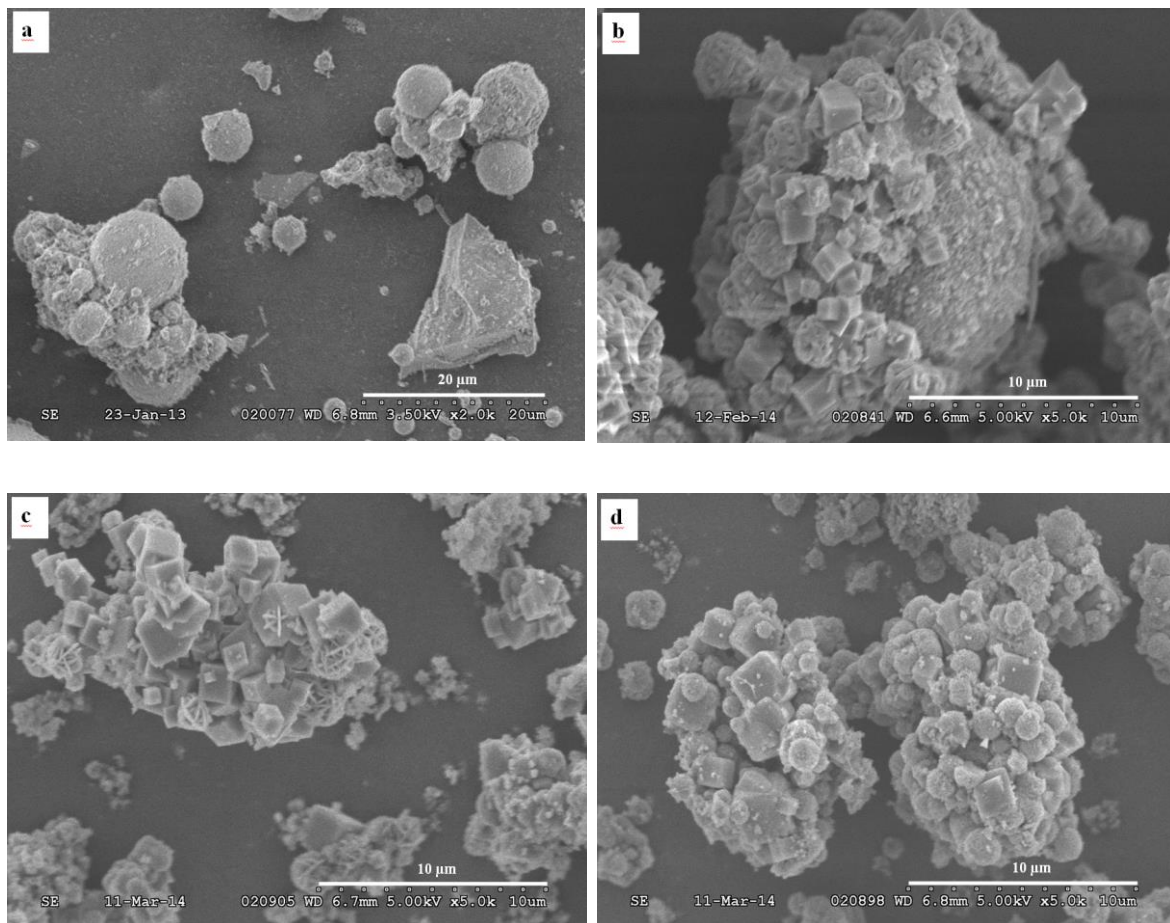
Figure 4-4. SEM image of CFA and the synthesized zeolites a) CFA b) Hydrothermal CFAZA c) Zeolite-A produced with pure chemical precursors d) Fusion CFAZA

4.3.4 Thermal Analysis (TGA)

Thermo-gravimetric analysis (TGA) curve of the CFA and its zeolitized counterpart are illustrated in Figure 4-5. The samples were subjected to TGA test without special pre-treatment. The CFA showed a weight loss of 6.1 %, in which most of the weight loss occurs at 105 ℃. This gentle slope weight variation and the trend of heat flow changes are a particular behavior of CFA and attributed to the reversible adsorption of atmospheric moisture on external surface and macropore of CFA. TGA curves of both CFAZA produced from direct hydrothermal method and indirect fusion a 10 % and 15 % weight loss, respectively, while sharing a point of inflection at approximately 158 ℃.

This weight loss indicates that the water content in these samples is higher than CFA sample confirming the obtained BET micropore surface area. It could be attributed to evaporation of adsorbed water molecules on the porous structure of the synthesized zeolite.
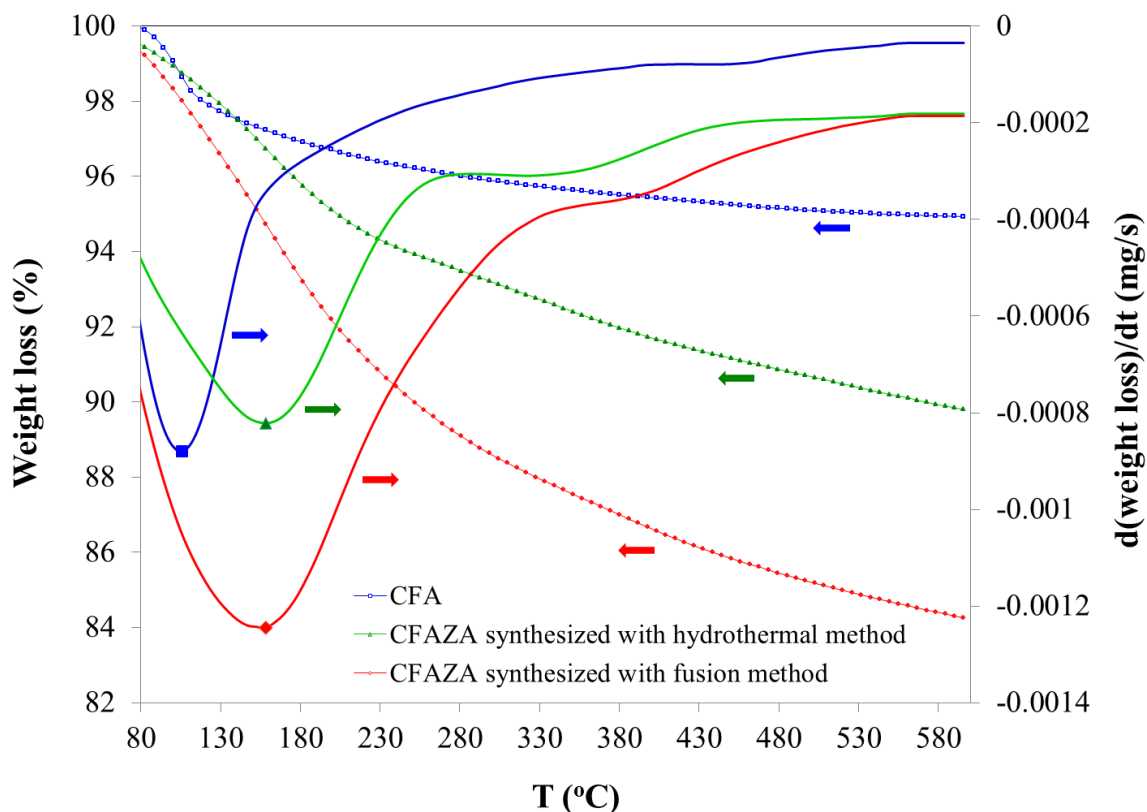
Figure 4-5. TGA Thermo-gravimetric analysis of CFA, hydrothermal CFAZA and fusion CFAZA

4.3.5 Surface area and N_2 adsorption tests (BET)

BET surface areas of the CFAZA sample synthesized utilizing hydrothermal and fusion methods at 300 W for 30 min with mole ratio of 4.714 Na_2O:1 Al_2O_3:1.780 SiO_2:192 H_2O were 42 m^2/g. and 641 m^2/g, respectively. The BET surface areas of CFAZA synthesized were a dramatic improvement over the BET surface area of 15 m^2/g for raw CFA, however, the surface area of zeolite synthesized from pure chemicals still had the highest BET surface area of 127 m^2/g. The BET adsorption and desorption curves are illustrated in Figure 4-6 (a-d). The shape of the adsorption/desorption isotherm and its

hysteresis pattern provide useful information about the physisorption mechanism, which can be used to qualitatively predict the types of pores present in the adsorbent. The hysteresis between the adsorption isotherm and desorption isotherm is thought to be due to the different size pores being combined. The obtained adsorption-desorption curve of CFAZA sample is a special type of isotherm shape, classified as Type IIB [35]. Based on International Union of Pure and Applied Chemistry (IUPAC) isotherm classification [36], the adsorption branch of the isotherm has a general shape like Type II isotherms such as nonporous aluminosilicate. This adsorption isotherm profile represents a monolayer-multilayer adsorption mechanism of the gas on the open and stable solid surface. A type II isotherm is normally associated with monolayer-multilayer adsorption on an open and stable external surface of a powder, which may be non-porous, macroporous or even to a limited extent microporous. The desorption branch of the isotherm is a distinct H3-type hysteresis loop indicating mesoporous aluminosilicate [35]. The H3 hysteresis loop type is mostly found in materials with platy particles having slit-shaped mesopores. These materials are not purely mesoporous as there is no indication of the completion of mesopore filling that would result in a plateau at higher relative pressures as in a typical Type IV isotherm. Characteristic features of the type IV isotherm are its hysteresis loop, which is associated with capillary condensation taking place in mesopores, and the limiting uptake over a range of high relative pressures. A significant volume of macropores in these materials results in the absence of the isotherm plateau at high relative pressures as seen in Type IV isotherms.

Another important feature observed in BET isotherm like many hysteresis patterns is the forced closure of desorption branch to adsorption one where relative pressures is low. Disappearance of the hysteresis (Tensile Strength Effect) is due to the instability of the hemispherical meniscus during capillary evaporation in pores with diameters smaller than approximately 4 nm. In these pores, the surface tension forces are stronger than the tensile strength of the liquid causing the meniscus collapse which leads to a spontaneous evaporation of the bulk liquid phase. The presence of "forced closure" in the isotherm shape may indicate a significant volume of pores with diameters smaller than 4 nm.
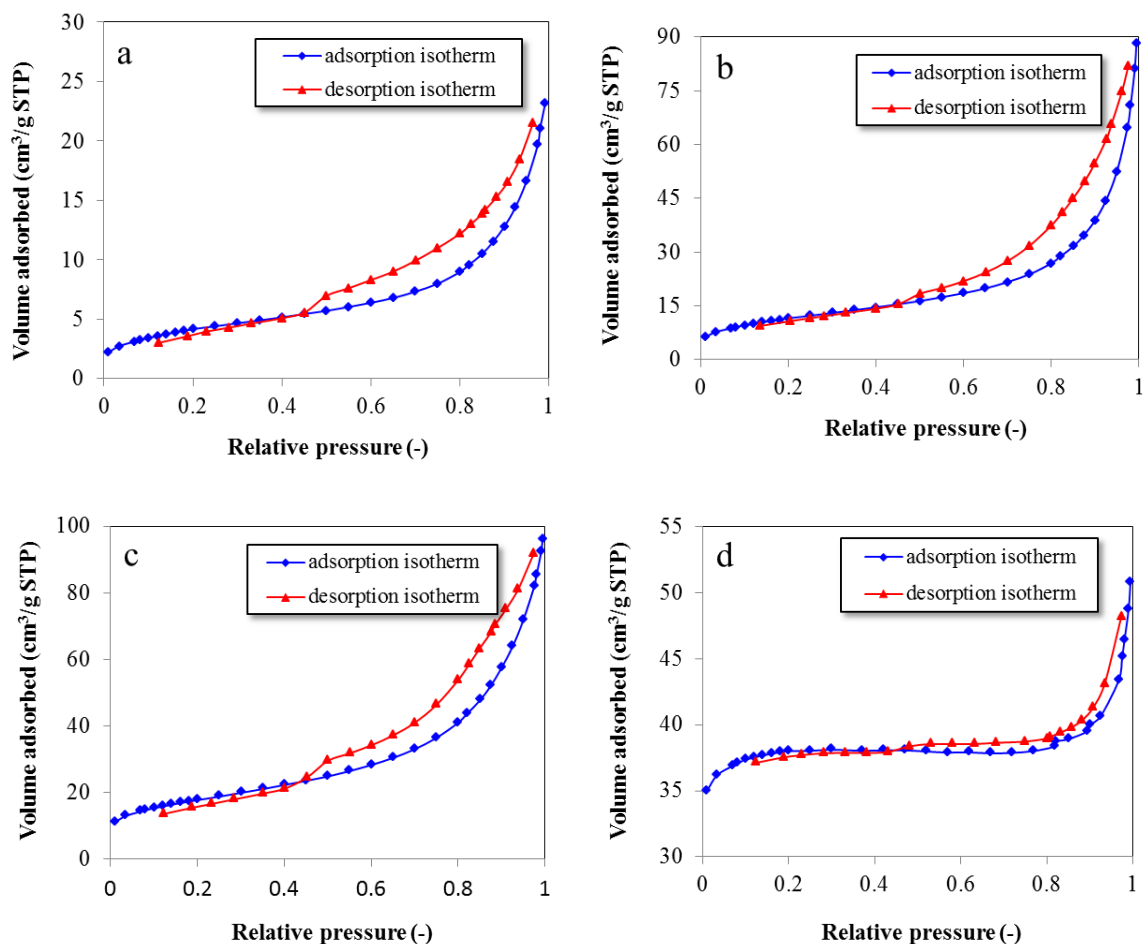
Figure 4-6. Adsorption and desorption isotherms of CFA and the synthesized zeolites a) CFA b) Hydrothermal CFAZA c) Fusion CFAZA d) Zeolite-A synthesized from pure chemical precursors

4.3.6 Leach Test

Results of typical leaching tests obtained using elemental analysis data of the leached ions after soaking the CFA and zeolite samples in ammonium accelerate solution for 7 days 25 ºC are summarized in Table 4-4. The concentration of different elements such as Fe, V, B, Be, Cr, Se, Co, and Pb, which were analyzed using ICP technique were remarkable lower in the leachate solution of the synthesized zeolitic product compared to the original coal fly ash. Hydrothermal conversion performed better than fusion conversion in immobilizing the heavy metal ions in the CFAZA framework. The summary of these results are given in Table 4-4. Hydrothermal CFAZA was better at

immobilizing all the observed heavy metal ions including Boron, Barium, Chromium, Manganese, and Nickel. While it performed just as good at immobilizing other ions as the CFAZA produced through fusion method. This immobilization maybe explained by the deposition difference of the two CFAZA. In the case of hydrothermal CFAZA, it is observed that the zeolite crystals deposit on the surface of the amorphous CFA particles thus sorbing heavy metal ions before they are liberated into the solution, however, in the case of fusion CFA it can be observed that the zeolite particles are agglomerated in the solution and therefore cannot come in contact with the CFA particles directly.

Table 4-4. ICP results from CFA and zeolite produced from fusion and hydrothermal method

Element	CFA (ppm)	Fusion (ppm)	Hydrothermal (ppm)
Al	1.450	0.05272	1.835
As	0.03390	0.03271	0.03330
B	4.317	0.4359	0.1374
Ba	1.965	2.987	1.961
Ca	448.96	424.42	486.71
Cu	0.06876	0.1860	0.2360
Cr	0.1505	0.0389	0.00516
Fe	0.3936	0.05753	0.3347
Mn	0.01544	0.01296	0.008547
Ni	0.05112	0.07892	0.04978
Pb	0.2700	0.2438	0.2525

V	0.02411	0.01231	0.01032

4.3.7 Cation Exchange Capacity (CEC)

The cation exchange capacities (CEC) synthesized CFAZA through hydrothermal and fusion method were found to be 2.43 meq/g and 2.22 meq/g, respectively. This was a dramatic improvement over the CEC of raw CFA of 0.3 meq/g. These CEC values are comparable to the zeolitized CFA reported by other researchers [37,38] indicating that the produced zeolite has a great potential to be used as adsorbent in different environmental remediation processes. The CEC values are given in Figure 4-7.
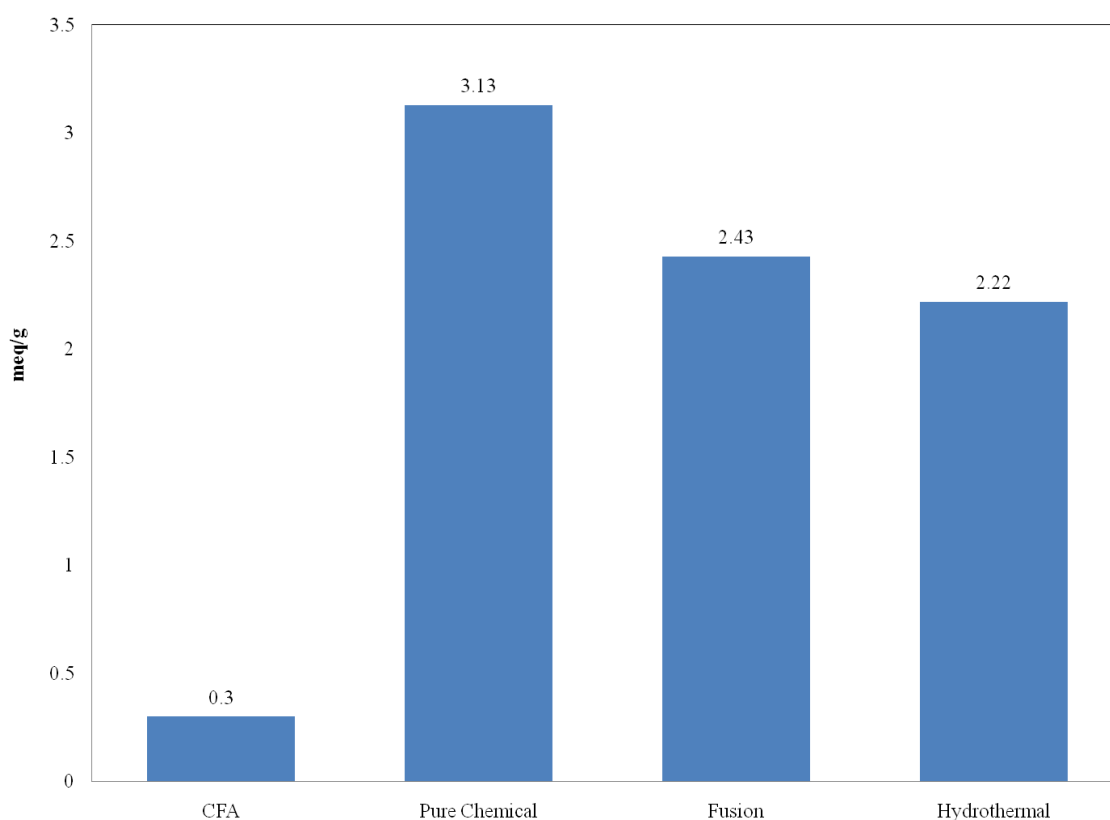
Figure 4-7. Cation Exchange (CEC) of different zeolite-A produced compared with CFA

4.3.8 Design of Experiment (DOE)

Analysis of variance (ANOVA) was used to study the variables that significantly influence crystallinity of the zeolite produced from CFA. Empirical models were constructed and assigned alphabetically coded input factors (i.e. α for the conversion method, P for MW Power, θ for MW irradiation time, δ for sodium aluminate concentration). Summary of the ANOVA of the model equation can be found in Table 4-5.

Table 4-5. Summary of the ANOVA of the model equation for the product yield as a function of conversion method, microwave irradiation power, time and sodium aluminate concentration

Source	Sum of Squares	Degrees of Freedom	Mean Square	F value	p value
Model	7.531×10^6	12	6.276×10^5	33.53	0.0073
α	2.159×10^6	1	2.159×10^6	115.33	0.0017
P	8.359×10^5	1	8.359×10^5	44.66	0.0068
θ	8.982×10^5	1	8.982×10^5	47.99	0.0062
δ	1.846×10^6	1	1.846×10^6	98.64	0.0022
$\alpha \cdot P$	1.178×10^5	1	1.178×10^5	6.29	0.0870
$\alpha \cdot \theta$	9.250×10^5	1	9.250×10^5	49.42	0.0059
$\alpha \cdot \delta$	13053.036	1	13053.06	0.70	0.4649
$P \cdot \theta$	55342.56	1	55342.56	2.96	0.1840
$P \cdot \delta$	19951.56	1	19951.56	1.07	0.3778
$\theta \cdot \delta$	31240.56	1	31240.56	1.67	0.2869

$\alpha \cdot P \cdot \theta$	4.228×10^5	1	4.228×10^5	22.59	0.0177
$\alpha \cdot \theta \cdot \delta$	2.073×10^5	1	2.073×10^5	11.07	0.0448

The Model F-value of 33.53 implies the model is significant. There is only a 0.73% chance that a "Model F-Value" this large could occur due to noise. The p values of less than 0.0500 indicate model terms are significant. In this case α (conversion method), P (power), θ (irradiation time), δ (aluminate concentration), and the interactions of $\alpha \cdot \theta$, $\alpha \cdot P \cdot \delta$, $\alpha \cdot \theta \cdot \delta$ are significant model terms. Values greater than 0.1000 indicate the model terms are not significant. However, some of the insignificant model terms are needed to be included to preserve the hierarchical design of the model.

Significance of $\alpha \cdot \theta$, $\alpha \cdot P \cdot \delta$ and $\alpha \cdot \theta \cdot \delta$ in the model indicate strong interaction between α (conversion method) and θ (time) and the interaction of α with P·θ and $\theta \cdot \delta$ indicate that conversion method plays significantly impacts the irradiation time, combination of power with time and time with the aluminate concentration in the precursor gel on zeolite crystallinity. The interactions of P·θ and $\theta \cdot \delta$ on peak area has p-values of 0.0870 and 0.4649, respectively, are greater than 0.05, therefore, insignificant in the absence of categorical factor of conversion method (α). It can be concluded that conversion method not only affects the crystallinity of the product but also affects factors such as time, power and aluminate concentration on the crystallinity of the zeolite produced.

When the peak areas of the two methods are compared it can statistically be stated with a 97% confidence that two data are different. It can be observed that the peak area observed in the hydrothermal method of conversion is statistically higher than in fusion conversion. Therefore, hydrothermal conversion can yield a better crystalline product than indirect fusion conversion.

Furthermore, the empirical equations Eq. (4-1)-Eq. (4-3) have been calculated. Equation (Eq. 2-1) gives the continuous equation for the model whereas equations Eq. (4-2) and Eq. (4-3) separate the two categorical factors hydrothermal method and fusion method into two different categorical equations, respectively.

$$Peak\ Area = 1225.44 + 367.31 \cdot \alpha + 228.56 \cdot P + 236.94 \cdot \theta + 339.69 \cdot \delta -$$
$$85.81 \cdot \alpha \cdot P - 240.44\ \alpha \cdot \theta + 28.56 \cdot \alpha \cdot \delta + 58.81 \cdot P \cdot \theta + 35.31 \cdot P \cdot \delta + 44.19 \cdot \theta \cdot \delta -$$
$$162.56 \cdot \alpha \cdot P \cdot \delta - 113.81 \cdot \alpha \cdot \theta \cdot \delta$$

Eq. (4-1)

$$Peak\ Area = 936.81 + 2.79 \cdot P - 43.67 \cdot \theta + 3237.47 \cdot \delta + 0.0588 \cdot P \cdot \theta - 13.43 \cdot P \cdot \delta$$
$$+ 166.75 \cdot \theta \cdot \delta$$

Eq. (4-2)

$$Peak\ Area = -599.23 - 1.98 \cdot P + 49.88 \cdot \theta + 576.51 \cdot \delta + 0.0588 \cdot P \cdot \theta +$$
$$20.88 \cdot P \cdot \delta - 73.48 \cdot \delta$$

Eq. (4-3)

4.4   Conclusions

CFA was converted into Na-A zeolite using a single mode microwave heating. Two method of converting CFA were investigated (direct hydrothermal and indirect fusion) along with three other factors (power, time, aluminate concentration). The synthesis solution with composition of 4.714 Na_2O:1 Al_2O_3:1.780 SiO_2:192 H_2O for high level aluminum mole composition and 4.714 Na_2O: 0.582 Al_2O_3:1.780 SiO_2:192 H_2O for low level aluminum mole composition in factorial design of experiment were used. It was demonstrated that the microwave energy released to a synthesis mixture at atmospheric pressure can produce pure zeolite A from CFA at atmospheric pressure. Zeolite produced from CFA (CFAZA) was characterized using FTIR, XRD, BET, TGA, and Cation Exchange Capacity (CEC). The hydrothermal and fusion products were comparable to each other in their characteristics, however, hydrothermal CFAZA performed better at immobilizing heavy metal ions and showed better crystalline structure whereas, fusion CFAZA had a higher BET surface area and a slightly higher CEC. The differences between the properties of the two different CFAZA are suggested to be due to the difference in the dissolution of aluminum and silicon content of CFA into the reaction gel. It is also observed that the XRD peaks for hydrothermal conversion are sharper higher and with bigger area under the peaks indicating a better crystallinity. The empirical equations found using the DOE shows that the method of conversion plays a

significant role in the crystallinity of CFAZA, while interacts with other numerical factors such as microwave irradiation power & time and the concentration of aluminum in the gel precursor. It is found that CFAZA produced by direct hydrothermal is comparable with the properties of CFAZA produced through indirect fusion conversion under microwave irradiation at atmospheric pressure. Indicating that a direct hydrothermal conversion would be efficient method of converting CFA into zeolite-A under atmospheric condition.

4.5   References

[1]   Heidrich C, Feuerborn, H, Weir, A. Coal Combustion Products: a Global Perspective. World Coal Ash WOCA, Lexington, KY: 2013.

[2]   Querol X, Moreno N, Umana J t, Alastuey A, Hernández E, López-Soler A, et al. Synthesis of zeolites from coal fly ash: an overview. Int J Coal Geol 2002;50:413–23.

[3]   Garrabrants AC, Kosson DS, DeLapp R, van der Sloot HA. Effect of coal combustion fly ash use in concrete on the mass transport release of constituents of potential concern. Chemosphere 2014;103:131–9.

[4]   Liu R, Durham SA, Rens KL. Effects of post-mercury-control fly ash on fresh and hardened concrete properties. Constr Build Mater 2011;25:3283–90.

[5]   Poon CS, Lam L, Wong YL. A study on high strength concrete prepared with large volumes of low calcium fly ash. Cem Concr Res 2000;30:447–55.

[6]   Duran-Herrera A, Juarez CA, Valdez P, Bentz DP. Evaluation of sustainable high-volume fly ash concretes. Cem Concr Compos 2011;33:39–45.

[7]   Borm PJA. Toxicity and occupational health hazards of coal fly ash (CFA) A review of data and comparison to coal mine dust. Ann Occup Hyg 1997;41:659–76.

[8]   Gordon J, Kazemian H, Rohani S. Rapid and efficient crystallization of MIL-53 (Fe) by ultrasound and microwave irradiation. Microporous Mesoporous Mater 2012;162:36–43.

[9]   Sabouni R, Kazemian H, Rohani S. A novel combined manufacturing technique for rapid production of IRMOF-1 using ultrasound and microwave energies. Chem Eng J 2010;165:966–73.

[10]   Shah BA, Shah AV, Jadav PY. Extractive efficacy for acephate of microwave synthesized zeolitic materials: equilibrium and kinetics. J Serbian Chem Soc 2013;78:1055–77.

[11]   Chindaprasirt P, Rattanasak U, Taebuanhuad S. Role of microwave radiation in curing the fly ash geopolymer. Adv Powder Technol 2013;24:703–7.

[12]   Holler H, Wirsching U. Zeolite formation from fly ash. Fortschr Mineral 1985;63:21–43.

[13]   Kazemian H, Naghdali Z, Ghaffari Kashani T, Farhadi F. Conversion of high silicon fly ash to Na-P1 zeolite: Alkaline fusion followed by hydrothermal crystallization. Adv Powder Technol 2010;21:279–83.

[14]   Shigemoto N, Hayashi H, Miyaura K. Selective formation of Na-X zeolite from coal fly ash by fusion with sodium hydroxide prior to hydrothermal reaction. J Mater Sci 1993;28:4781–6.

[15]   Hollman GG, Steenbruggen G, Janssen-Jurkovičová M. A two-step process for the synthesis of zeolites from coal fly ash. Fuel 1999;78:1225–30.

[16]   Park M, Choi CL, Lim WT, Kim MC, Choi J, Heo NH. Molten-salt method for the synthesis of zeolitic materials: I. Zeolite formation in alkaline molten-salt system. Microporous Mesoporous Mater 2000;37:81–9.

[17]   Murayama N, Takahashi T, Shuku K, Lee H, Shibata J. Effect of reaction temperature on hydrothermal syntheses of potassium type zeolites from coal fly ash. Int J Miner Process 2008;87:129–33.

[18]   Musyoka NM, Petrik LF, Fatoba OO, Hums E. Synthesis of zeolites from coal fly ash using mine waters. Miner Eng 2013;53:9–15.

[19]   Shoumkova A, Stoyanova V. Zeolites formation by hydrothermal alkali activation of coal fly ash from thermal power station "Maritsa 3", Bulgaria. Fuel 2013;103:533–41.

[20]   Tanaka H, Fujii A. Effect of stirring on the dissolution of coal fly ash and synthesis of pure-form Na-A and -X zeolites by two-step process. Adv Powder Technol 2009;20:473–9.

[21]   Musyoka NM, Petrik LF, Balfour G, Gitari WM, Hums E. Synthesis of hydroxy sodalite from coal fly ash using waste industrial brine solution. J Environ Sci Health Part A 2011;46:1699–707.

[22]   Yaping Y, Xiaoqiang Z, Weilan Q, Mingwen W. Synthesis of pure zeolites from supersaturated silicon and aluminum alkali extracts from fused coal fly ash. Fuel 2008;87:1880–6.

[23]   Molina A, Poole C. A comparative study using two methods to produce zeolites from fly ash. Miner Eng 2004;17:167–73.

[24]   Sakthivel T, Reid D, Goldstein I, Hench L, Seal S. Hydrophobic High Surface Area Zeolites Derived from Fly Ash for Oil Spill Remediation. Environ Sci Technol 2013.

[25]   Morschhäuser R, Krull M, Kayser C, Boberski C, Bierbaum R, P. A. Püschner, T. Glasnov, K.C. Oliver. Microwave-assisted continuous flow synthesis on industrial scale. Green Process Synth 2012;1:281–90.

[26]   Musyoka NM, Petrik L, Hums E. Synthesis of Zeolite A, X and P from a South African Coal Fly Ash. Adv Mater Res 2012;512:1757–62.

[27]   Robson HE, Lillerud KP. Verified syntheses of zeolitic materials. 2nd ed. Amsterdam, The Netherlands: Elsevier; 2001.

[28]   Treacy MMJ, Higgins JB. Collection of simulated XRD powder patterns for zeolites. Amsterdam, The Netherlands: Elsevier; 2007.

[29]   Bain DC, Smith BFL. Chemical analysis. Handb. Determinative Methods Clay Mineral., Glasgow: Blackie; 1987, p. 248–74.

[30]   Musyoka NM, Petrik LF, Hums E. Ultrasonic assisted synthesis of zeolite A from coal fly ash using mine waters (acid mine drainage and circumneutral mine water) as a substitute for ultra pure water. Int. Mine Water Assoc., Aachen, Germany: 2011, p. 423–8.

[31]   De Man AJM, Van Santen RA. The relation between zeolite framework structure and vibrational spectra. Zeolites 1992;12:269–79.

[32]   Stojkovic SR, Adnadjevic B. Investigation of the NaA zeolite crystallization mechanism by i.r. spectroscopy. Zeolites 1988;8:523–5.

[33]   Davis KM, Tomozawa M. An infrared spectroscopic study of water-related species in silica glasses. J Non-Cryst Solids 1996;201:177–98.

[34]   Efimov AM, Pogareva VG. IR absorption spectra of vitreous silica and silicate glasses: The nature of bands in the 1300 to 5000 cm- 1 region. Chem Geol 2006;229:198–217.

[35]   Rouquerol F, Rouquerol J, Sing K. Adsorption by Powder & Porous Solid. London: Academic Press; 1999.

[36]   Sing K, Everett D, Haul R, Moscou L, Peirotti R, Rouquerol J. IUPAC commission on colloid and surface chemistry including catalysis. Pure Appl Chem 1985;57:603–19.

[37]   Tanaka H, Fujii A, Fujimoto S, Tanaka Y. Microwave-Assisted Two-Step Process for the Synthesis of a Single-Phase Na-A Zeolite from Coal Fly Ash. Adv Powder Technol 2008;19:83–94.

[38]   Kazemian H, Ghaffari Kashani T, Noorian SM. Synthesis and characterization of zeolite A, using fly ash of the Iran Ferrosilice Company and investigating its ion-exchange properties. Iran J Crystallogr Mineral 2005;13:329–36.

Chapter 5

5 EFFECT OF ULTRASOUND ENERGY ON THE ZEOLITIZATION OF CHEMICAL EXTRACTS FROM FUSED COAL FLY ASH[1]

Abstract

This paper investigates the effects of ultrasound (UTS) energy at different temperatures on the zeolitization of aluminosilicate constituents of coal fly ash. UTS energy was irradiated utilizing probe immersed into the reaction mixture unlike previously reported works that have used UTS baths. Controlled synthesis was also conducted at constant stirring and at the same temperatures using conventional heating. The precursor reaction solution was obtained by first fusing the coal fly ash with sodium hydroxide at 550°C followed by dissolution in water and filtration. The synthesized samples were characterized by XRF, XRD, SEM and TGA. The crystallinity of crystals produced with UTS assisted conversion compared to conventional conversion at 85°C was twice as high. UTS energy also reduced the induction time from 60 min to 40 min and from 80 min to 60 min for reaction temperatures of 95°C and 85°C, respectively. Prolonging the UTS irradiation at 95°C resulted in the conversion of zeolite-A crystals to hydroxysodalite, which is a more stable zeolitic phase. It was found that at 85°C coupled with ultrasound energy produced the best crystalline structure with a pure single phase of zeolite-A. It has been shown that crystallization using UTS energy can produce zeolitic crystals at lower temperatures and within one hour, dramatically cutting the synthesis time of zeolite.

5.1 Introduction

Ultrasound (UTS) energy has been utilized in many chemical syntheses ranging from synthesis of metal and semiconductor particles, polymers, organic compounds, cleaning

---

of industrial equipment, leather processing, drug delivery, inter-particle collisions and coupled with electrochemical reactions [1]. The reason for its extensive use is because UTS energy can initiate reactions more easily; furthermore, UTS can accelerate chemical reactions. There are two types of sonochemical reactions, homogenous sonochemistry that results from the formation of radicals or radical intermediates, and heterogeneous sonochemistry that is influenced primarily through the mechanical effects of cavitation, such as surface cleaning, particle size reduction, and improved mass transfer [2]. The sonochemical effects do not come from a direct interaction between sound field and molecular species, but due to acoustic cavitation [3]. The cavitation is produced when gas nuclei that are present in the liquid go through oscillations expanding and compressing during the expansion of the ultrasonic field, creating a vacuum into which gas in the liquid diffuses. During the compression half of the cycle, the gas within the bubbles diffuses back into the host liquid, however, due to the smaller surface area, not all the gas that diffused into the bubble diffuses out. After multiple expansion and compression, micro-bubbles reach a critical size resulting in bubble collapse during one compression cycle. Collapse of these bubbles results in adiabatic heating of gas and vapour inside the bubble. These cavitations produce radicals inducing sonochemical reactions. The hot spots produced due to these cavitations can reach a temperature of 5000°C, the local pressure can go as high as 20 MPa with high cooling rates of 107 °C/s these cavitations result in particle collisions at high velocities [4–6]. There have been many reported works where zeolites have been synthesized utilizing UTS energy [7–14].

Musyoka et al. have converted aluminate and silicate extracts from coal fly ash fused with NaOH at elevated temperatures into zeolites. The progression of these reactions was observed utilizing UTS attenuation technique [15,16]. However, the UTS impulses used in their experiments were 2 MHz so there was no energy input and thus no effect on the zeolitization was expected [17]. It is hypothesized that dissipation of UTS energy in the reaction mixture obtained from fused CFA extracts would shorten the reaction time as observed in experiments conducted using pure chemical precursors [7]. All the previous experiments have investigated the effects of UTS energy on zeolitization from either pure chemical precursors [7–9,13,14] or CFA precursors [10,11]. The brief descriptions of the experimental procedures reported in literature are summarized in Table 5-1.

Table 5-1. Ultrasound assisted zeolite synthesis from literature

Ultrasound				Conventional				
Frequency	Power	Treatment		Crystallization				
ν (kHz)	P (W)	T (ºC)	t (h)	T (ºC)	t (h)	Zeolite	Remarks	Reference
47	n/a	60-70	4-6	n/a	n/a	Na-4A	Pretreated Kaolin at 800°C for 3h	Jin Park et al. [23]
35	n/a	50-60	2-15	n/a	n/a	Na-A	No treatment followed by UTS	Andaç et al. [7]
40	50	50	1	135-150	24-96	MCM-49	--	Wu et al. [14]
40	50	50	0.5-1	135-150	48-400	MCM-22	--	Wang et al. [13]
40	50	n/a	0.5	180	18-72	BZSM-5	--	Abrishamkar et al. [8]
40	50	25	0.5-1.5	160	48-72	ANA	--	Azizi and Yousefpour [9]
35	240	21-46	1	25-60	96	Na-X	CFA fused with NaOH prior to UTS	Belviso et al. [10]
35	240	21-46	1	25-60	96	Na-X	Fused CFA with NaOH, Sea Water	Belviso et al. [11]
n/a	100	30	0.67	800	3	Na-P1	Perlite precursor used	Azizi et al. [8]

To the best of our knowledge, there has been no work reported on the zeolitization process utilizing a UTS probe irradiating energy directly into the reaction solution. It is observed that irradiated UTS energy directly into the reaction solution can dramatically decrease the zeolitization time and form pure single phase crystals at lower temperatures.

5.2   Materials and Methods

5.2.1 Materials

Coal fly ash was procured from a coal fired power plant (OPG, Nanticoke) located in Ontario, Canada, and was stored in seal container before use. Sodium hydroxide (Alphachem, Canada), sodium aluminate anhydrous (Sigma-Aldrich, USA) and sodium metasilicate, (Sigma-Aldrich, USA) were of analytical grade and used as received. Deionized (DI) water was used for the preparation of the solutions.

5.2.2 Method of Conversion of CFA to Zeolite

The method used for converting CFA to zeolite was first introduced by Shigemoto et al. [18]. In this method a dry fusion step is introduced prior to hydrothermal treatment. The procedure outlined in the previous works was followed with few amendments [19]. CFA was fused with sodium hydroxide (granules) at a ratio of 1:1.2 by weight. The solid mixture was treated at 550°C for two hours. The fused substrate was milled to a greenish-yellow powder. The powder was mixed with DI water at a ratio of 1:5 by weight. The slurry mixture was stirred mechanically at 540 rpm for two hours to extract the aluminosilicate components of CFA into the aqueous phase. The slurry was filtered and sodium aluminate solution (0.155 g/mL) was added to the filtrate at volumetric ratio of 3:17. The mixture was aged for two hours at room temperature prior to crystallization.

The reaction mixture was crystallized at varied temperature of 75, 85 and 95°C, and different reaction times of 20, 40, 60, 80, 100, 120 min utilizing UTS probe (Vibra Cell VCX-500, Sonics & Materials, USA) and with conventional heating. A Jacketed crystallizer with re-circulating water system was used to control the temperature during the reaction. Figure 5-1 illustrates the reaction setup with UTS irradiation and without UTS irradiation.

Figure 5-1. Photograph of the experimental setup used for reaction a) temperature control and water circulator b) 500 Watt ultrasonic processor c) noise cancellation box d) ultrasound probe e) crystallizer #1 with UTS assistance f) mixer g) crystallizer #2 conventional heating h) piping for temperature control water circulation

Two identical crystallizers were used for UTS assisted synthesis and conventional synthesis. The experiments were run simultaneously under identical temperature and reaction time. The UTS conversion was conducted by immersing UTS probe into the reaction mixture while conventional conversion synthesis was conducted by utilizing mechanical mixer. The temperature in both crystallizing vessel was by temperature controlled water circulator.

5.2.3 Characterization

Chemical composition of the Coal Fly Ash (CFA) sample was determined by means of X-ray fluorescence spectroscopy (XRF) utilizing a PANalytical PW2400 Wavelength Dispersive System. A MiniFlex powder diffractometer (Rigaku, Woodlands, USA) was

used to collect XRD data of the synthesized samples using CuKα (λ for Kα = 1.54059 Å) over the range of 5°<2θ<40° with step width of 0.02°. ICP-AES (Perkin Elmer Optima-3000 DV System) was utilized to analyze the metal elemental concentration in the reaction mixture. The net intensity was calculated through peak area integration minus the backgrounds. Crystal size distribution and morphology of zeolite were studied by scanning electron microscope (SEM) JSM 600F (Japan) operating at 10 keV of acceleration voltage. The thermal analyses were performed using a Mettler Toledo TGA/SDTA 851e model (Mettler-Toledo Inc., Schwerzenbach, Switzerland) with version 6.1 Stare software. The samples were heated from 30°C to 600°C at a heating rate of 10 °C/min under nitrogen purge of 40 mL/min.

5.3   Results and discussion

5.3.1 X-ray analysis (XRF and XRD)

The chemical compositions of the raw CFA, the fused CFA after ageing and filtration and the produced zeolite were determined using X-ray fluorescence spectroscopy. The results are summarized in Table 5-2. The results show that the chemical composition of raw CFA and aged and filtered CFA are similar with the exception of the presence of sodium in the aged and filtered CFA. The presence of sodium is the result of the addition of NaOH in the fusion step. However, the chemical composition of zeolite produced was dramatically different. The zeolite produced composed mostly of aluminum, silicon and sodium. Silicon to aluminum ratio of the zeolitic crystals produced was close to one and the zeolitic crystal charge was balanced by sodium present in the structure. The other elements present in the CFA samples, such as calcium and iron, were incorporated, however, in limited amount in the zeolitic crystals while magnesium, titanium and potassium were incorporated in the zeolitic composition but in lower amounts compared to the original CFA. The incorporation of titanium in the zeolite structure might be of interest as TiO_2 is extensively researched for its photocatalytic properties for detoxification of organic and inorganic compounds in the purification of polluted air and industrial wastewater [20].

Table 5-2. Chemical composition of the raw CFA, intermediate and final product determined using XRF techniques

Major Oxides	CFA (%)	Post-Ageing (%)	Zeolite-A (%)
SiO_2	33.96	23.64	29.16
Al_2O_3	16.49	12.66	26.07
CaO	11.28	9.37	0.01
Fe_2O_3	4.65	3.66	0.00
MgO	2.72	2.13	0.33
TiO_2	1.16	0.91	0.10
K_2O	0.87	0.26	0.20
Na_2O	0.84	20.66	18.85
SiO_2/Al_2O_3	2.06	1.87	1.12
Loss on Ignition	26.05	26.04	25.28

ICP-AES was conducted to quantify the amount of metallic elements extracted from the CFA into the reaction mixture and the amount left in the supernatant after crystallization and retrieval of the zeolitic product through filtration. The ICP results are summarized in Table 5-3 indicate that the elemental constituents of the CFA dissolved into the reaction mixture. Post crystallization the elemental concentration decreases for all the metallic elements indicating that these elements have been incorporated into the zeolitic product

in varying concentrations that can corroborated with the XRF results. The only exception is aluminum, as the concentration of aluminum increases from post ageing and post crystallization. The reason for this increase is the addition of sodium aluminate into the reaction mixture during the ageing step. This addition of extra sodium aluminate is necessary to the reaction otherwise zeolitic products do not crystallize even though the silica and alumina ratio is close to 1:1 in the reactant mixture. Addition of extra alumina may be required to induce supersaturation in the reaction mixture to drive the crystallization process.

Table 5-3. ICP Elemental concentration of the reaction mixture pre-ageing and post-crystallization

Major Elements	Pre-Ageing (mg/L)	Post-Crystallization
Si	1976.63	536.60
Al	1557.87	7092.63
Ca	2.51	0.63
Fe	17.48	15.80
Mg	0.40	0.07
Ti	2.11	1.34
K	547.03	525.74

*Na concentration was over the equipment's detection limit

XRD analysis was conducted for the zeolite samples produced. It was observed that the zeolite-A (LTA) and hydroxysodalite (SOD) were the two major zeolitic phases present

in the products. The areas of the characteristic peaks for both LTA and SOD were calculated to compare the crystallinities of the products. The XRD results and the calculated peak areas are illustrated in Figure 5-2 and Figure 5-3, respectively.
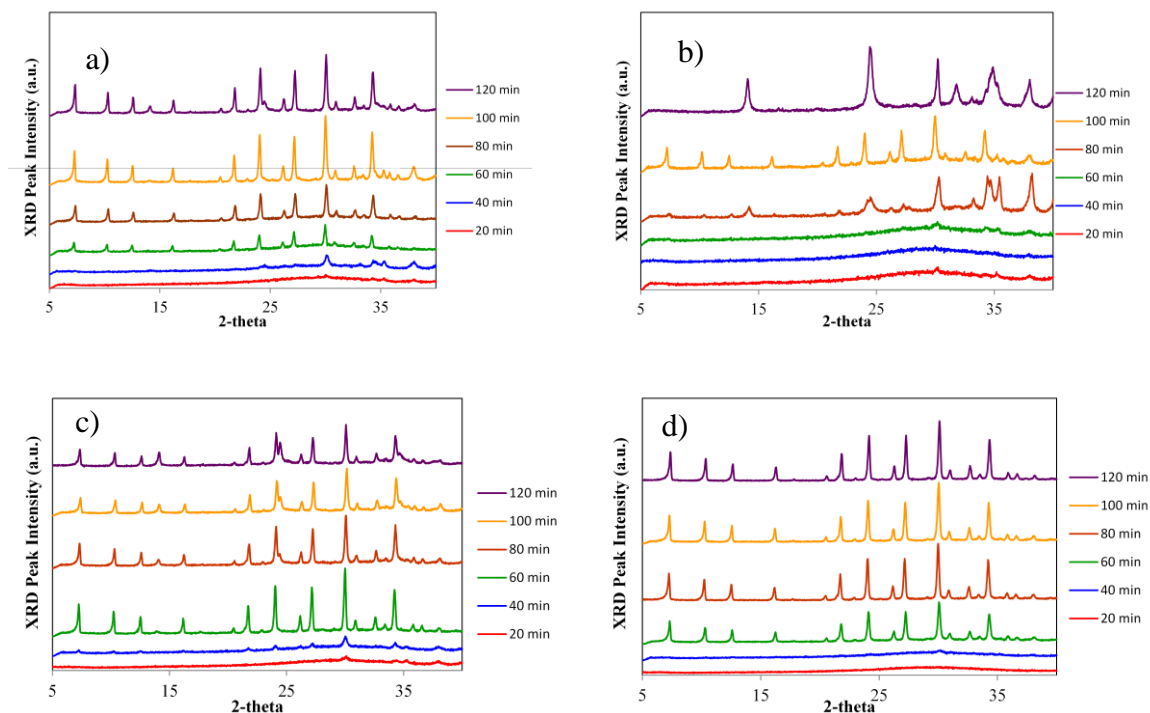
Figure 5-2. XRD patterns of synthesized zeolites with conventional heating a) 95°C b) 85°C and ultrasound assisted synthesis c) 95°C d) 85°C

XRD patterns of the synthesized products were compared with the simulated XRD powder patterns for zeolites [21] and it was concluded that only two zeolitic phases were present in the zeolitic products synthesized, namely LTA zeolite-A and SOD hydroxysodalite. The XRD patterns in Figure 5-2 (a)-(d) indicate that zeolitic crystals are not observed for the first 40 min of the reaction; however, there is a rapid formation of zeolite crystals between 40 min and 60 min reaction time. After 60 min of reaction, sharp peaks belonging to zeolite crystals are observed. Comparing conventional synthesis with UTS assisted synthesis; it is observed that the UTS energy produces sharper XRD peaks at lower reaction time. Figure 5-2 (a) indicates the XRD pattern that belongs to the crystals produced utilizing conventional heating at 95°C. Zeolite peaks can be observed at 60 min reaction time, however these peaks are shorter compared to the XRD peaks

observed for the same reaction conditions for UTS assisted synthesis in Figure 5-2 (c). As the reaction progresses SOD peaks are observable for both conventional and UTS assisted conversion. For conventional conversion in Figure 5-2 (a) the SOD peaks appears at 120 min of reaction time while for UTS assisted conversion SOD peaks are observable at 80 min reaction time for the reaction temperature of 95°C (Figure 5-2 (c)). It can be concluded that the UTS induction not only produces sharper LTA peaks but also promotes the conversion of LTA to SOD as the reaction progresses.

The conventional and UTS assisted conversion at 85°C are compared in Figure 5-2 (b) and Figure 5-2 (c), respectively. Conventional synthesis produces any discernable peaks after 80 min of reaction time while UTS assisted synthesis shows zeolite peaks after 60 min of reaction time. The XRD peaks for the UTS synthesis are sharper and produce a single phase of zeolite (zeolite-A). UTS conversion is most effective at 85°C because it produces the highest XRD peaks and a pure single phase zeolite-A compared to conventional synthesis at both 85°C and 95°C and also compared to UTS assisted synthesis at 95°C.

The characteristic peak areas of LTA and SOD in the zeolitic products for different reaction conditions are indicated in Figure 5-3.
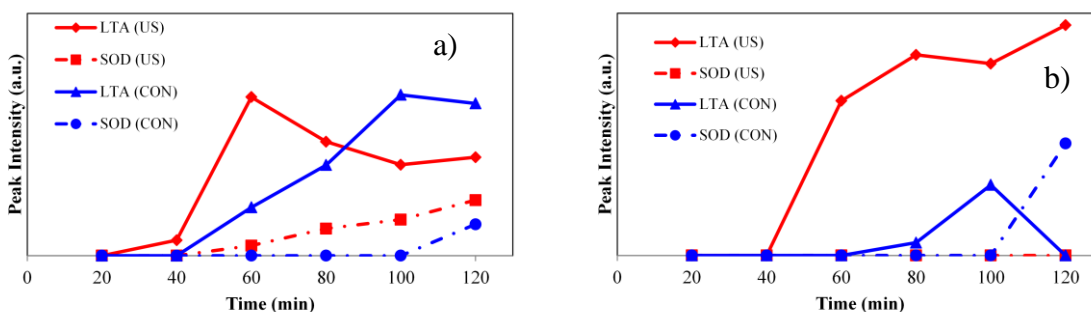
Figure 5-3. Characteristic peak area of zeolitic phases LTA and SOD in the products vs reaction time at reaction temperature a) 95°C b) 85°C

Figure 5-3 (a) indicates the difference between the characteristic peaks of the zeolitic products. At 40 min reaction time we can observe the emergence of zeolitic peaks for UTS induced synthesis while the same is not true for the conventional synthesis. From

the aforementioned observation, it can be concluded that the UTS energy helps reduce the induction time for the zeolite synthesis. Furthermore, Figure 5-3 (a) indicates a sharp growth of zeolite-A for UTS assisted synthesis crystals compared to the conventional heating. Therefore, in addition to reducing the induction time for zeolitization, UTS energy also dramatically increases the crystal growth rate. Reduced induction period and linear growth rate of zeolite-A corroborates with previously conducted experiments [22]. It can also be observed that as the reaction progresses, zeolite-A characteristic peaks area decreases while hydroxysodalite peaks area increases. It can be inferred that zeolite-A converts to the more stable hydroxysodalite phase. This conversion is much faster and more dramatic under UTS induced condition.

Figure 5-3 (b) shows a more dramatic difference between the products synthesized with UTS assistance and conventional synthesis. The crystal growth is faster after induction time for the UTS assisted reaction at lower temperature of 85°C compared to 95°C, while the crystal growth for conventional synthesis is much slower. Furthermore it is observed that the two phases of zeolite products (i.e. zeolite-A and hydroxysodalite) are competing phases in the conventional synthesis, while for UTS induced synthesis of pure zeolite-A. The UTS induced synthesis at 85°C leads to the formation of pure zeolite-A phase compared to UTS induced synthesis at 95°C.

5.3.2 Scanning Electron Microscope (SEM)

Scanning electron microscope (SEM) images of the zeolites produced through conventional and UTS assisted syntheses at varying temperatures are illustrated in Figure 5-4.
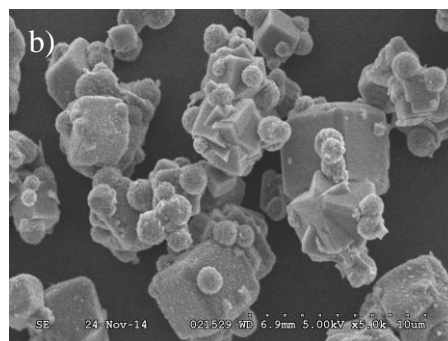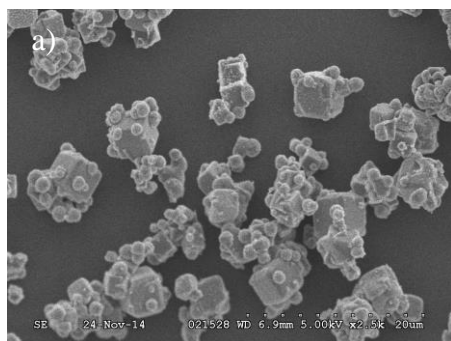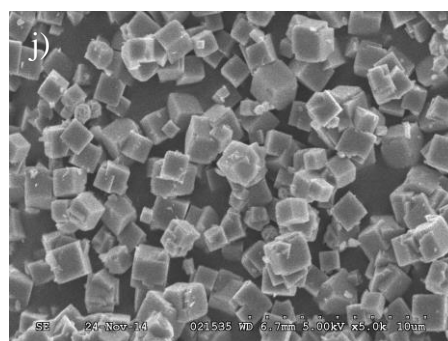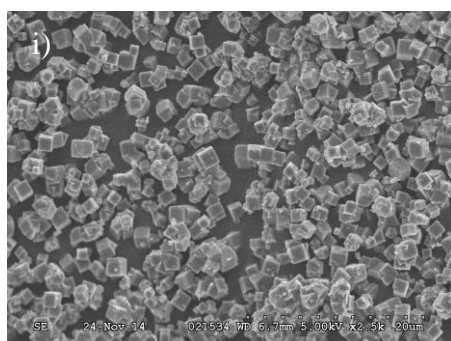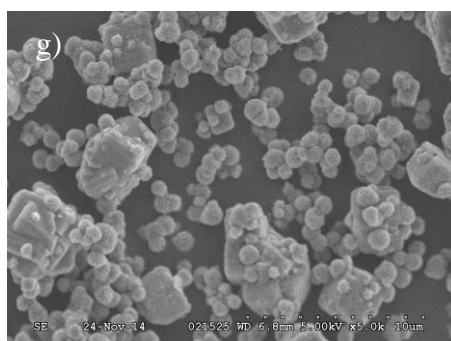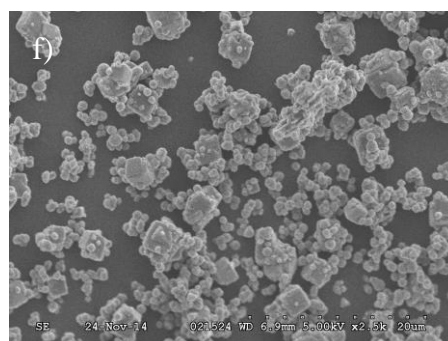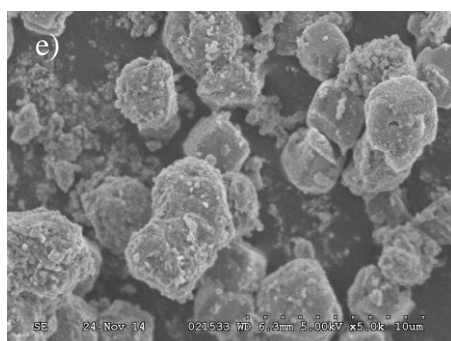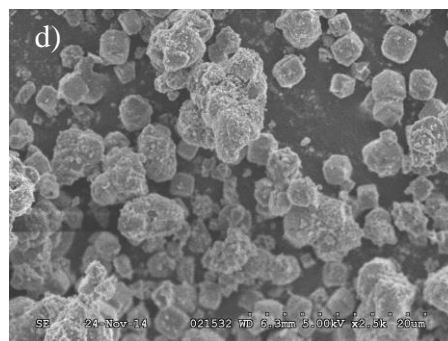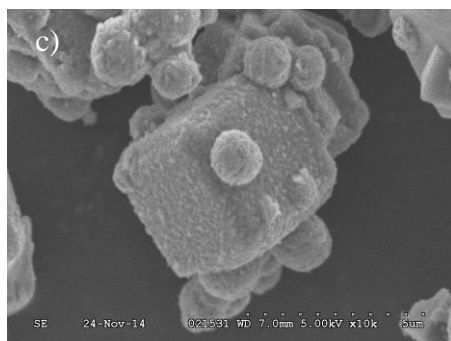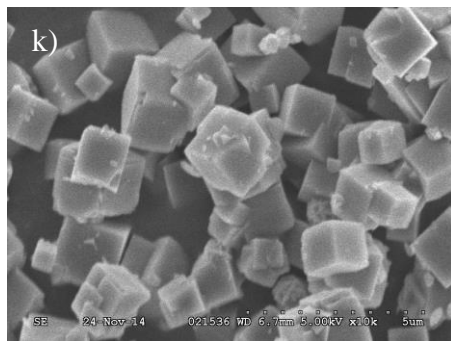
Figure 5-4. SEM micrographs of the zeolite produced utilizing conventional heating at a) to c) at 95°C, d) to e) at 85°C, f) to h) ultrasound assisted synthesis at 95°C, and i) to k) ultrasound assisted synthesis at 85°C

Conventional synthesis at higher temperatures produces zeolite-A with better crystalline structure. The cubic structures observed in Figure 5-4 belong to zeolite-A while spherical structures with protruding surface are hydroxysodalite surface. The crystalline structure is more developed during the conventional synthesis at 95°C compared to the reaction temperature of 85°C. Figure 5-4 (d) to (e) indicate a poor crystalline structure with ample amorphous gel attached to the surface of the zeolitic product. Therefore, suggesting lower temperatures are not conducive to the production of pure zeolite-A crystals. UTS induced synthesis at 95°C show similar results to the conventional synthesis at 95°C. Crystalline zeolite-A is observed with hydroxysodalite product alongside it. More spherical hydroxysodalite crystals are observed in the UTS induced products compared to the conventional synthesis. Indicating that UTS energy is conducive to the conversion of zeolite-A to hydroxysodalite at 95°C. However, a complete opposite trend is observed at 85°C. UTS assisted synthesis at 85°C produces single phase zeolite-A. The crystalline structure of zeolite produced with UTS assistance at 85°C has cubic structure with smooth faces and also produces smaller crystals. It can be concluded that lower temperature of 85°C with the assistance of UTS is the optimized condition for converting the aluminosilicate gel to zeolite-A structure. Compared to UTS assisted synthesis at 85°C; all other synthesis conditions yield zeolites with some undesirable amorphous phase. This difference is most discernable between Figure 5-4 (c) and (k). The induction period of the reaction is decreased at higher temperatures and the difference in induction

time from UTS assistance is smaller as it can be seen in Figure 3. UTS energy plays the most significant role in the crystal growth rate and crystal phase purity.

Further, it is noteworthy that several experiments were conducted with both conventional synthesis and UTS assistance at temperatures lower than 85°C; however, no zeolitic products were observed in those cases. This indicates that elevated temperature is important for the rapid synthesis of zeolite-A and hydroxysodalite regardless of UTS assistance during the reaction.

5.3.3 Thermal Analysis (TGA)

Thermo-gravimetric analysis (TGA) curves of the zeolites produced using conventional heating and ultrasound energy with the highest crystallinity for each method are illustrated in Figure 5-5. The samples were subjected to TGA after drying at 100°C overnight. TGA curves of both zeolites produced from conventional heating and with ultrasound show a 17 % and 20 % weight loss, respectively, while sharing a point of inflection at approximately 200ºC. The weight loss at this temperature indicates that the water content in the produced zeolites. The water loss from the zeolitic crystals is at higher temperature than 100°C therefore; this water content can be attributed to evaporation of adsorbed water molecules on the porous structure of the synthesized zeolite.
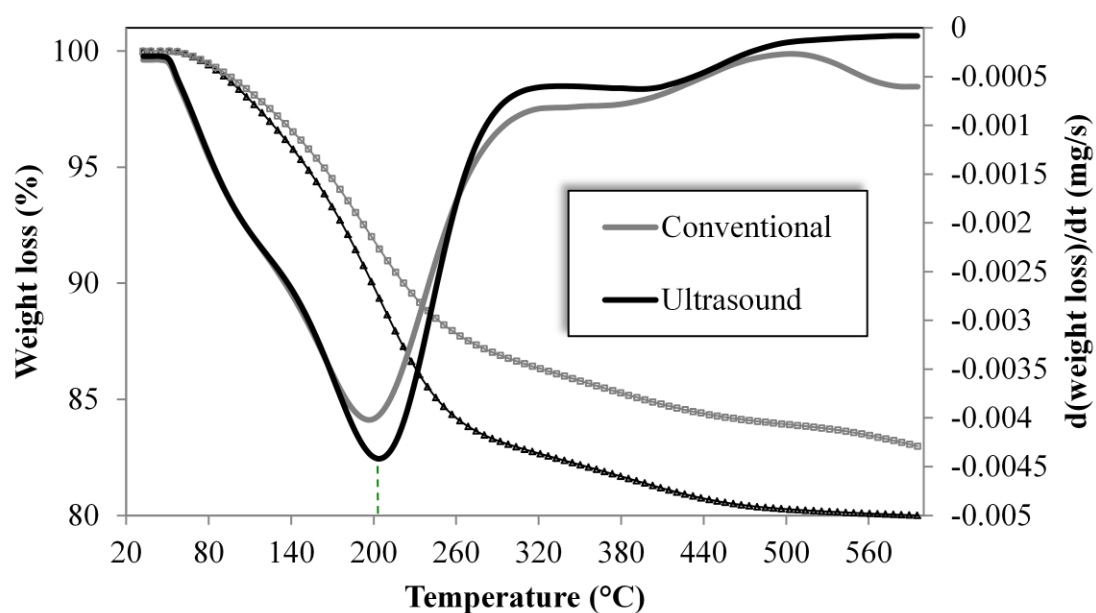
Figure 5-5. TGA Thermogravimetric analysis of zeolite produced through conventional heating and through ultrasound assistance

5.3.4 Induced UTS Energy

The amount of UTS energy irradiated into the reaction solution is illustrated in Figure 5-6.
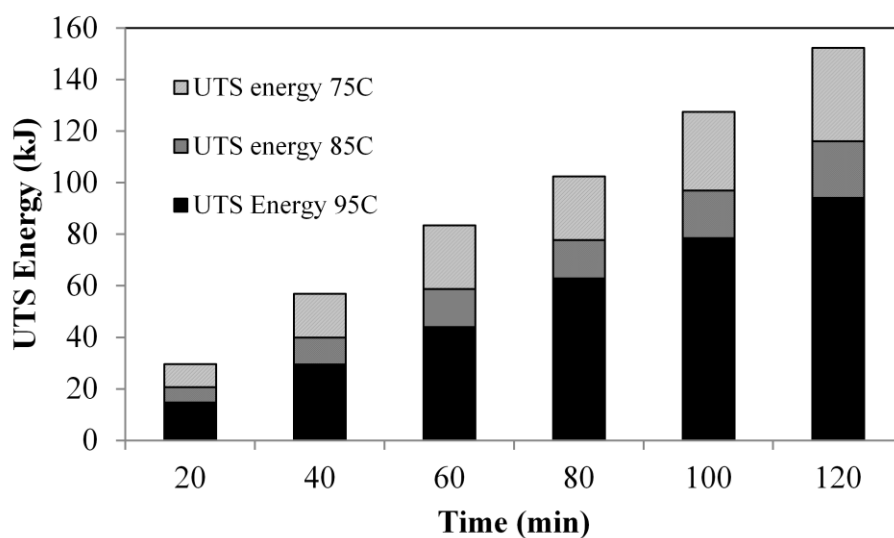
Figure 5-6. Comparison of UTS energy irradiation into the reaction mixture vs time at different temperatures

Figure 5-6 reveals that the amount of energy dissipated by the UTS probe depends on the temperature of the reaction mixture. UTS power irradiation follows a linear trend with respect to the temperature of reaction mixture as indicated in Figure 5-7.
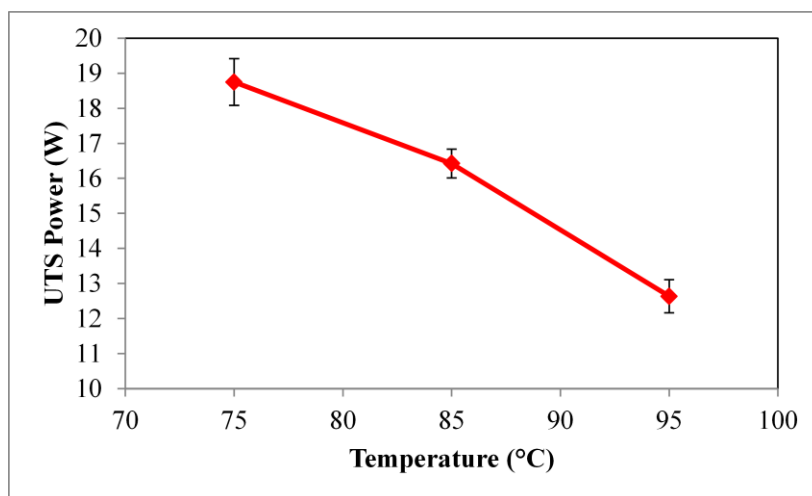
Figure 5-7. UTS power irradiation into the reaction mixture vs reaction temperature

The amount of UTS energy plays a significant role in the zeolitization process. However, the amount of UTS irradiation is strongly coupled with the temperature of the reaction mixture. Figure 5-3 shows that UTS energy irradiation plays a positive role in increasing the induction time of zeolitization process and significantly increases the crystal growth rate. It has also been observed that at 75°C regardless of the amount of energy irradiated, no zeolitic crystals have been observed. Thus it can be concluded that while UTS energy is conducive to the zeolitization process by reducing the induction time, reducing the crystal size, increasing the crystal growth rate, however, the temperature of the reaction mixture is of utmost importance.

5.4 Conclusion

The UTS energy has been successfully utilized for many types of chemical synthesis. UTS energy has also been used to assist with zeolitization process. However, these attempts have been limited to the use of UTS bath. The UTS waves are produced and induced into the water bath; the energy is further transferred from the water into the solution through the reaction vessel. This paper explores the effect of UTS induced utilizing a UTS probe immersed into the reaction solution. A probe immersed in the reaction solution transfers the UTS energy directly to the reaction and the amount of energy induced is observed throughout the reaction. The technique of immersing the UTS probe directly into the reaction mixture produced Na-A in 1 hour, whereas previous works reported 97 hours of reaction time to convert CFA to zeolite [10,11], while other works reported reaction time ranging from 3-6 hours when other precursors such as kaolin [23] and perlite [24] were used. Furthermore, reaction times varied from 2-400 hours for different zeolites synthesized from pure chemical precursors such as Na-A [7], MCM-49 [14], MCM-22 [13] and ANA [8].

The precursor reaction solution was prepared by extracting the constituents of CFA by fusing it with sodium hydroxide at 550°C followed by dissolving it in deionized water. The clear filtered liquid was used as the precursor reaction solution. The zeolitization process was conducted with conventional heating and with the assistance of UTS energy. The differences found in the reaction products for the two methods were significant. Conducting the experiments at 75°C resulted in no crystalline products after two hours of

heat treatment both with and without UTS assistance. UTS assisted synthesis at 95°C reduced the induction time of the zeolitization process by 20 min and also increased the crystal growth rate compared to conventional heating. However, as the reaction progresses, the synthesized zeolite-A converts to a more stable zeolite phase, namely hydroxysodalite. This conversion is discernable sooner and much more rapid in the case of the UTS assisted synthesis. Hydroxysodalite XRD peaks are detectable at and after 60 min of reaction time for UTS synthesis at 95°C and these peaks gradually increase in height linearly as the peaks for zeolite-A decrease exponentially. Whereas, hydroxysodalite peaks are not observable until after 100 min into the reaction for conventional synthesis at 95°C. Reaction conducted at 85°C showed that UTS energy in addition to reduction of induction time and an increase in the crystal growth rate, produces a single phase zeolite-A, while the conventional heating showed production of both small amounts of both zeolite-A and hydroxysodalite. SEM images showed that UTS energy at 85°C produced the purest single phase zeolite-A with smooth crystalline surface and smaller crystal sizes. However, conventional synthesis at 85°C resulted in zeolitic crystals with amorphous debris on the surface, generally with larger crystal sizes and presence of hydroxysodalite crystals. TGA analysis showed that the products have high water content. The zeolites produced by UTS had 3 % higher water carrying capacity by weight compared to zeolite synthesized conventionally.

UTS energy plays a positive role in the production of zeolite. It can not only expedite the production of zeolitic crystals but can also do it at a lower temperature and at a more rapid pace while producing a pure single phase crystals of smaller size.

5.5 References

[1]   Ashokkumar M, Grieser F. Ultrasound assisted chemical processes. Rev Chem Eng 1999;15:41–83.

[2]   Baig RN, Varma RS. Alternative energy input: mechanochemical, microwave and ultrasound-assisted organic synthesis. Chem Soc Rev 2012;41:1559–84.

[3]   Suslick KS, Hyeon T, Fang M. Nanostructured materials generated by high-intensity ultrasound: sonochemical synthesis and catalytic studies. Chem Mater 1996;8:2172–9.

[4]   Sabouni R, Kazemian H, Rohani S. A novel combined manufacturing technique for rapid production of IRMOF-1 using ultrasound and microwave energies. Chem Eng J 2010;165:966–73.

[5]   Suslick KS. Sonochemistry. Science 1990;247:1439–45.

[6]   Flint EB, Suslick KS. The temperature of cavitation. Science 1991;253:1397–9.

[7]   Andaç Ö, Tatlıer M, Sirkecioğlu A, Ece I, Erdem-Şenatalar A. Effects of ultrasound on zeolite A synthesis. Microporous Mesoporous Mater 2005;79:225–33.

[8]   Abrishamkar M, Azizi SN, Kazemian H. Ultrasonic-Assistance and Aging Time Effects on the Zeolitation Process of BZSM-5 Zeolite. Z Für Anorg Allg Chem 2010;636:2686–90.

[9]   Azizi SN, Yousefpour M. Static and Ultrasonic-assisted Aging Effects on the Synthesis of Analcime Zeolite. Z Für Anorg Allg Chem 2010;636:886–90.

[10]   Belviso C, Cavalcante F, Lettino A, Fiore S. Effects of ultrasonic treatment on zeolite synthesized from coal fly ash. Ultrason Sonochem 2011;18:661–8.

[11]   Belviso C, Cavalcante F, Fiore S. Ultrasonic waves induce rapid zeolite synthesis in a seawater solution. Ultrason Sonochem 2013;20:32–6.

[12]   Bukhari SS, Behin J, Kazemian H, Rohani S. Conversion of coal fly ash to zeolite utilizing microwave and ultrasound energies: A review. Fuel 2015;140:250–66.

[13]   Wang B, Wu J, Yuan Z-Y, Li N, Xiang S. Synthesis of MCM-22 zeolite by an ultrasonic-assisted aging procedure. Ultrason Sonochem 2008;15:334–8.

[14]   Wu J, Wang B, Li N, Xiang S. Effect of Aging with Ultrasound on the Synthesis of MCM-49 Zeolite. Chin J Catal 2006;27:375–7.

[15]   Musyoka NM, Petrik LF, Hums E, Baser H, Schwieger W. In situ ultrasonic diagnostic of zeolite X crystallization with novel (hierarchical) morphology from coal fly ash. Ultrasonics 2014;54:537–43.

[16]   Musyoka NM, Petrik LF, Hums E, Baser H, Schwieger W. In situ ultrasonic monitoring of zeolite A crystallization from coal fly ash. Catal Today 2012;190:38–46.

[17]   Hums E, Musyoka NM, Baser H, Inayat A, Schwieger W. In-situ ultrasound study of the kinetics of formation of zeolites Na–A and Na–X from coal fly ash. Ultrasonics 2014;54:537–43.

[18]   Shigemoto N, Hayashi H, Miyaura K. Selective formation of Na-X zeolite from coal fly ash by fusion with sodium hydroxide prior to hydrothermal reaction. J Mater Sci 1993;28:4781–6.

[19]   Bukhari SS, Behin J, Kazemian H, Rohani S. A comparative study using direct hydrothermal and indirect fusion methods to produce zeolites from coal fly ash utilizing single-mode microwave energy. J Mater Sci 2014;49:8261–71.

[20]   Yu Y. Preparation of nanocrystalline TiO2-coated coal fly ash and effect of iron oxides in coal fly ash on photocatalytic activity. Powder Technol 2004;146:154–9.

[21]   Treacy MMJ, Higgins JB. Collection of simulated XRD powder patterns for zeolites. Amsterdam, The Netherlands: Elsevier; 2007.

[22]   Cundy CS, Cox PA. The hydrothermal synthesis of zeolites: Precursors, intermediates and reaction mechanism. Microporous Mesoporous Mater 2005;82:1–78.

[23]   Park J, Kim BC, Park SS, Park HC. Conventional versus ultrasonic synthesis of zeolite 4A from kaolin. J Mater Sci Lett 2001;20:531–3.

[24]   Azizi SN, Asemi N. The Effect of Ultrasonic and Microwave-Assisted Aging on the Synthesis of Zeolite P From Iranian Perlite Using Box-Behnken Experimental Design. Chem Eng Commun 2014;201.

Chapter 6

6 Microwave assisted zeolitization of coal fly ash using landfill leachate as the solvent

Abstract

Coal fly ash (CFA) was converted to zeolite using microwave energy. Landfill leachate was used as the solvent, after increasing its pH with sodium hydroxide to precipitate the heavy metals contents, in three modes: filtered using a 0.45 µm filter (fine-filtered), filtered using a 1 µm filter (coarse filtered) and unfiltered. The experiments were performed using a self-adjusting microwave source (single-mode, 2.45 GHz, CEM cooperation, Discover, USA) in a cylindrical batch PTFE vessel (28 mm ID × 108 mm). The XRD analysis of the product showed that using leachate inhibited the production of zeolite A (LTA) and favoured the production of hydroxysodalite (SOD). More heavy metals removal from leachate by precipitation and filtration favoured LTA production. Samples synthesized at 300 W of microwave irradiation for 30 minutes had a SOD/LTA ratio of 1.00, 1.06, and 2.28 for fine-filtered, coarse filtered and unfiltered leachate samples. SEM, TGA and CEC analyses further confirmed that more heavy metal precipitation and filtration favoured LTA over SOD production. CECs for zeolites synthesized using fine-filtered, coarse filtered and unfiltered leachate were 0.80, 0.72 and 0.67 meq/g, respectively. SOD production increased with increased microwave irradiation energy. There was an optimal microwave irradiation energy level per g of CFA (65.9 kJ/g) in which the most LTA was produced.

6.1   Introduction

Coal-fired energy production has gradually decreased in recent years. Despite this fact, due to the growth in population and world development, coal-fired energy still remains a very large segment of the energy production market. Coal-fired power plants burn pulverized coal to produce electricity. One of the waste products produced upon the combustion of coal is a particulate material called coal fly ash (CFA). Coal fly ash is potentially carcinogenic and has to be disposed of or used safely to mitigate the potential

risks [1]. CFA contains silicon and aluminum which can be utilized to synthesize zeolites. Zeolites are used as catalysts (mainly in the petroleum/petrochemical industry), to purify air and water, as well as other uses in industrial settings. Many studies have been conducted [2–12] and reviews written [13,14] on the production of zeolites from CFA.

Zeolitization of CFA involves the use of high quantities of water. Production of one metric ton of zeolite from CFA requires 20 metric tons of fresh water [15]. Most of the studies utilized pure water during the synthesis process. However, there has been growing interest in utilizing liquid waste streams in the production of zeolite. Eliminating the use of fresh water can significantly reduce the cost and environmental impact associated with the zeolitization process. Furthermore, if a source of wastewater is used instead of fresh water, two waste streams (CFA and wastewater) are used for the production of a value added material. Belviso et al. [16] synthesized zeolite X from CFA and seawater as the solvent by fusion with NaOH followed by hydrothermal crystallization. A comparison was done between the results obtained from the use of seawater and distilled water. The synthesis yield was higher using seawater than using distilled water at different crystallization temperatures. Hussar et al. [17] synthesized zeolite A by a hydrothermal process using sodium silicate, sodium aluminate and the by-product of an aluminum etching process. The chemical composition of the aluminum etching by-product consisted of the following main oxides expressed as percentage by weight; Al_2O_3, 92%; Na_2O, 6%; SiO_2, 0.5%. Their results indicated that a higher synthesis reaction temperature and longer reaction time favored synthesis of zeolite A. The effect of using industrial waste brine solution instead of ultra-pure water was investigated during the synthesis of zeolite by Musyoka [18]. They used coal fly ash as the Si feedstock and high halide brine obtained from the retentate effluent of a reverse osmosis water treatment plant of a mine, as the solvent. The brine contained high sodium and potassium and low concentrations of toxic elements. Also there was trace amounts of aluminum equal to 48.38 μg/L and no silicon. The use of brine as a solvent resulted in the formation of hydroxysodalite zeolite although unconverted mullite and hematite from the fly ash feedstock were also present in the product. Musyoka et al. [5] used two types of mine waters (acidic and circumneutral). The important cationic species of circumneutral water were: Na: 952

mg/L, Mg: 38 mg/L, Ca: 19 mg/L and Si: 1.2 mg/L (no detectable Al); and in the acidic drainage water were: Fe: 4694 mg/L, Na: 68 mg/L, Mg: 386 mg/L, Ca: 458 mg/L, Al: 613 mg/L and Si: 31 mg/L. Zeolites Na-X and Na-P1 were synthesized by fusion and hydrothermal method, respectively. The use of circumneutral mine water resulted in similar zeolite forms, i.e. Na-P1 and X, whereas the use of acidic mine drainage led to the formation of a single phase hydroxysodalite zeolite. Studies were also conducted by Behin et al. [19] utilizing a liquid waste stream from plasma electrolytic oxidation (PEO), which is a relatively novel technique to produce functional oxide coatings on the surface of metals such as aluminum, magnesium, and titanium alloys [20]. The wastewater from the PEO process had a pH of 12 and contained Na (63 mg/L), K (497 mg/L), Si (295 mg/L) and Al (10 mL/g) metal cations. The zeolite produced with PEO wastewater was comparable with the zeolite produced with fresh water in terms of BET surface area, water carrying capacity and cation exchange capacity (CEC). The wastewater streams used in the above experiments did not contain any heavy metals. Landfill leachates, however may contain heavy metal ions and would be an interesting study to conduct on the zeolitization process of CFA.

Landfill leachate is produced when water infiltrates a landfill and leaches out from the landfill. Depending on the composition of the waste, leachate can contain soluble organic, inorganic, bacteriological constituents, heavy metals and suspended solids [21]. It presents many potential environmental hazards and due to its complex nature is difficult and expensive to treat. A significant portion of the landfilling cost is due to leachate treatment. Many studies have been conducted [22–25] and reviews written [26–28] on leachate treatment. Here the goal is to use leachate instead of water for the production of zeolite A. There have been studies conducted using wastewater to synthesize zeolites, however, in these studies the major constituents have been alkali and alkali-earth metals. The use of leachate in this experiment helps to shed light on the effects of heavy metal ions in the reaction mixture on the zeolitization process.

6.2　Materials and Methods

6.2.1 Materials

Coal fly ash was obtained from a coal fired power plant (Ontario Power Generation, Nanticoke, Canada) and was stored in a sealed container before use. Sodium hydroxide (Alphachem, Mississauga, Canada) and sodium aluminate anhydrous (Sigma-Aldrich, USA) were of analytical grade and used as received. The leachate was obtained from the W12A Landfill (London, Canada). Upon collection of the leachate, the leachate was filtered through VWR Grade 415 Filter Paper (Mississauga, Canada) to remove any particulate matter present in the leachate. When not in use, the leachate was stored at 4°C to limit degradation of the leachate. When used during experiments, the leachate was allowed to reach room temperature before each experiment. The unused leachate was subsequently refrigerated after use. Other chemicals used for characterization tests were of analytical grade. Other chemicals used for characterization tests were of analytical grade.

6.2.2 Experimental procedure

Coal fly ash was converted into zeolite by a single step hydrothermal alkaline treatment [2]. Zeolitization of coal fly ash was carried out as follows: 2.18 g of sodium hydroxide granules with 1.82 g of fly ash (NaOH/CFA ratio of 1.2) were dissolved in 17 mL of leachate. Upon increase of pH (required for digestion of CFA) using NaOH, heavy metal hydroxides precipitated. One set of experiments was conducted with leachate that was filtered through 0.45 µm polyethersulfone syringe filters (VWR, Canada) (fine-filtered). Another set of experiments was conducted with the leachate filtered through 1 µm filter paper (coarse filtered). A third set using the unfiltered leachate. The digestion of CFA was conducted at 60ºC for 12 h using an end-over-end shaker in a cylindrical PPCO vessel (25.5 mm ID × 104.5 mm). After digestion, 3 mL of the aqueous sodium aluminate solution (0.155 g/mL) were added and the reaction solution aged for 2 hours. Subsequently, the mixture was subjected to microwave radiation for crystallization. The experiments were performed using a self-adjusting microwave source (single-mode, 2.45 GHz, CEM cooperation, Discover, USA) at atmospheric pressure. A cylindrical batch

PTFE vessel (28 mm ID × 108 mm) equipped with a reflux condenser was placed in the microwave chamber for varied periods of time (10, 20 and 30 min) and microwave power (100, 200, 300 W). In a single mode microwave, electromagnetic irradiation is directed through a precisely-designed wave guide that produces a standing wave, whereas in multimode microwave there is a mixture of many waves with different phase shifts. The microwave field density in a single mode microwave is much higher compared to a multimode microwave. Therefore, similar results can be achieved in a single-mode microwave using lower power input [29]. After a given period of MW irradiation, the solid products were filtered, washed with deionized water and dried overnight.

6.2.3 Characterization

Inductively coupled plasma atomic emission spectroscopy (ICP-AES) was used to measure the concentration of different ions in the leachate. Concentrations were found using a Perkin-Elmer Optima-3300 DV ICP-Atomic Emission Spectrometer (USA). Chemical composition of the CFA sample was determined by means of X-ray fluorescence spectroscopy (XRF) utilizing PANalytical PW2400 Wavelength Dispersive. Rigaku–Miniflex powder diffractometer (Japan) was used to collect XRD data of the synthesized zeolites using CuKα (λ for Kα = 1.54059 Å) over the range of 5°<2θ<25° with a step width of 0.02°. The obtained crystalline phase was identified based on standard peaks in literature [30]. The thermogravimetric analysis (TGA) of the samples was performed using a Mettler Toledo TGA/SDTA 851e model (Switzerland) with version 6.1 STARe software. The samples were heated from 25°C to 600°C at a heating rate of 10°C/min under nitrogen purge. The crystal size distribution and morphology of the zeolites were studied by scanning electron microscope (SEM); Hitachi S 2600N SEM (Tokyo, Japan) operating at 5 kV of acceleration voltage. CEC was measured using ammonium acetate saturation method (5 days) based on Bain and Smith [31]. The zeolite samples were soaked in a 1 N solution of ammonium acetate for 5 days in the same end-over-end shaker. After 5 days, the zeolite samples were filtered and allowed to air dry. The dried samples were then washed using 100 mL (5 x 20 mL) of an aqueous solution of 10 wt% NaCl and 1 vol% HCl to remove the fixated ammonium. The ammonium concentration in the supernatant was then measured. The ammonium concentration was

correlated to peak absorbance intensity between 550 and 800 nm measured using UV-VIS spectroscopy. To prepare the samples for the UV-VIS spectroscopy, sodium salicylate, sodium hydroxide and sodium hypochlorite were added and 5 minutes allowed to elapse for the reaction to proceed to completion.

6.3   Results and Discussion

6.3.1 Inductively coupled plasma atomic emission spectroscopy (ICP-AES)

The ions concentrations and pH of the leachate are found in Table 6-1.

Table 6-1. Cation concentration (mg/L) and pH of leachate

Cation	Concentration (mg/L)
Ag	< 0.01
Al	0.14
As	< 0.01
B	3.95
Be	< 0.01
Ca	206.08
Cd	4.15
Co	0.03
Cr	0.27
Cu	1.71
Fe	0.62

Hg	< 0.01
K	252.27
Li	0.05
Mg	141.46
Mn	1.01
Mo	< 0.01
Na	810.80
Ni	5.92
P	0.53
Pb	0.62
S	99.13
Sb	< 0.01
Se	< 0.01
Si	21.94
Sn	< 0.01
Tl	< 0.01
V	< 0.01
Zn	7.61
pH*	7.56

* Unitless

The leachate contained high levels of Ca (206.08 mg/L), K (252.27 mg/L), Mg (141.46 mg/L), Na (810.80 mg/L) and S (99.13 mg/L). Ca, K, Mg and Na are most likely a result of the leaching of salts from the soil covers of the landfill [32]. Sulfur is most likely from the leaching of the landfill waste [33]. Silicon and Al are required for the synthesis of zeolites. The landfill leachate had only trace amounts of both elements; concentrations of Si and Al were 21.94 and 0.14 mg/L, respectively.

6.3.2 X-ray analysis (XRF and XRD)

The chemical compositions of the CFA that was used as the main source of Si and Al for hydrothermal zeolitization process are summarized in Table 2. The SiO2/Al2O3 ratio was found to be 2.13, which was appropriate for the synthesis of low silica zeolite crystallites such as LTA type zeolite. According to the XRD data, the main components of the CFA were amorphous aluminosilicate as well as quartz and mullite that existed as crystalline structures as indicated in Table 6-2.

Table 6-2. XRF analysis of chemical composition of CFA

Parameter	Weight percent (%)
Major oxide	
SiO_2	41.78
Al_2O_3	19.61
CaO	13.64
Fe_2O_3	5.79
MgO	3.23
TiO_2	1.39
K_2O	1.1
Na_2O	0.94
P_2O_5	0.71
BaO	0.36
SrO	0.25
Cr_2O_3	0.01

MnO	0.02
Loss On Ignition	10.89
Total	99.72

Phases analysis

Amorphous aluminosilicate

Quartz (SiO_2)

Mullite ($3Al_2O_3.2SiO_2$)

*SiO_2/Al_2O_3: 2.13

The XRD analysis was conducted for all the samples after microwave irradiation in order to identify the zeolite phases present. Two major zeolitic phases were observed, namely zeolite A (LTA) and hydroxysodalite (SOD). The XRD patterns for the different leachates are shown in Figure 6-1.
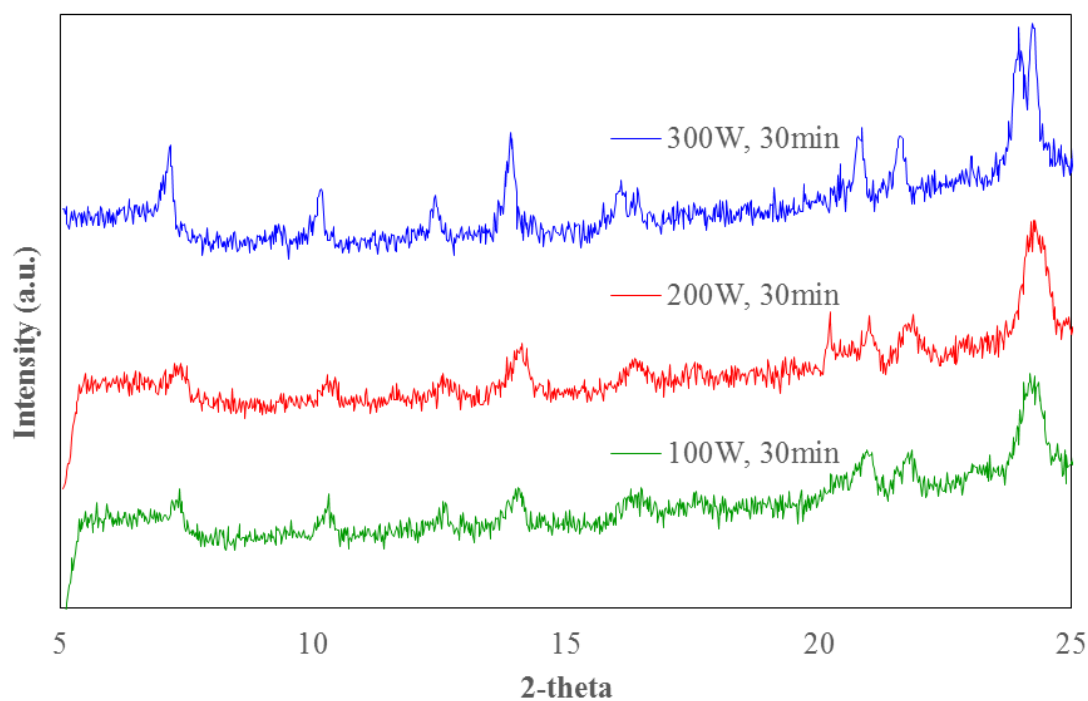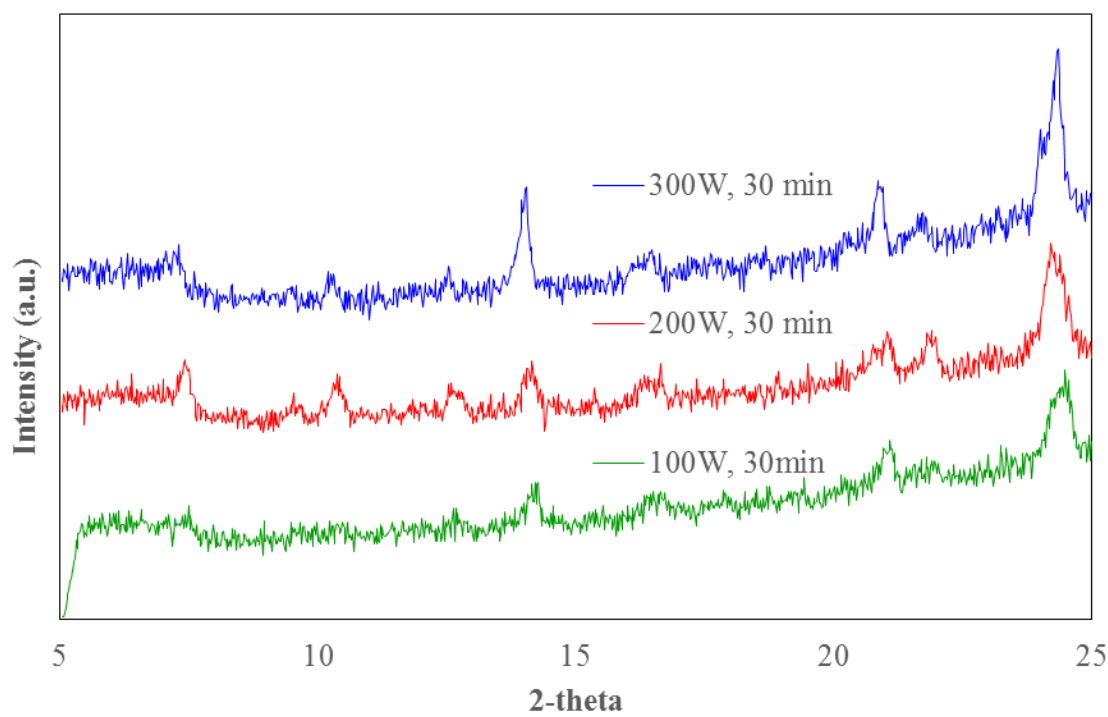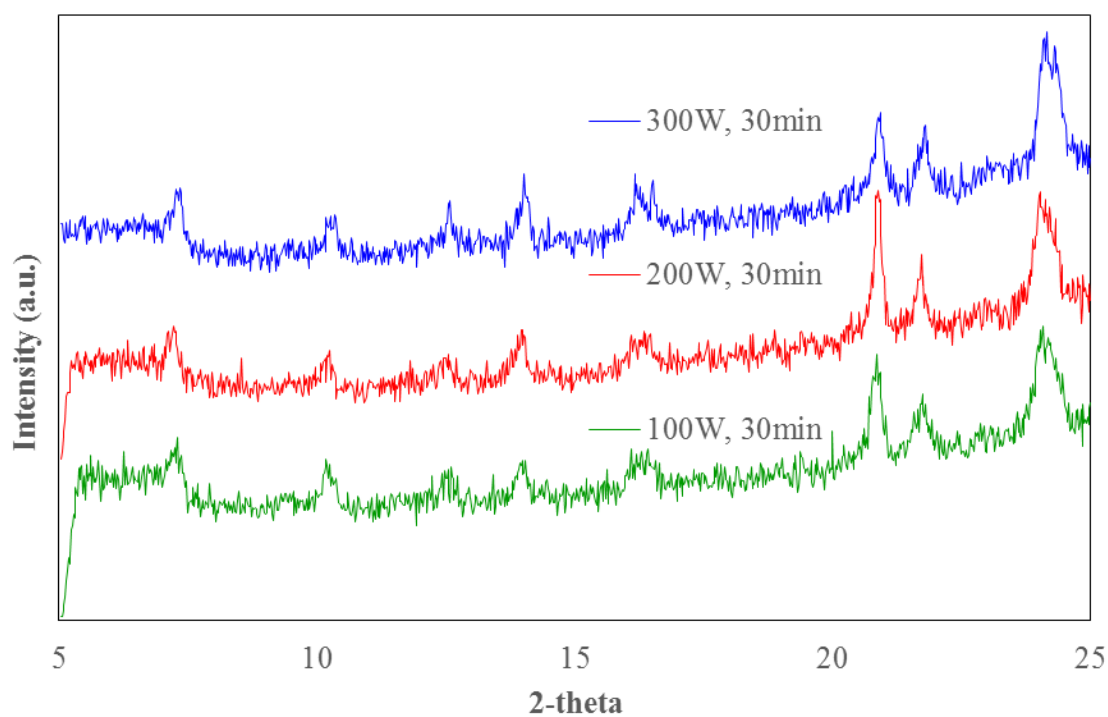
Figure 6-1. The XRD patterns of zeolitized coal fly ash a) fine0filtered leachate b) coarse filtered leachate and c) unfiltered leachate as the reaction solvent

The relative peak intensities were defined as the ratio of the characteristic peak of each product species to the highest characteristic peak observed.

$$RI_{LTA} = \frac{I_{LTA,Sample}}{I_{LTA,Max}}$$ **Eq 6-1**

$$RI_{SOD} = \frac{I_{SOD,Sample}}{I_{SOD,Max}}$$ **Eq 6-2**

Table 6-3 shows the relative peak intensities of the samples irradiated with different microwave power and using different leachates as the reaction solvent. It was observed that higher microwave power for 30 min irradiation time favoured the production of SOD over LTA. Furthermore, the fine-filtered leachate solvent produced more zeolite A and higher crystallinity. This indicates that microwave irradiation favours the production of SOD which has also been reported by previous works [34]. It can also be concluded that the presence of cations other than Na^+ can disrupt the production of zeolite A thus lowering the crystallinity of the product and strongly favouring the production of SOD over LTA.

Table 6-3. Relative characteristic XRD Peak Intensity for fine-filtered, coarse filtered and unfiltered synthesis after 30 minutes of Microwave Irradiation

Leachate	Power (W), time (min)	LTA	SOD
	300, 30	1.00	1.00
Fine-filtered	200, 30	0.346	0.471
	100, 30	0.495	0.345
	300, 30	0.495	0.525
Coarse filtered	200, 30	0.407	0.404

	100, 30	0.445	0.318
	300, 30	0.390	0.888
Unfiltered	200, 30	0.495	0.444
	100, 30	0.297	0.395

In order to study the effect of total microwave energy irradiation on the zeolite phase produced, relative intensities of characteristic peaks of both LTA and SOD were plotted against microwave irradiation energy. Figure 6-2 illustrates the results for both coarse filtered and unfiltered leachate used as the zeolitization reaction solvent. In both cases it is observed that there is an optimal microwave irradiation energy level for the production of LTA, however as the amount of irradiation energy is increased, more SOD was produced. While the production of LTA plateaus, the production of SOD increases linearly.
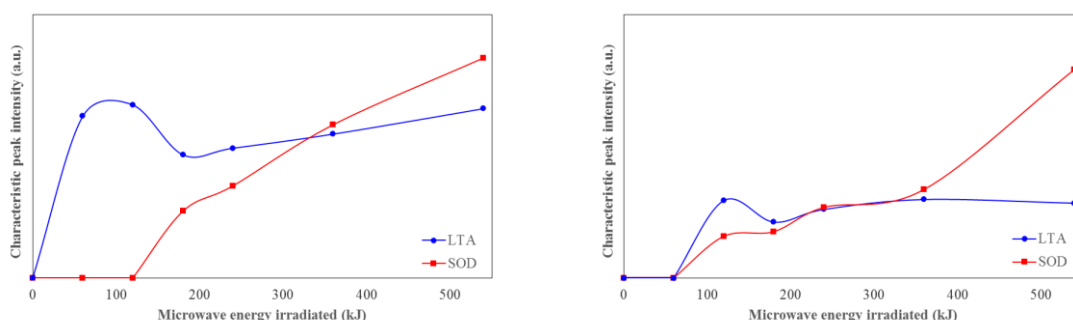
Figure 6-2. The characteristic XRD peak intensities with respect to microwave irradiation utilizing a) coarse filtered leachate and b) unfiltered leachate as reaction solvent

This trend is more pronounced for the zeolite synthesized in the unfiltered leachate. Much more SOD is produced compared to LTA for unfiltered leachate experiments than the coarse filtered leachate. This again indicates that the heavy metals in the reaction solution retard the production of LTA and significantly favour the production of SOD.

From Figure 6-2, it is observed that zeolitic characteristic peaks occur sooner for coarse filtered leachate solvent experiments compared to the unfiltered leachate solvent experiments. This indicates that heavy metal constituents prevent nucleation of LTA zeolite crystals. Our research group has earlier conducted similar experiments with pure water [35] and wastewater produced from plasma electrolytic oxidation process [19] (both lacking heavy metal ions) and produced pure LTA unlike for leachate experiments that produced a mixture of LTA and SOD. This indicates the significant role that heavy metal ions play in suppressing the nucleation of LTA.

The presence of various alkali metal cations in otherwise identical gels, results in the synthesis of different zeolites. For example, Na+, K+, Cs+ result in crystallization of zeolite A, chabazite, and edingtonite, respectively [36]. The interactions between negatively charged silicate, aluminate and aluminosilicate species and the cation species are extremely important in determining the zeolite crystallized. ,LTA is a less stable phase compared to SOD [11] and requires germination of multiple composite building units (CBU's) as opposed to SOD which has only one CBU (beta cage). The presence of heavy metal oxides may favour the production of a stable phase by preventing the germination of "d4r" and "lta" cages which are the CBU's required for LTA synthesis [37]. Abundance of beta cages ("sod" CBU) in the solution in lieu of "d4r" and "lta" favours the production of stable SOD phase.

6.3.3 Scanning electron microscope (SEM)

The scanning electron microscope (SEM) images of the synthesized zeolites utilizing unfiltered, coarse filtered and fine-filtered leachate as zeolitization solvent are illustrated in Figure 6-3 (a-f). In all of the SEM images, two distinct main structures can be observed, cubic and rough surfaced spheres. The cubic structures are associated with LTA framework, while the rough sphere are SOD framework [10,38,39]. The zeolitic frameworks are crystallized on the surface of the undissolved coal fly ash particles in accordance with an earlier suggested mechanism [13,35].
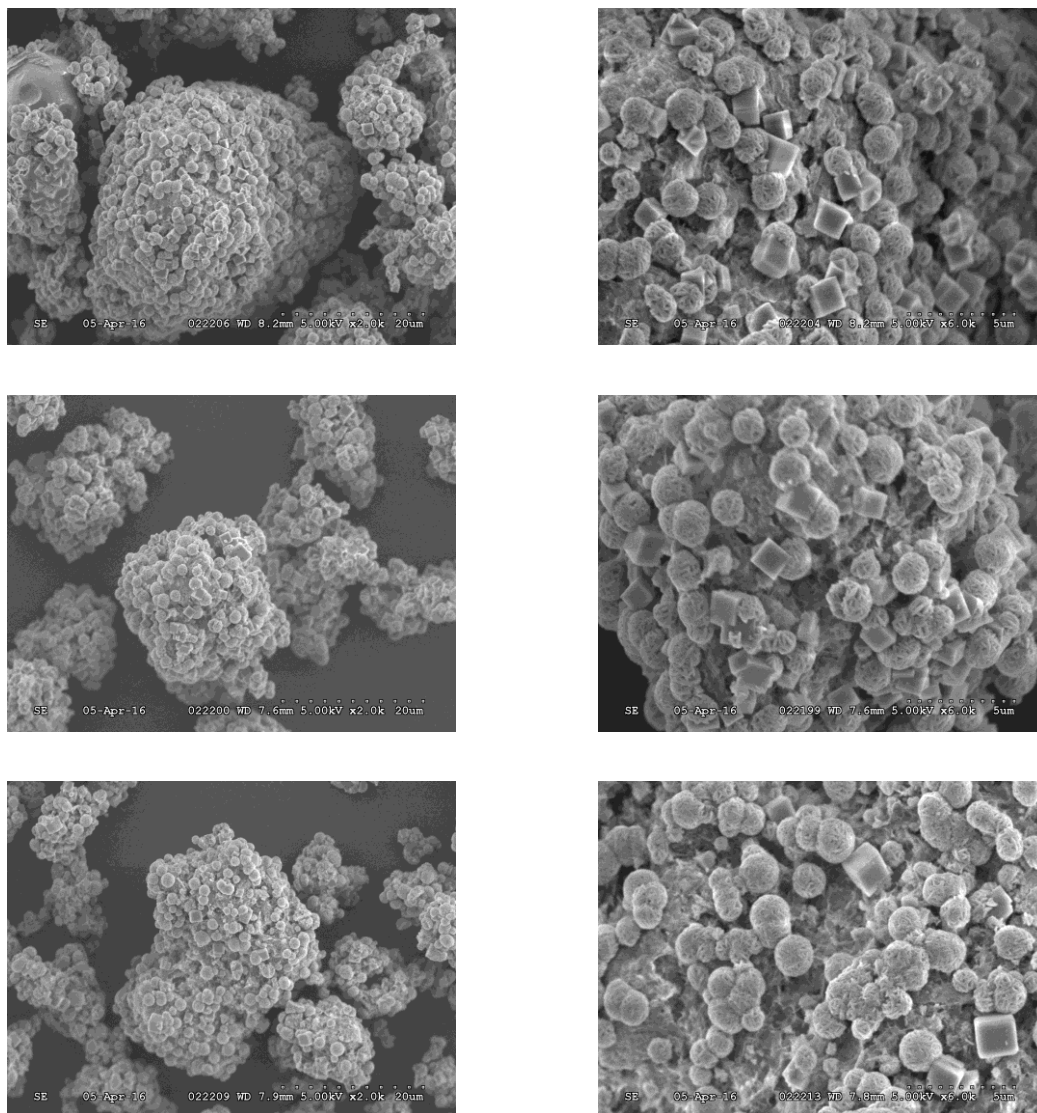
Figure 6-3. The SEM images of zeolitized coal fly ash utilizing a, b) fine-filtered c, d) coarse filtered and e, f) unfiltered leachate as solvent

The SEM images indicate that the cubic structures associated with the LTA are more abundant than spherical structures in both fine-filtered and coarse filtered leachate experiments. In the case of unfiltered experiments, the spherical SOD crystals clearly outnumber the cubic LTA. These results corroborate the results and conclusions drawn from XRD analysis.

6.3.4 Thermogravimetric analysis (TGA)

The TGA curves of the synthesized zeolites using unfiltered, coarse filtered and fine-filtered leachate as reaction solvent are shown in Figure 6-4.
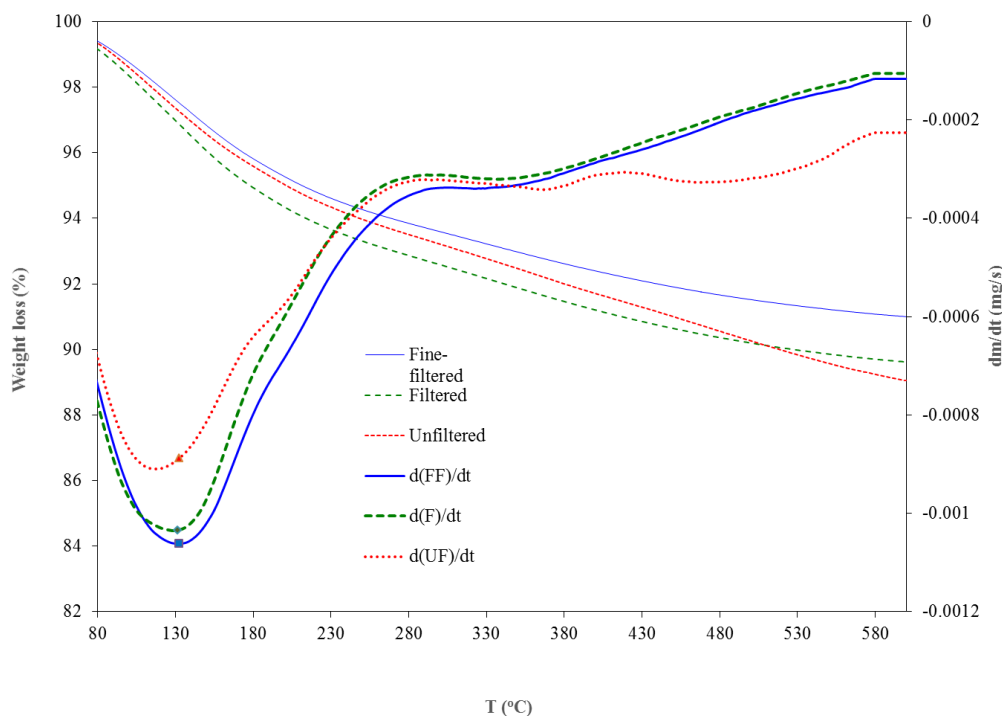
Figure 6-4. The TGA of synthesized zeolites using fine-filtered, coarse filtered and unfiltered leachate as solvent

All three samples showed major weight loss at approximately 120-130°C (shown by the derivative lines). The synthesized zeolite using fine-filtered leachate, coarse filtered leachate, and unfiltered leachate lost approximately 9.0%, 10.4% and 11.0%, respectively (shown by the weight loss lines of the three samples; Figure 6-4). The derivative of the weight loss of the synthesized zeolites samples using coarse filtered and fine-filtered leachates decreased in magnitude at approximately 340-350°C (seen as an upward trend in the derivative curves), whereas that of the synthesized zeolite using unfiltered leachate was relatively flat after 340-350°C. This indicates that more weight was lost by the zeolite produced using unfiltered leachate. A possible explanation for the higher weight loss of the zeolite synthesized using unfiltered leachate is due to the thermal

decomposition of heavy metal hydroxides present in the unfiltered leachate. The difference between the three synthesized zeolite samples was the amount of heavy metal precipitate in the leachate. Upon filtration of the precipitates, the concentration of heavy metal hydroxide decreased. The unfiltered leachate had the highest heavy metal hydroxides concentration.

Another result of the heavy metal hydroxides concentration difference between the samples was the water carrying capacity. This is shown in Figure 6-4 by the depth of the large peak of the first derivatives at approximately 100-140°C.The lower the peak, the more water is held in the zeolite structure. This can be ascribed to an increase in surface area compared to the initial CFA [10]. The lowest peak in the first derivatives (most negative), was that of the zeolite synthesized using fine-filtered leachate, showing the most water carrying capacity. The highest peak (least negative) was that of the zeolite synthesized using unfiltered leachate, showing the least water carrying capacity.

6.3.5 Cation exchange capacity (CEC)

Figure 6-5 shows the correlation between ammonium concentration and peak absorbance intensity. The R^2 value was found to be 0.9991 indicating a very strong linear correlation between ammonium concentration and peak absorbance intensity. After removal of the ammonium ions from the zeolite, the ammonium concentration was measured using UV-VIS method as explained in 6.2.

$$C_{NH_4} = 2.005A - 0.2277$$
$$R^2 = 0.9991$$
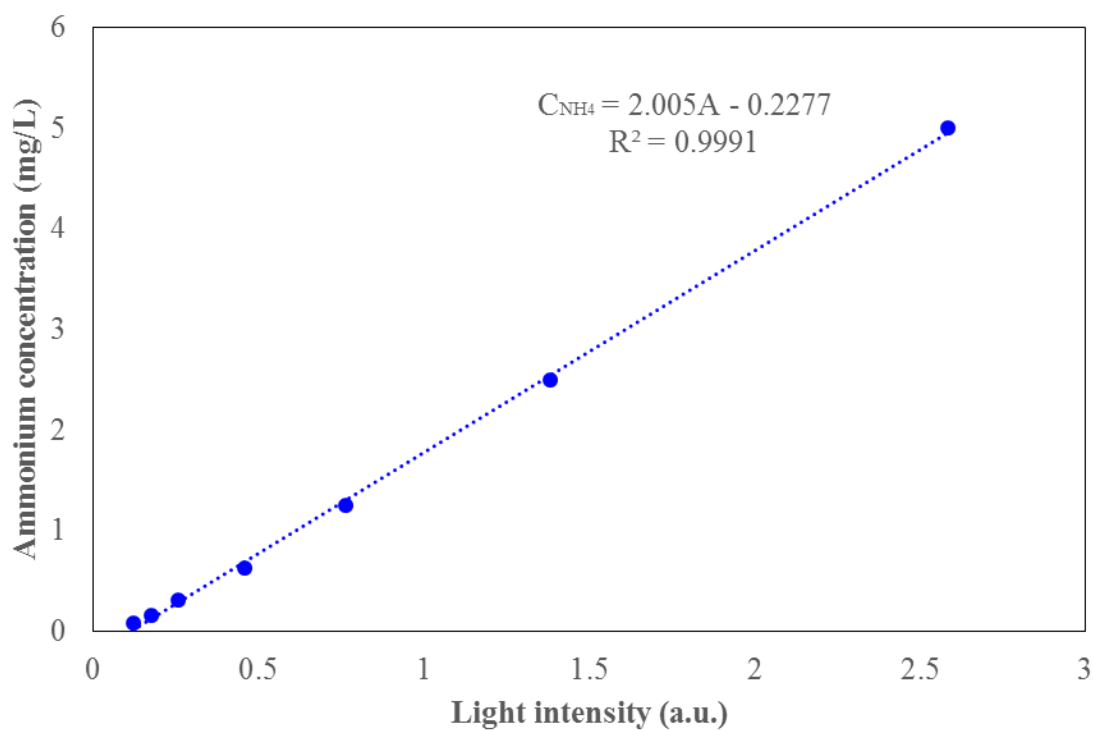
Figure 6-5. The correlation between the NH$_4^+$ concentration and peak absorbance intensity

The CEC values of the zeolites synthesized using fine-filtered, coarse filtered and unfiltered leachate are shown in Figure 6-6. The CEC values of the zeolites synthesized using fine-filtered, coarse filtered and unfiltered leachate were 0.80, 0.72 and 0.67 meq/g, respectively.
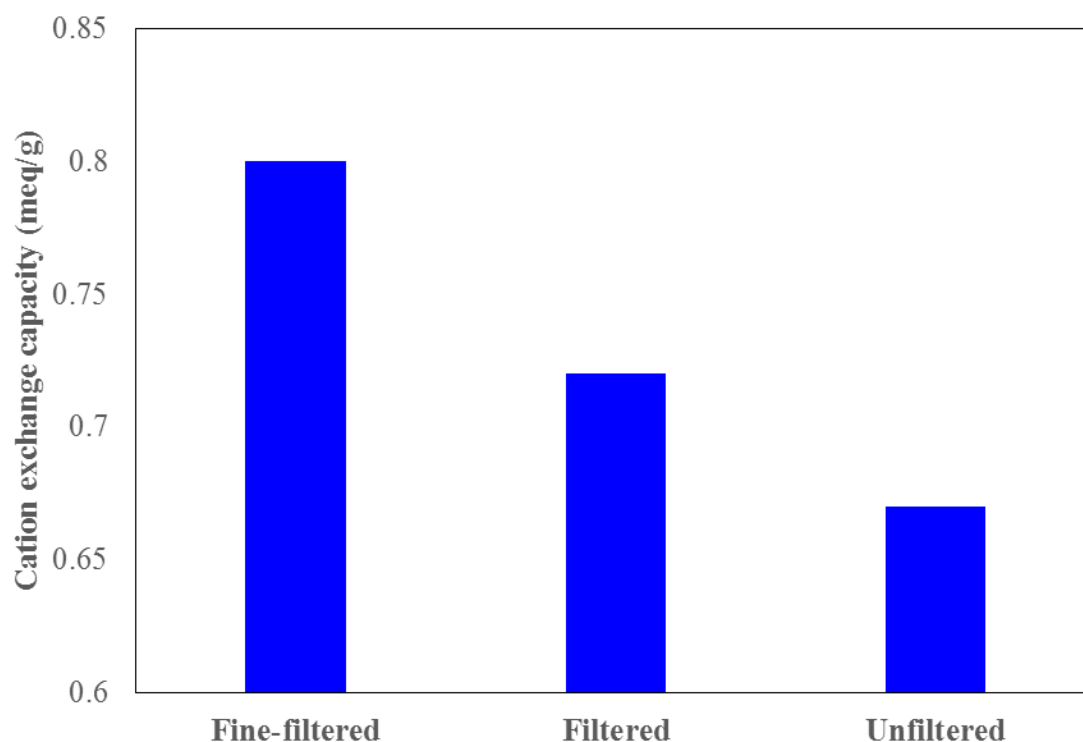
Figure 6-6. The CEC values of fine-filtered, coarse filtered and unfiltered leachate prepared zeolites

The CEC value depends on the amount of zeolite A produced. Raw CFA has a CEC value of 0.3 meq/g [10]. Whereas CEC values of zeolite A are reported in the range of 2-5 meq/g [10,40,41]. Sodalite has a CEC value ranging from 0.099-1.22 meq/g (various ions were used to determine the CEC of sodalite in literature) [42]. Since, raw CFA and sodalite have lower CEC values than zeolite A, the presence of either of these will decrease the CEC of the produced sample. Table 6-3 shows that the zeolite synthesized using fine-filtered leachate had the highest amount of zeolite A. The zeolite synthesized using coarse filtered leachate had more zeolite A than the zeolite synthesized using unfiltered leachate and this corresponds to a higher CEC value (0.72 and 0.67 meq/g, respectively; Figure 6-6). The SEM micrographs (Figure 6-3) also confirm the larger quantity of zeolite A using fine-filtered and coarse filtered leachate compared to the zeolite synthesized using unfiltered leachate.

6.4 Conclusions

Landfill leachate was used for coal fly ash zeolitization. Sodium hydroxide added to the leachate solution resulted in a large amount of heavy metal precipitation. In order to investigate the effects of the presence of heavy metal cations and precipitation on the zeolitization process, three sets of experiments were performed. In one set, the precipitate was removed using 0.45 μm filters. In another set, filtration was performed with 1 μm filters. In a third set of experiments, no filtration was performed. After the zeolitization process utilizing single mode microwave, multiple analyses, including XRD, SEM, CEC and TGA were conducted.

The XRD analysis indicated that utilizing leachate for the synthesis of zeolites suppressed the production of LTA and favoured the production of SOD. Unfiltered leachate produced the highest ratio of SOD to LTA. Whereas, fine-filtered leachate, with the least amount of heavy metal precipitate, produced the highest amount of LTA even though there was still SOD present. This indicated that the presence of heavy metal ions leads to the production of SOD; the higher the amount of heavy metal in the solution, the higher the ratio of SOD to LTA.

Microwave power was associated with both higher crystallinity and production of SOD. There was an optimal level of microwave energy irradiated for the production of LTA. Further increasing the irradiated energy, reduced the production of LTA which eventually plateaued while SOD production increased linearly. This trend was more pronounced for experiments conducted with unfiltered leachate.

The SEM, CEC and TGA results corroborated the XRD results. The SEM micrographs showed approximately equal amounts of LTA and SOD structures deposited on CFA particles for both zeolites produced using coarse filtered and fine-filtered leachate solutions while zeolite produced using unfiltered leachate samples showed more SOD structures. The CEC values were the highest for the zeolite synthesized using fine-filtered leachate followed by the zeolite synthesized using coarse filtered leachate and lowest for the unfiltered leachate. The TGA results showed the same trend for the water carrying capacity.

References

[1]   G.L. Fisher, C.E. Chrisp, O.G. Raabe, Physical Factors Affecting the Mutagenicity of Fly Ash from a Coal-Fired Power Plant, Science. 204 (1979) 879–881.

[2]   H. Holler, U. Wirsching, Zeolite formation from fly ash, Fortschr. Mineral. 63 (1985) 21–43.

[3]   H. Kazemian, Z. Naghdali, T. Ghaffari Kashani, F. Farhadi, Conversion of high silicon fly ash to Na-P1 zeolite: Alkaline fusion followed by hydrothermal crystallization, Adv. Powder Technol. 21 (2010) 279–283.

[4]   N. Murayama, T. Takahashi, K. Shuku, H. Lee, J. Shibata, Effect of reaction temperature on hydrothermal syntheses of potassium type zeolites from coal fly ash, Int. J. Miner. Process. 87 (2008) 129–133.

[5]   N.M. Musyoka, L.F. Petrik, O.O. Fatoba, E. Hums, Synthesis of zeolites from coal fly ash using mine waters, Miner. Eng. 53 (2013) 9–15.

[6]   M. Park, C.L. Choi, W.T. Lim, M.C. Kim, J. Choi, N.H. Heo, Molten-salt method for the synthesis of zeolitic materials: I. Zeolite formation in alkaline molten-salt system, Microporous Mesoporous Mater. 37 (2000) 81–89.

[7]   N. Shigemoto, H. Hayashi, K. Miyaura, Selective formation of Na-X zeolite from coal fly ash by fusion with sodium hydroxide prior to hydrothermal reaction, J. Mater. Sci. 28 (1993) 4781–4786.

[8]   A. Shoumkova, V. Stoyanova, Zeolites formation by hydrothermal alkali activation of coal fly ash from thermal power station "Maritsa 3", Bulgaria, Fuel. 103 (2013) 533–541.

[9]   H. Tanaka, A. Fujii, Effect of stirring on the dissolution of coal fly ash and synthesis of pure-form Na-A and -X zeolites by two-step process, Adv. Powder Technol. 20 (2009) 473–479.

[10]   S.S. Bukhari, J. Behin, H. Kazemian, S. Rohani, A comparative study using direct hydrothermal and indirect fusion methods to produce zeolites from coal fly ash utilizing single-mode microwave energy, J. Mater. Sci. 49 (2014) 8261–8271. doi:10.1007/s10853-014-8535-2.

[11]   S.S. Bukhari, S. Rohani, H. Kazemian, Effect of ultrasound energy on the zeolitization of chemical extracts from fused coal fly ash, Ultrason. Sonochem. 28 (2016) 47–53. doi:10.1016/j.ultsonch.2015.06.031.

[12]   Y. Chen, T. Xu, C. Xie, H. Han, F. Zhao, J. Zhang, et al., Pure zeolite Na-P and Na-X prepared from coal fly ash under the effect of steric hindrance, J. Chem. Technol. Biotechnol. (2015) n/a–n/a. doi:10.1002/jctb.4794.

[13]   S.S. Bukhari, J. Behin, H. Kazemian, S. Rohani, Conversion of coal fly ash to zeolite utilizing microwave and ultrasound energies: A review, Fuel. 140 (2015) 250–266.

[14]   X. Querol, N. Moreno, J.C. Umaña, A. Alastuey, E. Hernández, A. López-Soler, et al., Synthesis of zeolites from coal fly ash: an overview, Int. J. Coal Geol. 50 (2002) 413–423. doi:10.1016/S0166-5162(02)00124-6.

[15]   J. Behin, S.S. Bukhari, H. Kazemian, S. Rohani, Developing a zero liquid discharge process for zeolitization of coal fly ash to synthetic NaP zeolite, Fuel. 171 (2016) 195–202.

[16]   C. Belviso, F. Cavalcante, A. Lettino, S. Fiore, Zeolite synthesised from fused coal fly ash at low temperature using seawater for crystallization, Coal Combust. Gasifica-Tion Prod. 1 (2009) 8–13.

[17]   K. Hussar, S. Teekasap, N. Somsuk, Synthesis of Zeolite A from By-Product of Aluminum Etching Process: Effects of Reaction Temperature and Reaction Time on Pore Volume, Am. J. Environ. Sci. 7 (2011) 35.

[18]   N.M. Musyoka, L.F. Petrik, G. Balfour, W.M. Gitari, E. Hums, Synthesis of hydroxy sodalite from coal fly ash using waste industrial brine solution, J. Environ. Sci. Health Part A. 46 (2011) 1699–1707.

[19]   J. Behin, S.S. Bukhari, V. Dehnavi, H. Kazemian, S. Rohani, Using Coal Fly Ash and Wastewater for Microwave Synthesis of LTA Zeolite, Chem. Eng. Technol. 37 (2014) 1532–1540. doi:10.1002/ceat.201400225.

[20]   V. Dehnavi, B.L. Luan, D.W. Shoesmith, X.Y. Liu, S. Rohani, Effect of duty cycle and applied current frequency on plasma electrolytic oxidation (PEO) coating growth behavior, Surf. Coat. Technol. 226 (2013) 100–107.

[21]   E. Senior, ed., Microbiology of Landfill Sites, Second, Lewis Publishers, Boca Raton, 1995.

[22]   F.J. Rivas, F. Beltrán, F. Carvalho, B. Acedo, O. Gimeno, Stabilized leachates: sequential coagulation–flocculation + chemical oxidation process, J. Hazard. Mater. 116 (2004) 95–102. doi:10.1016/j.jhazmat.2004.07.022.

[23]   S. Ghafari, H.A. Aziz, M.H. Isa, A.A. Zinatizadeh, Application of response surface methodology (RSM) to optimize coagulation–flocculation treatment of leachate using poly-aluminum chloride (PAC) and alum, J. Hazard. Mater. 163 (2009) 650–656. doi:10.1016/j.jhazmat.2008.07.090.

[24]   N.G. Turan, O.N. Ergun, Removal of Cu(II) from leachate using natural zeolite as a landfill liner material, J. Hazard. Mater. 167 (2009) 696–700.

[25]   K.Y. Foo, B.H. Hameed, An overview of landfill leachate treatment via activated carbon adsorption process, J. Hazard. Mater. 171 (2009) 54–60. doi:10.1016/j.jhazmat.2009.06.038.

[26]   J. Wiszniowski, D. Robert, J. Surmacz-Gorska, K. Miksch, J.V. Weber, Landfill leachate treatment methods: A review, Environ. Chem. Lett. 4 (2006) 51–61. doi:10.1007/s10311-005-0016-z.

[27]   S. Renou, J.G. Givaudan, S. Poulain, F. Dirassouyan, P. Moulin, Landfill leachate treatment: Review and opportunity, J. Hazard. Mater. 150 (2008) 468–493. doi:10.1016/j.jhazmat.2007.09.077.

[28]   H. Omar, S. Rohani, Treatment of landfill waste, leachate and landfill gas: A review, Front. Chem. Sci. Eng. 9 (2015) 15–32. doi:10.1007/s11705-015-1501-y.

[29]   R. Morschhäuser, M. Krull, C. Kayser, C. Boberski, R. Bierbaum, P. A. Püschner, T. Glasnov, K.C. Oliver, Microwave-assisted continuous flow synthesis on industrial scale, Green Process. Synth. 1 (2012) 281–290.

[30]   M.M.J. Treacy, J.B. Higgins, Collection of simulated XRD powder patterns for zeolites, Elsevier, Amsterdam, The Netherlands, 2007.

[31]   D.C. Bain, B.F.L. Smith, Chemical analysis, in: Handb. Determinative Methods Clay Mineral., Blackie, Glasgow, 1987: pp. 248–274.

[32]   E.K. Miller, J.D. Blum, A.J. Friedland, Determination of soil exchangeable-cation loss and weathering rates using Sr isotopes, Nature. 362 (1993) 438–441. doi:10.1038/362438a0.

[33]   P. Kjeldsen, M.A. Barlaz, A.P. Rooker, A. Baun, A. Ledin, T.H. Christensen, Present and Long-Term Composition of MSW Landfill Leachate: A Review, Crit. Rev. Environ. Sci. Technol. 32 (2002) 297–336. doi:10.1080/10643380290813462.

[34]   M. Inada, H. Tsujimoto, Y. Eguchi, N. Enomoto, J. Hojo, Microwave-assisted zeolite synthesis from coal fly ash in hydrothermal process, Fuel. 84 (2005) 1482–1486.

[35]   S.S. Bukhari, J. Behin, H. Kazemian, S. Rohani, A comparative study using direct hydrothermal and indirect fusion methods to produce zeolites from coal fly ash utilizing single-mode microwave energy, J. Mater. Sci. 49 (2014) 8261–8271.

[36]   S. Khodabandeh, Synthesis of Alkaline-Earth Zeolites, California Institute of Technology, 1997.

[37]   Baerlocher, Ch., McCusker, L.B., Olson, D.H., Atlas of Zeolite Framework types, 6th ed., Elsevier Science, New York, NY, USA, 2007.

[38]   E. Hums, N.M. Musyoka, H. Baser, A. Inayat, W. Schwieger, In-situ ultrasound study of the kinetics of formation of zeolites Na–A and Na–X from coal fly ash, Ultrasonics. 54 (2014) 537–543.

[39]   S.S. Bukhari, J. Behin, H. Kazemian, S. Rohani, Synthesis of zeolite NA-A using single mode microwave irradiation at atmospheric pressure: The effect of microwave power, Can. J. Chem. Eng. 93 (2015) 1081–1090.

[40]   H. Tanaka, A. Fujii, S. Fujimoto, Y. Tanaka, Microwave-Assisted Two-Step Process for the Synthesis of a Single-Phase Na-A Zeolite from Coal Fly Ash, Adv. Powder Technol. 19 (2008) 83–94. doi:10.1163/156855208X291783.

[41]   H. Kazemian, T. Ghaffari Kashani, M. Noorian, Synthesis and characterization of Zeolite A, using fly ash of the Iran ferrosilice company and investigating its ion-exchange properties, Iran. J. Crystallogr. Mineral. 13 (2005) 329–336.

[42]   A. Derkowski, W. Franus, H. Waniak-Nowicka, A. Czimerova, Textural properties vs. CEC and EGME retention of Na-X zeolite prepared from fly ash at room temperature, Int. J. Miner. Process. 82 (n.d.) 57–68. doi:10.1016/j.minpro.2006.10.001.

Chapter 7

7 Continuous Flow Large Scale Synthesis of Zeolite-A Utilizing Microwave Irradiation with Recycled Liquid Stream

Abstract

Coal fly ash (CFA) was converted to zeolite using continuous microwave reactors at bench and pilot scales while minimizing the wastewater produced during the zeolitization process. At bench scale, a continuous flow tubular microwave reactor was used to explore the effect of microwave irradiation on the crystallinity of the product. The waste water was reused in consecutive runs and ICP (inductively coupled plasma) analysis was conducted during and after each run to observe the concentration of cations. An increase in the production of hydroxysodalite compared to zeolite-A was noted at higher levels of microwave energy. The XRD and SEM analyses were also conducted to corroborate the results. The CEC measurement showed the highest value of 0.405 meq/g when deionized (DI) water was used, the CEC dropped to 0.177 meq/g for thrice recycled waste stream. It was also found that higher microwave irradiation resulted in faster crystal growth, and the product crystallinity reached its maximum at 810 W of microwave irradiation in 60 min while 335 W of microwave irradiation resulted in the same crystallinity after 120 min of reaction. The design and specification of a pilot plant MW-based reactor system capable of converting CFA to zeolite, are presented at the end.

7.1 Introduction

Despite public and private investments and advances in renewable energies, coal remains the leading source of electricity generation in the world. Currently about 40% of the global electricity is produced by coal and predicted to account for 33% by 2035 according to International Energy Agency [1]. Even with this reduced share, coal will stay a major source of electricity production around the world. In 2010 alone, coal fired power plants produce about 780 million ton coal combustion products such as Coal Fly Ash (CFA) worldwide. Only about 50% of these products were recycled [2]. There has been much research conducted on producing value added products such as zeolites [3] from the accumulated CFA. Pioneering studies in zeolitization of CFA was reported using conventional heating [4–6], however, recently many researchers have focused their efforts on utilizing novel energy sources such as microwave [7–9] and ultrasound [10–13].

Most of the studies conducted in the field of zeolitization of CFA have utilized deionized, distilled or industrial water, however, there have been a few reports which studied different sources of water. Belviso et al. [14] synthesized zeolite X from CFA and seawater by pre-treatment fusion with NaOH followed by hydrothermal crystallization.. The synthesis yield at different crystallization temperature was higher using seawater. Hussar et al. [15] synthesized zeolite A by hydrothermal process using sodium silicate, sodium aluminate and the by-product of an aluminum etching process. Chemical composition of the aluminum etching by-product consisted mainly of oxides Al2O3 (92 %), Na2O (6 %) and SiO2 (0.5 %). Their results indicated that higher synthesis reaction temperature and reaction time resulted in synthesis of zeolite A with a higher crystallinity. The effect of using industrial waste brine solution instead of ultrapure water, was investigated by Musyoka et al. [16]. They used coal fly ash as silicon feedstock and high halide brine obtained from the retentate effluent of a reverse osmosis mine water treatment plant, as the solvent. The brine contained a high sodium and potassium levels and low concentrations of toxic elements. In addition, there was a trace of aluminum equal to 48.38 µg/L. The use of brine as a solvent resulted in the formation of hydroxysodalite zeolite. Musyoka et al. [17] used two types of mine waters (i.e. acid and

circumneutral) obtained from coal mining operation instead of pure water to manufacture zeolites Na-X and Na-P by means of a two step indirect (fusion followed by hydrothermal crystallization) and a direct method, respectively. The important cationic species of circumneutral water were: (Na: 952 mg/L, Mg: 38 mg/L, and Ca: 19 mg/L and Si: 1.2 mg/L without any Al) and acid drainage water contained: (Fe: 4694 mg/L, Na: 68 mg/L, Mg: 386 mg/L, and Ca: 458 mg/L, Al: 613 mg/L and Si: 31 mg/L). The use of circumneutral mine water resulted in similar quality zeolite Na-P and X, whereas the use of acidic mine drainage led to the formation of hydroxysodalite zeolite. Behin et al. [7] utilized liquid waste stream from a Plasma Electrolytic Oxidation (PEO) process. The electrolytes used in PEO typically contained low concentrations of alkaline solutions [18]. The waste stream of PEO contained Na (673 mg/L), K (497 mg/L), Si (295 mg/L) and Al (10 mg/L) cations and the zeolite synthesized with this waste stream had a lower CEC and water carrying capacity compared to zeolite synthesized with DI water.

In addition to using waste water as mentioned above, Behin et al. [19] reused and recycled the waste stream from zeolitization process. It was found that the product was zeolite-P utilizing waste water stream as opposed to zeolite-P produced with DI water.

The present work explores the utilizing of recycled waste water for the production of zeolite-A at larger scale unlike previous works focusing on microwave zeolitization of CFA that were limited to lab scale [7,8,14,17,19].

There has been some researched done on a larger scale. Moriyama et al. [20] used a 0.6 L reactor for the conversion of CFA to zeolite-P at an elevated pressure of 0.48 MPa and 153°C. The liquid to solid ratio was 1.1 L/kg in NaOH solution (3 M). The zeolite-P produced had a CEC ranging from 1.25-2.0 meq/g. Querol et al. [21] produced zeolite-P in a 10,000 L reactor. The reaction was conducted at 149.5°C and 0.35 MPa. The liquid to solid ratio in the slurry was 1.68 L/kg in 2.4 M NaOH solution.

This Chapter reports the work conducted in a bench MW reactor with a volume of 0.2 L and also introduces a pilot scale reactor system with an 80 L MW reactor.

7.2   Materials and Method

7.2.1 Materials

Coal fly ash was obtained from a coal fired power plant (OPG, Nanticoke) located in the Ontario province of Canada and was stored in a seal container before use. Sodium hydroxide (Alphachem, Canada), sodium aluminate anhydrous (Sigma-Aldrich, USA) were of analytical grade and used as received. Deionized (DI) water was used for the preparation of the solutions. Other chemicals used for characterization tests were of analytical grade.

7.2.2 Methods

Two sets of experiments were conducted; the first set of experiments were conducted to study the effects of MW power while the second set of experiments were conducted utilizing a recycled stream. The Milestone FlowSynth MW (Milestone, Italy) reactor was used to conduct direct conversion of CFA to zeolite similar to [8], but at a larger scale (1 L of reaction slurry compared to 20 mL).

7.2.2.1   MW power experiments

The first set of experiment was carried out by adding 109 g of sodium hydroxide granules with 91 g of fly ash (NaOH/CFA ratio of 1.2) to 850 mL deionized water, and mixed at 60 ℃ for 16 h. Afterwards, 150 mL aqueous sodium aluminate solution (concentration: 0.155 g/mL) was also added. The slurry with extra sodium aluminate was aged for two hours at room temperature and mixed in the tank attached to the MW reactor. The schematic diagram of the experimental apparatus is illustrated in Figure 7-1.
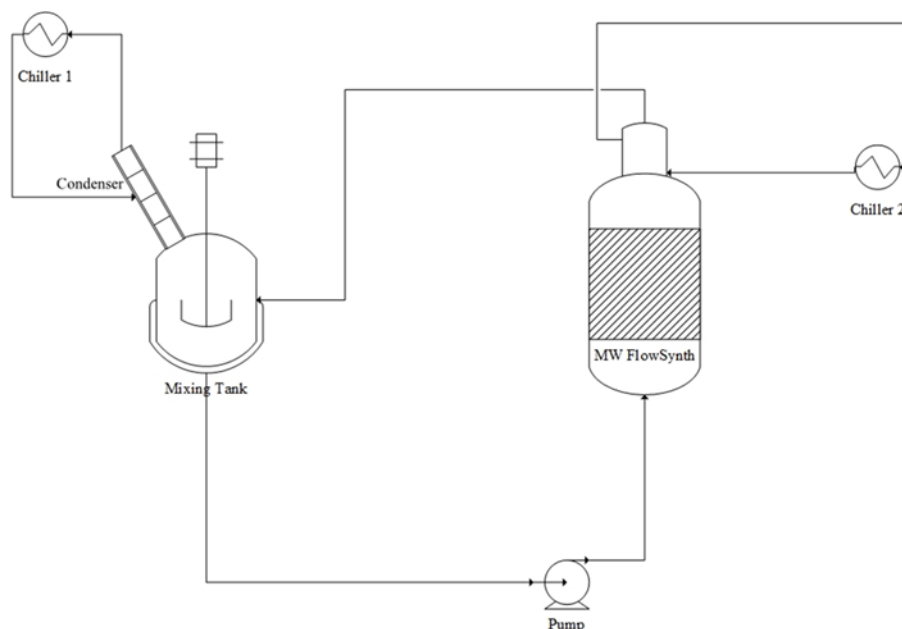
Figure 7-1. Schematic of experimental setup

The system was kept at atmospheric pressure at 95°C with the use of a condenser. The slurry was circulated through the MW reactor and samples were withdrawn from the mixing tank at predetermined times. The slurry flow was adjusted to increase the total or cumulative MW irradiation to the reaction slurry to study the effect s of MW irradiation on the zeolitization process. The experimental runs with different flow rates and corresponding MW power are outlined in Table 7-1. The block diagram of the runs without the overall recycle stream to the digestion tank is shown in Figure 7-2.

Table 7-1. Microwave power experiment samples with corresponding MW power and flow rates

Sample	Average MW Power (W)	Flow rate (mL/min)
P-300	335	130
P-400	395	150

| P-600 | 600 | 200 |
| P-800 | 810 | 250 |
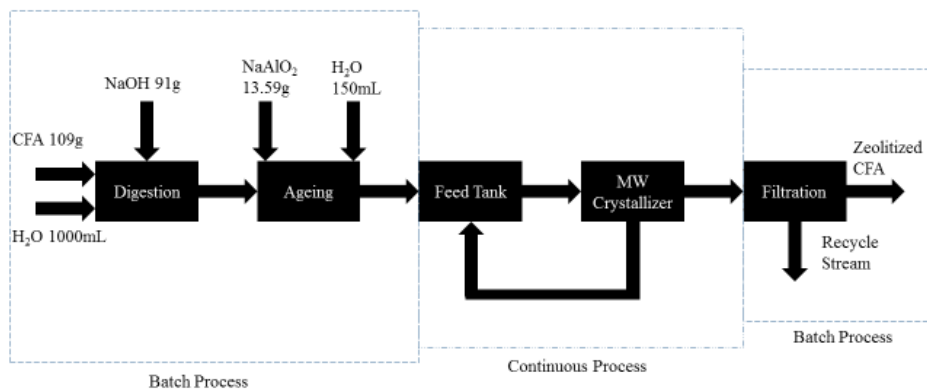
Figure 7-2. The block diagram of runs without the overall recycle stream from the MW reactor/crystallizer to the digestion tank

7.2.2.2   Recycled stream experiments

The slurry for the first run was prepared with DI water according to the procedure discussed above. For the successive runs with an overall recycled stream, the slurry was withdrawn from the FlowSynth MW crystallizer/reactor after removing the product zeolitized CFA in the filtration system, was mixed of the DI water. Seven hundred fifty mL of the effluent stream from the Flow Synth MW reactor/crystallizer was recovered and mixed with the DI water to replenish the solvent. The loss of 250 mL in each run was associated with two major factors, some of the liquid remained in the zeolitized CFA, and the liquid content inside the reactor could not be completely removed. The block diagram of the runs with the overall recycled stream is illustrated in Figure 7-3.
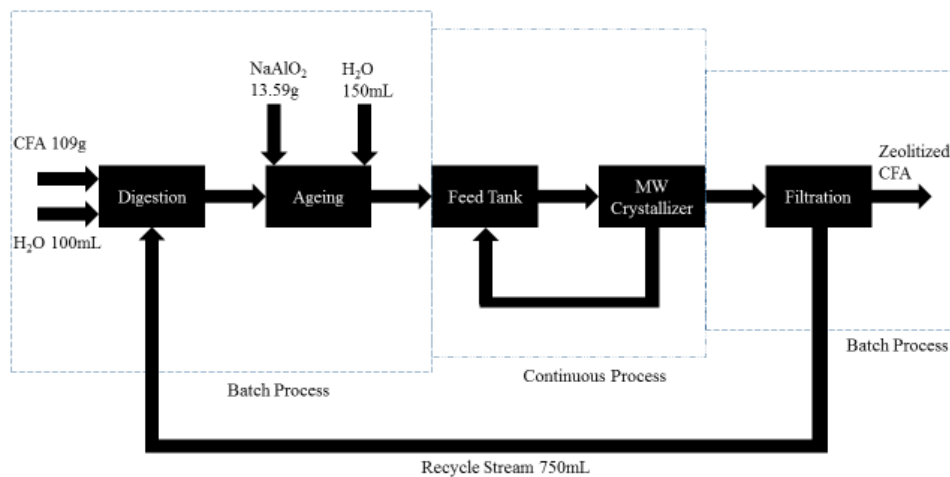
Figure 7-3. The block diagram of runs with the overall recycle stream from the MW reactor/crystallizer to the digestion tank

Samples were withdrawn after each digestion and microwave treatment (crystallization) to observe the metal ion concentration in the solution throughout the experiments.

7.2.3 Characterization

Inductively coupled plasma atomic emission spectroscopy (ICP-AES) was used to measure the concentration of different ions in the solution both after digestion and microwave reaction. Concentrations were found using a Perkin-Elmer Optima-3300 DV ICP-Atomic Emission Spectrometer (USA). Chemical composition of the CFA sample was determined by means of X-ray fluorescence spectroscopy (XRF) utilizing PANalytical PW2400 Wavelength Dispersive. Rigaku–Miniflex powder diffractometer (Japan) was used to collect XRD data of the synthesized zeolites using CuKα (λ for Kα = 1.54059 Å) over the range of 5°<2θ<25° with a step width of 0.02°. The characteristic peaks of zeolitized CFA were at the 2θ of 7.20°, 10.19°, 12.49°, 16.14°and 24° [22]. The peak areas were calculated using MDI-Jade v 7.5 software. The crystal size distribution and morphology of the zeolites were studied by scanning electron microscope (SEM); Hitachi S 2600N SEM (Tokyo, Japan) operating at 5 kV of acceleration voltage. CEC was measured using ammonium acetate saturation method (over a 5 day period) based on

Bain and Smith [23]. The zeolite samples were soaked in a 1 N solution of ammonium acetate for 5 days in the same end-over-end shaker. After 5 days, the zeolite samples were filtered and allowed to air dry. The dried samples were then washed using 100 mL (5 x 20 mL) of an aqueous solution of 10 wt% NaCl and 1 vol% HCl to remove the fixated ammonium. The ammonium concentration in the supernatant was then measured. The ammonium concentration was correlated to peak absorbance intensity between 550 and 800 nm measured using UV-VIS spectroscopy. To prepare the samples for the UV-VIS spectroscopy, sodium salicylate, sodium hydroxide and sodium hypochlorite were added and 5 minutes allowed to elapse for the reaction to proceed to completion.

7.3 Results and Discussion

7.3.1 X-ray analysis (XRD and XRD)

The main sources of Si and Al from CFA for hydrothermal zeolitization process are summarized in Table 7-2. The XRD data indicated that the main components of the CFA were amorphous aluminosilicate as well as quartz and mullite that existed as crystalline structures.

Table 7-2. XRF analysis of chemical composition of CFA

Parameter	Weight percent (%)
Major oxide	
SiO_2	41.78
Al_2O_3	19.61
CaO	13.64
Fe_2O_3	5.79
MgO	3.23
TiO_2	1.39
K_2O	1.1
Na_2O	0.94
P_2O_5	0.71
BaO	0.36

SrO	0.25
Cr_2O_3	0.01
MnO	0.02
Loss On Ignition	10.89
Total	99.72

Phases analysis
     Amorphous aluminosilicate
     Quartz (SiO_2)
     Mullite ($3Al_2O_3.2SiO_2$)

*SiO_2/Al_2O_3: 2.13

7.3.2 MW power experiments

7.3.2.1　X-ray Diffraction Analysis (XRD)

After the digestion in the mixing tank, the feed pump was turned on at a predetermined speed indicated in Table 7-1 to continuously supply the CFA slurry through the microwave reactor. It took the system about ten min to reach steady state. Following steady state, samples were collected every 30 min to conduct XRD analysis. The characteristic peaks area of the samples collected are indicated in Figure 7-4.
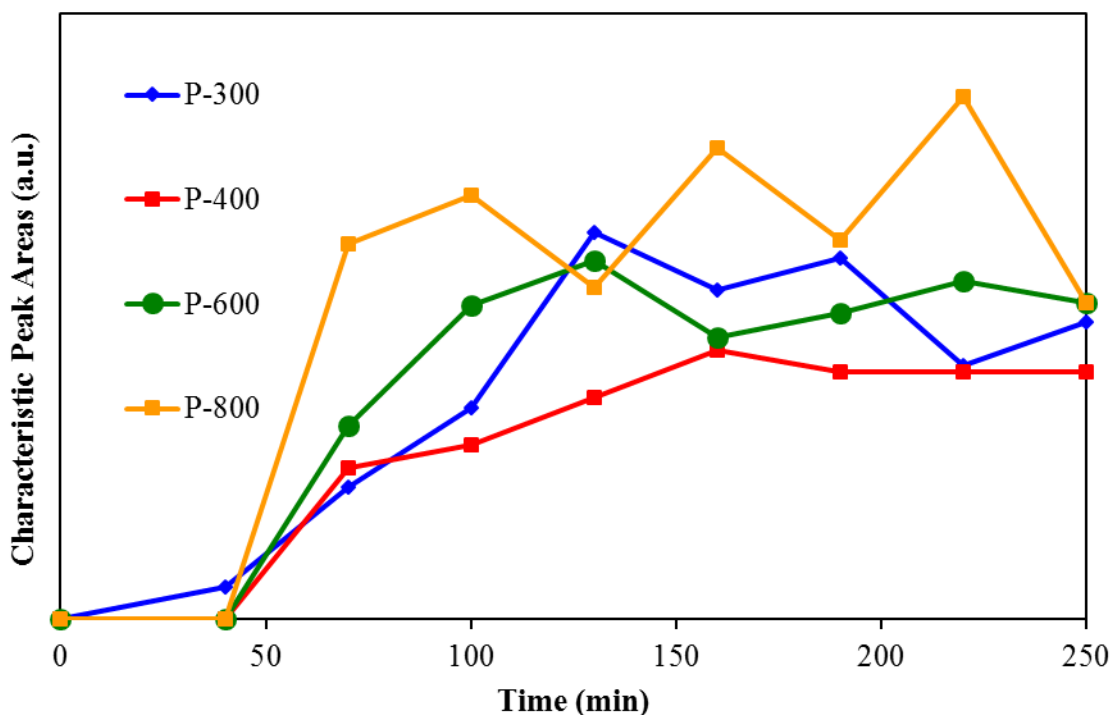
Figure 7-4. XRD characteristic peak areas with respect to time

The XRD analysis indicate that irrespective of MW power all the samples require at least 30 min before zeolitic crystals can be registered by XRD. Therefore, it indicates that the nucleation of zeolitic crystals is not a strong function of the MW power. However, once crystal growth starts, the samples irradiated under higher MW power grow faster compared to samples irradiated with lower power. Once the characteristic peak of a sample area reached a maximum, it did not increase with the increases MW power input. All of the samples eventually had the similar crystallinity irrespective of the MW power input level.

7.3.2.2   Scanning Electron Microscope (SEM)

The SEM images of the solids were taken over the four h of microwave irradiation. The SEM images are illustrated in Figure 7-5 (a-e).
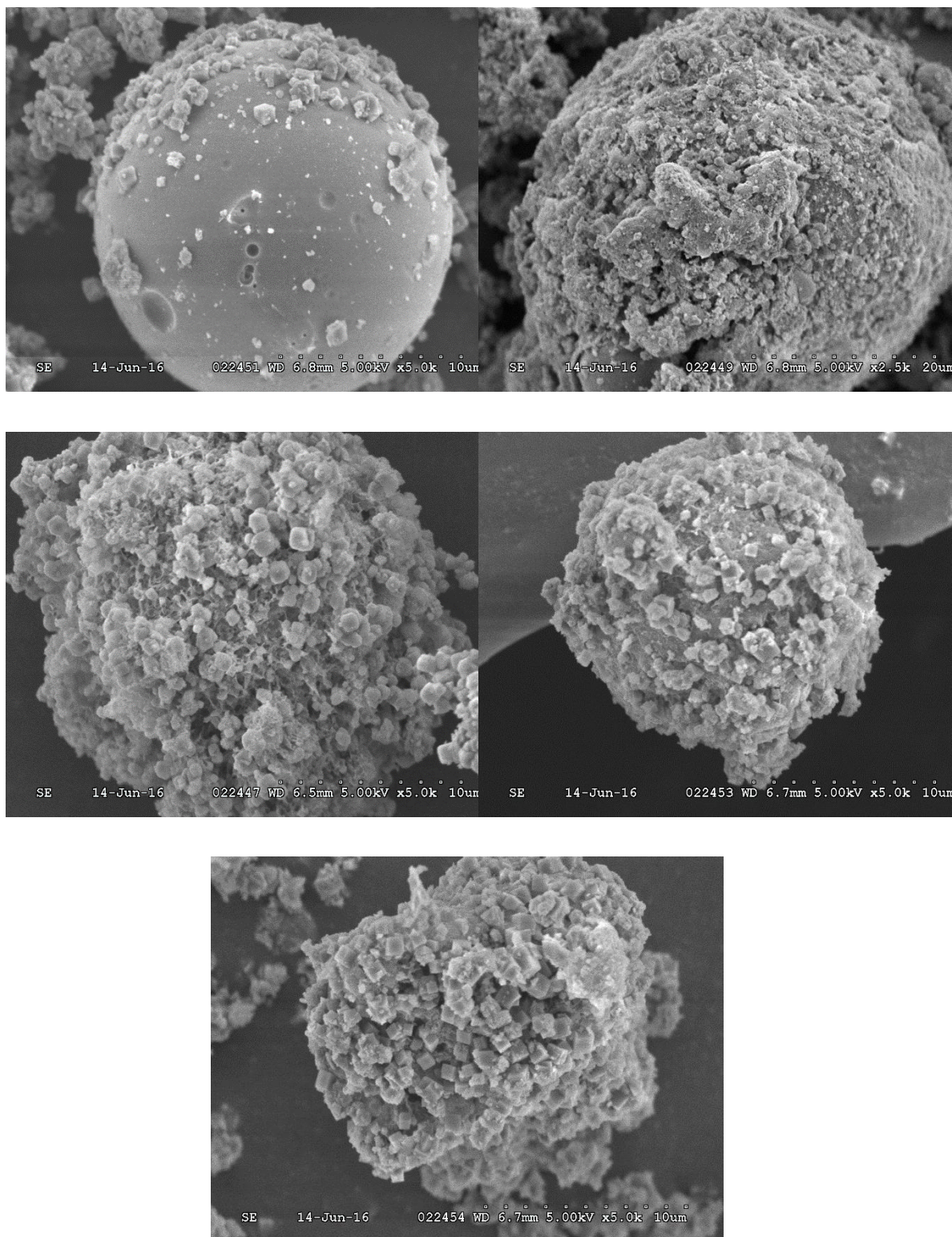
Figure 7-5. SEM images of zeolitized CFA at a) 30 min b) 60 min c) 90 min d) 120 min e) 150 min

The SEM analysis of the microwave irradiated experiments show that the surface of CFA is the nucleation and crystal growth site for the zeolites. As the reaction progresses small cubic LTA zeolitic crystals can be deciphered in the SEM images. These structures grow larger with increase in the time of microwave irradiation.

7.3.3 Recycled stream experiments

7.3.3.1   X-ray Diffraction analysis (XRD)

The XRD analyses for the recycled stream experiments were conducted after the end of each run. The results are indicated in Figure 7-6.
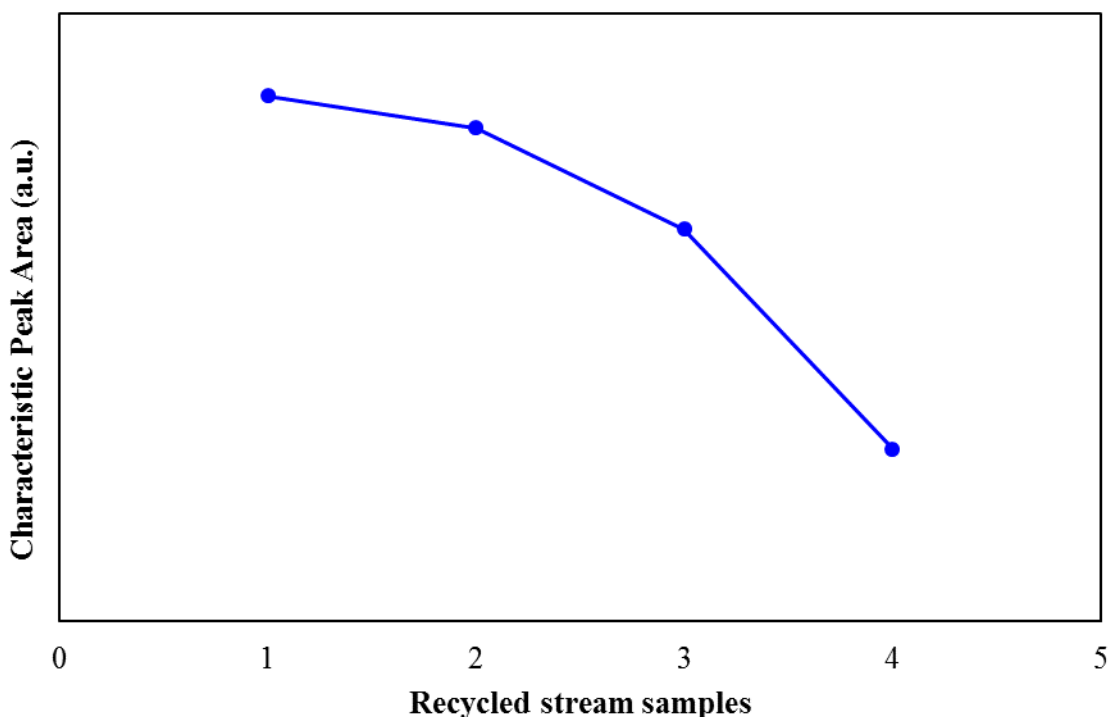
Figure 7-6. The XRD characteristic peak area results for recycled stream

It was observed that after each run the crystallinity of the final product was reduced. Indicating that the recycled stream as the precursor reactant solvent produces a lower quality of zeolitic crystals compared to using fresh water. As the recycle stream is re-used the crystallinity of the product is further decreased. This can be explained due to the

increased concentration of metallic ions with each run. This is later corroborated with the ICP results.

7.3.3.2 Inductively coupled plasma atomic emission spectroscopy (ICP-AES)

The ICP analysis was conducted for recycle stream experiments in order to track the concentration of metallic ions in the solvent over the length of the whole experiment. Samples for the ICP analysis were drawn after digestion (designated by D in Figure 7-7) and crystallization (designated by C in Figure 7-7).

Metallic ions including Al, As, Fe, K, Si, and V were detected in the solvent. The concentration of both light and heavy metals increased with each run as indicated in Figure 7-7 (a-c). The solid bars represent the ICP result after digestion and the shaded bars represent ICP results after digestion.
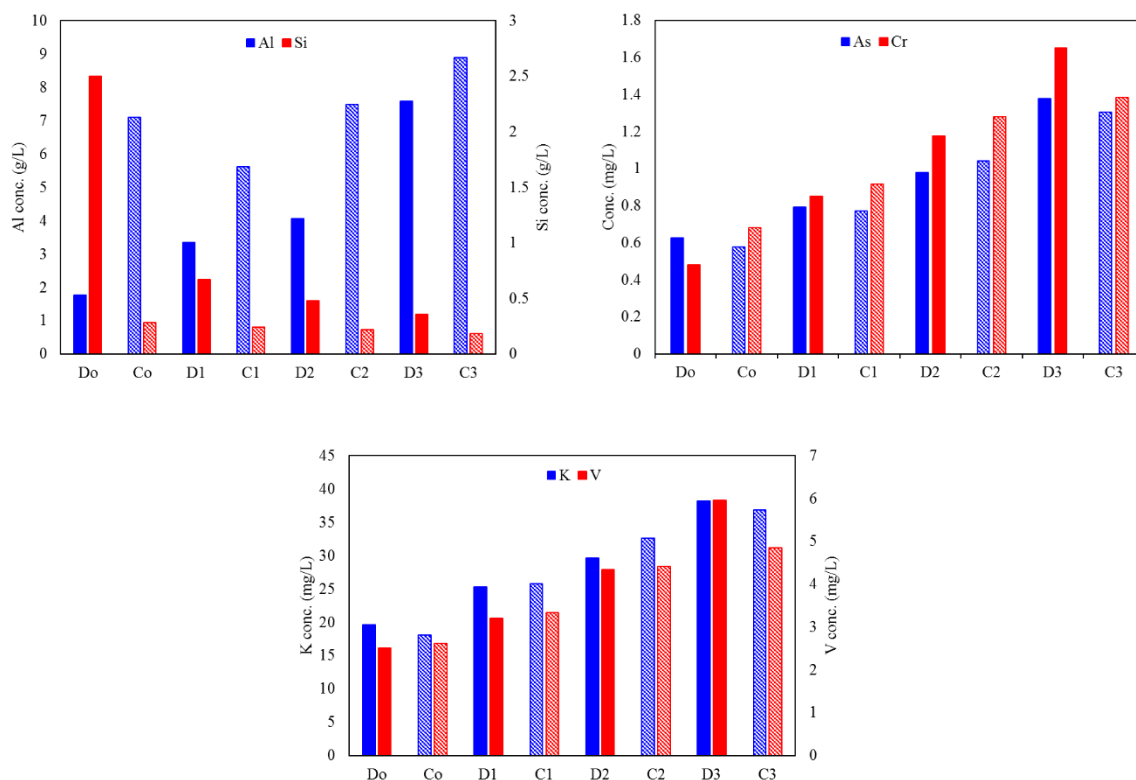
Figure 7-7. ICP analysis of a) Al, Si b) As, Cr and c) K, V

Figure 7-7 a) indicates that after digestion in the first run (D_0) both the aluminum and silicon concentration can be detected which indicates the dissolution of aluminosilicate contents of CFA into the reactant solvent. Aluminum content is seen to increase in each ICP samples after crystallization (C_0 to C_3) due to the addition of extra aluminum before crystallization step. Addition of extra aluminum is necessary for the crystallization of LTA framework as it is observed that without extra aluminum zeolite-P is obtained [19,24].

Each ICP after crystallization shows lower concentration of Si compared to the corresponding digestion step, indicating that the Si constituents in the reactant solvent crystallize as part of zeolitic framework. It can be further noted that each consecutive digestive step results in lower concentration of Si compared to the last digestion step signifying that recycle stream is not as capable of dissolving CFA contents compared to fresh water. This effect becomes more significant as the liquid stream is recycled. This could be due to the saturation of the reactant solvent with metallic ions.

Figure 7-7 b and c show the concentration of As, Cr, K, and V over the recycled stream run. It can be observed that the concentration of these metallic ions constantly increases as the recycled stream is reused, indicating continuous dissolution of metallic constituents of CFA into the reactant solvent.

7.3.3.3   Scanning Electron Microscope (SEM)

The SEM images of the recycled stream experiments were obtained for samples at the end of each 4 hour run. The images showed cubic LTA and rough spherical sodalite (SOD) structure. The amount of zeolitic crystals present, depended on the reactant solvent and how many times the reactant solvent stream was recycled. The first two samples, one crystallized in DI water and the other in once recycled stream had significantly higher cubic structures. However, successive experiments had fewer cubic LTA structures and significantly more rough spherical SOD structures. The presence of heavy metal ions can be a cause for the preference of SOD crystals.
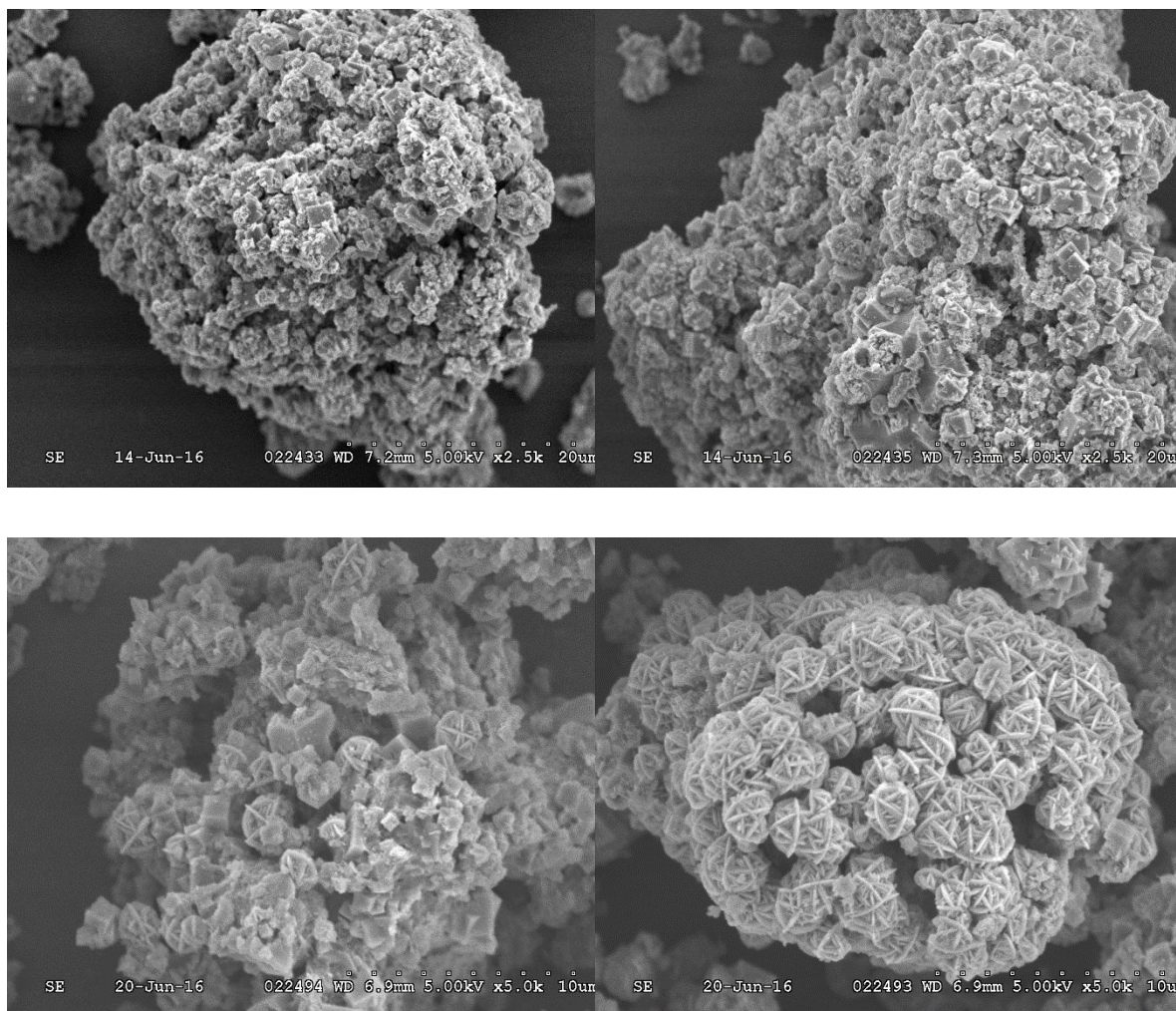
Figure 7-8. SEM images of zeolitized CFA with a) Deionized Water b) first recycled stream c) Second recycled stream d) Third recycled stream

7.3.3.4   Cation Exchange Capacity (CEC)

The cation exchange capacity (CEC) is an important physical property of zeolite that determines its quality. Figure 7-9 illustrates the CEC of the zeolitized CFA synthesized with various reaction solvents.
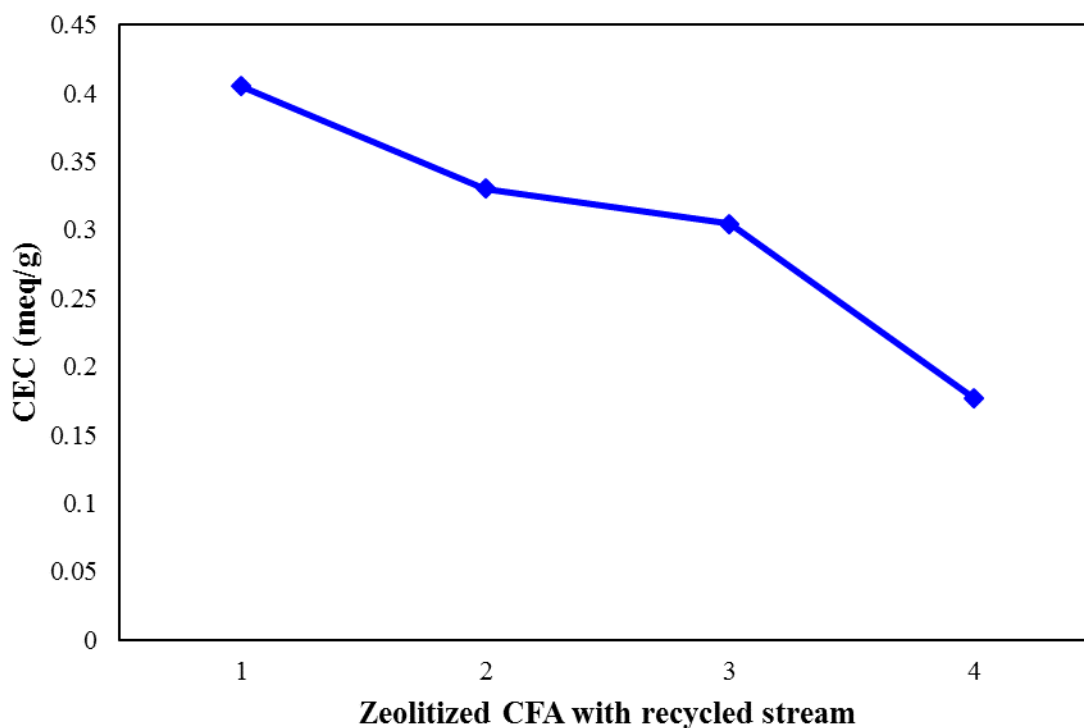
**Figure 7-9. CEC of zeolitized CFA with Deionized water, First recycled stream,
Second recycled stream, Third recycled stream**

The zeolitized CFA synthesized with DI water had the highest CEC with 0.405 meq/g, and as the consecutive recycled stream is used the resulting product had lower CEC, 0.330, 0.305 and 0.177 meq/g, respectively. The decrease in the CEC of the synthesized samples can be attributed to the higher production of hydroxysodalite when the solvent has a higher concentration of metallic cations.

7.3.4 Pilot reactor system

Penetration depth of microwave irradiation is a measure of its efficiency to heat up a bulk material. It is defined as the depth at which the intensity of the radiation inside the material falls to 1/e (about 37%) of its original value at the surface. The penetration depth can be calculated using the following equation

$$D_P = \frac{\lambda}{2\,\pi\,\sqrt{2\epsilon'}} \cdot \frac{1}{\sqrt{\sqrt{1 + \left(\frac{\epsilon''}{\epsilon'}\right)^2} - 1}}$$

Eq. 7-4

Where D_p is the penetration depth, λ is the wave length of the MW, ϵ', is the dielectric constant, which represents stored energy when the material is exposed to an electric field, ϵ'' is the dielectric loss factor which is the imaginary part, influences energy absorption and attenuation. Penetration depth was calculated assuming dielectric properties of water and was found to be 4.86 cm, however this penetration depth decreases with the introduction of ions in the solution because of the dramatic change in dielectric [25,26].

Penetration depth of MW is low in most materials which leads to difficulty in the scaling up of a microwave reactor. It is difficult to realize a continuous flow microwave system that can operate for volumes big enough to be compatible with the use of heterogeneous reaction condition and prevent the problem of line clogging. This has led to a stop-flow technique development, where reagent mixtures are pumped into a batch reactor under atmospheric pressure. The reaction takes place in autogenous pressure and a back regulating valve is used to keep the reactor mixture from escaping the reactor. After the completion of the reaction the product is pumped out [27]. However, this technic is not truly a continuous system.

In order to envision a truly continuous system two issues have to be resolved. First, the penetration depth has to be increased and secondly, heat has to be removed from the reactor to keep reaction mixture from boiling and producing higher pressure thus eliminating a need for a stop-flow reactor. The pilot scale reactor system was designed with these two issues in mind.

The reactor system was commissioned at Institute for Chemicals and Fuels from Alternative Resources (ICFAR) in Ilderton.

7.3.4.1   MW reactor overview

The MW reactor was designed as a continuous stirred tank reactor (CSTR) with the microwave introduced through slotted antenna. Utilizing MW antenna has the benefit of introduces MW irradiation radially inside the reaction mixture unlike most MW system where the electromagnetic waves travel across planar. This design of slotted antenna immersed in the reaction solution increases the surface with which MW come in direct contact with the slurry. Furthermore, the MW reactor vigorously mixes the reaction solution/suspension resulting in a homogenous MW heating. The design of the MW reactor with the slotted antenna and mixer is illustrated in Figure 7-10.
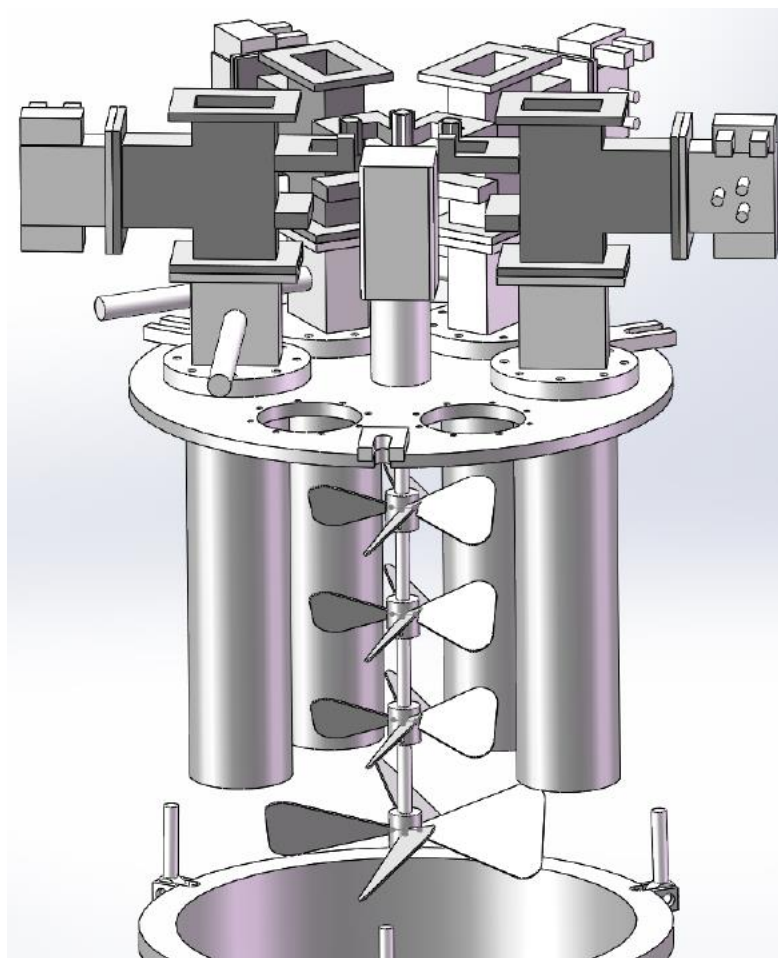
Figure 7-10. 3-D illustration of the MW reactor with slotted antenna

This system is designed to utilize both single mode and multimode microwaves. The reaction can also be conducted with a combination of both multimode and single mode regimes. In a single mode microwave, electromagnetic irradiation is directed through a precisely-designed wave guide that produces a standing wave, whereas in multimode microwave there is no single standing wave but a mixture of many waves with different phase shifts. The microwave field density in a single mode microwave is much higher compared to multimode microwave, therefore similar results can be achieved in single-mode microwave using lower power than in high power multimode microwave [26].

Six specially designed slotted antenna produce 8 kW of microwaves. The reactor is jacketed and a heavy duty chiller is installed in order to control the temperature and prevent a temperature and pressure spike.

7.3.4.2   Reactor system electrical specifications

The system is designed to separate electrical power supplies, three phase 380 V and 208 V. The electrical specifications for the chiller and MW reactor system are outline in Table 7-3.

Table 7-3. Electrical supply and specification for MW reactor system and chiller

Electrical Supply	Voltage (V)	Phase	Frequency (Hz)	Power (kW)	Current (A)
Reactor System	208	3	60	18	50
	380	3	60	20	33
	220	1	50	20	33
Chiller	380	3	60	5.6	13.5

The electrical supply to the main reactor system used to power pumps, mechanical stirrers, MW magnetrons and water pump. The chiller electrical supply powers the

compressor and cooling fans in the chiller. The electrical line diagrams for the chiller and reactor system power supply are shown in Figure 7-11 and Figure 7-12.
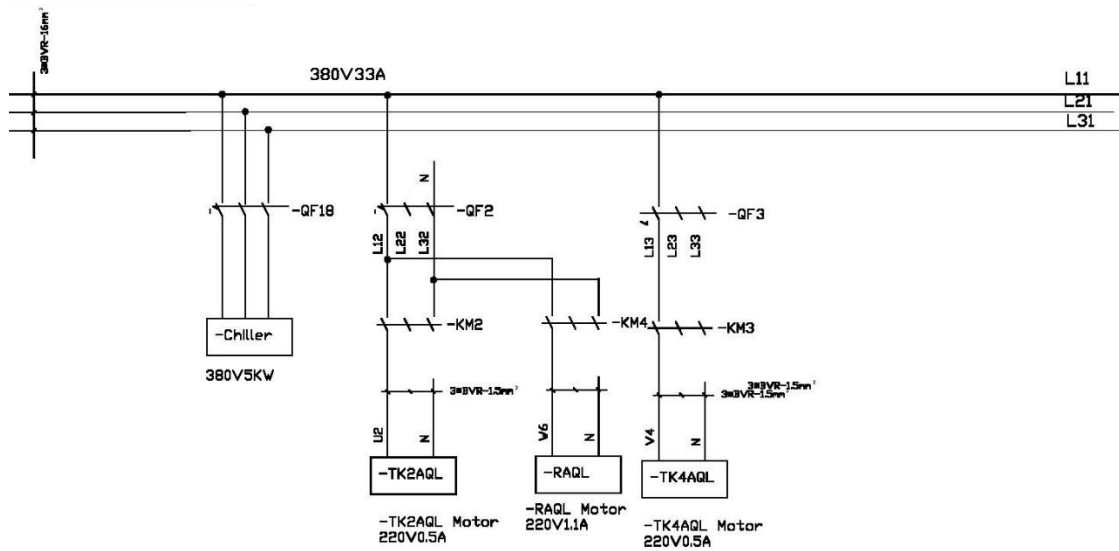
Figure 7-11. Electrical line diagram for chiller with a 3-phase 380 V power supply
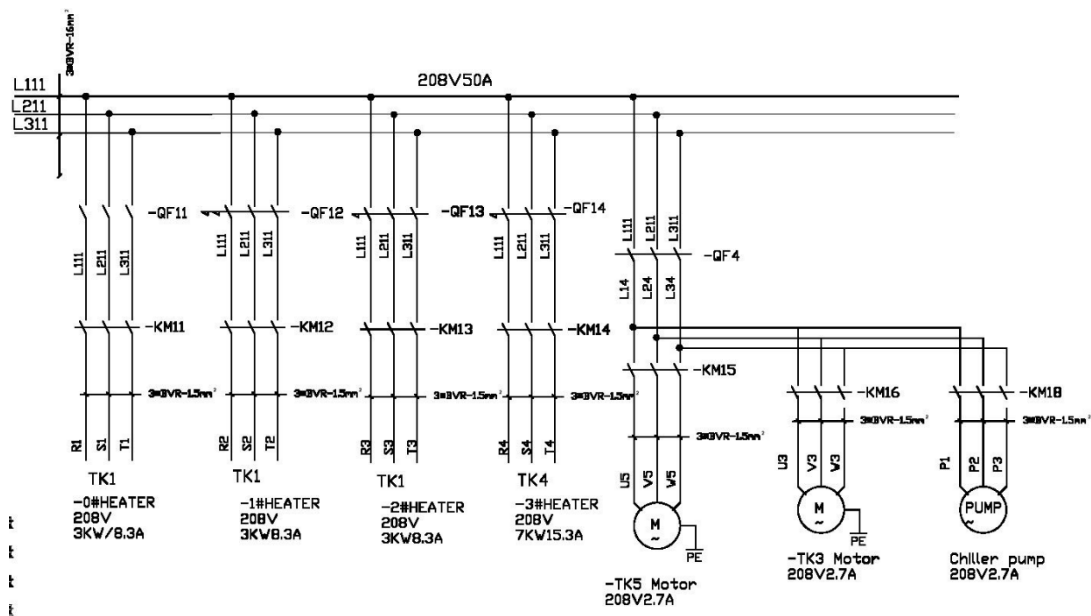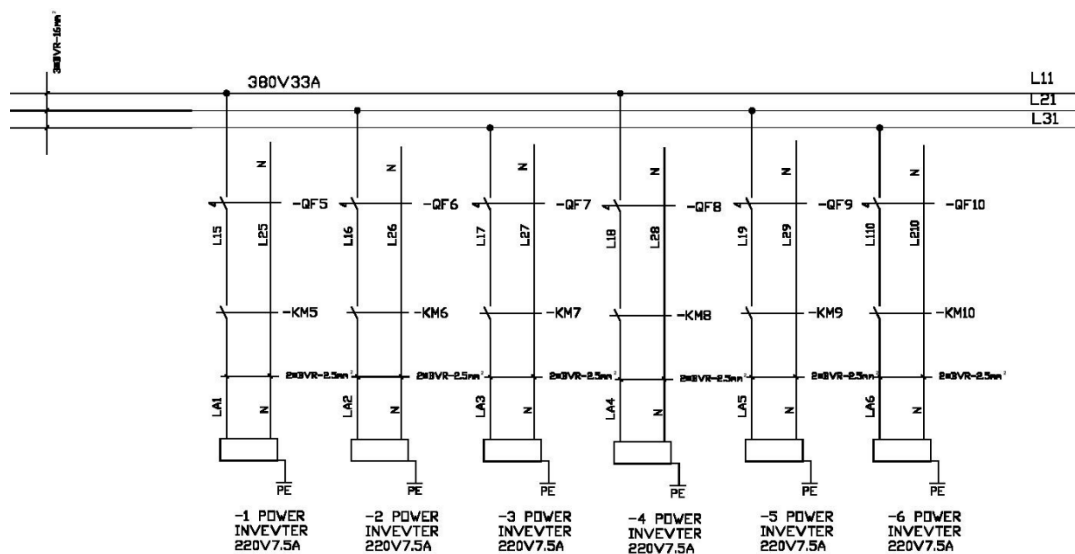
Figure 7-12. Electric line diagram of MW reactor system a) 3 phase 208 V powering heaters, pumps and mechanical stirrers b) 1 phase 220 V powering six MW antenna

7.3.4.3   Reactor system specifications

The reactor system consists of five tanks and one microwave reactor. There are also six peristaltic pumps. The process flow diagram is illustrated in Figure 7-13 while the commissioned reactor system is shown in Figure 7-14.
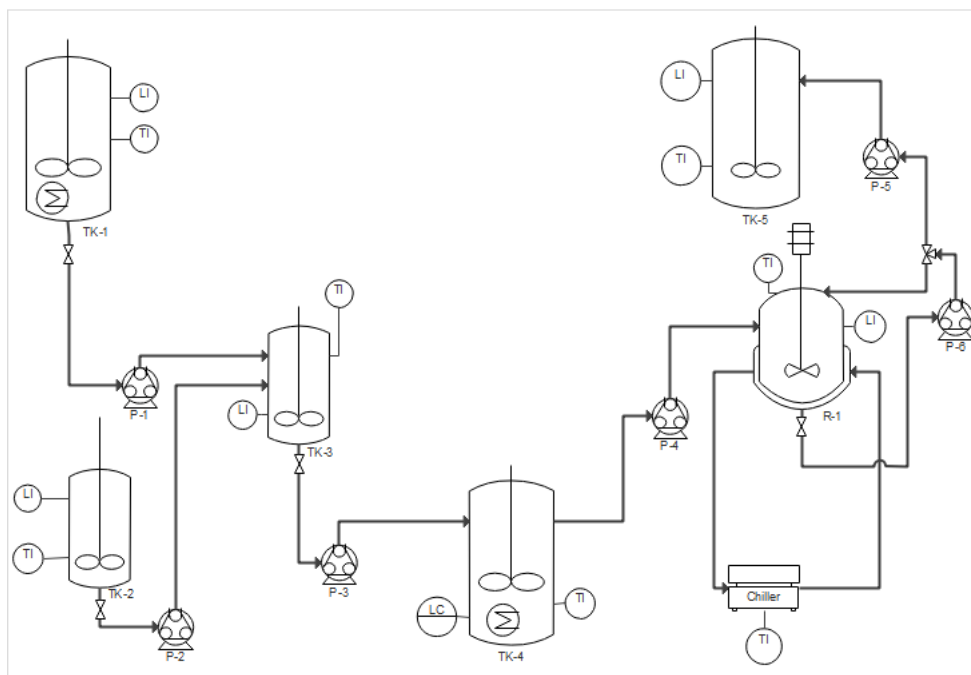
Figure 7-13. Process Flow Diagram of the MW reactor system
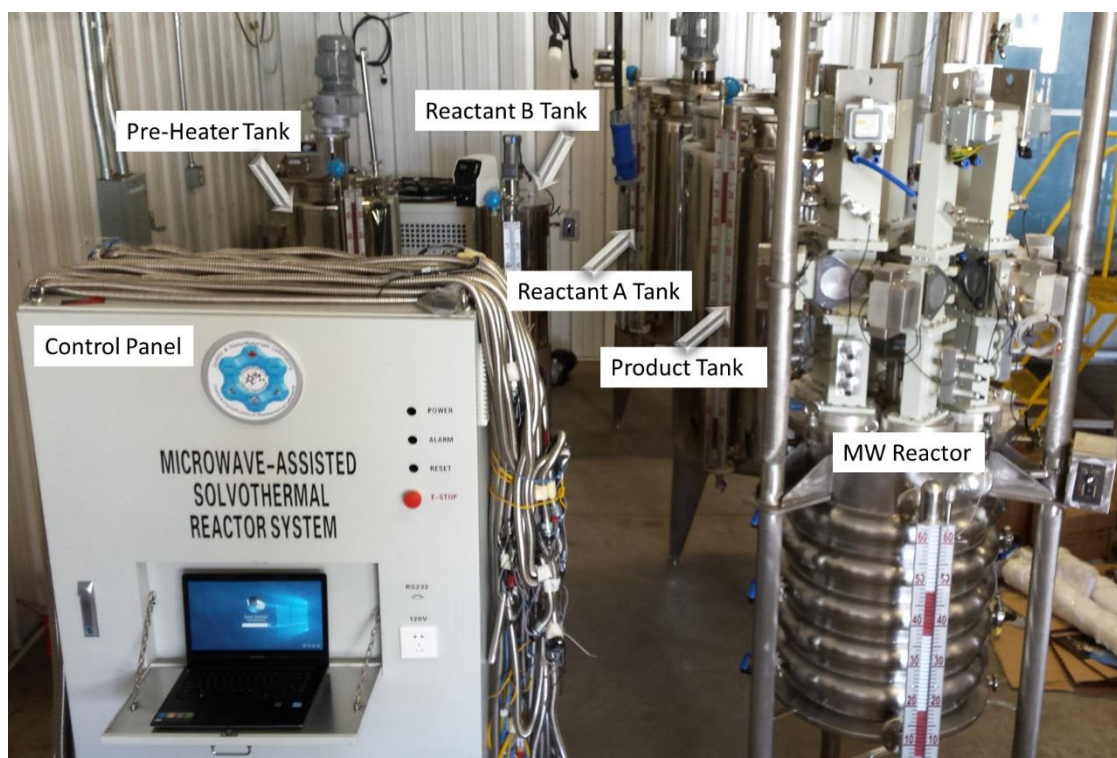
Figure 7-14. Commissioned MW reactor system

All the tanks and the MW reactor have bypass level indicators. One of the limitation of this type of indicator is that there is a minimum level of liquid required in the tank before a signal can be registered. The minimum and maximum operating volume of each tank and MW reactor are indicated in Table 7-4.

Table 7-4. The minimum and maximum operating conditions for each tank and MW reactor

	Min. Volume (L)	Max. Volume (L)	Heating Capacity (kW)	Role
TK-1	110	500	9 kW	Reactant A
TK-2	30	80	N/A	Reactant B
TK-3	60	180	N/A	Mixing tank
TK-4	N/A	N/A	7 kW	Pre-heater
TK-5	110	600	N/A	Product tank
R-1	20	80	8 kW (MW)	MW Reactor

Tank 4 (TK-4) uses a float level to work at a constant level that can be set through the user interface. The user interface runs on the software King View 7.0 (WellinTech) and this interface is illustrated in Figure 7-15.
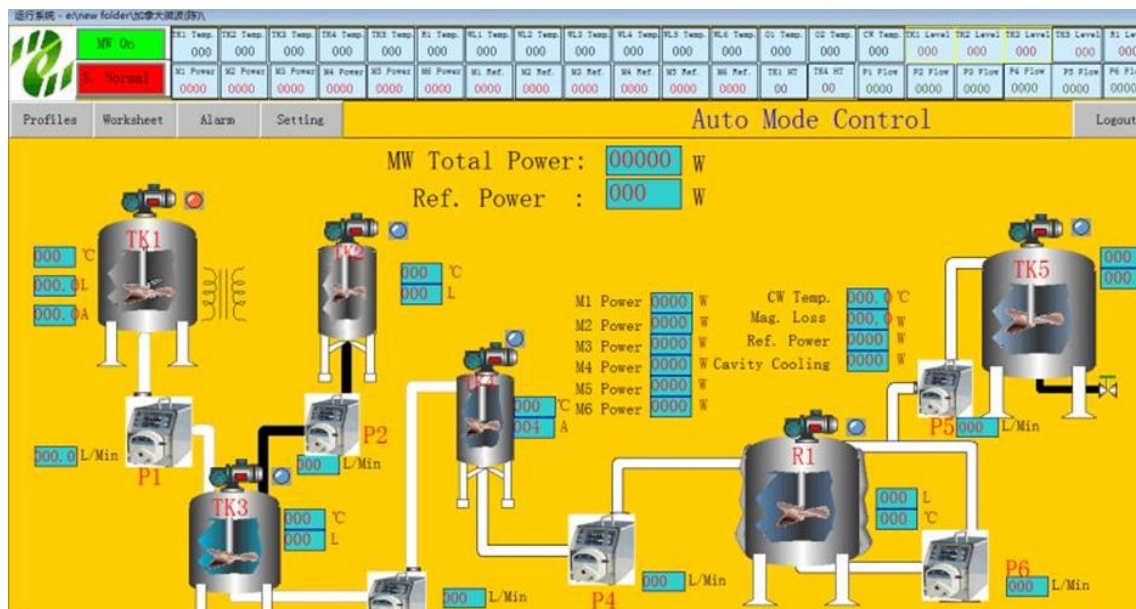
Figure 7-15. The software user interface for the MW reactor system

The calibration for the tanks and pumps are given in Figure D-1 and Figure D-2, respectively. These calibrations can be used to set the flowrate of each pump to vary the reaction parameters.

7.3.4.4 Recommendations

A filtration system should be introduced after TK-1 to separate the undissolved CFA. The pumps are capable of pumping slurry, however, pipes and elbows would be prone to clogging if slurry solution is used. Furthermore, filtering out the undissolved CFA particles would produce a higher purity zeolite.

Source of water should be installed near the reactor system instead of manually filling the system with water. This will save a lot of man hour.

A dyke with a sink is required in case of a spill to safely operate the system. A shower needs to be installed for emergency cases.

7.4 Conclusions

Two sets of experiments converting CFA to zeolite were conducted utilizing the continuous flow microwave reactor. The first set of experiment was conducted to investigate the effects of microwave power on the zeolitization. It was observed that higher power of microwave irradiation resulted in a faster crystal growth while after 150 min of reaction it was observed that the crystallinity reached a maximum regardless of microwave power.

The second set of experiment was conducted with recycled waste liquid stream from the process for the zeolitization process. The ICP analysis was conducted after digestion and after crystallization for each run. The concentration of silicon and aluminum significantly increased after each digestion step and decreased after crystallization. This signifies the dissolution of aluminosilicate constituents of CFA and the subsequent decrease of silicon and aluminum concentration in the liquid result from aluminosilicates crystallizing as zeolitic crystals on the surface of CFA particles. However, each consecutive recycled stream shows the amount of aluminosilicate constituents of CFA dissolved are lower than previous successive runs. This indicates that the waste stream produced by the zeolitization process cannot be recycled indefinitely. This is also observed through XRD and SEM analysis. The XRD analysis indicates that the crystallinity of the zeolite produced with successive recycled streams is lower while the SEM shows a higher production of hydroxysodalite compared to zeolite-A. The CEC analysis further indicates that the zeolite produced with DI water has higher CEC of 0.405 meq/g compared to recycled streams of 0.330, 0.305, and 0.177 meq/g.

This Chapter also discusses the design and specification of a pilot plant MW reactor system that is capable of converting CFA to zeolite.

7.5 References

[1]   Agency IE, International Energy Agency, editors. World energy outlook 2013. Paris: International Energy Agency; 2013.

[2]   Heidrich C, Feuerborn, H, Weir, A. Coal Combustion Products: a Global Perspective. World Coal Ash WOCA, Lexington, KY: 2013.

[3]   Bukhari SS, Behin J, Kazemian H, Rohani S. Conversion of coal fly ash to zeolite utilizing microwave and ultrasound energies: A review. Fuel 2015;140:250–66.

[4]   Holler H, Wirsching U. Zeolite formation from fly ash. Fortschr Mineral 1985;63:21–43.

[5]   Shigemoto N, Hayashi H, Miyaura K. Selective formation of Na-X zeolite from coal fly ash by fusion with sodium hydroxide prior to hydrothermal reaction. J Mater Sci 1993;28:4781–4786.

[6]   Hollman GG, Steenbruggen G, Janssen-Jurkovičová M. A two-step process for the synthesis of zeolites from coal fly ash. Fuel 1999;78:1225–1230.

[7]   Behin J, Bukhari SS, Dehnavi V, Kazemian H, Rohani S. Using Coal Fly Ash and Wastewater for Microwave Synthesis of LTA Zeolite. Chem Eng Technol 2014;37:1532–40. doi:10.1002/ceat.201400225.

[8]   Bukhari SS, Behin J, Kazemian H, Rohani S. A comparative study using direct hydrothermal and indirect fusion methods to produce zeolites from coal fly ash utilizing single-mode microwave energy. J Mater Sci 2014;49:8261–71.

[9]   Querol X, Alastuey A, López-Soler A, Plana F, Andrés JM, Juan R, et al. A fast method for recycling fly ash: microwave-assisted zeolite synthesis. Environ Sci Technol 1997;31:2527–2533.

[10]   Bukhari SS, Rohani S, Kazemian H. Effect of ultrasound energy on the zeolitization of chemical extracts from fused coal fly ash. Ultrason Sonochem 2016;28:47–53. doi:10.1016/j.ultsonch.2015.06.031.

[11]   Belviso C, Cavalcante F, Lettino A, Fiore S. Effects of ultrasonic treatment on zeolite synthesized from coal fly ash. Ultrason Sonochem 2011;18:661–8.

[12]   Wang S, Zhu ZH. Sonochemical treatment of fly ash for dye removal from wastewater. J Hazard Mater 2005;126:91–5.

[13]   Musyoka NM, Petrik LF, Hums E. Ultrasonic assisted synthesis of zeolite A from coal fly ash using mine waters (acid mine drainage and circumneutral mine water) as a substitute for ultra pure water. Int. Mine Water Assoc., Aachen, Germany: 2011, p. 423–8.

[14]   Belviso C, Cavalcante F, Lettino A, Fiore S. Zeolite synthesised from fused coal fly ash at low temperature using seawater for crystallization. Coal Combust Gasifica-Tion Prod 2009;1:8–13.

[15]   Hussar K, Teekasap S, Somsuk N. Synthesis of Zeolite A from By-Product of Aluminum Etching Process: Effects of Reaction Temperature and Reaction Time on Pore Volume. Am J Environ Sci 2011;7:35.

[16]   Musyoka NM, Petrik LF, Balfour G, Gitari WM, Hums E. Synthesis of hydroxy sodalite from coal fly ash using waste industrial brine solution. J Environ Sci Health Part A 2011;46:1699–1707.

[17]   Musyoka NM, Petrik LF, Fatoba OO, Hums E. Synthesis of zeolites from coal fly ash using mine waters. Miner Eng 2013;53:9–15.

[18]   Dehnavi V, Luan BL, Shoesmith DW, Liu XY, Rohani S. Effect of duty cycle and applied current frequency on plasma electrolytic oxidation (PEO) coating growth behavior. Surf Coat Technol 2013.

[19]   Behin J, Bukhari SS, Kazemian H, Rohani S. Developing a zero liquid discharge process for zeolitization of coal fly ash to synthetic NaP zeolite. Fuel 2016;171:195–202.

[20]   Moriyama R, Takeda S, Onozaki M, Katayama Y, Shiota K, Fukuda T, et al. Large-scale synthesis of artificial zeolite from coal fly ash with a small charge of alkaline solution. Fuel 2005;84:1455–61.

[21]   Querol X, Umaña JC, Plana F, Alastuey A, Lopez-Soler A, Medinaceli A, et al. Synthesis of zeolites from fly ash at pilot plant scale. Examples of potential applications. Fuel 2001;80:857–865.

[22]   Treacy MMJ, Higgins JB. Collection of simulated XRD powder patterns for zeolites. Amsterdam, The Netherlands: Elsevier; 2007.

[23]   Bain DC, Smith BFL. Chemical analysis. Handb. Determinative Methods Clay Mineral., Glasgow: Blackie; 1987, p. 248–74.

[24]   Aldahri T, Behin J, Kazemian H, Rohani S. Synthesis of zeolite Na-P from coal fly ash by thermo-sonochemical treatment. Fuel 2016;182:494–501.

[25]   Hasted JB. Liquid water: Dielectric properties. Phys. Phys. Chem. Water, Springer; 1972, p. 255–309.

[26]   Buchner R, Barthel J, Stauber J. The dielectric relaxation of water between 0 C and 35 C. Chem Phys Lett 1999;306:57–63.

[27]   Glasnov TN, Kappe CO. Microwave-Assisted Synthesis under Continuous-Flow Conditions. Macromol Rapid Commun 2007;28:395–410.

[28]   Morschhäuser R, Krull M, Kayser C, Boberski C, Bierbaum R, P. A. Püschner, T. Glasnov, K.C. Oliver. Microwave-assisted continuous flow synthesis on industrial scale. Green Process Synth 2012;1:281–90.

Chapter 8

8   Conclusions and recommendations

8.1   Conclusions

The research of this thesis focused on the synthesis of zeolite from pure precursors and coal fly ash utilizing a single mode microwave unit and an ultrasound horn. The product samples were analyzed and characterized using XRD, FTIR, TGA, BET, CEC, SEM. Following are the main conclusions from this work

1) Na-A zeolite was synthesized from pure chemicals using a single mode microwave heating method. The presence of zeolite Na-A and Na-X crystals was verified by both XRD and SEM. Producing zeolite through microwave synthesis significantly shortens the production time (by approximately 50%) of the zeolite compared to the conventional hydrothermal process. The microwave irradiation power plays a significant role in producing a single phase zeolite, furthermore, the total amount of microwave irradiated energy also strongly influences the purity of the zeolite produced. Higher power and total energy irradiation produce pure Na-A compared to a mixture of Na-X and Na-A at lower power and energy irradiation. Single mode microwave is also more effective in the production of zeolite as relatively low power is required to achieve the same results. In this study powers of 100 W and 300 W were used from a single mode microwave source compared to many previous studies where the power source was as high as 1000 W in a multimode microwave.

2) Coal fly ash (CFA) was converted into Na-A zeolite using a single mode microwave heating at atmospheric pressure. Two methods of converting CFA were investigated (direct hydrothermal and indirect fusion). The effects of three factors (power, time, aluminate concentration) were investigated. Zeolite produced from CFA (CFAZA) was characterized using FTIR, XRD, BET, TGA, and CEC. The hydrothermal and fusion products were comparable to each other in their characteristics. The empirical equations found using the design of experiment (DOE) show that the method of conversion plays a significant role in the crystallinity of the CFAZA, while interacts with other factors such

as microwave irradiation power & time and the concentration of aluminum in the gel precursor. It is found that CFAZA produced by direct hydrothermal is comparable to the CFAZA produced through indirect fusion conversion under microwave irradiation at atmospheric pressure. The direct hydrothermal conversion proved to be more economically attractive for converting CFA to zeolite-A as it is less energy intensive compared to indirect fusion conversion.

3) The technique of immersing the ultrasound (UTS) probe directly into the reaction mixture prepared by extracting the constituents of CFA produced Na-A in 1 hour. The UTS assisted synthesis at 95°C reduced the induction time of the zeolitization process by 20 min and also increased the crystal growth rate compared to the conventional heating. However, as the reaction progressed, the synthesized zeolite-A converted to a more stable zeolite phase, namely hydroxysodalite. Reaction conducted at 85°C showed that the UTS energy in addition to reduction of induction time and an increase in the crystal growth rate, produces a single phase zeolite-A, while the conventional heating produced small amounts of both zeolite-A and hydroxysodalite. The SEM images showed that the UTS energy at 85°C produced the purest single phase zeolite-A with smooth crystalline surface and smaller crystal sizes. However, conventional synthesis at 85°C resulted in zeolitic crystals with amorphous debris on the surface, generally with larger crystal sizes and in the presence of hydroxysodalite crystals.

4) Landfill leachate was used for coal fly ash zeolitization, as a solvent. Sodium hydroxide added to the leachate solution resulted in a large amount of heavy metal precipitation. The presence of heavy metal ions led to the production of hydroxysodalite; the higher the amount of heavy metals in the solution, the higher the ratio of hydroxysodalite to Na-A. Higher microwave power was associated with both higher crystallinity and production of hydroxysodalite. There was an optimal level of the total or cumulative microwave energy irradiated for the production of Na-A. Further increase of the irradiated energy, reduced the production of Na-A which eventually plateaued while hydroxysodalite production increased linearly.

5) In the bench scale zeolitization experiments, it was observed that higher power of microwave irradiation resulted in a faster crystal growth while after 150 min of reaction it was observed that the crystallinity did not change regardless of MW power. In order to decrease the amount of waste produced during this process, the liquid waste stream was recycled. Consecutive recycled stream shows lower amounts of aluminosilicate constituents of CFA. Therefore, this indicates that the waste stream produced by the zeolitization process cannot be recycled indefinitely.

6) The CEC detection method utilizing salicylate-based ammonia assay proved to save time and be less prone to experimental errors as compared to Kjeldahl method as the latter method requires careful back titration.

8.2   Recommendations and further research

8.2.1 Single mode microwave

Experiments conducted utilizing single mode microwave have shown that zeolites can be produced at a much lower power level (100-300 W) compared to multimode microwave (1000 W). It is recommended that any industrial conversion process of CFA using microwaves should focus on a single mode microwave reactor.

8.2.2 Ultrasound probe

Irradiation of ultrasound energy directly into the reaction system using an ultrasound probe has shown to be much more effective than water bath ultrasound systems used in studies conducted previously. Ultrasound probe has shown that zeolite can be readily produced at a lower temperature and at a faster rate, therefore, the ultrasound irradiation should be directly introduced in the reaction sample.

8.2.3 Direct and indirect zeolitization of CFA

Design of experiment (DOE) methodology was used to compare the direct and indirect zeolitization of CFA in Chapter 4. It was concluded that the characteristics of zeolitized CFA produced from these two methods were comparable. The BET surface area was 42 m^2/g for direct method and 64 m^2/g for indirect method, whereas, CEC was 2.43 meq/g

and 2.252 meq/g, respectively. Therefore, it is recommended that the direct conversion method should be preferred over the indirect conversion. The indirect conversion method is also more energy intensive method.

8.2.4 Extraction of aluminosilicate constituents from CFA

The amount of aluminum and silicon extracted from the digestion process is an important parameter and needs much focus. Through ICP analysis of the solution after digestion it was calculated that only 13.75% of Si and 17.35% of Al content of CFA (data from Chapter 4) were extracted during the indirect fusion conversion, while during the direct conversion 17.3% of Si and 22.3% of Al content were extracted (data from Chapter 7). This indicates that both methods are highly inefficient in the extraction of the aluminum and silicon content of CFA. Future research should focus on increasing the amount of aluminosilicate content that is extracted from CFA.

8.2.5 Filtration of CFA prior to zeolitization

The SEM data conclusively show that during the direct hydrothermal conversion zeolite particles are formed on the surface of the undissolved CFA particles. Therefore, the zeolitized CFA has a core of unreacted CFA particle, however, the work in Chapter 6 has shown that after the digestion step the undissolved CFA particles can be separated from the clear solution and zeolites be formed using the extracted aluminum and silicon in the clear solution. The zeolites formed in the clear solution do not have heavy metal content and they can be used for more diverse applications compared to the zeolitized CFA. It is recommended that when a higher quality of zeolite is desired a filtration step be introduced remove the undissolved CFA particles.

8.2.6 Waste utilization

Work conducted in Chapter 6 and Appendix A shows that different liquid waste streams can be utilized for zeolitization process. This can result in the use of both solid waste from coal fired power plants and liquid wastes from other industries. Further research can be conducted to utilize waste stream from other processes in the CFA zeolitization.

8.2.7 Applications of zeolitized CFA

The zeolitized CFA can have a core of undissolved CFA particle which are rich in heavy metals. In order to fully utilize these zeolitized CFA further studies have to conducted on effects of using these zeolites in agricultural and environmental applications. However, XRF results of zeolites produced after filtration of undissolved CFA show that heavy metals were not imbedded in the zeolite crystals. These zeolites might be more promising for agricultural and environmental applications.

8.2.8 Pilot scale reactor

A pilot scale plant was designed, fabricated and commissioned at the end of this project. This reactor system is capable of converting CFA to zeolite utilizing both single mode and multimode microwave irradiation. It is recommended that this reactor system be used in the future to produce zeolites from CFA at a much larger scale than this work was able to accomplish.

Appendix A

A Using coal fly ash and wastewater for microwave synthesis of LTA zeolite[1]

Abstract

This study was motivated to re-use industrial wastes from coal-fired power plant and plasma electrolytic oxidation (PEO) process to utilize two waste stream to produce zeolite. The batch composition was adjusted by adding sodium hydroxide and sodium aluminate. A single mode microwave oven equipped with reflux condenser was used for crystallization under atmospheric pressure. The synthesized samples were then characterized using XRD, SEM, BET, TGA, and CEC measurement. Analytical results indicated that zeolite Na-A with a maximum crystallinity of 67.24 % was successfully synthesized by a hydrothermal treatment of fly ash with wastewater at 300 W for 30 min. Due to the high CEC (i.e. 182 meq/100g), the product can be used for gas purification and soil remediation processes.

A.1   Introduction

The abundance of amorphous aluminosilicate in fly ash, a by-product of coal-fired power stations, makes it an important source material for synthetic zeolites. Over the last few decades, the synthesis of different zeolites from fly ash has been of great interest to many researchers. Two well-known activation processes are generally used for the conversion of coal fly ash (CFA) to zeolite. The first one is a two-step process, in which pre-treatment fusion at high temperature is followed by hydrothermal process. Different zeolites including Na-A [1–3], Na-X [4–8] and Na-P [6,9] were synthesized by means of this indirect two-stage method. The second method is a direct hydrothermal process, in

---

which the fusion step is eliminated [10] and different zeolite such as Na-A [11,12], Na-Y [13], Na-P [14–17] and hydroxysodalite [18] are synthesized. The direct and indirect zeolitization processes of CFA are being studied in terms of the type and concentration of the alkaline solutions, the solution/solid ratio, aging time, mixing technique; and time, temperature and pressure of the crystallization reaction using different thermal sources such as conventional and microwave techniques. Numerous publications including reviews articles [19–21] indicate the increasing interest in using fly ash as a source of Si and Al for manufacturing different porous zeolitic aluminosilicate.

All of the methodologies used for zeolitization of CFA involve three major stages of dissolution, nucleation, and crystal growth. The conventional techniques for synthesis of different zeolites from coal fly ash are very time consuming taking 12-48 hours on average. Currently microwave-assisted hydrothermal processes are being considered as one of the most effective techniques for chemical synthesis including zeolite crystallization [22–24].

Although, most of the studies utilized deionized, distilled or industrial water during the synthesis, few reports studied different sources of water. Belviso et al. [4] synthesized zeolite X from CFA and seawater by pre-treatment fusion with NaOH followed by hydrothermal crystallization. A comparison between the results obtained from the use of seawater and distilled water was reported [4]. The synthesis yield at different crystallization temperature was higher using seawater. Hussar et al. [25] synthesized zeolite A by hydrothermal process using sodium silicate, sodium aluminate and the by-product of an aluminum etching process. Chemical composition of the aluminum etching by-product consisted of the main oxides of Al2O3 (92 %), Na2O (6 %) and SiO2 (0.5 %). Their results indicated that higher synthesis reaction temperature and higher reaction time resulted in better synthesis of zeolite A. The effect of using industrial waste brine solution instead of ultra-pure water was investigated during the synthesis of zeolite by Musyoka et al. [18]. They used coal fly ash as silicon feedstock and high halide brine obtained from the retentate effluent of a reverse osmosis mine water treatment plant. The brine contained a high sodium and potassium levels and low concentrations of toxic elements. In addition, there was a trace of aluminum equal to 48.38 µg/L and no silicon.

The use of brine as a solvent resulted in the formation of hydroxysodalite zeolite. Unconverted mineral phase of mullite and hematite from the fly ash feedstock were found in the synthesis product. Musyoka et al. [6] used two types of mine waters (i.e. acid and circumneutral) obtained from coal mining operation instead of pure water to manufacture zeolites Na-X and Na-P by means of two step indirect (fusion followed by hydrothermal crystallization) and direct method, respectively. The important cationic species of circumneutral water were: (Na: 952 mg/L, Mg: 38 mg/L, and Ca: 19 mg/L and Si: 1.2 mg/L without any Al) and acid drainage water contained: (Fe: 4694 mg/L, Na: 68 mg/L, Mg: 386 mg/L, and Ca: 458 mg/L, Al: 613 mg/L and Si: 31 mg/L). The use of circumneutral mine water resulted in similar quality zeolite Na-P and X whereas the use of acidic mine drainage led to the formation of hydroxy sodalite zeolite.

Plasma electrolytic oxidation (PEO) is a relatively novel technique to produce functional oxide coatings on the surface of metals such as aluminum, magnesium, and titanium and their alloys. As a result of the increasing application of light metals, namely aluminum and magnesium, in different industries due to their strength to weight ratio, low density and ease of fabrication, together with the ability of the PEO process to create coatings on these substrates with considerably improved wear and corrosion resistance compared to anodizing, the PEO process has attracted a lot of interest recently. The configuration used in PEO is similar to conventional anodizing but the coating process is performed at much higher potentials. The electrolytes used in PEO typically contain low concentrations of alkaline solutions [26].

CFA is not only a waste and environmental hazard, but also, its disposal is a financial liability. Wastewater of plasma electrolytic oxidation process is also considered an environmental liability and requires expensive technologies to treat and dispose. The volume of generated industrial waste will continue to grow with the increased industrial and domestic energy demand. In order to reduce the environmental impacts of industrial wastes, potential utilization of the waste toward value added product should be explored. The use of industrial wastewater is considered as a solution for high water consumption demand of zeolite synthesis technologies. Furthermore, it is a potential capital saving option for handling these two industrial solid and liquid wastes. Using a single-mode

microwave irradiation shortens the zeolitization time leading toward a facile and efficient process at larger scale.

A.2   Experimental

A.2.1 Materials

Coal fly ash was obtained from Nanticoke coal fired power plant, Ontario, Canada (owned by Ontario Power Generation; OPG). The CFA sample was stored in a sealed container before use. All of the chemicals including sodium hydroxide (Alphachem, Canada) and anhydrous sodium aluminate (Sigma-Aldrich, USA) were analytical grade and used as received without further purification. Wastewater of plasma electrolytic oxidation process [26] was used instead of distilled water for the preparation of the solutions.

A.2.2 Hydrothermal Synthesis

The reaction mechanism of the hydrothermal microwave-assisted zeolitization of CFA involves three stages of dissolution, nucleation and crystallization [16], which is shown in Figure A-1. A typical synthesis experiment for production of zeolite Na-A from coal fly ash (CFAZA) involved the addition of 1.82 g of sodium hydroxide (granules) and 1.82 g of fly ash to 17 mL wastewater (i.e. NaOH/CFA ratio was 1). The mixture was then mixed using a mechanical stirrer for 12h at 60 ℃ (Sol A). Afterwards, in order to balance Si/Al molar ratio to 1; 3 mL of sodium aluminate solution (Sol B) (0.155 g/L in the PEO wastewater) was added to the Sol A and mixed thoroughly for 2 h by means of a mechanical stirrer. The molar composition of the final aluminosilicate gel was 4.45 Na_2O: 1 Al_2O_3: 1.79 SiO_2: 193.78 H_2O. The mixture was subjected to microwave radiation at different power levels and time for crystallization of zeolite LTA. The crystallization experiments were carried out using a single mode microwave device equipped with a condenser system for reaction heating under atmospheric pressure. A cylindrical PTFE reactor (28 mm ID, 108 mm length) was used to conduct the reaction inside the microwave chamber at various MW power, reaction time and reaction temperature.
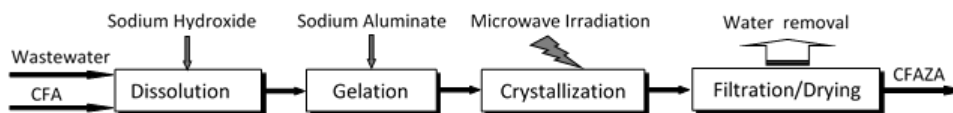
Figure A-1. Different steps of synthesized CFAZA from CFA

The experiments were performed in a self-adjusting, microwave oven (single-mode, 2.45 GHz, CEM cooperation, Discover, USA), where the reaction temperature and power were recorded using a real time monitoring system. The temperature was measured using infrared pyrometer installed in the microwave chamber. Figure A-2 shows the overview of the crystallization system. After a given period of MW irradiation, the solid products were filtered, thoroughly washed with deionized water to remove unreacted and water soluble components, dried overnight at 100 ºC in an electric oven, then characterized.
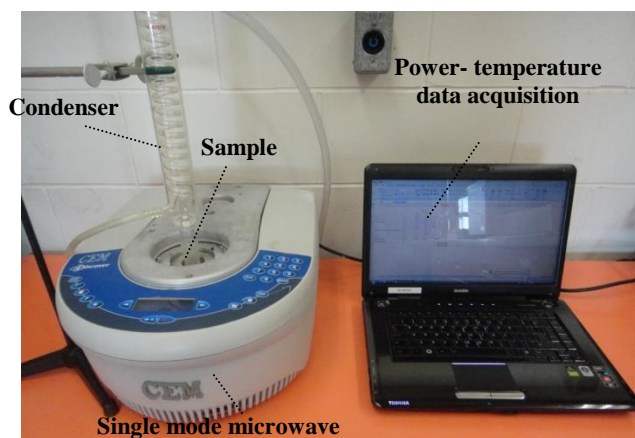
Figure A-2. Single-mode microwave reactor setup

A.2.3 Characterization

A Rigaku-MiniFlex powder diffractometer (Japon) was used to collect XRD data of the synthesized samples using CuKα (λ for Kα = 1.54059 Å) over the range of 5°<2θ<40° with step width of 0.02°. The obtained zeolite crystalline phase was compared with the

standard peaks of a reference zeolite [27]. The crystallinity of the products was determined by "peak fitting" algorithm in the MDI-Jade v 7.5 software. Crystal size distribution and morphology of zeolite were studied by scanning electron microscope (SEM) JSM 600F (Joel, Japan) operating at 10 keV of acceleration voltage. Specific surface area and pore size of the prepared samples were measured by means of a BET analyzer (Micrometrics ASAP 2010). Known amounts of samples (e.g. 50-80 mg) were loaded into the BET sample tube and degassed under vacuum (10-5 Torr) at 125 °C for 6 h. The thermal analyses were performed using a Mettler Toledo TGA/SDTA 851e model (Switzerland) with version 6.1 Stare software. The samples were heated from 30 °C to 600 °C at heating rate of 10 °C/min under nitrogen purge. Cation exchange capacity (CEC) is the maximum quantity of total cations, of any class, that a zeolite is capable of holding, available for exchange with the solution. It is expressed as milliequivalent of hydrogen per gram of dry zeolite, it is a specific characteristic of each zeolite, which depends on the structural chemistry of a particular zeolite. Theoretically, the Si /Al molar ratio determines the number of exchangeable cations and the CEC. The CEC values of the zeolitized CFA samples were measured using the "ammonium acetate saturation" standard procedure (5 days) [28]. The whole process consists of three basic steps: (1) replacing exchangeable ions of 1 g zeolite with ammonium ($NH4^+$) in the material through saturation using 20 ml of neutral 1 N solution of ammonium acetate (2) release of NH4+ ions through washing dry sample (0.2 g) with 50 mL of 10 % NaCl solution acidified to 0.005 M in HCl and (3) measurement of NH_4^+ released in form of NH3 in Kjeldahl apparatus. In order to measure the concentration of leached ions from the tested samples, the supernatant solution of the CEC tests was tested by means of an inductively coupled plasma atomic emission spectrometer (ICP-AES) (Varian, Australia) using ICP expert software (version: v 4.0). The product yield of the zeolitization process demonstrating the efficiency of the zeolite synthesis procedure was calculated by [7]:

$$\text{Yield}(\%) = \frac{W_{CFAZA}}{W_{CFA}} \times 100 \qquad \text{(Eq. A-1)}$$

Where W_CFAZA is the weight of the zeolite product (g) and W_CFA is the weight of the CFA (g).

A.2.4 Experimental design

The CFAZA synthesis was optimized by the means of a statistical approach using a two-level (central composite), double-factorial design. Design-Expert 7.1.5 software (StatEase, Minneapolis, USA) was used to examine the influence of each reaction parameter on the crystallinity of Na-A (as a response). The effects of two most important variables, microwave power (at three levels of 100, 200 and 300 W) and irradiation time (at three levels of 10, 20 and 30 min) for continuous MW irradiation at atmospheric pressure were investigated.

A.3 Results and Discussion

A.3.1 The chemical composition

The chemical and mineralogical compositions of the CFA used as starting materials and main source of Si and Al are given in Table A-1. According to the XRD data, the main components of the CFA are amorphous aluminosilicate as well as quartz and mullite that exist as crystalline phases. The SiO_2/Al_2O_3 ratio was found to be 2.06 which is good for the synthesis of low silica zeolite crystallites such as LTA type zeolite. The loss on ignition is mainly associated with the unburnt carbon present in the CFA.

Table A-1. Chemical composition (XRF analysis) of the CFA used in this study (particle size $\leq$ 600 µm)*

Parameter	Weight percent (%)
Major oxide	
SiO_2	41.78
Al_2O_3	19.61
CaO	13.64
Fe_2O_3	5.79
MgO	3.23
TiO_2	1.39

K_2O	1.10
Na_2O	0.94
P_2O_5	0.71
BaO	0.36
SrO	0.25
Cr_2O_3	0.01
MnO	0.02
Loss On Ignition	10.89
Total	99.72
Phases analysis	
Amorphous aluminosilicate	88
Quartz (SiO_2)	8
Mullite ($3Al_2O_3.2SiO_2$)	3
Others	1

*SiO_2/Al_2O_3: 2.13

The chemical composition of the wastewater used in this study (measured by ICP-AES) is reported in Table A-2. The alkaline pH of the wastewater (i.e. 12) due to the presence of NaOH and KOH as well as trace amounts of Si and Al, makes this waste suitable medium for zeolite synthesis.

Table A-2. Major elemental composition of the used PEO wastewater (pH=12)

Parameter	Quantity (mg/l)
Na	673
K	497
Si	295
Al	10

A.3.2 The XRD analysis

The NaOH to CFA ratio was set at a minimum value of one due based on the amount of alkaline source presented in the wastewater. Figure A-3 illustrates the XRD pattern of raw and alkaline treated coal fly ash before subjecting to microwave irradiation. Quartz, mulite, calcite and hematite are the main crystalline phases presented in CFA. During the process of alkaline treatment of CFA with sodium hydroxide, calcite phase was removed (dissolved) and no relevant peak was observed. No noticeable dissolution of quartz happened at the mild alkaline conditions indicating the resistance of quartz during direct hydrothermal treatment.

The low intensity peaks show the residual amounts of mullite and hematite phases after alkaline treatment. Low levels of the mullite phase is attributed to the fact that mullite is resistant to dissolution during direct hydrothermal treatment.

The kinetics of dissolution of silicon and aluminum strongly depends on the concentration of hydroxyl ion (OH⁻), which is responsible for hydrolysis and dissolution of the reagents. There is no significant difference between XRD results of CFA before and after gelation with sodium aluminate solution.
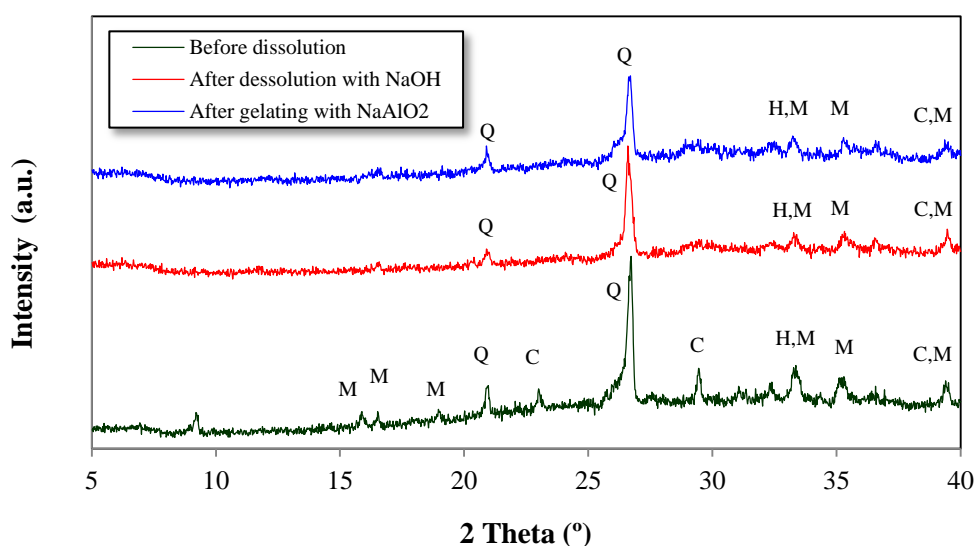
Figure A-3. XRD patterns of the raw and treated CFA smaples prior to the microwave irradiation. M; mullite, Q; quartz, H; hematite, C; calcite

The XRD patterns of the zeolite synthesized by microwave crystallization are presented in Figure A-4. Most of the peaks appear at 2θ ranging from 5 to 40 degrees and well-match with those for zeolite Na-A, confirming the successful formation of LTA zeolite as the major crystalline phase of the zeolitized CFA [29]. It can be seen that the majority of quartz phase in the CFA remained intact when the digestion (dissolution) process is carried out at 60 ℃ for 12 h. As reviewed by Querol et al. [21], the main limitation of the processes for synthesizing zeolites from fly ash is the slow reaction rate and the relatively high temperatures (125-200 ℃) needed to dissolve Si and Al from fly ash particles. Under these conditions, many of the high-CEC and large pore zeolites such as zeolites Na-A cannot be synthesized. If temperature is reduced, then synthesis yield is reduced considerably and a very long activation time (24-48 h) is required. The advantage of microwave-assisted crystallization process is to reduce the activation time from hours to f minutes when complete dissolution of Si and Al happen. Increasing both power and time, increases the crystallinity of the product. At a constant power of 100 W, the average temperature of activation solution was 116 ℃ (Figure A-4a). The quantities of mullite and hematite were low because not all of the coal fly ash had been converted to zeolite and the presence of unconverted mullite and hematite in the products was also confirmed by XRD. Increasing power to a level of 300 W resulted in a solution temperature of 127 ℃ (Figure A-4c). The zeolite synthesis from the coal ash is therefore an equilibrium reaction between the alkaline solution and solid phase. By raising the temperature, the solubility of silica and alumina ions increases and the formation of crystal nuclei is initiated. The crystal growth leads to a complete dissolution of the original material for the formation of crystalline phases zeolite.
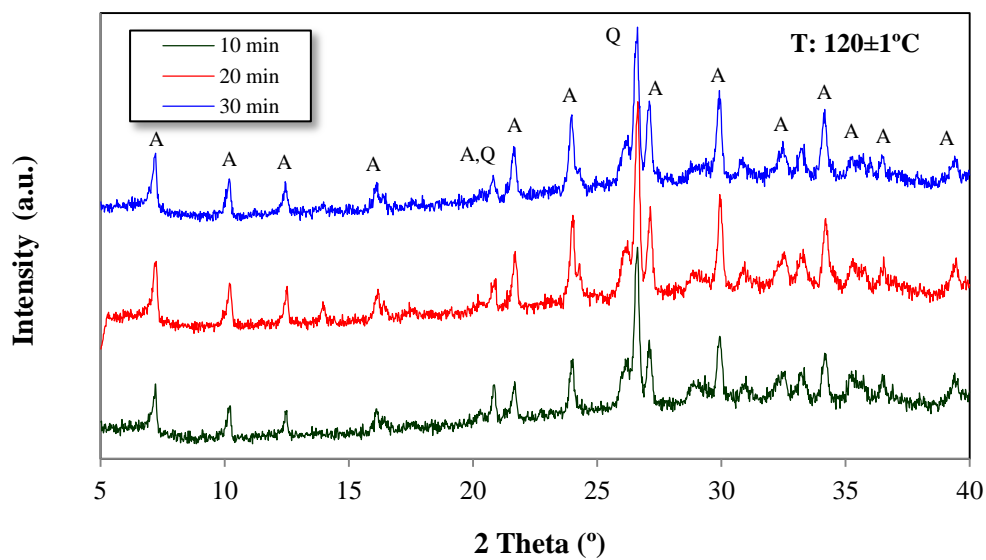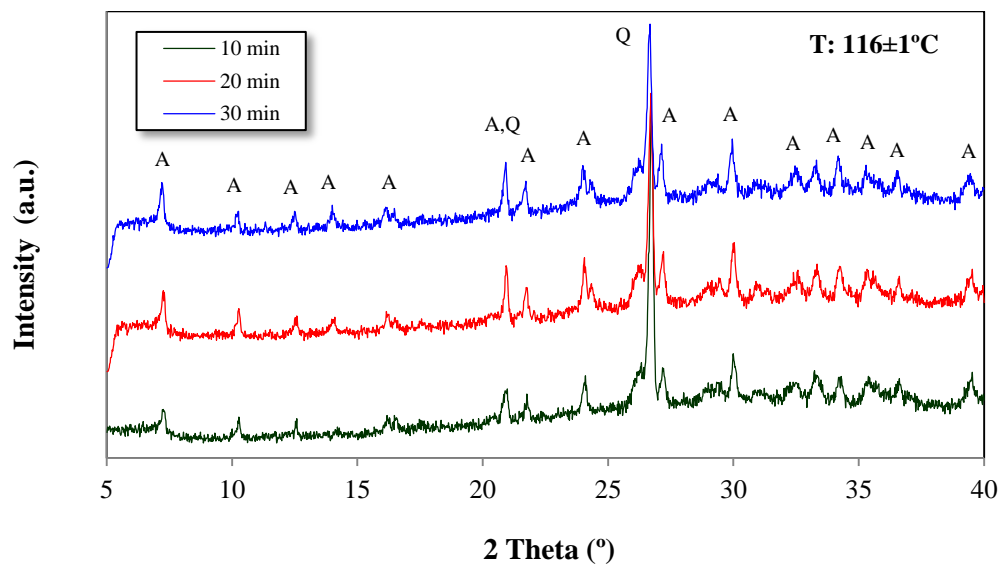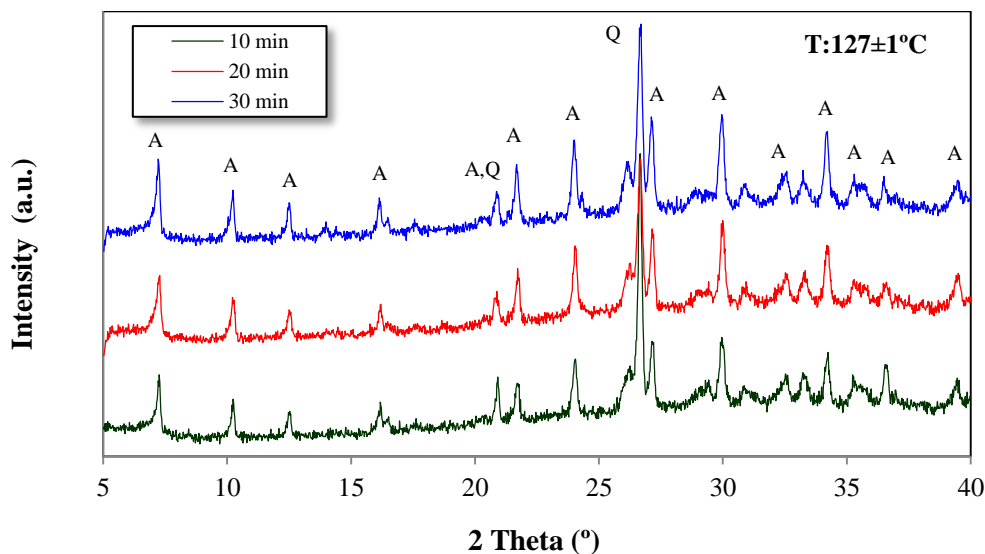
Figure A-4. XRD patterns of synthesized CFA at three levels of microwave power versus time. Power: a) 100 W, b) 200 W, c) 300W

The characteristics of CFAZA synthesized using CFA and wastewater as starting materials by means of microwave-assisted hydrothermal technique were compared with the synthesized samples using distilled water. The XRD patterns of the samples synthesized under experimental conditions of 300 W and 30 min are illustrated in Figure A-5. Most of the peaks match well with those obtained for distilled water. The height of peaks corresponding to distilled water is stronger showing more crystallinity.
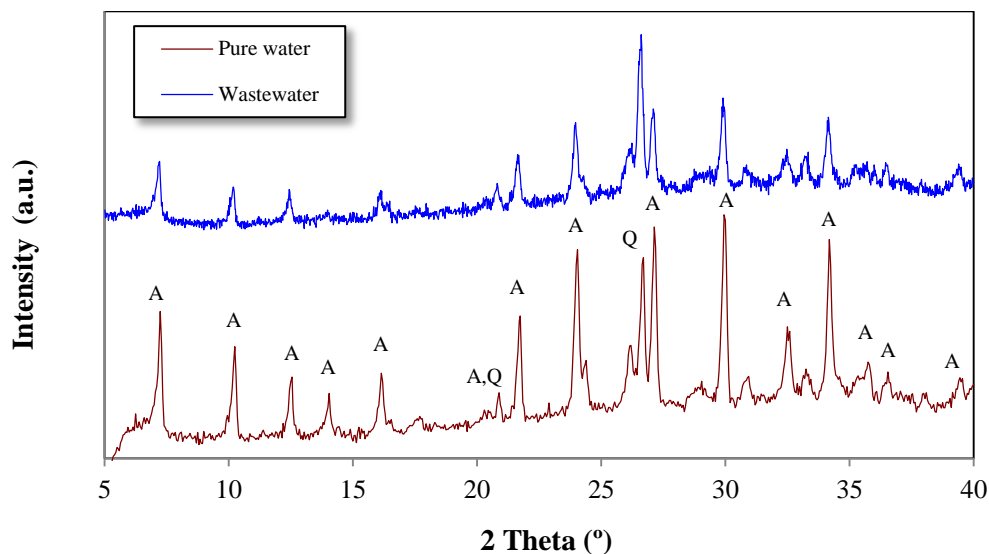
Figure A-5. XRD patterns of CFAZA obtained with distilled water and wastewater under microwave power of 300 W for 30 min

A statistical method based on a two-level full-factorial design with center point per block (i.e. 9 experimental runs in total) was used to optimize the synthesis conditions. Design-Expert 7.1.5 software employed to study the effect of microwave irradiation power and time on crystallinity. Table A-3 summarizes the effect of MW power and irradiation time on the crystallinity and yield of the final product. According to the XRD data, zeolite Na-A with a maximum crystallinity of 67.24 % was successfully synthesized by a hydrothermal treatment of fly ash with wastewater at 300 W for 30 min, which is very close to the crystallinity of the zeolitic product obtained by distilled water under similar reaction conditions (i.e. 73.47 %). It is noteworthy that the yields of all synthesized CFAZA were quite similar to the product yield of the zeolite produced by CFA and distilled water and it was in the range of 82.0-84.1 %.

Table A-3. Crystallinity and yield for the Synthesis of Zeolite Na-A from CFA

Power (W)	Time (min)	Crystallinity (%)	Yield (%)
100	10	47.57	82.0
	20	50.41	84.1
	30	54.09	83.4
200	10	57.15	83.5
	20	62.30	83.7
	30	64.63	83.8
300	10	58.14	83.2
	20	66.20	84.1
	30	67.24	83.7

Analysis of variance (ANOVA) was used to evaluate the influence of different variables on the crystallinity. Table A-4 shows the results of preliminary statistical analysis and the effects of the variables. The F-test was used to identify the most significant variables in the hydrothermal microwave assisted process. The significance level (p-value) adopted was 0.05. A mathematical polynomial model (quadratic design) was constructed in terms of the alphabetically coded input significant variables (i.e. P for MW Power, θ for MW time). According to the data reported in Table 4, the crystallinity is affected by both microwave power and time. The higher F-value (150.3) of the microwave power indicates that crystallinity is strongly affected by microwave power rather than microwave irradiation time with an F-value of 51.38.

Table A-4 Summary of the ANOVA of the model equation for the product crystallinity as a function of MW irradiation and time

Source	Sum of squares	Degrees of freedom	Mean square	F value	p value
Model	388.65	5	77.73	44.91	0.0051
P	260.17	1	260.17	150.31	0.0012
θ	88.94	1	88.94	51.38	0.0056
P.θ	1.66	1	1.66	0.96	0.3991
P^2	33.37	1	33.37	19.28	0.0219
$θ^2$	4.50	1	4.50	2.60	0.2053

$$*\text{Crystallinity} = 62.36 + 6.59\,P + 3.85\,θ + 0.64\,P.θ - 4.09\,P^2 - 1.50\,θ^2$$

A.3.3 The scanning electron microscope (SEM) analysis

Scanning electron microscope (SEM) images of the raw CFA and the synthesized zeolitic products are illustrated in Figure A-6. The presence of characteristic cubic crystallites of Na-A zeolite validates the XRD data. It can be seen that the amount of amorphous phase decreases and more cubic crystals appear as the microwave power is increased. It seems that the zeolite crystallization takes place at the interface between the un-dissolved CFA particle and the alkali solution leading to the deposition of zeolite crystallites. This means that the nucleation mechanism of the CFA zeolitization is heterogeneous. After 30 min of MW irradiation at 100 W, a few cubic structure appears, however, the cubic structure is not abundant and is embedded in the flower-like (ball-of-yarn-like) crystalline structure. Furthermore, the size of the zeolite crystallites is increased at higher microwave power. The Na-A zeolite morphology is characterized by regulated cubic shaped crystals with approximate dimensions of 2-5 μm. The morphology of the CFAZA was chamfered-edged cube due to the initial SiO2/Al2O3 concentration used in the production process.

As the MW irradiation power increases the abundance and size of cubic zeolite crystals increase, indicating crystal growth is strongly related to MW irradiation power.
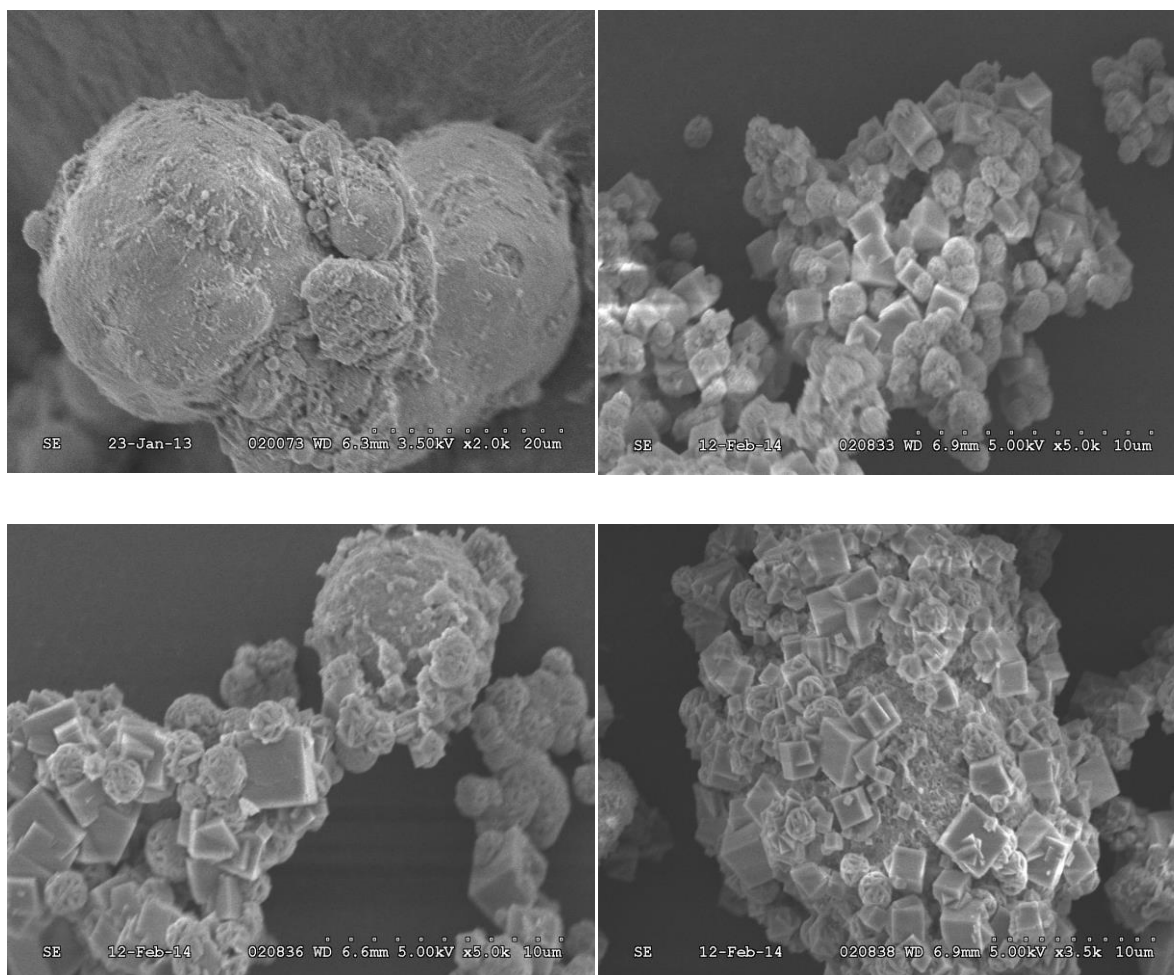
Figure A-6. SEM images of the raw CFA and microwave-assisted synthesized CFAZA samples after 30 min microwave irradiation at different power values. A) CFA, b) CFAZA (100 W), c) CFAZA (200 W), d) CFAZA (300 W)

A.3.4 The scanning electron microscope (SEM) analysis

The BET surface area of the CFAZA sample synthesized under optimized condition of 300 W for 30 min, was 47.14 m^2/g. This surface area is 10% larger than surface area of the sample synthesized at 100 W, which was 43.8 m^2/g. On the other hand, micropore area and external surface area of the sample produced at 300 W were 5.69 m^2/g and 41.45 m^2/g, respectively. The pore volume and the mean pore diameter for the best sample were

$0.132 \text{ cm}^3/\text{g}$ and 8.274 nm, respectively (Table A-5). The specific surface area of CFAZA obtained by wastewater is three times larger than that of CFA.

Table A-5. Pores structure specification of CFA and CFAZA samples

Sample	S_{BET} (m^2/g)	V_{BET} (cm^3/g)	Mean pore diameter (nm)
CFA	15.47	0.068	7.871
CFAZA Synthesized by wastewater	47.14	0.132	8.274
CFAZA Synthesized by distilled water	42.43	0.138	9.448

The shape of the adsorption/desorption isotherm and its hysteresis pattern provide useful information about the physisorption mechanism, which can be used to qualitatively predict the type of pores present in the adsorbent. The hysteresis between the adsorption isotherm and desorption isotherm is thought to be due to the different size pores being combined. The obtained adsorption-desorption curve of CFAZA sample is a special type of isotherm shape, classified as Type IIB [30]. Based on International Union of Pure and Applied Chemistry (IUPAC) isotherm classification [31], the adsorption branch of the isotherm has a general shape like Type II isotherms typical of nonporous aluminosilicate. This adsorption isotherm profile represents a monolayer-multilayer adsorption mechanism of the gas on the open and stable solid surface. A type II isotherm is normally associated with monolayer-multilayer adsorption on an open and stable external surface of a powder, which may be non-porous, macroporous or even to a limited extent microporous. The desorption branch of the isotherm is a distinct H3-type hysteresis loop indicating mesoporous aluminosilicate [30]. The H3 hysteresis loop type is mostly found in materials with platy particles having slit-shaped mesopores. These materials are not purely mesoporous as there is no indication of the completion of mesopore filling that would result in a plateau at higher relative pressures as in a typical Type IV isotherm. Characteristic features of the type IV isotherm are its hysteresis loop, which is associated

with capillary condensation taking place in mesopores, and the limiting uptake over a range of high relative pressures. A significant volume of macropores in these materials results in the absence of the isotherm plateau at high relative pressures as seen in Type IV isotherms.

Another important feature observed in BET isotherm is the forced closure of desorption branch to adsorption one where relative pressures is low. Disappearance of the hysteresis (Tensile Strength Effect) is due to the instability of the hemispherical meniscus during capillary evaporation in pores with diameters smaller than approximately 4 nm. In these pores, the surface tension forces are stronger than the tensile strength of the liquid causing the meniscus collapse which leads to a spontaneous evaporation of the bulk liquid phase. The presence of "forced closure" in the isotherm shape may indicate a significant volume of pores with diameters smaller than 4 nm.

A.3.5 The thermo-gravimetric analysis (TGA)

Thermo-gravimetric analysis (TGA) curve of the CFA and its zeolitized counterpart are shown in Figure A-7. The CFA showed a weight loss of 6.1%, in which most of the weight loss occurs at 105ºC. The gentle slope associated with the weight variations and the trend of heat flow changes are a particular behavior of CFA and attributed to the reversible adsorption of atmospheric moisture on the external surface and macropore of CFA. The TGA curves of both CFAZA samples show a 10 % weight loses with a point of inflection at approximately 160ºC. This weight loss indicates that the water content in these samples is higher than CFA sample confirming the obtained BET micropore surface area. It could be attributed to the evaporation of adsorbed water molecules on the porous structure of the synthesised zeolite.
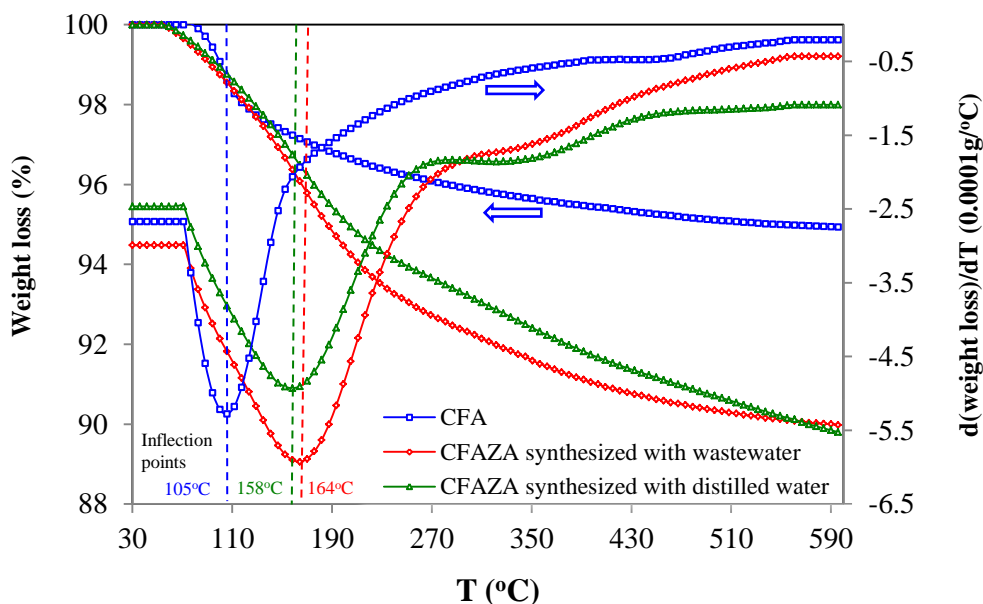
Figure A-7. TGA pattern of CFA and CFAZA

A.3.6 The cation exchange capacity (CEC) and heavy metals in the leachate

The cation exchange capacities (CEC) of the CFA and synthesized CFAZA samples were found to be 0.30 meq/g and 1.82 meq/g, respectively. This very high CEC, which is comparable to the zeolitized CFA reported by other researchers [2,24] indicated that the produced zeolite has a great potential to be used as adsorbent in different environmental remediation processes.

Results of typical leaching tests obtained using elemental analysis data of the leached ions after soaking the CFA and zeolite samples in ammonium accelerate solution for 7 days 25 °C are summarized in Table A-6. Composition of supernatant liquids obtained by soaking CFA and synthesized CFAZA in distilled water (mg/L). The concentration of different elements such as Fe, V, B, Be, Cr, Se, Co, and Pb, which were analyzed using ICP technique, were remarkably lower in the leachate solution of the synthesized zeolitic product compared to the original coal fly ash. Accordingly, the leach resistance of the zeolitized sample toward the studied ions is as follows: Fe > V > B > Be > Cr > Se > Co > Pb. Due to the initial composition of used wastewater, the concentration of some

elements such as K, Na, Ba, Cu, and Ni in supernatant liquid is higher for CFAZA than CFA [32]. Aluminum concentration of the leachate solution of the zeolitized sample by means of wastewater was higher than of the distilled water.

Table A-6. Composition of supernatant liquids obtained by soaking CFA and synthesized CFAZA in distilled water (mg/L)

Element	CFA	CFAZA	
	Non treated	Distilled water	Wastewater
Al	1.446	0.526	1.399
As	0.059	0.060	0.058
B	4.278	0.423	0.547
Ba	2.028	3.000	5.832
Be	0.00015	0.00003	0.00002
Ca	469.75	470.76	613.88
Cd	0.0011	0.0013	0.0010
Co	0.0021	0.0012	0.0010
Cr	0.141	0.036	0.049
Cu	0.064	0.166	0.185
Fe	0.364	0.041	0.032
K	8.860	12.944	24.548
Mg	73.144	54.064	72.911
Mn	0.011	0.009	0.008

Na	22.185	909.79	605.28
Ni	0.042	0.046	0.060
Pb	0.270	0.244	0.255
Se	0.110	0.023	0.045
Tl	0.031	0.022	0.025
V	0.016	0.002	0.002
Zn	0.016	0.018	0.018

Hydrothermal microwave-assisted zeolitization is fast and energy-effective reaction. The MW irradiation energy which is a function of both MW power and MW irradiation time influences the crystallinity of the final product. The required energy for CFAZA crystalization was between 9.1 Wh/g CFA (correspond to 10 W for 10 min) and 82.4 Wh/g CFA (correspond to 300 W for 30 min). Comparing with high conduction heating energy requirement for 2-90 h ordinary crystallization process, low microwave energy consumption makes this technology more economic.

Microwave energy has found general, commercial application in very few areas including food processing, analytical chemistry, and heating and vulcanization of rubber. Food processing and rubber manufacture involve relatively high-volume, continuous processing. Analytical chemistry applications are broad in scope and involve high-volume, repetitive, batch processing, often with long intermediate drying and reaction steps that can be shortened using microwave heating. Despite the considerable effort that has been expended in microwave process development in zeolite synthesis, there has been no industrial application to date, with most of the effort still in the laboratory stage. Some of the more significant problems that have inhibited industrial application of microwave processing to synthesis CFA-ZA from CFA include the relatively high capital cost of equipment, design of microwave transparent reactor and variation in dielectric properties of reactant with temperature and composition. Therefore, much work has to be

undertaken to overcome the existing limitations in terms of capabilities and scaling and will lead to identification of promising processes.

From an environmental and economic point of view, the process developed in this study can only reduce the environmental burden associated with these wastes as well as could also offer extra income generated from the reusing wastewater instead of water. Further studied should also be conducted on the residuals of this procedure and the possible environmental impact. It will also be of interest to investigate the potential for recyclability of the resulting post-synthesis supernatant back to synthesis process.

A.4   Conclusions

This research focuses on a novel approach to address environmental concerns related to the CFA and PEO wastewater as a solid and a liquid industrial waste streams. In this regard, production of a value added zeolitic product (i.e. Na-A zeolite) is studied using CFA and PEO wastewater. This process can be considered for large scale conversion of CFA. The MW-assisted production of the LTA zeolite using CFA and PEO wastewater as starting materials was systematically studied and optimized using a two-level full-factorial design with center point per block technique. Using microwave irradiation at relatively low power of 100-300 W for short period of time (i.e. 10-30 min) renders a feasible technique for scale up. The process developed in this study will help to reduce the environmental burden associated with these wastes and also offer a new source of revenue for the coal-fired power plant. The zeolitized coal fly ash produced in this research showed a relatively high CEC and good water adsorption capacity and high leaching resistance to toxic elements make in value-added product as a promising candidate for environmental remediation applications.

A.5   References

[1]   F. Fotovat, H. Kazemian, M. Kazemeini, Synthesis of Na-A and faujasitic zeolites from high silicon fly ash, Mater. Res. Bull. 44 (2009) 913–917.

[2]   H. Kazemian, T. Ghaffari Kashani, S.M. Noorian, Synthesis and characterization of zeolite A, using fly ash of the Iran Ferrosilice Company and investigating its ion-exchange properties, Iran. J. Crystallogr. Mineral. 13 (2005) 329–336.

[3]   T. Klamrassamee, P. Pavasant, N. Laosiripojana, Synthesis of Zeolite from Coal Fly Ash: Its Application as Water Sorbent, Eng. J. 14 (2010) 37–44.

[4]   C. Belviso, F. Cavalcante, A. Lettino, S. Fiore, Zeolite synthesised from fused coal fly ash at low temperature using seawater for crystallization, Coal Combust. Gasifica-Tion Prod. 1 (2009) 8–13.

[5]   A. Molina, C. Poole, A comparative study using two methods to produce zeolites from fly ash, Miner. Eng. 17 (2004) 167–173.

[6]   N.M. Musyoka, L.F. Petrik, O.O. Fatoba, E. Hums, Synthesis of zeolites from coal fly ash using mine waters, Miner. Eng. 53 (2013) 9–15.

[7]   D. Ruen-ngam, D. Rungsuk, R. Apiratikul, P. Pavasant, Zeolite formation from coal fly ash and its adsorption potential, J. Air Waste Manag. Assoc. 59 (2009) 1140–1147.

[8]   N. Shigemoto, H. Hayashi, K. Miyaura, Selective formation of Na-X zeolite from coal fly ash by fusion with sodium hydroxide prior to hydrothermal reaction, J. Mater. Sci. 28 (1993) 4781–4786.

[9]   H. Kazemian, Z. Naghdali, T. Ghaffari Kashani, F. Farhadi, Conversion of high silicon fly ash to Na-P1 zeolite: Alkaline fusion followed by hydrothermal crystallization, Adv. Powder Technol. 21 (2010) 279–283.

[10]   R. Moriyama, S. Takeda, M. Onozaki, Y. Katayama, K. Shiota, T. Fukuda, et al., Large-scale synthesis of artificial zeolite from coal fly ash with a small charge of alkaline solution, Fuel. 84 (2005) 1455–1461.

[11]   K.S. Hui, C.Y.H. Chao, Pure, single phase, high crystalline, chamfered-edge zeolite 4A synthesized from coal fly ash for use as a builder in detergents, J. Hazard. Mater. 137 (2006) 401–409.

[12]   M. Nascimento, P.F. Prado, P.S.M. Soares, V.P. de Souza, Thermodynamic Study of the Synthesis of Zeolites from Coal Ash and Its Use as Sorbents for Heavy Metals, (2012).

[13]   X.S. Zhao, G.Q. Lu, H.Y. Zhu, Effects of ageing and seeding on the formation of zeolite Y from coal fly ash, J. Porous Mater. 4 (1997) 245–251.

[14]   G.G. Hollman, G. Steenbruggen, M. Janssen-Jurkovi\vcová, A two-step process for the synthesis of zeolites from coal fly ash, Fuel. 78 (1999) 1225–1230.

[15]   M. Inada, Y. Eguchi, N. Enomoto, J. Hojo, Synthesis of zeolite from coal fly ashes with different silica–alumina composition, Fuel. 84 (2005) 299–304.

[16]   N. Murayama, H. Yamamoto, J. Shibata, Mechanism of zeolite synthesis from coal fly ash by alkali hydrothermal reaction, Int. J. Miner. Process. 64 (2002) 1–17.

[17]   N.M. Musyoka, L.F. Petrik, W.M. Gitari, G. Balfour, E. Hums, Optimization of hydrothermal synthesis of pure phase zeolite Na-P1 from South African coal fly ashes, J. Environ. Sci. Health Part A. 47 (2012) 337–350.

[18]   N.M. Musyoka, L.F. Petrik, G. Balfour, W.M. Gitari, E. Hums, Synthesis of hydroxy sodalite from coal fly ash using waste industrial brine solution, J. Environ. Sci. Health Part A. 46 (2011) 1699–1707.

[19]   M. Ahmaruzzaman, A review on the utilization of fly ash, Prog. Energy Combust. Sci. 36 (2010) 327–363.

[20]   Y. Chauhan, M. Talib, A novel and green approach of synthesis and characterization of nano-adzorbents (zeolites) from coal fly ash: A review, Sci. Rev. Chem. Commun. 2 (2012) 12–19.

[21]   X. Querol, N. Moreno, J. t Umana, A. Alastuey, E. Hernández, A. López-Soler, et al., Synthesis of zeolites from coal fly ash: an overview, Int. J. Coal Geol. 50 (2002) 413–423.

[22]   M. Inada, H. Tsujimoto, Y. Eguchi, N. Enomoto, J. Hojo, Microwave-assisted zeolite synthesis from coal fly ash in hydrothermal process, Fuel. 84 (2005) 1482–1486.

[23]   X. Querol, A. Alastuey, A. López-Soler, F. Plana, J.M. Andrés, R. Juan, et al., A fast method for recycling fly ash: microwave-assisted zeolite synthesis, Environ. Sci. Technol. 31 (1997) 2527–2533.

[24]   H. Tanaka, A. Fujii, S. Fujimoto, Y. Tanaka, Microwave-Assisted Two-Step Process for the Synthesis of a Single-Phase Na-A Zeolite from Coal Fly Ash, Adv. Powder Technol. 19 (2008) 83–94.

[25]   K. Hussar, S. Teekasap, N. Somsuk, Synthesis of Zeolite A from By-Product of Aluminum Etching Process: Effects of Reaction Temperature and Reaction Time on Pore Volume, Am. J. Environ. Sci. 7 (2011) 35.

[26]   V. Dehnavi, B.L. Luan, D.W. Shoesmith, X.Y. Liu, S. Rohani, Effect of duty cycle and applied current frequency on plasma electrolytic oxidation (PEO) coating growth behavior, Surf. Coat. Technol. (2013).

[27]   M.M.J. Treacy, J.B. Higgins, Collection of simulated XRD powder patterns for zeolites, Elsevier, 2007.

[28]   D.C. Bain, B.F.L. Smith, Chemical analysis, in: Handb. Determinative Methods Clay Mineral., Blackie, Glasgow, 1987: pp. 248–274.

[29]   H.E. Robson, K.P. Lillerud, Verified syntheses of zeolitic materials, 2nd ed., Elsevier, Amsterdam, The Netherlands, 2001.

[30]   F. Rouquerol, J. Rouquerol, K. Sing, Adsorption by Powder & Porous Solid, Academic Press, London, 1999.

[31]   K. Sing, D. Everett, R. Haul, L. Moscou, R. Peirotti, J. Rouquerol, IUPAC commission on colloid and surface chemistry including catalysis, Pure Appl. Chem. 57 (1985) 603–619.

[32]   K.S. Hui, C.Y.H. Chao, S.C. Kot, Removal of mixed heavy metal ions in wastewater by zeolite 4A and residual products from recycled coal fly ash, J. Hazard. Mater. 127 (2005) 89–101.

Appendix B

B Developing a zero liquid discharge process for zeolitization of coal fly ash to synthetic NaP zeolite[1]

Abstract

The present work reports the conversion of coal fly ash (CFA) to synthetic NaP zeolite with zero liquid discharge. The process eliminates the need for large amounts of water and the need for a big wastewater treatment unit. The need for water, as a make-up stream, is only to compensate water losses during filtering, drying and sampling for analysis. The process reduces the sodium hydroxide consumption by 60% and the quality of Na-P zeolite (CFA-ZP) obtained from this process is comparable to conventional method. The zeolitized product had a high crystalline quality and was leach resistance toward heavy metal and trace element content of the product. Concentrations of trace elements in leachate of CFA-ZP were less than threshold limit for landfill leachate and wastewater effluent for discharging into river and surface water. Savings associated with minimizing make-up water and eliminating wastewater treatment unit can be substantial.

B.1 Introduction

CFA is a by-product of coal fired power plants, which is considered as a solid waste [1-3]. The recycling of CFA to be used for other applications is rather low [4, 5]. Currently less than 50 % of worldwide produced CFA is being re-used for different applications [6]. Coal Fly ash is mainly used as a construction material, in which majority of the CFA utilization is in concrete production as pozzolan. More than 50% of the world production of CFA is disposed into landfills or ponds at significant cost for the coal-fired power plants. Furthermore, there have been accidents that landfills leachates found their ways to the environment causing millions of dollars of damage [7]. It seems that production rate of CFA is much faster than the development of cement production; which means larger

---

[1] This Appendix has been published in the journal Fuel. J. Behin, S.S. Bukhari, H. Kazemian, S. Rohani, Fuel 171 (2016) 195–202.

volume of CFA are expected to accumulate even more in the future that increases the risk of environmental disasters as a result releasing of toxic compounds to the water bodies and soil [8].

CFA contains trace concentrations of toxic compounds and heavy metals such as arsenic, beryllium, cadmium, barium, chromium, copper, lead, molybdenum, nickel, selenium and vanadium, in which some of them are known to be detrimental to the human health [9]. Leachate of the CFA landfills may cause huge risk of contaminating ground/surface water that leads to entering some of the toxic elements into the food chain affecting human health. Safe and efficient disposal of CFA is a global issue because of its massive production rate and its harmful effects on the environment [1,10,11]. It has been found that the surface layer of coal fly ash particles of micrometers in diameter contain a significant amount of readily leachable material, which are deposited during cooling after combustion [5,12,13].

In order to minimize the problem associated with CFA disposal, in the past four decades, researchers have focused on the conversion of coal ash, as a source of aluminosilicate, to value-added materials such as different types of synthetic zeolites including Na-P [14-23], Na-A [24-29], Na-X [24, 29-33], hydroxysodalite [17, 34-37], Na-Y [38] and mixture of zeolitic phases [39-41]. Wide range of the CFA zeolitization variables such as, temperature, pressure, conversion time, Si/Al ratio, solution alkalinity, liquid/solid ratio were optimized to achieve higher yield, purity, cation exchange capacity and crystallinity [42-44]. Moreover, to make the process more cost effective, novel sources of energy such as microwave and ultrasound method were used along with the conventional hydrothermal process to reduce conversion/synthesis time [45-52]. Despite suggesting different applications for the synthesized zeolite such as catalyst, adsorbent, molecular sieve, water softener and detergent builder, to the best of the authors' knowledge no significant investment has been done to commercialize the process.

Some of the technical barriers toward scale up of the CFA zeolitization process are: a) presence of trace amounts of toxic compounds like mercury, arsenic and other heavy metals in the final products, b) the darker color of the zeolitized CFA compared to the

synthetic zeolite manufactured from other industrial source of Si and Al, and c) last but not least, the liquid discharge from a CFA zeolitization operation contains heavy metals and other trace elements.

Overall, a suggested process for recycling a solid waste by-product (i.e. CFA), produces a stream of liquid waste that could be more harmful than the starting material in some cases and even more difficult to deal with. The liquid discharge is because of excessive use of water in filtering and washing processes that must be discharged from the operation. In the existing systems, for instance, to convert 1.5 ton/hour of CFA, 30 ton/hour of industrial water are used for washing (i.e.20 ton water per ton of CFA) [5]. The liquid effluent from the washing process, which contains metallic elements, must be treated before it can be discharged to the ecosystem or to be reused for other applications. Evaporation of this liquid effluent is not feasible due to the tremendous volume of effluent.

In this research a process of zeolitization of coal fly ash with zero liquid discharge is developed. The effluent from the filtration and washing steps is fed to the zeolitization process to minimize the hazardous liquid waste and increase the potential of commercialization of the coal fly ash zeolitization process. Recycling of aqueous waste by means of reusing into the zeolitization process resulted in almost a zero liquid discharge production line.

B.2 Materials and method

Coal fly ash was obtained from Nanticoke coal fired power plant, Ontario, Canada (owned by Ontario Power Generation; OPG). The CFA sample was stored in a sealed container before use. Sodium hydroxide (Alphachem, Canada) was analytical grade and used as received without further purification. Deionised water was used for washing of synthesized zeolite.

B.2.1   Zeolitization process

A mixture of a 1 M NaOH alkali solution (0.8 g sodium hydroxide in 20 mL deionised water) and 3 g of CFA is heated in a Teflon vessel in an end-over-end rotary oven at115

ºC for 6 h. Process flow diagram of the developed zero discharge process is illustrated in Figure B-1. The molar composition of the final aluminosilicate gel adjusted to $1Na_2O$: $1Al_2O_3$: $3.62SiO_2$: $195.46H_2O$. During the course of heating, dissolution of silicon and aluminum occurs first. When the concentration of aluminate ions reaches to a threshold, condensation takes place and aluminosilicate gel rapidly starts to deposit on the surface of CFA particulates. The temperature increases during the process leads to the transformation of aluminosilicate gel to crystalline zeolitic phase (i.e. crystallization) [45]. In brief, the first step of dissolution is followed by the condensation and crystallization of Na-P zeoilte on the surface of the CFA particles (i.e. CFA-ZP, coal fly ash zeolite P bearing particles). Synthetic NaP belongs to the Gismondine framework of zeolites.

The product was filtered to separate zeolitized CFA (CFA-ZP) from alkaline supernatant solution. Five mL of the filtrate that mainly contains sodium hydroxide, residual dissolved Si and Al and trace concentrations of heavy metals was subjected to testing with Inductively Coupled Plasma Atomic Emission Spectrometer (ICP-AES) analysis.
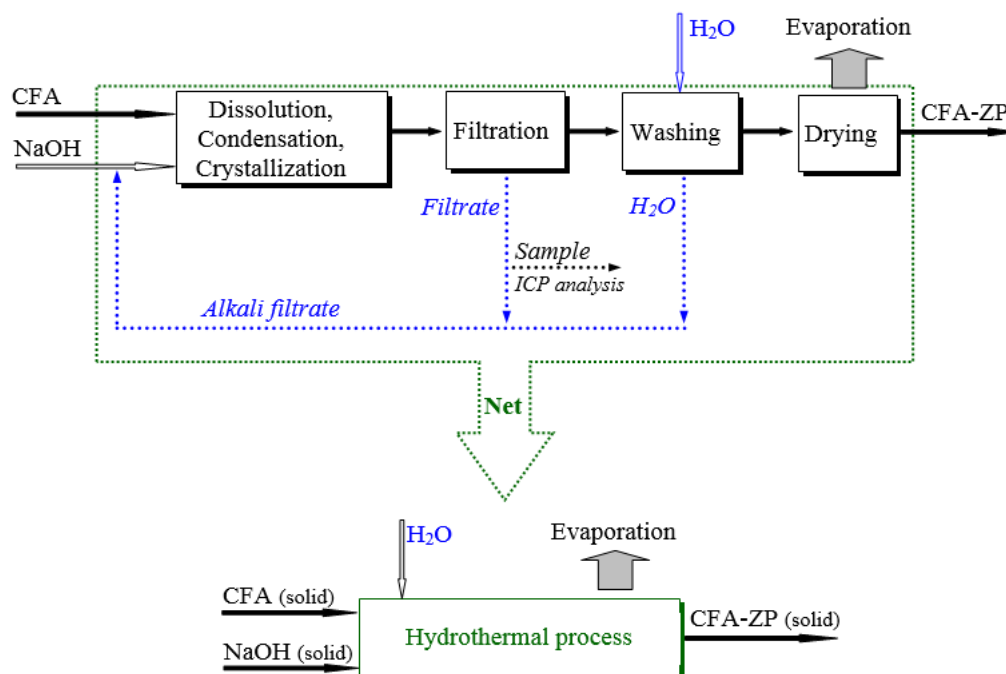

Figure B-1. Process flow diagram of the developed zero discharge process

B.2.1.1 Washing

In the next step, CFA-ZP particles were subjected to a stage-wise counter-current washing with de-ionized (DI) water. The CFA-ZP was washed with deionised water in 5 stages (each stage with 5 mLof DI-water). Multiple stage counter-current washing process removes majority of soluble and unreacted sodium hydroxide from the CFA-ZP product. A properly designed washing procedure with an efficient segregated water system effectively removes most of the toxic components, such as cadmium and arsenic, from synthesized zeolite. Fresh DI-water was used in each washing stage only for the first washing. The filtrate of the first washing stage was recovered to be used for the next stages under steady-state operation. Details of washing steps are shown in Figure B-2. The filtrate pH decreased in each washing stage from stage 1 to stage 5. The five stages washing step was chosen to assure that alkalinity of the final solid product decrease to an acceptable level. Filtrate collected from the first washing (i.e. stage 1) (5 mL), which had the highest pH was mixed with filtrate of filtering stage (i.e. 15 mL) and recycled back to the dissolution (digestion) step as the alkali solution source of the next synthesis. This operation is integrated to reuse water and minimizes process water consumption and eliminates the need for the wastewater treatment unit, as well as minimizes chemicals consumption. The recycled filtrate is initially subjected to a zeolitization operation with fresh CFA.
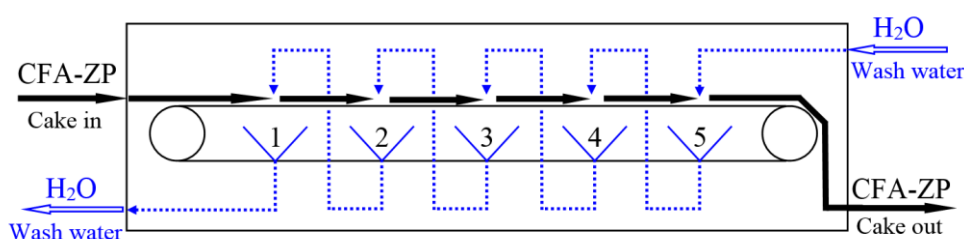

Figure B-2. Details of washing in 5 stage in a counter-current manner

B.2.1.2 Steady-state Operation

At the steady state, 0.35 g of sodium hydroxide was added to the alkali filtrate collected from the first operation (start-up) to make up and adjust the alkalinity of solution for the

next zeolitization run. It should be noted that the need for sodium hydroxide in the steady state operation and successive runs (i.e. 0.35 g) is much less compared to what is needed for the start-up operation (i.e. 0.8 grams) because of residual sodium hydroxide existing in the alkali filtrate collected from the preceding runs. The steady-state operation was started with adding 3 g CFA to the recycled alkali filtrate and subjecting the suspension to the dissolution step. In the steady-state washing step, the water collected from the second washing stage of the preceding run served as washing water in the first stage of current run; the water collected from third stage served as the washing water of the second stage and so on. Only 5 mL of fresh water was used in the fifth stage of washing as make-up water. This make-up water compensated the water loss during filtration, drying and sampling stages.

The washed zeolitized CFA undergoes normal drying process. Overall, the developed zero liquid discharge zeolitization process of coal fly ash comprises of a main start-up step that uses fresh solution of sodium hydroxide and fresh DI-water followed by a steady-state stage, in which only 5ml of fresh water is used for the entire process.

For better understanding of the developed technology, the mass balance around the system for water is summarized in Table B-1. From total needed water (i.e. 45 mL) for the whole starting process including washing stages, more than 88.8% was recycled back to the process (i.e. 40 mL) and only 11.2% (5 mL) was lost because of sampling and drying process. During zeolitization of CFA, the molarity of the alkaline solution was decreased from 1 M to 0.56 M. Therefore, to achieve the proper molarity of 1 M for the next consecutive recycle, the adding of 0.35 g of sodium hydroxide to the solution was necessary. This amount was calculated based on material balance on sodium hydroxide.

Table B-1. Water balance (mL) for the whole zeolitization process

Process	Operation						
	Start-up			*Steady-state*			
	Fresh water	**Recycle (generated)**	**water loss**	**Fresh water**	**recycle (used)**	**Recycle (generated)**	**Water loss**
Zeolitization							
Source of alkali solution	20	-	-	-	20[1]	-	-
Filtrate	-	15	-	-	-	15	-
Sample volume for ICP test	-	-	3	-	-	-	3
Moisture in solid	-	-	2	-	-	-	2
Washing							
Stage 1	5	5	-	-	5	5	-
Stage 2	5	5	-	-	5	5	-
Stage 3	5	5	-	-	5	5	-
Stage 4	5	5	-	-	5	5	-
Stage 5	5	5	-	5		5	-

Total	45	40	5	5	40	40	5

[1]Sum of filtrate (15 mL) and washing water (5mL) of stage 1 generated in precedent step

The developed procedure was continued for 10 consecutive cycles, in order to achieve the steady state conditions to prove feasibility of the concept. Composition of the recycled alkali filtrate reached to a quasi-steady-state after the forth recycling; the effect of recycled alkali filtrate on quality of zeolitized CFA was studied up to 10 consecutive recycles. The pH of the filtrate resulted from washing at different stages was chosen as a criterion of reaching the steady-state condition

In order to characterize the phase purity of the zeolitized CFA, a Rigaku-MiniFlex powder diffractometer (Japan) was used to collect XRD data of the synthesized samples using CuKα (λ for Kα = 1.54059 Å) over the range of 5°<2θ<40° with step width of 0.02°. Crystallite size distribution and morphology of zeolite were studied by scanning electron microscope (SEM) JSM 600F (Joel, Japan) operating at 10keV of acceleration voltage. The CFA-ZP samples were subjected to a leaching test using the European Committee for standardization (CEN) procedure (EU-CEN/TC292/WG2) [53] to evaluate the evolution of the concentrations of different metals leached from the zeolitzed products. The leaching solutions were analyzed by means of inductively coupled plasma ICP-AESfor the metals of interest.

B.3 Results and discussion

To find out the numbers of recycling stages that were needed to achieve the steady state conditions, the variation of pH of filtrates of each washing steps were measured, which are illustrated in Figure B-3. The pH of filtrate increases as the number of recycling goes up. The most variations were observed for the stages 3 to 5. Although after 4 times of recycling, the composition of filtrate (in each stage) reaches to a quasi-steady-state level.
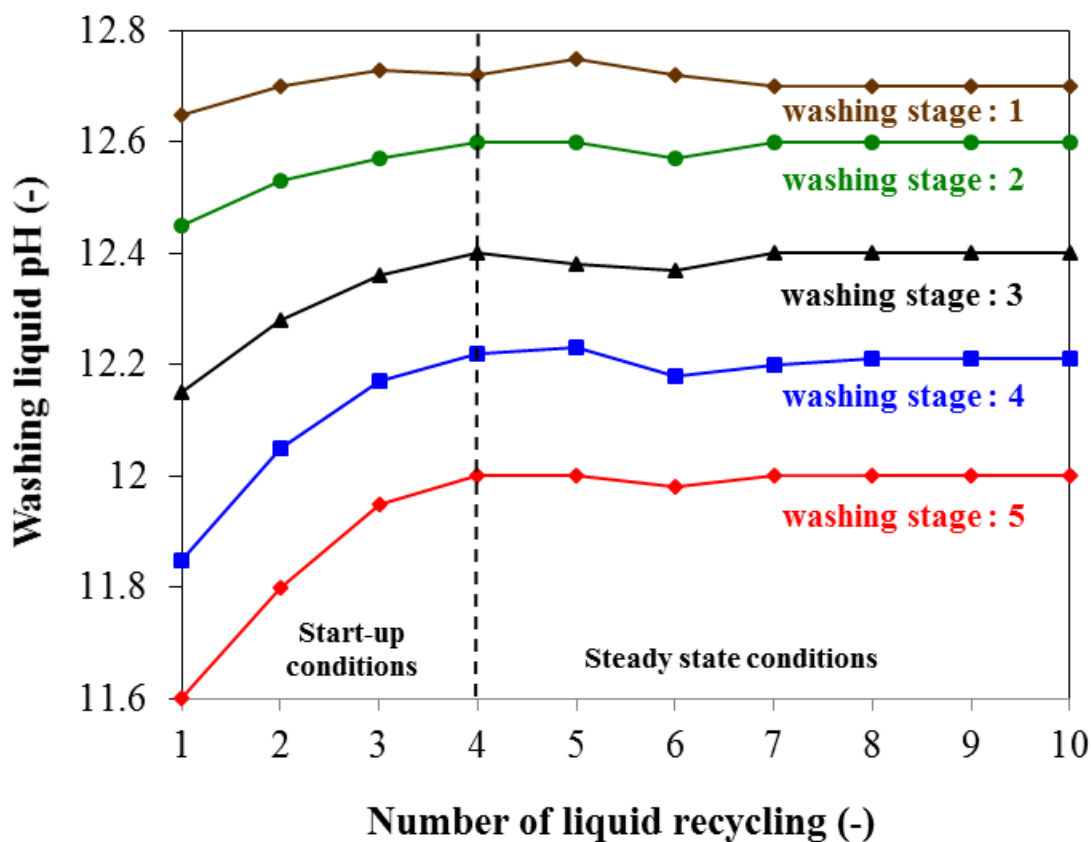
Figure B-3. Alkalinity of washing liquid in different stages of washing process

The XRD pattern of the parent coal fly ash and the zeolitized products are illustrated in Figure B-4. Quartz, mulite, calcite and hematite are the main crystalline phases present in the CFA. During the process of CFA hydrothermal zeolitization with sodium hydroxide; it can be concluded that calcite phase was dissolved because all of its characteristic peaks are disappeared. The crystallinity of the produced zeolitic phase was compared with the standard peaks of the reference Na-P zeolite confirming the type of synthesized zeolitic framework. No noticeable dissolution of quartz occurred at the mild alkaline conditions indicating the resistance of quartz during direct hydrothermal conversion of CFA to zeolite. As it can be seen from the XRD patterns, phase purity and crystallinity of the synthesized zeolites for 10 consecutive experimental runs by means of the developed zero liquid discharge technique, in which the recycled filtrate is used show no significant difference.
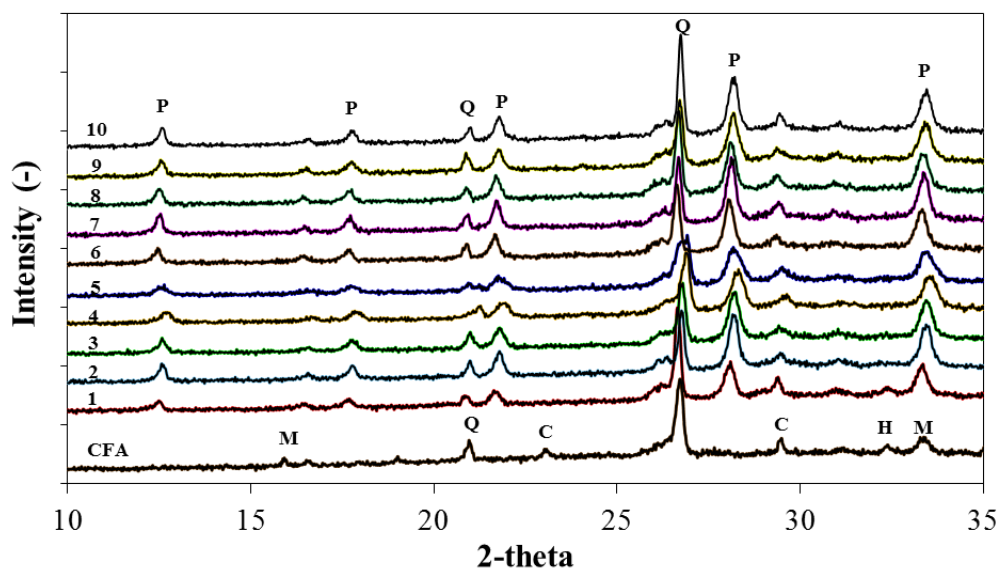
Figure B-4. XRD patterns of the CFA and resulted zeolitized products of CFA-ZP

The chemical and mineralogical compositions of the CFA used as the starting materials and main source of Si and Al are summarized in Table B-0-2. According to the XRD data, the main components of the CFA are amorphous aluminosilicate (88%) and crystalline phases of quartz (8%) and mullite (3%).

Table B-0-2. Chemical composition (XRF analysis) of the CFA used in this study (particle size ≤ 600 μm)*

Parameter	Weight percent (%)
Major oxide	
SiO_2	41.78
Al_2O_3	19.61
CaO	13.64
Fe_2O_3	5.79
MgO	3.23
TiO_2	1.39
K_2O	1.10
Na_2O	0.94

P$_2$O$_5$	0.71
BaO	0.36
SrO	0.25
Cr$_2$O$_3$	0.01
MnO	0.02
Loss On Ignition	10.89
Total	99.72
Phases analysis	
Amorphous aluminosilicate	88
Quartz (SiO$_2$)	8
Mullite (3Al$_2$O$_3$.2SiO$_2$)	3
Others	1

*SiO$_2$/Al$_2$O$_3$: 2.13

Figure B-5 depicts the variations of crystallinity of product versus number of recycled filtrate. The crystallinity of the products was determined by "peak fitting" algorithm in the MDI-Jade v 7.5 software. The variations are in an erratic manner around a mean value. The mean crystallinity of CFA-ZP is 55% with a tolerance of 5%. Therefore, it can be concluded that permanent recycled filtrate, in steady state operation, has no significant influence on the quality of the synthesized zeolite.
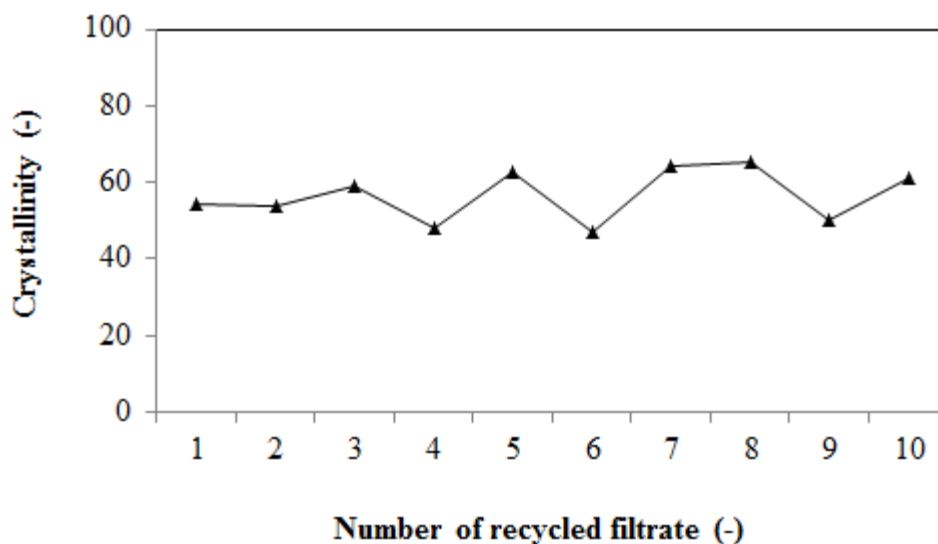
Figure B-5. The variations of peak intensity and crystallinity of product versus number of recycling

Scanning electron microscope (SEM) images of the raw CFA and the synthesized zeolitic products are illustrated in Figure 6. The existence of macro-pores at surface of CFA after dissolution step (Figure 6 b) shows the dissolution of surface Si and Al at a relatively high rate. The SEM images illustrate pseudo-spherical forms constituted by small plates, which is a typical characteristic morphology of synthetic Na-P zeolite (Figure 6c) and is in good agreement with the images of Na-P zeolite synthesised with conventional method using fresh alkali solution [14-23]. The results ascertain that using of the recycled filtrate show no adverse effect on crystal structure of the synthesized zeolite.

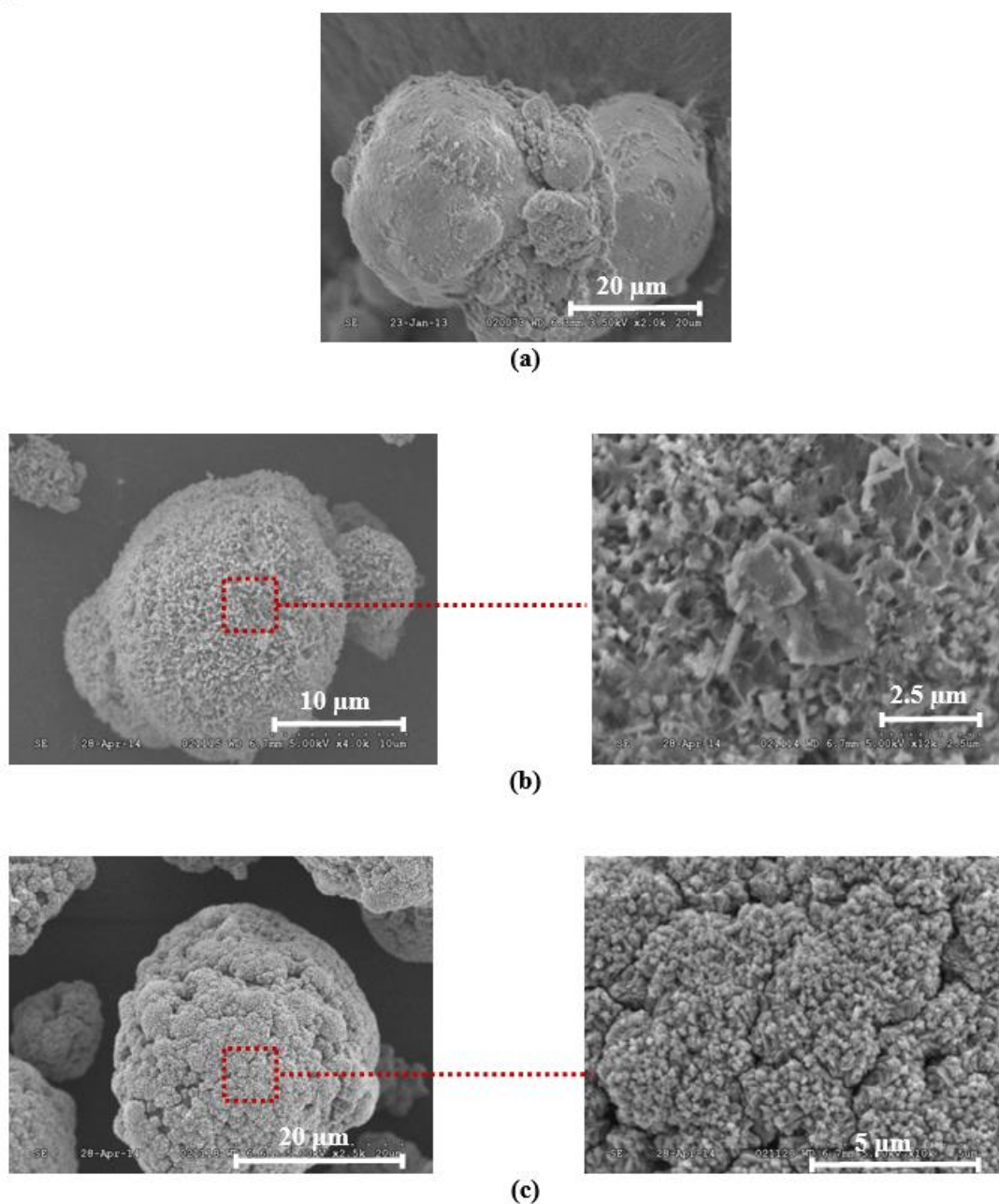**Figure B-6. SEM images of CFA and synthesized zeolite; a) CFA before treatment, b) CFA after dissolution of SI and Al, c) CFA-ZP after 10 recycled filtrate**

The BET surface area of the raw CFA and the CFA-ZP sample synthesized after 1-consecutive cycles was 15.47 m^2/g and 62.01 m^2/g, respectively. A remarkable increase of the surface area was achieved by zeolitization of CFA. Micro-pore area and external

surface area of the produced sample were 8.07 m^2/g and 53.25 m^2/g, respectively. The synthetic zeolite was formed on the surface of CFA, which attributes to the increase of the surface area due to the higher porosity of CFA-ZP. The pore volume and the mean pore diameter of the sample were 0.12 cm^3/g and 10.92 Å, respectively.

According to the regulations, if concentrations of heavy metals and certain elements (i.e. As, Ba, Cd, Cr, Hg, Pb, Se, and Ag) of a CFA leachate exceed regulatory limits, it will be classified as hazardous waste, complicating landfill disposal [54]. Our experimental data revealed that the levels of Hg and Ag of the CFA used in this research were below detection limits.

Figure B-7 a) illustrates the inductively coupled plasma atomic emission spectrometer (ICP-AES) analysis of recycled filtrate in 10 consecutive runs. The concentration of most of elements especially Na, Si, Al, remained relatively constant, which is desirable because our goal was to keep their concentration constant and without accumulation during the steady-state operation. It can be concluded that under the experimental conditions, silicon and aluminum supplied by CFA were totally utilized to form Na-P zeolite. Constant and stable concentration of sodium in the filtrate indicates that the amount of sodium hydroxide that was added to the system (as make up) was enough to regulate the solution pH and provide the proper condition for formation Na-P zeolite. Figure B-7 b) illustrates the concentration of Na, Si and Al ions in leachate solution of the CFA-ZP product. The results show the same trend for concentration of elements in recycled filtrate, but with lower order of magnitude in comparison to the recycled filtrate. Level of Na, Si, and K ions were the highest in the leachate. It could be due to re-condensation of mentioned dissolved ions in the crystallization process. Most likely, the stable yellowish color of alkali filtrate is because Fe (III).The color of filtrate after 5 and 9 recycling further confirmed the steady-state conditions (Figure B-7 c).

The concentration of K increased with small slope indicating dissolution of potassium content of CFA. Its concentration didn't change for the leachate of CFA-ZP. Although it does not hinder the production; however, it indicates that the zeolite produced prefers sodium as a cation in its framework over potassium. The same trend was observed for Cr,

and more slightly for V and Ni, as their concentrations increased to 4.5, 35 and 1.5 ppm, respectively after 6-8 consecutive runs and kept relatively constant. However, no significant change was observed in their concentrations in leachate of the CFA-ZP product.
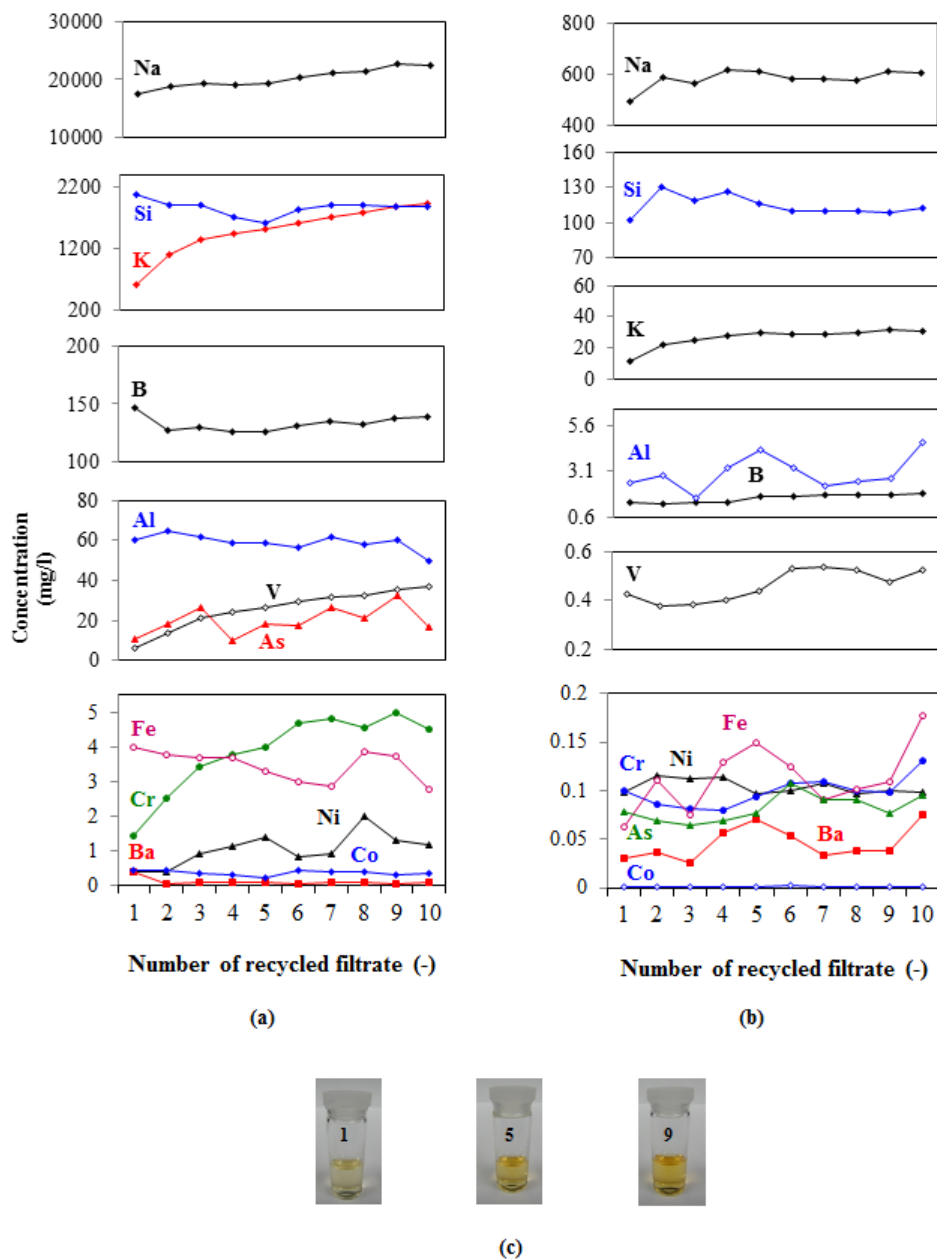
Figure B-7. Inductively coupled plasma atomic emission spectrometer (ICP-AES) analysis of a function of recycling number a) recycled filtrate, b) leachate of CFA-ZP, c) colour of recycled filtrate.

Elemental analysis (major and trace elements) of the collected leachate of the CFA-ZP (after 10 consecutive run of filtrate recycling) and the raw CFA sample, is compared in Table B-3. It is noteworthy that pH of the leachates from CFA-ZP samples was in the

range of 11.80-11.95, which was comparable with that from CFA (i.e. 11.45). Therefore, it can be concluded that the difference between leaching rates could not be considered as the result of pH of the solution. The concentrations of non-hazardous elements (Na, K and Si) in leachate of CFA-ZP were higher than those in leachate of CFA. The measured Al, Fe, Cr, Ba, Mg, Se, Co and Mn concentrations were found to be considerably below the specified characteristic toxicity levels. Co and Mn concentration in the leachate of CFA-ZP sample were remarkably low. The results showed that during the zeolitization process, heavy metals retained in the zeolitized product, either because they were adsorbed by the Na-P zeolite or precipitated as hydroxides at high pH of the solution [55-59]. Relatively high cations exchange capacity (CEC) and high specific surface area are two main factors that can be considered as contributors to the lower concentrations of cations in leachate of CFA-ZP. Average boron level in soil was reported to be approximately 10 ppm [54]. Elevated levels of boron in leachates may be of environmental interest [60].

Table B-3. Leachate analysis of CFA and CFA-ZP

Element	Concentration (ppm)		
	CFA-ZP		**Raw CFA**
Na	608	>	70.016
Si	113	>	0.757
K	30.8	>	16.3
B*	1.850	>	1.098
V	0.520	>	0.051
Ni*	0.100	>	0.027
As*	0.096	>	0.023
Al	4.68	<	33.91
Fe	0.180	<	0.475
Cr	0.130	<	0.271

Ba	0.075	<	0.251
Mg	0.039	<	0.238
Se	0.023	<	0.095
Pb	UD	<	0.024
Co	0.002	<	0.006
Mn	0.0005	<	0.0008

* Less than threshold (maximum permissible limit) for landfill leachate and wastewater effluent for discharge into river and surface water (5 ppm for Al, 4 ppm for B, 0.2 ppm for Ni, 0.1 ppm for As,, 0.05 ppm for Co, 2 ppm for Fe, 0.05 ppm for Pb, 0.2 ppm for Mn, 0.02 ppm for Se, 0.05 ppm for Cr: and 0.1 for V) [54, 56]

The results of leachate tests showed the leaching of some elements (i.e. As, Ni, and V) still poses a problem regarding the regulatory levels. These elements have a greater tendency to leach out from the synthesized zeolite. Most anion-forming elements proved to be quite mobile and were to a large extent extracted during the process. This trend was expected, since zeolites have a permanent negative charge on their surface with no affinity for anions. These elements are soluble usually in anionic form such as arsenite (AsO_3^{3-}), arsenate (AsO_4^{3-}), borate (BO_3^{3-}) and metavanadate (VO_3^-). Therefore during the zeolitization process, cationic heavy metals are mostly immobilized while anionic species are largely leached. This finding is in agreement with literature [62]. Anionic species were largely extracted by the process water during the course of filtration. Arsenic was released initially from the solid phase mostly in the trivalent oxidation state but was unstable to either oxidation or adsorption. Solution pH also affects adsorption of As on surface active solids. From a biological perspective, the oxidation state of arsenic in coal ash and its leachate, and the ease of transformation between these states, are of considerable concern. The inorganic trivalent forms of arsenic are more toxic than inorganic pentavalent and organic trivalent forms. Analytical data gathered during the course of leaching tests revealed that the selectivity of the CFA-ZP toward tested cations is as following:

Pb>Al>Mg>Se>Ba>Co>Fe>Cr
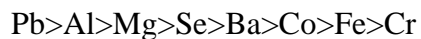
B.3.1   Economical aspect

Developing of cost effective and eco-friendly techniques to treat CFA is of great importance. Efficient zeolitization of CFA will reduce the risks associated with the disposal of this industrial solid waste. One of the main objectives of this work was to reduce that pollution associated with coal fly ash and the conversion techniques, in which the produced second waste may contaminate the surface and underground water. Heavy metals of CFA are hazardous to the environment because of their contribution to the formation of toxic compounds. This contamination could lead to health and environmental problems. In economical point of view, the relationship between cost of recycling process (capital investment), cost of fresh DI-water, cost of sodium hydroxide as the main chemicals needed for the zeolitization process (apart from CFA that can be considered very cheap) and huge cost associated with the treatment of the produced industrial wastewater streams should be considered as the main factors determining economic feasibility of the developed zero liquid discharge technique. Table B-4 shows a preliminary cost estimation and profitability of zero discharge process.

Table B-4. Preliminary cost tabulation based on production of one metric ton of CFA-ZP from CFA by total recycling of washing liquid (cased on: $400-450/metric ton NaOH (min. order 20 Ton) [Alibaba] and $1.52 cubic meter H_2O [Canada-Ontario]

Item	Without recycling	With recycling	Reduction in raw material	
			%	$
Sodium hydroxide (ton)	0.27	0.12	55.5	63.7
Fresh water (ton)	20	1.70	91.5	27.8
Waste water treatment Installation	Required	-	-	-
Liquid recycling Installation	-	Required	-	-

B.4 Conclusions

This work presents the feasibility of using a zero liquid discharge technique for continuous zeolitization of Coal fly ash in a lab scale, which is techno-economically feasible for implementation at larger scales. Zero liquid discharge minimizes the consumption of freshwater and sodium hydroxide remarkably. In addition, elimination of liquid discharge will obviate the need to comply with increasingly stringent environmental restrictions with very costly large wastewater treatment units

Quality of the zeolitized coal fly ash products didn't change significantly, after the consecutive zeolitization process with recycled filtrates from filtering and washing stages. In comparison to the parent raw CFA, leach resistance of the products are very promising, which shows their high capacity to immobilize environmental pollutants such as heavy metals. Although the leaching of the elements V, Ni and As is slightly higher

than CFA, however, it is still lower than the threshold value of the wastewater and landfill leachate before discharge into the environment.

Scaling up of the developed zero liquid discharge technique seems to be techno-economically feasible and the zeolitic product can be used in environmental friendly technology to immobilize different pollutants.

B.5   References

[1] Querol X, Moreno N, Umaña JC, Alastuey A, Hernández E, López-Soler A, Plana F. Synthesis of zeolites from coal fly ash: an overview. Int J Coal Geol 2002; 50: 413-423.

[2] Siddique R. Performance characteristics of high-volume class F fly ash concrete. Cem Concr Res 2004; 34: 487-493.

[3] Blissett RS, Rowson NA. A review of the multi-component utilization of coal fly ash. Fuel 2012; 97: 1-23.

[4] E.P.A. US, Using coal fly ash in highway construction, a guide to benefits and impacts, EPA-530, K-05-002 (2005).

[5] Kikuchi R. Application of coal ash to environmental improvement transformation into zeolite, potassium fertilizer, and FGD absorbent. Resour Conserv Recy 1999; 27: 333-346.

[6] Heidrich C, Feuerborn H, Weir A. Coal combustion products: a global perspective. World Coal Ash WOCA, Lexington, KY: 2013.

[7] Ahmaruzzaman M. A review on the utilization of fly ash. Progress in Energy and Combustion Science, 2010; 36: 327-363.

[8] Sheps-Pelleg S, Cohen H. Evaluation of the leaching potential of trace elements from coal ash to the (groundwater) aquifer, International Ash utilization Symposium. Center for Applied Energy Research, University of Kentucky.Paper # 110, 1999.

[9] Coal ash handbook, Kankyo Gijyutsu Kyokai and Nippon Fly Ash Kyokai, Tokyo (2000).

[10] Twardowska I, Szczepanska J. Solid waste, terminological and long-term environmental risk assessment problems exemplified in a power plant fly ash study. Sci Total Environ 2002; 285: 29-51.

[11] Borm PJA. Toxicity and occupational health hazards of coal fly ash (CFA): A review of data and comparison to coal mine dust. Ann Occup Hyg 1997; 41: 659-676.

[12] Popovic A, Djordjevic D, Polic P. Trace and major element pollution originating from coal ash suspension and transport processes. Environ Int 2001; 26: 251-255.

[13] Lokeshappa B, Dikshit AK. Disposal and management of fly ash, 2011, International Conference on Life science and Technology, IPCBEE vol. 3, IACSIT Press, Singapore.

[14] Berkgaout V, Singer A. High capacity cation exchanger by hydrothermal zeolitization of coal fly ash. Appl Clay Sci 1996; 10: 369-378.

[15] Querol X, Plana F, Alastuey A, López-Soler A. Synthesis of Na-zeolites from fly ash. Fuel 1997; 76: 793-799.

[16] Hollman GG, Steenbruggen G, Janssen-Jurkovičová M, A two-step process for the synthesis of zeolites from coal fly ash. Fuel 1999; 78: 1225-1230.

[17] Park M, Choi CL, Lim WT, Kim MC, Choi J, Heo NH. Molten-salt method for the synthesis of zeolitic materials: II. Characterization of zeolitic materials. Microporous Mesoporous Mater 2000; 37:91-98.

[18] Moreno N, Pereira CF, Junssen- Jurkovičová M. Utilization of zeolites synthesized from coal fly ash for the purification of acid mine waters. Environ Sci Technol 2001; 35: 3526-3534.

[19] Querol X, Umaña JC, Plana F, Alastuey A, Lopez-Soler A, Medinaceli A, Valero A, Domingo MJ, Garcia-Rojo E. Synthesis of zeolites from fly ash at pilot plant scale. Examples of potential applications. Fuel 2001; 80: 857-865.

[20] Moreno N, Querol X, Plana F, Andres JM, Janssen M, Nugteren H., Pure zeolite synthesis from silica extracted from coal fly ashes. J Chem Technol Biotechnol 2002; 77:274-279.

[21] Inada M, Eguchi Y, Enomoto N, Hojo J. Synthesis of zeolite from coal fly ashes with different silica-alumina composition. Fuel 2005; 84: 299-304.

[22] Wdowin M, Franus M, Panek R, Badura L, Franus W. The conversion technology of fly ash into zeolites. Clean Technol Envir 2014; 16: 1217-1223.

[23] Wałek TT, Saito F, Zhang Q. The effect of low solid/liquid ratio on hydrothermal synthesis of zeolites from fly ash. Fuel 2008; 87: 3194-3199.

[24] Chang HL, Shih WH., Synthesis of zeolite A and X from fly ashes and their ion-exchange behaviour with cobalt ions, Ind Eng Chem Res 2000; 39: 4185-4191.

[25] Nascimento M, Soares PSM, de Souza VP. Adsorption of heavy metal cations using coal fly ash modified by hydrothermal method. Fuel 2009; 88:1714-1719.

[26] Hui KS, Chao CYH. Effects of step-change of synthesis temperature on synthesis of zeolite 4A from coal fly ash. Microporous Mesoporous Mater 2006; 88:145-151.

[27] Rayalu SS, Udhoji JS, Munshi KN, Hasan MZ. Highly crystalline zeolite-A from fly ash of bituminous and lignite coal combustion. J Hazard Mater 2001; 88:107-121.

[28] Chauhan YP, Talib M. A novel and green approach of synthesis and characterization of nano-adsorbents (zeolites) from coal fly ash: a review. Sci Rev Commun 2012; 2: 12-19.

[29] de C. Izidoro J, Fungaro DA, Abbott JE, Wang S. Synthesis of zeolites X and A from coal fly ashes for cadmium and zinc removal from aqueous solutions in single and binary ion systems. Fuel 2013; 103: 827-834.

[30] Shigemoto N, Hayashi H, Miyaura K. Selective formation of Na-X zeolite from coal fly ash by fusion with sodium hydroxide prior to hydrothermal reaction. J Mater Sci 1993; 28: 4781-4786.

[31] Belviso C, Cavalcante F, Lettino A, Fiore S. Zeolite synthesized from fused coal fly ash at low temperature using seawater for crystallization. Coal combustion and Gasification Products 2009; 1: 1-13.

[32] Ruen-ngam D, Rungsuk D, Apiratikul R, Pavasant P. Zeolite formation from coal fly ash and its adsorption potential. J Air and Waste Manage Assoc 2009; 59: 1140-1147.

[33] Srinivasan A, Grutzeck MW. The Adsorption of SO2 by Zeolites Synthesized from fly ash. Environ Sci Technol 1999; 33:1464-1469.

[34] Woolard CD, Strong J, Erasmus CR. Evaluation of the use of modified coal ash as a potential sorbent for organic waste streams. Appl Geochem 2002; 17: 1159-1164.

[35] Musyoka NM, Petrik LF, Balfour G, Gitari WM, Hums E, Synthesis of hydroxyl sodalite from coal fly ash using waste industrial brine solution. J Environ Sci Health, Part A 2011; 46: 1699-1707.

[36] Shoumkova A, Stoyanova V. Zeolites formation by hydrothermal alkali activation of coal fly ash from thermal power station "Maritsa 3", Bulgaria. Fuel 2013; 103:533-541.

[37] Klamrassamee T, Pavasant P, Laosiripojana N. Synthesis of zeolite from coal fly ash: Its application as water sorbent. Eng J 2010;14:37-44.

[38] Zhao XS, Lu GQ, Zhu HY. Effects of ageing and seeding on the formation of zeolite Y from coal fly ash, J Porous Mat 1997; 4: 245-251.

[39] Molina A, Poole C. A comparative study using two methods to produce zeolites from fly ash. Miner Eng 2004; 17:167-173.

[40] Rios CA, Williams CD, Roberts CL. A comparative study of two methods for the synthesis of fly ash-based sodium and potassium type zeolites. Fuel 2009; 88: 1403-1416.

[41] Musyoka NM, Petrik LF, Fatoba OO, Hums E. Synthesis of zeolites from coal fly ash using mine waters. Miner Eng 2013; 53: 9-15.

[42] Tanaka H, Fujii A, Fujimoto S, Tanaka Y. Microwave-assisted two-step process for the synthesis of a single-phase Na-A zeolite from coal fly ash. Adv Powder Technol 2008; 19: 83-94.

[43] Musyoka NM, Petrik LF, Gitari WM, Balfour G, Hums E. Optimization of hydrothermal synthesis of pure zeolite Na-P1 from South African coal fly ashes. J Environ Sci Health Part A 47, 2012; 337-350.

[44] Mainganye D, Ojumu TV, Petrik L. Synthesis of zeolites Na-P1 from South African coal fly ash: Effect of impeller design and agitation. Materials 2013; 6: 2074-2089.

[45] Bukhari SS, Behin J, Kazemian H, Rohani S. Conversion of coal fly ash to zeolite utilizing microwave and ultrasound energies: A review. Fuel 2015; 140: 250-266.

[46] Inada M, Tsujimoto H, Eguchi Y, Enomoto N, Hojo J. Microwave-assisted zeolite synthesis from coal fly ash in hydrothermal process. Fuel 2005; 84: 1482-1486.

[47] Juan R, Hernández S, André JM, Ruiz C., Synthesis of granular zeolitic materials with high cation exchange capacity from agglomerated coal fly ash. Fuel 2007; 86: 1811-1821.

[48] Fukui K, Katoh M, Yamamoto T, Yoshida H. Utilization of NaCl for phillipsite synthesis from fly ash by hydrothermal treatment with microwave heating. Adv Powder Technol 2009; 20: 35-40.

[49] Azizi SN, Asemi N. The effect of ultrasonic and microwave-assisted aging on the synthesis of zeolite P from Iranian perlite using Box-Behnken experimental design. Chem Eng Comm 2014; 201: 909-925.

[50] Belviso C, Cavalcante F, Lettino A, Fiore S. Effects of ultrasonic treatment on zeolite synthesized from coal fly ash. Ultrason Sonochem 2011; 18: 661-668.

[51] Bukhari SS, Rohani S, Kazemian H. Effect of ultrasound energy on the zeolitization of chemical extracts from fused coal fly ash. Ultrason Sonochem 2016; 28: 47-53.

[52] Slangen PM, Jansen JC, Van Bekkum H., The effect of ageing on the microwave synthesis of zeolite NaA. Microporous Mater 1997; 9:259-65.

[53] CEN/TC292/WG2 Leaching Test Procedure: 1994, Compliance test for leaching of granular waste materials and sludges.

[54] Landsberger S, Cerbus JF, Larson S. elemental characterization of coal fly ash and its leachate using sequential extraction techniques. J Radioan Nucl Ch 1995; 192: 265-274.

[55] Mohan S, Gandhimathi R. Removal of heavy metal ions from municipal solid waste leachate using coal fly ash as an adsorbent, J Hazard Mater 2009; 16:351-350.

[56] Koukouzas N, Vasilatos C, Itskos G., Mitsis I, Moutsatsou A. Removal of heavy metals from wastewater using CFB-coal fly asf zeolitic materials. J Hazard Mater 2010; 173:581-588.

[57] Itskos G., Koukouzas N, Vasilatos C, Megremi I, Moutsatsou A. Comparative uptake study of toxic elements from aqueous media by the different particle-size-fraction of fly ash. J Hazard Mater 2010; 183:787-792.

[58] Cho H, Oh D, Kim K. Astudy on emoval characteristics of heveay metals from aqueous solution by fly ash. J Hazard Mater 2005; B127:187-195.

[59] Wang S, Soudi M, Li L, Zhu ZH. Coal ash conversion into effective adsorbents for removal of heavy metals and dyes from wastewater ash. J Hazard Mater 2006; B133:243-251.

[60] Bowen HJM. Trace Elements in Biochemistry, Academic Press, New York (1966).

[61] Zandi M, Russell NV, Edyvean RGJ, Hand RJ, Ward P. Interpretation of standard leaching test BS EN 12457-2: is your sample hazardous or inert? J Environ Monitor 2007; 9: 1426-1429.

[62] Steenbruggen G, Hollman GG. The synthesis of zeolites from fly ash and the properties of the zeolite products. J Geochem Explor 1998; 62: 305-309.

Appendix C

C Measurement of cation exchange capacity of zeolites using Kjeladhl method and UV-VIS spectroscopy

Abstract

The cation exchange capacity of three different zeolite-A samples was measured using two different NH4+ techniques; Kjeldahl method and UV-VIS spectroscopy. The zeolite samples were saturated with ammonium acetate and then washed by a 10% NaCl (by weight) and 1% (by volume) of HCl. The NH_4^+ rich supernatant was then analyzed for NH_4^+ concentration using the two methods. Kjeldahl method involved two neutralization reactions and titration, whereas, UV-VIS spectroscopy involved the treatment of the NH_4^+ rich supernatant with sodium salicylate and sodium hypochlorite. The addition of these two chemicals in the presence of ammonium ions resulted in a colour change that was detected by UV-VIS spectrometer. The cation exchange capacities for the three samples were calculated using both methods which were within 10% of each other. Using UV-VIS spectrometry took only ten minutes to conduct after ammonium saturation and washing step compared to two hours for Kjeldahl method. Using sodium salicylate and sodium hypochlorite for the calculation of CEC is a more efficient method when access to a UV-VIS spectrometer is readily available.

C.1 Introduction

Zeolites have become an invaluable part of the chemical industry. They are multifunctional crystalline structures that have a variety of applications including the catalysis of reactions (used heavily in the petroleum industry), gas separation, purification of air and water, among other uses [1–7].

Zeolite structure is based on silicate chemistry with tetrahedron structure similar to aliphatic carbon chemistry. Tetrahedron is a polyhedron composed of four triangular faces. Three of these triangular faces meet at the vertex while the forth triangle composes the base of the structure. Silicate (SiO_4) unit within a structure is linked to other silicate

through shared oxygen atoms. Zeolite frameworks exclusively contain Al^{+3} and Si^{+4}, therefore producing a negative charge in the frameworks. These frameworks contain cations (mainly Na, K, Ca and Mg) to electrochemically balance the negative charge introduced by Al atoms present in aluminosilicates. It can be inferred that higher ratio of Al^{+3} would result in higher cation exchange capacity [1]. An important feature of zeolites is the ability of these surface cations to be exchanged with other cations (Figure C-1).
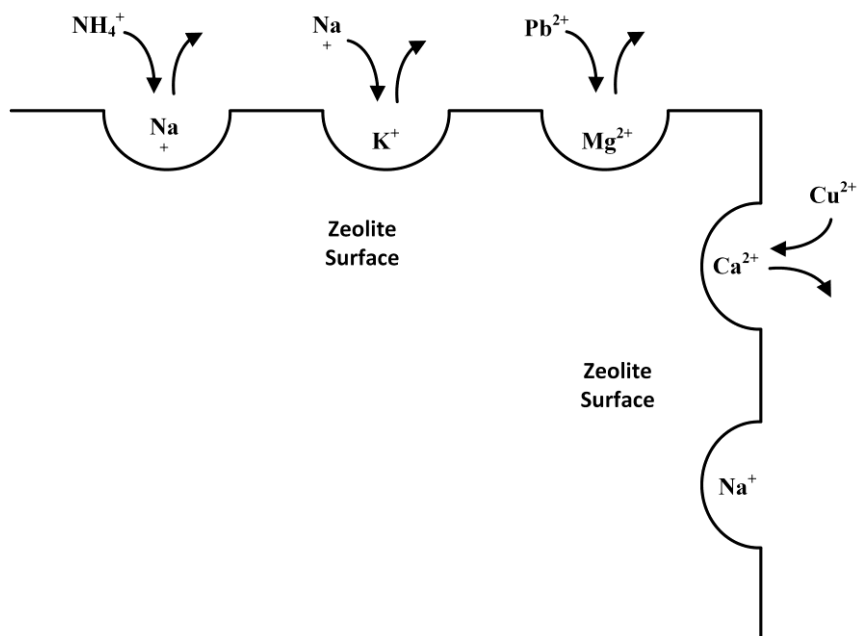

Figure C-1. Zeolite surface ion exchange

This has been exploited for water treatment [8–11]. Cation exchange capacity (CEC) is a measure reported that quantifies the amount of cations (typically reported as milliequivalent or meq) of cation that can be exchanged per gram of zeolite. Zeolites can be generally classified into two broad groups: natural and synthetic zeolites. Table C-1 reports the CEC of zeolites (both natural and synthetic).

Table C-1. CEC of different zeolites as reported in literature

Natural zeolite	CEC	Method	Reference
Clinoptilolite	1.84 meq/g	ammonium acetate	[12]
Clinoptilolite	1.03 meql/g	Na, Ca displaced by K	[11]
48% clinoptilolite – 30% mordenite	2.05 meq/g	-	[13]
Mordenite	2.29 meq/g	theoretical	[14]
44% phillipsite – 4% chabazite	2.12 meq/g	ammonium acetate	[15]
37% phillipsite – 17% chabazite	1.90 meq/g	cross-exchange	[12]

Synthetic zeolite	CEC		Reference
4A	3.59 meq/g	Cd-Na exchange	[16]
A	2.63 meq/g	ammonium acetate	[17]
Na-LTA (anhydrous)	7.0 meq/g	theoretical	[18]
Na-SOD (anhydrous)	6.4 meq/g	theoretical	[18]
NaCs-RHO (anhydrous)	3.1 meq/g	theoretical	[18]
P	2.49 meq/g	Cd-Na exchange	[16]
X	2.79 meq/g	ammonium acetate	[19]
Y	1.69 meq/g	Cd-Na exchange	[16]

In general, synthetic zeolites have higher CEC values than natural zeolites (Table C-1). However, due to the relative high cost compared to natural zeolites, natural zeolites are used more often in water treatment applications.

The general procedure for the measurement of CEC is as follows: (1) the zeolite is soaked in a cationic solution of high selectivity (many different cations reported in literature [20–22]) for a specified period of time to allow for the zeolite to be completely saturated in the cation; (2) after saturation, the zeolite is allowed to dry thoroughly, typically in air to allow the cations to remain fixated to the zeolite; (3) once dry, the zeolite is thoroughly rinsed or soaked in a solution to remove the fixated cations (usually a high concentration NaCl solution due to zeolites' selectivity for Na+ ions); (4) the concentration of the now removed cation is measured and is back calculated to find how much cation was fixated to the specified mass of zeolite and related back to CEC.

The most common cation used to measure the CEC is NH4+ due to zeolites high selectivity to NH4+ (ammonium acetate method). Another advantage of NH4+ is its small molecular diameter allowing it to penetrate the small pores of the zeolite, giving a more representative CEC value. Many different methods can be used to measure NH4+. The two methods that are used in this work to measure NH4+ are the Kjeldahl method and UV-VIS spectroscopy.

C.2 Materials and methods

C.2.1   Zeolite synthesis

The chemical precursors used for the synthesis of zeolites were sodium aluminate Na2O:Al2O3:3H2O (Anachemia, Canada), sodium metasilicate, $Na_2SiO_3:5H_2O$ (Sigma-Aldrich, USA) and sodium hydroxide (Alphachem, Canada). The gel composition of 3.165 Na_2O:1 Al_2O_3:1.926 SiO_2:128 H_2O was used for synthesis of zeolite-A. The preparation procedure of the gel [23] was as follows: (a) Sodium aluminate (8.258 g) and sodium metasilicate (15.48 g) were dissolved in an 0.22 M solution of sodium hydroxide (40 mL), separately. After 30 min of stirring at room temperature, clear solutions were obtained. (b) The solutions were mixed to form the precursor gel. Four different procedures were used to synthesize four different samples of zeolite-A.

Sample A was synthesized under conventional heating using an oven following the verified zeolite-A synthesis method published by the International Zeolite Association

[23]. For the rest of the samples the gel formed was aged at room temperature for 2 hours before further reaction. The constant aging time of 2 h was chosen as the optimum-short aging time mentioned in literature [24]. Sample B was synthesized under atmospheric pressure utilizing microwave irradiation. The experiments were performed in a self-adjusting, microwave oven (single-mode, 2.45 GHz, CEM cooperation, Discover, USA). After a given period of MW irradiation, the solid products were filtered off, washed with deionized water and dried overnight at 100 ºC in an electric oven. Sample B had a condenser affixed to conduct the experiment at atmospheric condition similar to experiments conducted by this group previously [25]. Sample C was synthesized utilizing an ultrasound probe (Vibra Cell VCX-500, Sonics & Materials, USA) that was immersed into the reaction mixture.

C.2.2   Ammonium acetate saturation method

The procedure to saturate the zeolite with NH4+ was based on the method of Bain and Smith (1987) [20]. A known amount of zeolite was added to 30 mL of 1 N ammonium acetate (NH4OAc) in a 50 mL cylindrical Nalgene vessel with dimensions of 28 mm ID × 108 mm. The samples were mixed in an end-over-end mixer for 5 days for saturation of the zeolite. After 5 days, the samples were filtered through 1 µm filter paper and allowed to air dry overnight. To extract the NH4+, the dried samples were washed using 100 mL (5 x 20 mL) of an aqueous solution of 10% NaCl (by weight) and 1% (by volume) of HCl. The NH4+ rich supernatant was then analyzed for NH4+ concentration.

C.2.2.1   Kjeldahl method

The Kjeldahl apparatus used included a round bottom flask placed over a heater which helped heat up the content of the round bottom flask. The flask was affixed with a funnel with a valve to introduce NaOH in the solution to convert ammonium in the solution to ammonia gas. This gas was carried through a tube to the other side of the apparatus where it was bubbled into an Erlenmeyer flask containing HCl of a known concentration and volume. The Erlenmeyer flask was also affixed with a condenser to prevent any gas from escaping. The ammonia bubbled into the flask reacted with the HCl which was back titrated to calculate the ammonium concentration in the solution in the round bottom

flask. The temperature was constantly raised at 2°C/min to 100°C in order to reduce the solubility of ammonium in the solution [26]. The Kjeldhal setup used is illustrated in Figure 2.
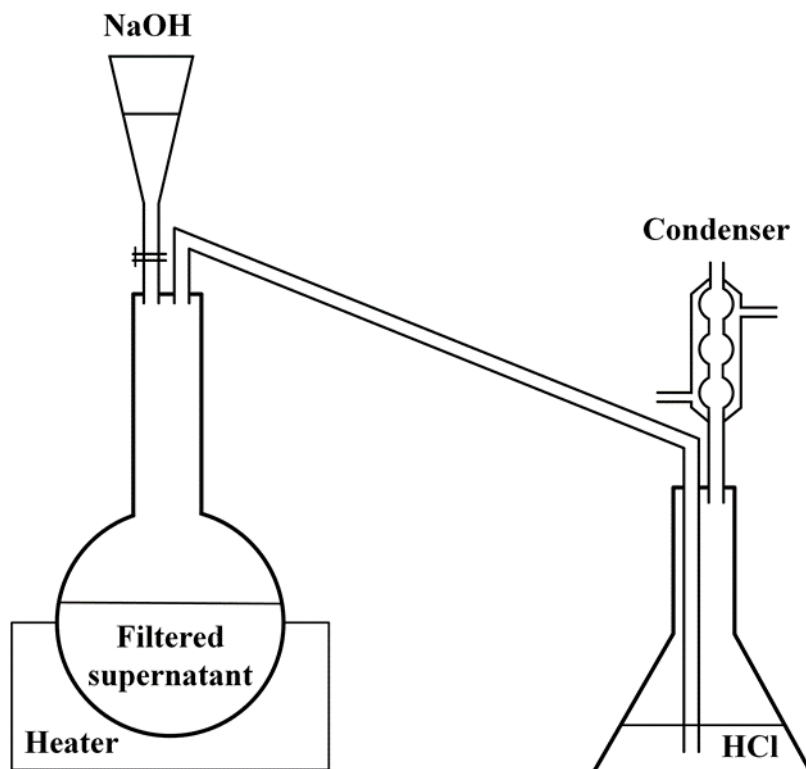

Figure C-0-2. The schematics of Kjeldahl apparatus

The ammonium in the solution in the round bottom flask is neutralized by NaOH and the resulting ammonia gas is neutralized by HCl in the Erlenmeyer flask back to ammonium. The overall ionic reaction on the extraction side in the round bottom flask and the dissolution side in the Erlenmeyer flask are given below.

$$NH_4^+{}_{(aq)} + OH^-{}_{(aq)} \rightarrow NH_{3(g)} + H_2O_{(l)}$$

$$NH_{3(g)} + H^+{}_{(aq)} \rightarrow NH_4^+{}_{(aq)}$$
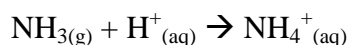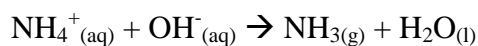
C.2.2.2   UV-VIS spectroscopy

The peak absorbance intensity was correlated to ammonium concentration by preparing known NH4+ concentrations. Sodium salicylate, sodium hydroxide and sodium

hypochlorite were added to the NH4+ standards. After addition of the reagents, the standards were allowed 5 minutes for completion of the reaction. This reaction results in the clear solution to change colour to a yellowish-green hue. The samples were then analyzed using UV-VIS spectroscopy (Cary 100 UV-Visible Spectrophotometer, Agilent, Santa Clara, USA) between 550 and 800 nm and fitted with a linear equation (Figure C-0-3(a) and (b)).
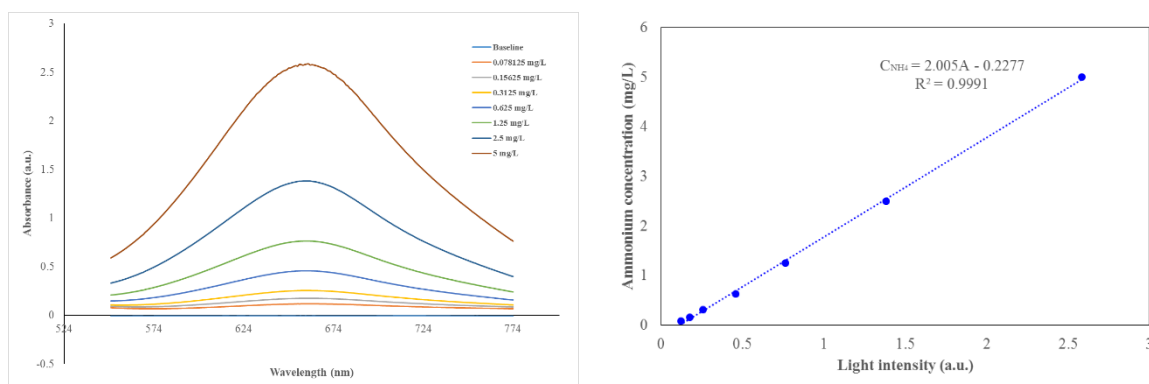

Figure C-0-3. (A) Wavelength (nm) vs. absorbance and (b) peak absorbance intensity vs NH$_4^+$ concentration (mg/L) with linear fit

From previous experience and literature data, the range of expected CEC was determined. After extraction of the fixated ammonium, the samples were diluted to a concentration that is in the range of the calibration curve (Figure C-0-3(b)). Sodium salicylate, sodium hydroxide and sodium hypochlorite were added to the diluted sample and allowed to react for 5 minutes. The samples were then analyzed using UV-VIS spectroscopy. The peak absorbance intensity was then used to determine the concentration of NH4+ and to determine the CEC.

C.3 Results and discussion

C.3.1   Cation exchange capacity

Table C-2 shows the CEC values measured using Kjeldahl method and UV-VIS method.

Table C-2. Comparison of CEC values using the two NH$_4^+$ measurement techniques

Method	Zeolite Samples		
	Sample A	Sample B	Sample C
Kjeldahl	3.13	2.63	2.97
UV-VIS	3.12	2.89	3.20

The above data shows that the two methods agree within 10%. Indicating UV-spectroscopy can be accurately used to measure CEC. Kjeldahl method involves back titration of a standardized HCl solution. Titration is prone to errors because the end point has to be visually discerned which is a qualitative observation. However, using salicylate based ammonium assay results in a colour change that is quantitatively detected by UV-VIS Spectroscopy.

Kjeldahl method also requires considerable more time compared to UV-VIS Spectroscopy. The saturated ammonium solution in the Kjeldahl method has to go through two neutralization reactions and a careful titration for the determination of the CEC in the zeolite sample. These steps can take more than two hours. In the case of UV-VIS Spectroscopy, the ammonium assay only takes ten minutes before a reading can be taken. The ease of using UV-VIS Spectroscopy over back titration saves considerable time for measuring CEC.

C.4 Conclusion

Three different zeolite-A samples were synthesized using different synthesis schemes. The cation exchange capacity (CEC) of all the samples was determined both my Kjeldahl method and UV-spectroscopy. The measurement of CEC was found to be within 10% of each other. Use of the UV-VIS spectroscopy was determined to save time and less prone to experimental errors as compared to Kjeldahl method as the later method requires two neutralization reactions followed by a careful back titration.

C.5 References

[1]   S.S. Bukhari, J. Behin, H. Kazemian, S. Rohani, Conversion of coal fly ash to zeolite utilizing microwave and ultrasound energies: A review, Fuel. 140 (2015) 250–266.

[2]   N. Moreno, X. Querol, C. Ayora, A. Alastuey, C. Fernández-Pereira, M. Janssen-Jurkovicová, Potential Environmental Applications of Pure Zeolitic Material Synthesized from Fly Ash, J. Environ. Eng. 127 (2001) 994–1002.

[3]   A. Malekpour, M.R. Millani, M. Kheirkhah, Synthesis and characterization of a NaA zeolite membrane and its applications for desalination of radioactive solutions, Desalination. 225 (2008) 199–208. doi:10.1016/j.desal.2007.02.096.

[4]   P.K. Sinha, P.K. Panicker, R.V. Amalraj, V. Krishnasamy, Treatment of radioactive liquid waste containing caesium by indigenously available synthetic zeolites: A comparative study, Waste Manag. 15 (1995) 149–157. doi:10.1016/0956-053X(95)00014-Q.

[5]   M.V. Landau, L. Vradman, V. Valtchev, J. Lezervant, E. Liubich, M. Talianker, Hydrocracking of heavy vacuum gas oil with a Pt/H-beta-Al2O3 catalyst: Effect of zeolite crystal size in the nanoscale range, Ind. Eng. Chem. Res. 42 (2003) 2773–2782.

[6]   O. Babajide, N. Musyoka, L. Petrik, F. Ameer, Novel zeolite Na-X synthesized from fly ash as a heterogeneous catalyst in biodiesel production, Catal. Today. 190 (2012) 54–60.

[7]   M. Wdowin, M.M. Wiatros-Motyka, R. Panek, L.A. Stevens, W. Franus, C.E. Snape, Experimental study of mercury removal from exhaust gases, Fuel. 128 (2014) 451–457.

[8]   E. Erdem, N. Karapinar, R. Donat, The removal of heavy metal cations by natural zeolites, J. Colloid Interface Sci. 280 (2004) 309–314. doi:10.1016/j.jcis.2004.08.028.

[9]   M.J. Zamzow, B.R. Eichbaum, K.R. Sandgren, D.E. Shanks, Removal of Heavy Metals and Other Cations from Wastewater Using Zeolites, Sep. Sci. Technol. 25 (1990) 1555–1569. doi:10.1080/01496399008050409.

[10]   A. Langella, M. Pansini, P. Cappelletti, B. de Gennaro, M. de' Gennaro, C. Colella, NH+4, Cu2+, Zn2+, Cd2+ and Pb2+ exchange for Na+ in a sedimentary

clinoptilolite, North Sardinia, Italy, Microporous Mesoporous Mater. 37 (2000) 337–343. doi:10.1016/S1387-1811(99)00276-0.

[11] Q. Du, S. Liu, Z. Cao, Y. Wang, Ammonia removal from aqueous solution using natural Chinese clinoptilolite, Sep. Purif. Technol. 44 (2005) 229–234. doi:10.1016/j.seppur.2004.04.011.

[12] S. Capasso, E. Coppola, P. Iovino, S. Salvestrini, C. Colella, Sorption of humic acids on zeolitic tuffs, Microporous Mesoporous Mater. 105 (2007) 324–328. doi:10.1016/j.micromeso.2007.04.017.

[13] A.H. Englert, J. Rubio, Characterization and environmental application of a Chilean natural zeolite, Int. J. Miner. Process. 75 (2005) 21–29. doi:10.1016/j.minpro.2004.01.003.

[14] V. Campos, L.C. Morais, P.M. Buchler, Removal of chromate from aqueous solution using treated natural zeolite, Environ. Geol. 52 (2006) 1521–1525. doi:10.1007/s00254-006-0596-3.

[15] S. Capasso, S. Salvestrini, E. Coppola, A. Buondonno, C. Colella, Sorption of humic acid on zeolitic tuff: a preliminary investigation, Appl. Clay Sci. 28 (2005) 159–165. doi:10.1016/j.clay.2004.01.010.

[16] B. Singh, B.J. Alloway, F.J.M. Bochereau, Cadmium sorption behavior of natural and synthetic zeolites, Commun. Soil Sci. Plant Anal. 31 (2000) 2775–2786. doi:10.1080/00103620009370626.

[17] S.S. Bukhari, J. Behin, H. Kazemian, S. Rohani, Synthesis of zeolite NA-A using single mode microwave irradiation at atmospheric pressure: The effect of microwave power, Can. J. Chem. Eng. 93 (2015) 1081–1090. doi:10.1002/cjce.22194.

[18] Y. Watanabe, H. Yamada, J. Tanaka, Y. Komatsu, Y. Moriyoshi, Ammonium Ion Exchange of Synthetic Zeolites: The Effect of Their Open-Window Sizes, Pore Structures, and Cation Exchange Capacities, Sep. Sci. Technol. 39 (2005) 2091–2104. doi:10.1081/SS-120039306.

[19] M. Zhang, H. Zhang, D. Xu, L. Han, D. Niu, B. Tian, J. Zhang, L. Zhang, W. Wu, Removal of ammonium from aqueous solutions using zeolite synthesized from fly ash by a fusion method, Desalination. 271 (2011) 111–121. doi:10.1016/j.desal.2010.12.021.

[20]   D.C. Bain, B.F.L. Smith, A Handbook of Determinative Methods in Clay Mineralogy, in: Handb. Determinative Methods Clay Mineral., Blackie & Son Ltd., Glasgow, 1987: pp. 248–274.

[21]   A. Derkowski, W. Franus, H. Waniak-Nowicka, A. Czimerova, Textural properties vs. CEC and EGME retention of Na-X zeolite prepared from fly ash at room temperature, Int. J. Miner. Process. 82 (n.d.) 57–68. doi:10.1016/j.minpro.2006.10.001.

[22]   W. Franus, M. Wdowin, M. Franus, Synthesis and characterization of zeolites prepared from industrial fly ash, Environ. Monit. Assess. 186 (2014) 5721–5729. doi:10.1007/s10661-014-3815-5.

[23]   H.E. Robson, K.P. Lillerud, Verified syntheses of zeolitic materials, 2nd ed., Elsevier, Amsterdam, The Netherlands, 2001.

[24]   W. Yuan, H. Chen, R. Chang, L. Li, Synthesis and characterization of NaA zeolite particle as intumescent flame retardant in chloroprene rubber system, Particuology. 9 (2011) 248–252.

[25]   S.S. Bukhari, J. Behin, H. Kazemian, S. Rohani, Synthesis of zeolite NA-A using single mode microwave irradiation at atmospheric pressure: The effect of microwave power, Can. J. Chem. Eng. 93 (2015) 1081–1090.

[26]   M.J. O'Neil, The Merck index: an encyclopedia of chemicals, drugs, and biologicals, RSC Publishing, 2013.

[27]   M.M.J. Treacy, J.B. Higgins, Collection of simulated XRD powder patterns for zeolites, Elsevier, Amsterdam, The Netherlands, 2007.

[28]   D.C. Bain, B.F.L. Smith, Chemical analysis, in: Handb. Determinative Methods Clay Mineral., Blackie, Glasgow, 1987: pp. 248–274.

Appendix D

D Pilot scale reactor system calibration curves for tanks and pumps
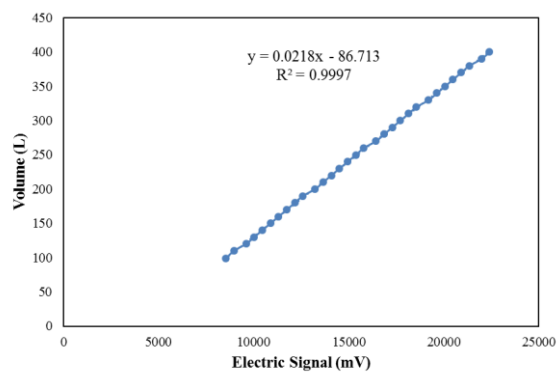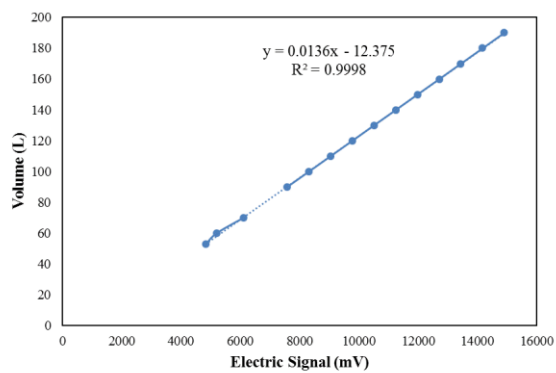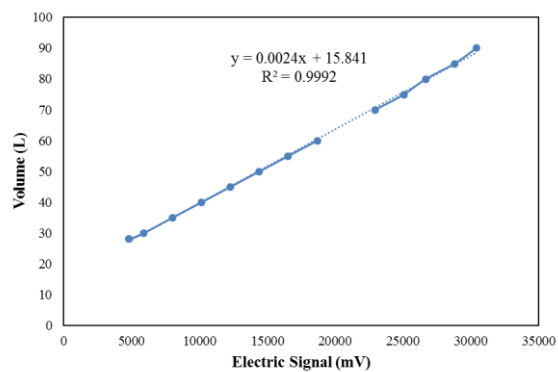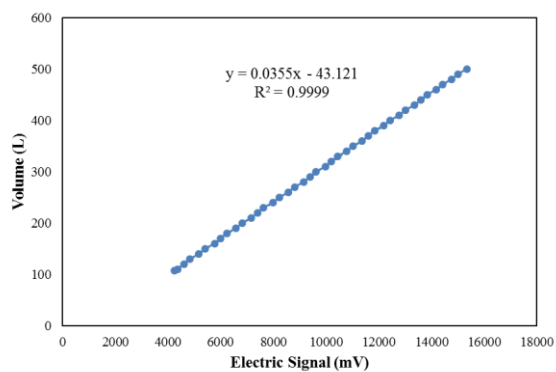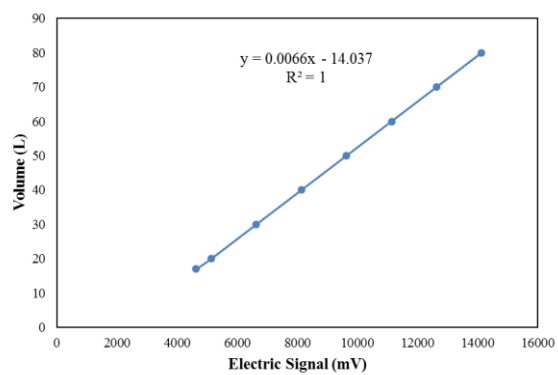
Figure D-1. Calibration curves and line of best fit for tanks a) TK-1 b) TK-2 c) TK-3 d) TK-5 e) R-1
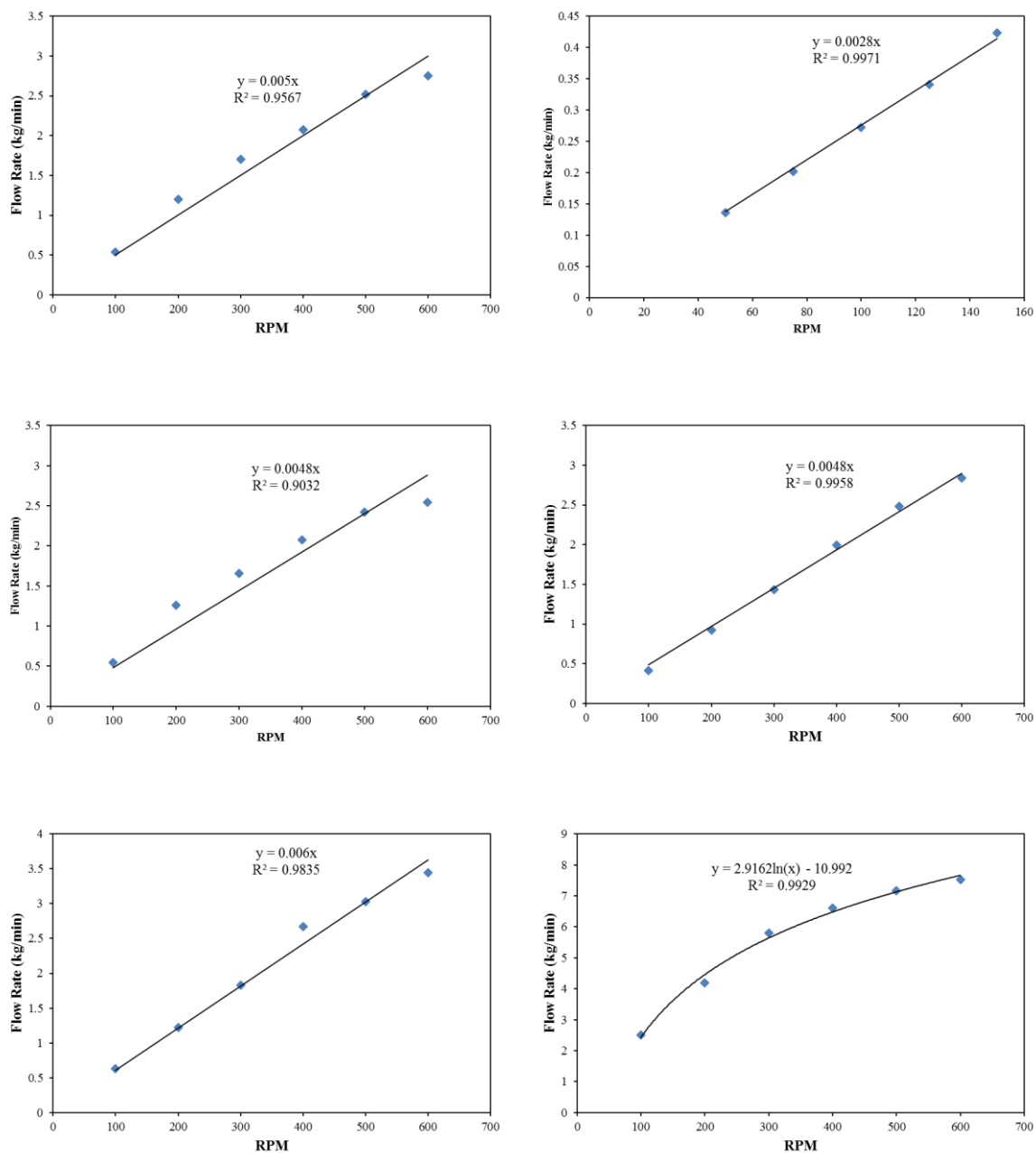
Figure D-2. Calibration curves and lines of best fir for a) P-1 b) P-2 c) P-3 d) P-4 e) P-5 f) P-6

Curriculum Vitae

Name:	Syed Salman Raza Bukhari

Post-secondary Education and Degrees:

University of Florida
Gainesville, Florida, USA
2005-2007 B.Sc.

University of Florida
Gainesville, Florida, Canada
2007-2009 M.E.

The University of Western Ontario
London, Ontario, Canada
2012-2016 Ph.D.

Honours and Awards:

Queen Elizabeth II Graduate Scholarship in Science &Technology
2015 – 2016

Florida Bright Future Scholarship
2003 – 2007

President's Honor Scholarship
2003 – 2005

Related Work Experience

Teaching Assistant
The University of Western Ontario
2012-2016

Publications:

[1]   Bukhari SS, Rohani S. Continuous Flow Synthesis of Zeolite-A from Coal Fly Ash Utilizing Microwave Irradiation with Recycled Liquid Stream. Fuel Under Review.

[2]   Bukhari SS, Omar H, Rohani S. Microwave assisted zeolitization of coal fly ash using landfill leachate as the solvent. J Hazard Mater Under Review.

[3]   Attari M, Bukhari SS, Kazemian H, Rohani S. Mercury Removal from Aqueous Solution by Zeolitized Coal Fly Ash: Equilibrium and Kinetic Study. Chemosphere Under Review.

[4]   Behin J, Bukhari SS, Kazemian H, Rohani S. Developing a zero liquid discharge process for zeolitization of coal fly ash to synthetic NaP zeolite. Fuel 2016;171:195–202.

[5]   Bukhari SS, Rohani S, Kazemian H. Effect of ultrasound energy on the zeolitization of chemical extracts from fused coal fly ash. Ultrason Sonochem 2016;28:47–53. doi:10.1016/j.ultsonch.2015.06.031.

[6]   Bukhari SS, Behin J, Kazemian H, Rohani S. Synthesis of zeolite NA-A using single mode microwave irradiation at atmospheric pressure: The effect of microwave power. Can J Chem Eng 2015;93:1081–1090.

[7]   Bukhari SS, Behin J, Kazemian H, Rohani S. Conversion of coal fly ash to zeolite utilizing microwave and ultrasound energies: A review. Fuel 2015;140:250–66.

[8]   Bukhari SS, Behin J, Kazemian H, Rohani S. A comparative study using direct hydrothermal and indirect fusion methods to produce zeolites from coal fly ash utilizing single-mode microwave energy. J Mater Sci 2014;49:8261–71.

[9]   Behin J, Bukhari SS, Dehnavi V, Kazemian H, Rohani S. Using Coal Fly Ash and Wastewater for Microwave Synthesis of LTA Zeolite. Chem Eng Technol 2014;37:1532–40.